

THÈSE DE DOCTORAT  
de l'École Nationale des Ponts

## Mathematical and numerical analysis of embedding methods in quantum mechanics

École doctorale MSTIC

Discipline: Mathématiques

Thèse préparée au CERMICS, au sein de l'équipe Inria MATERIALS

Thèse soutenue le 18 novembre 2024, par

**Alfred KIRSCH**

### Composition du jury

Zied AMMARI Maître de conférence, Université Rennes 1	<i>Rapporteur</i>
Michael LINDSEY Associate professor, UC Berkeley	<i>Rapporteur</i>
Volker BACH Full Professor, Technische Universität Braunschweig	<i>Examinateur</i>
Virginie EHRLACHER Professeure, École des Ponts ParisTech	<i>Examinaterice</i>
Michel FERRERO Chargé de recherche, École Polytechnique	<i>Examinateur</i>
Lucia REINING Directrice de recherche, École Polytechnique	<i>Examinaterice</i>
Éric CANCÈS Professeur, École des Ponts ParisTech	<i>Directeur de thèse</i>
David GONTIER Maître de conférence, Université Paris-Dauphine	<i>Co-directeur de thèse</i>



## Résumé succinct

Dans cette thèse, on se propose d'étudier les propriétés mathématiques et numériques de certaines *méthodes de plongement* en mécanique quantique. Le principe de ces dernières réside dans l'approximation d'un grand système quantique en une collection de sous-systèmes auto-cohérents. Cette stratégie permet d'outrepasser les limitations pratiques inhérentes du problème à  $N$ -corps, et de décrire certaines propriétés de systèmes électroniques fortement corrélés.

La première partie pose le cadre mathématique et introduit les deux méthodes étudiées dans cette thèse : d'une part la Théorie du Champ Moyen Dynamique (Dynamical Mean-Field Theory (DMFT)), s'intéressant aux fonctions de Green quantiques à un corps, et d'autre part la Théorie du Plongement de la Matrice Densité (Density Matrix Embedding Theory (DMET)), portant sur la matrice densité réduite à un corps.

On présente alors une analyse des équations DMET, où l'on démontre l'existence et l'unicité d'une solution "physique" dans la limite faiblement interagissante. La qualité de l'approximation réalisée est aussi étudiée dans cette limite : on montre l'exactitude au premier ordre, en le paramètre d'interaction entre les électrons, de l'approximation DMET. Des résultats numériques présentent l'applicabilité des théorèmes démontrés, et soulignent l'importance des hypothèses formulées.

Les équations DMFT sont étudiées dans la partie suivante, dans le cadre de l'approximation du solveur d'impureté "Iterated Perturbation Theory (IPT)". Notre analyse montre l'existence de solutions à ces équations, à l'aide d'une reformulation originale de ces dernières en termes d'un problème de point-fixe dans l'espace de certaines mesures positives.

Enfin, on étudie les propriétés d'une version discrète des équations IPT-DMFT, en donnant des résultats d'existence et d'unicité de la solution. Des simulations numériques réalisées sur un modèle de Hubbard révèlent l'intérêt et les propriétés de cette méthode dans l'étude d'un effet de fortes corrélations: la transition de Mott.

## Executive summary

In this thesis, we propose to study the mathematical and numerical properties of certain *embedding methods* in quantum mechanics. The principle of these methods lies in the approximation of a large quantum system into a collection of self-consistent subsystems. This strategy makes it possible to overcome the practical limitations inherent in the  $N$ -body problem, and to describe certain properties of strongly correlated electronic systems.

The first part sets out the mathematical framework and introduces the two methods studied in this thesis: Dynamical Mean-Field Theory (DMFT), which deals with one-body quantum Green's functions, and Density Matrix Embedding Theory (DMET), which deals with the one-body reduced density matrix.

We then present an analysis of the DMET equations, in which we demonstrate the existence and uniqueness of a "physical" solution in the weakly interacting limit. The quality of the approximation is also studied in this limit: the first-order accuracy of the DMET approximation in terms of the electron interaction parameter is shown. Numerical results show the applicability of the theorems demonstrated, and underline the importance of the assumptions formulated.

The DMFT equations are studied in the following section, in the framework of the approximation of the impurity solver "Iterated Perturbation Theory (IPT)". Our analysis shows the existence of solutions to these equations, using an original reformulation of the latter in terms of a fixed-point problem in the space of certain positive measures.

Finally, we study the properties of a discrete version of the IPT-DMFT equations, giving existence and uniqueness results for the solution. Numerical simulations implemented on the Hubbard model reveal the interest and properties of this method in the study of a strong correlations effect: the Mott transition.



## Résumé détaillé

Cette thèse se concentre sur l'analyse mathématique et numérique d'une classe d'approximations en mécanique quantique, les *méthodes de plongement* (*embedding methods*). Ces dernières s'intéressent plus précisément aux systèmes d'électrons en interaction, et sont motivées par des réalisations expérimentales dont l'explication théorique est un sujet actif de recherche, aussi bien en physique de la matière condensée (supraconductivité à haute température par exemple) qu'en chimie quantique (structure électronique par exemple).

### Vue d'ensemble

Avant de présenter ces approximations, rappelons que l'étude de systèmes quantiques impliquant un grand nombre de particules en interaction constitue un véritable défi pour le mathématicien appliqué, aussi bien analytique que numérique. Par exemple, connaître les états admissibles d'un système quantique isolé et composé d'une assemblée de  $N$  particules en interaction nécessite de résoudre d'un problème aux valeurs propres, *l'équation de Schrödinger à  $N$  corps*. Cette équation, dont l'inconnue est la fonction d'onde à  $N$  corps, est une équation aux dérivées partielles posée dans un espace fonctionnel dont la dépendance spatiale croît exponentiellement avec le nombre  $N$  de particules décrites, et pour laquelle la recherche de solutions explicites est très difficile. Des approches numériques issues de la simulation des équations aux dérivées partielles, comme celles des éléments ou des volumes finis, sont dès lors cantonnées à l'étude d'un faible nombre de particules, et échouent en particulier à décrire la situation limite d'un nombre infini de particules, aussi appelée limite thermodynamique.

Ce constat explique le recours à des *méthodes d'approximations spécifiques*, dont l'élaboration remonte à l'avènement de la théorie de la mécanique quantique elle-même. L'exemple archétypique et primordial de ces méthodes est certainement la *théorie de Hartree-Fock*, dont l'objet d'étude est l'état fondamental d'une assemblée de fermions en interaction. Sans entrer dans les détails ni le formalisme, indiquons en résumé que son principe consiste à trouver la meilleure solution approchée parmi les fonctions d'ondes représentant des électrons non interagissants, les *déterminants de Slater*. Une fois cette solution trouvée, l'écart entre celle-ci et la solution exacte décide du caractère *corrélé* du système : lorsque l'écart est faible, c'est-à-dire lorsque la solution calculée par la méthode de Hartree-Fock est proche de la solution exacte, le système est dit *faiblement corrélé*. Bien entendu, c'est la situation contraire, celle des systèmes dits *fortement corrélés* qui motive l'élaboration actuelle de nouvelles méthodes d'approximations, et en particulier celle des *méthodes de plongements*.

Bien que le sujet soit encore émergent et que ses contours soient à préciser, on peut dégager de la littérature existante le principe sur lequel cette nouvelle classe d'approximation repose. Contrairement à la méthode de Hartree-Fock, les méthodes de plongement approchent la solution exacte en considérant une collection de sous-problèmes d'électrons interagissant, appelés *problèmes d'impureté*. Ces derniers sont formés à la suite d'une *décomposition* du système original, et sont ainsi définis pour être résolus efficacement par des méthodes précises. En reportant les détails de la construction de ces problèmes d'impuretés (celle-ci dépend d'ailleurs de la méthode de plongement considérée), indiquons seulement que, par un procédé donné, chaque problème d'impureté est obtenu par *moyennisation* des interactions extérieures à celui-ci, donnant lieu à l'équivalent quantique d'un *champ moyen*, de façon analogue à celui que l'on présente lors de l'étude du modèle d'Ising. Toujours de façon informelle, les méthodes de plongement peuvent aussi être considérées comme un équivalent quantique des méthodes de décomposition de domaine des équations aux dérivées partielles.

En se concentrant sur la résolution d'une collection de sous-problèmes, les méthodes de plongement ont ainsi une complexité algorithmique bien moindre que les approches conventionnelles. C'est d'autant plus vrai lorsque le système possède une *invariance par translation* spatiale, réduisant alors la résolution à celle d'un *unique problème d'impureté*. Toutefois, et de la même façon que pour le modèle d'Ising, les méthodes de plongement imposent que les paramètres du champ moyen des problèmes d'impureté soient cohérents avec la solution obtenue : il s'agit d'une méthode auto-cohérente, qui, sur le plan de l'analyse mathématique, mène à la résolution d'une *équation de point-fixe*. La résolution pratique de ces équations utilise cette formulation, et fait donc appelle à des méthodes itératives, avec accélération ou non.

Malgré l'usage généralisé de ces méthodes, leur étude mathématique est très limitée. Dans cette thèse, nous nous intéressons en particulier à deux méthodes de plongement : la *théorie du plongement de la matrice densité* d'une part (*Density Matrix Embedding Theory (DMET)*), utilisée essentiellement en chimie quantique et s'intéressant à la matrice densité réduite à un corps, et la *théorie du champ moyen dynamique* d'autre part (*Dynamical Mean-Field Theory (DMFT)*), davantage utilisée en physique de la matière condensée et se concentrant sur la fonction de Green à un corps du système. Dans les

deux cas, l'objectif premier est de montrer leur caractère bien posé, c'est-à-dire l'existence et l'unicité d'une solution à l'équation de point fixe qui les définit mathématiquement. L'espace dans lequel cette équation est posée doit répondre à deux obligations: d'une part, il doit assurer le caractère bien posé de l'équation, et d'autre part, il doit se restreindre aux solutions dites "physiques", celles qui partagent certaines propriétés attendues de la solution exacte que la méthode se propose d'approcher.

Cette thèse s'organise donc comme suit. Le premier chapitre constitue une introduction générale, aux systèmes quantiques fortement corrélés. Il définit les quantités auxquelles les méthodes étudiées s'intéressent, et présente brièvement la structure de ces méthodes ainsi que les résultats mathématiques obtenus. Dans le deuxième chapitre, on étudie la théorie du plongement de la matrice densité (DMET). Le troisième et le quatrième chapitres sont quant à eux consacrés à l'étude de la théorie du champ moyen dynamique (DMFT), sans puis avec discréétisation. Cet ordre, anti-chronologique pour ce qui relève du développement des méthodes, est celui que l'auteur a suivi durant son doctorat. Il est motivé par le fait que les objets impliqués vont par abstraction croissante : l'approximation DMET se pose dans un espace de matrices bien décrit mathématiquement par des travaux antérieurs, alors que l'approximation DMFT nécessite l'introduction des fonctions de Nevanlinna-Pick, dont l'usage en mathématiques de la mécanique quantique est peu répandu.

## Chapitre 1 : introduction générale aux méthodes de plongement

Le premier chapitre introduit et motive les méthodes de plongement. Partant d'une expérience de lévitation d'un aimant au-dessus d'un supraconducteur, on présente d'abord un modèle minimaliste d'électrons en interaction, le modèle de Hubbard. Ce modèle est présenté pour deux raisons : d'une part, il intéresse aussi bien le champ de la matière condensée que celui de la chimie quantique, modèle plus connu par ce dernier sous le nom de Pariser-Parr-Pople, et d'autre part, c'est la résolution approchée de ce modèle qui a motivé l'élaboration de la première méthode de plongement, la théorie du champ moyen dynamique.

On présente ensuite les deux quantités d'intérêt des méthodes de plongement considérées. Le formalisme adéquat pour une présentation unifiée de ces dernières dans les situations qui intéressent les deux méthodes est celui de la seconde quantification pour un système fermionique, dont les grandes lignes sont rappelées. On introduit alors la matrice densité réduite à un corps d'un tel état, et on détaille les propriétés de cette dernière dans le cas d'un état déterminant de Slater et dans celui d'un état de Gibbs. La partie la plus importante de l'introduction se concentre alors sur le cadre mathématique des fonctions de Green quantiques à un corps : le formalisme introduit permet de voir cette dernière comme une généralisation dynamique de la matrice densité réduite à un corps. On introduit pour ce faire la notion d'état stationnaire d'un Hamiltonien donné, qui englobe les états propres de ce dernier ainsi que l'état de Gibbs associé, et on définit alors les propagateurs de particule et de trou. On calcule alors l'expression de ces derniers dans le cas d'un système de fermions non interagissant (le Hamiltonien à  $N$  corps est construit à partir d'un Hamiltonien à un corps), explicitant ainsi le lien entre les propagateurs et la matrice densité réduite à un corps. Cette situation est aussi celle dans laquelle les fonctions de Green quantiques à un corps (ordonnée en temps, avancée et retardée), introduites à cet endroit, sont effectivement des fonctions de Green de l'opérateur différentiel impliqué dans l'équation de Schrödinger à un corps. On introduit alors la transformée de Fourier généralisée de ces fonctions (définie dans le demi-plan complexe supérieur), qui, toujours dans le cadre d'un système de fermions non interagissant, se révèle être la résolvante de l'Hamiltonien à un corps. Dans le cas général d'un Hamiltonien quelconque, les fonctions de Green quantique à un corps ne sont plus les fonctions de Green d'un opérateur différentiel donné. Cependant, et pourvu que celle-ci soit bien définie, leur transformée de Fourier généralisée définit une fonction de Nevanlinna-Pick à valeur dans l'ensemble des opérateurs bornés. Cette propriété permet alors d'introduire et de discuter du contenu physique de la mesure spectrale associée, en comparant la représentation intégrale des fonctions de Nevanlinna-Pick et celle de Källen-Lehmann des fonctions de Green quantiques à un corps.

Cette introduction générale se conclut par une présentation des deux méthodes dans l'ordre inverse de celui choisi pour cette thèse, afin de proposer une perspective différente. Pour se démarquer plus encore des présentations individuelles de ces méthodes dans les chapitres qui leur sont dédiés, la théorie du plongement de la matrice densité est présentée d'une manière différente et plus concise, et que les lecteurs habitués aux méthodes issues du champ de l'information quantique apprécieront peut-être davantage. Les contributions mathématiques y sont alors résumées et un tableau récapitulatif permet de comparer les deux méthodes. Enfin, quelques perspectives sont dégagées, essentiellement concernant la théorie du champ moyen dynamique.

## Chapitre 2 : la théorie du plongement de la matrice densité (DMET)

Dans le deuxième chapitre, on s'intéresse à la théorie du plongement de la matrice densité. Ce chapitre est tiré d'un article coécrit avec Éric Cancès, Fabian Faulstich, Antoine Levitt et Éloïse Letournel.

Comme annoncé dans l'article introduisant cette méthode, la théorie du plongement de la matrice densité se veut être une “alternative plus simple” à la théorie du champ moyen dynamique. D'une part, elle se concentre sur la matrice densité réduite à un corps de l'état fondamental (une quantité statique, par opposition à la fonction de Green) D'autre part, les problèmes d'impureté sont de dimension finie. Cette approche permet de mobiliser, lors de l'étape de résolution de ces problèmes, des solveurs précis et bien connus de la communauté de la chimie quantique (méthode Full Configuration Interaction (FCI) par exemple). Pour cette raison, l'étape impliquant la résolution commune des problèmes d'impureté porte le nom de “solveur haut niveau” (high-level solver). Par opposition à ce dernier, la boucle de rétroaction (qui permet de définir le problème de point fixe) porte elle le nom de “solveur bas niveau” (low-level solver), car il est attendu que cette étape fasse appel à des méthodes moins précises et donc moins coûteuses (méthode de Hartree-Fock par exemple). Cette méthode s'applique à des problèmes issus de la chimie quantique, pour lequel le Hamiltonien est constitué de deux termes : l'un modélise le comportement individuel des électrons, l'autre les interactions entre ces électrons.

Dans cette partie, on introduit la première analyse mathématique de cette méthode. L'approche adoptée trouve son origine dans l'affirmation selon laquelle cette théorie serait exacte dans la limite non-interagissante (de façon analogue à la théorie du champ moyen dynamique) : l'analyse est d'abord entreprise dans cette limite, puis étendue à la limite faiblement interagissante.

Ainsi, après une introduction permettant de formaliser mathématiquement cette méthode, on prouve d'abord que, dans la limite non-interagissante et sous des hypothèses raisonnables, la matrice densité réduite à un corps exacte est effectivement solution de l'équation de point de fixe de cette méthode. Toutefois, rien n'indique que cette solution est unique (des résultats numériques vont d'ailleurs dans le sens contraire de cette affirmation) : on se contente donc, ensuite et sous deux hypothèses supplémentaires, de prouver l'existence et l'unicité d'une solution dans le voisinage de la solution exacte dans la limite faiblement interagissante. De plus, on montre que cette solution est analytique en le paramètre d'interaction, tout comme la solution exacte. Dans cette limite, la théorie du plongement de la matrice densité fournit donc une approximation “physique” de la matrice densité réduite à un corps, au sens où la solution approchée partage cette propriétés de la solution exacte. Toujours dans cette limite faiblement interagissante, on montre enfin que la solution fournie par la méthode est exacte au premier ordre en le paramètre d'interaction entre les électrons.

On complète alors cette analyse mathématique par une étude numérique pour deux systèmes, l'un impliquant dix atomes d'hydrogène et l'autre six. Pour le deuxième système, les atomes sont placés dans une configuration paramétrée par un angle donné : en faisant varier cet angle, on montre alors numériquement que, *a priori*, la solution approchée n'est exacte qu'au premier ordre en le paramètre d'interaction. Toujours en variant la configuration de ces atomes, on montre que pour certaines valeurs de l'angle violent les hypothèses nécessaires au théorème d'unicité, il existe plusieurs solutions à l'équation de point fixe posée.

## Chapitre 3 : la théorie du champ moyen dynamique (DMFT)

Le troisième chapitre porte sur la théorie du champ moyen dynamique. Ce chapitre est tiré d'une prépublication coécrite avec Éric Cancès et Solal Perrin-Roussel.

Par opposition au chapitre précédent, la théorie du champ moyen dynamique cherche elle à approcher une quantité réduite dépendante du temps d'un système quantique : la fonction de Green quantique à un corps associée à un état de Gibbs. Bien qu'elle ait été étendue par la suite à des modèles plus généraux, en particulier lorsqu'elle est combinée à d'autres méthodes telles que la théorie de la fonctionnelle de la densité , la DMFT cherche, dans sa version primitive, à approcher la fonction de Green d'un modèle de Hubbard. Pour ce faire, elle procède de façon analogue à la théorie de champ moyen du modèle de Ising. En premier lieu, on réalise une partition du graphe en une collection de sous-graphes. À chaque sous-graphe est ensuite associé un problème d'impureté de Anderson, pour lequel l'impureté est spécifiée par le sous-graphe, alors que le bain ainsi que son couplage à l'impureté sont les inconnues de la théorie. Ces derniers, représentés par leur fonction d'hybridation, sont choisis de sorte à satisfaire une équation d'auto-cohérence formulée à l'aide de la self-énergie des problèmes d'impureté et de la fonction de Green non-interagissante du modèle de Hubbard. Cette équation d'auto-cohérence garantit en outre le caractère exact de cette méthode dans les situations limites des électrons non interagissants et strictement interagissant.

Dans cette partie, on propose donc la première analyse mathématique des équations de la théorie du champ moyen dynamique, appliquée à un modèle de Hubbard et pour un solveur d'impureté spécifique, le solveur Iterated Perturbation Theory (IPT).

Après une remise en contexte dans la première partie, la cadre mathématique et l'approximation physique en question sont introduits. On y rappelle les définitions et les propriétés de la fonction de Green à un corps, puis on introduit la self-énergie pour un espace de Hilbert à une particule de dimension finie. Cette quantité intermédiaire est centrale dans la théorie du champ moyen dynamique : après avoir rappelé la définition du modèle de Hubbard, on présente le modèle d'impureté de Anderson, pour lequel la self-énergie se révèle être un opérateur localisé sur l'impureté. C'est cette propriété qui motive l'approximation de la théorie du champ moyen dynamique, qui, à un modèle de Hubbard, associe une collection de modèles d'impureté de Anderson. Cette association est présentée avec tout le formalisme mathématique nécessaire (en particulier, grâce au langage de la théorie des graphes), et discutée dans les limites triviales d'électrons non interagissants et strictement interagissants. On présente alors le solveur d'impureté IPT. Cette notion nécessite l'introduction d'un formalisme propre aux fonctions de Green associées aux états de Gibbs, le formalisme dit de Matsubara. On montre en particulier le lien qu'entretient ce dernier avec le formalisme des fonctions de Green introduites jusqu'ici, avant de présenter le solveur IPT pour un système invariant par translation et paramagnétique. Cette section se conclut par la présentation des équations IPT-DMFT, dont on se propose de faire l'analyse mathématique.

Dans la troisième partie, on commence par montrer le lien entre, d'une part, les fonctions de Green, la self-énergie et la fonction d'hybridation, et d'autre part, les fonctions de Nevanlinna-Pick : à un signe près, ces quantités issues de la physique sont des fonctions de Nevanlinna-Pick à valeurs opérateur. C'est cette propriété qui définit les solutions dites "physiques" aux équations auxquelles on s'intéresse. On montre ensuite l'absence de solutions définies par un bain de dimension finie. Cette proposition motive l'extension du domaine à celui de fonctions représentant un bain de dimension infinie, pour lequel on montre l'existence de solution(s). La preuve est basée sur un théorème de point fixe de Schauder, après avoir reformulé le problème en termes de mesures de probabilité via la représentation intégrale des fonctions de Nevanlinna-Pick. En corollaire de la preuve, on montre que toute solution aux équations IPT-DMFT ont une mesure de Nevanlinna Riesz admettant des moments à tout ordre.

## Chapitre 4 : étude d'un schéma de discréétisation des équations IPT-DMFT

Dans ce dernier chapitre, on s'intéresse à un schéma de discréétisation des équations IPT-DMFT. Ce chapitre est tiré d'un article en cours de rédaction avec Éric Cancès et Solal Perrin-Roussel.

L'intérêt majeur des méthodes de plongement réside dans leur capacité à fournir une approximation numérique des quantités auxquelles elles s'intéressent. C'est le cas de la théorie du plongement de la matrice densité, qui, telle que présentée et étudiée au chapitre 2, est formulée dans un espace de dimension finie et ne nécessite donc pas *a priori*, de schéma de discréétisation supplémentaire. En revanche, on a montré dans le chapitre précédent que les équations IPT-DMFT admettent une solution lorsqu'elles sont formulées dans un espace de fonctions de Nevanlinna-Pick. Cet espace n'est pas de dimension finie, et toute approche numérique nécessite donc une discréétisation des équations étudiées jusqu'ici.

On s'intéresse plus particulièrement aux équations discréétisées aux fréquences dites de Matsubara (aussi appelées "fréquences imaginaires") : les fonctions sont remplacées par leur évaluation en un ensemble discret de points également espacés sur l'axe imaginaire pur, les fréquences de Matsubara fermioniques. Cette méthode de discréétisation est naturelle lorsque l'on utilise le solveur IPT dans sa version continue : celui-ci ne nécessite que la donnée de la fonction d'hybridation en ces points, et fournit la self-énergie à partir de ces mêmes points. Elle permettrait, pour un nombre infini de fréquences de Matsubara, d'obtenir la solution dans le demi-plan complexe supérieur tout entier par prolongement analytique. En revanche, pour un nombre fini de fréquence, le solveur IPT n'a pas accès à l'intégralité des fréquences de Matsubara : on doit donc étudier une version approchée de ce dernier, pour lequel aucun résultat mathématique précédemment établi ne s'applique directement.

Dans ce chapitre, on présente d'abord la méthode et les équations étudiées. Après un bref rappel du formalisme de Matsubara, on définit les équations concernées sont définies. La différence essentielle avec le chapitre précédent réside dans le fait que ces équations ne sont pas adaptées au formalisme des fonctions de Nevanlinna-Pick. Pour cette raison, on relaxe le critère de solution "physique", en imposant seulement que les solutions soient (à un signe un près) des vecteurs aux composantes dans le demi-plan supérieur.

On montre dans la deuxième partie un théorème garantissant l'existence de solutions, uniformément en le paramètre d'interaction, pourvu que les autres paramètres du modèle et de l'approximation DMFT

respectent une certaine inégalité. La preuve est basée sur le théorème de Brouwer, ainsi que des estimations des différentes quantités impliquées dans ce formalisme, et ne fait aucun usage de la théorie des fonctions de Nevanlinna-Pick.

Dans la section qui suit, on effectue des tests numériques en implémentant un algorithme itératif basé sur cette discrétisation, grâce à la librairie TRIQS. On montre alors numériquement la transition de Mott ayant lieu pour un modèle de Hubbard, telle que prévue par l'approximation DMFT discrétisée. On s'intéresse ensuite à la convergence de l'algorithme: on discute en particulier du rôle de la température et du paramètre d'interaction entre les électrons dans celle-ci. Guidé par cette étude numérique, on exhibe d'ailleurs une solution aux équations qui ne satisfait pas au critère minimal de solution physique défini au préalable.

Cette étude est cohérente avec le résultat d'unicité présenté dans la dernière partie : on montre que, pourvu que la température soit suffisamment élevée (relativement aux autres grandeurs du système), la solution est unique et peut être obtenue à l'aide d'une méthode itérative directe. La preuve de ce dernier théorème repose sur le théorème de point fixe de Picard.



## Remerciements

Avant de plonger dans le vif du sujet, je voudrais remercier ici celles et ceux que j'ai eu la chance de côtoyer durant ces années d'études et de recherche, et qui, chacun à leur façon, ont contribué à l'élaboration de cette thèse.

Je remercie tout d'abord Éric, mon directeur de thèse, pour sa bienveillance, son approche au savoir et sa remarquable capacité à ne pas céder devant un problème difficile et vierge de toute empreinte mathématique. Je tire de ces trois années à tes côtés une grande confiance en la capacité des mathématiques à être utiles aux autres sciences, et bien entendu le plaisir nouveau et intellectuel de la recherche. Merci David d'avoir été là lorsqu'il fallait dégager les premières pistes, pour ton énergie et ton soutien régulier.

Michel, ces lignes refléteront difficilement ce que je te dois. Merci pour ton accueil de la première heure, pour ton appui constant tout au long de ce stage durant l'été 2019, pour les déjeuners au Collège, les écoles d'été et les conférences de physique où tu m'as toujours introduit. Je t'admire pour ton humeur inlassable, cet élan que tu insuffles à celles et ceux qui t'entourent, ton élégance et ta franchise, académique ou non. Le sujet de cette thèse ne te sera pas inconnu, et je mesure tout ce que l'intuition que j'ai pu gagner à cet endroit provient de tes conseils et de ton enseignement. Merci enfin pour ton amitié et ta participation au jury.

Je remercie également les autres membres de ce jury pour l'intérêt qu'ils portent à mes travaux. Thank you Michael for the review, you are one of the few who were already interested in the subject when I started this PhD, and your manuscript really guided me in the dark night of the first months. Merci aussi Zied pour le rapport. Connaissant ton travail par tes articles, dont j'apprécie beaucoup l'effort pédagogique, je mesure le temps qu'il t'a fallu pour te plonger dans le manuscrit, et je suis ravi que tu partages l'enthousiasme qu'est le nôtre au sujet des propriétés des fonctions de Green. Thank you Volker for the interest you show in this PhD, I am sure you will notice an influence of your work between the lines of it. Merci Lucia pour les discussions et pour nous rappeler combien les théoriciens simplifient parfois un peu trop l'expérience. Merci aussi pour ce mot, emprunté à ton éditeur : "On ne finit jamais un livre : on l'abandonne". Je pense que c'est aussi vrai pour une thèse : le croire m'aura en tout cas rassuré durant la phase de rédaction. Merci enfin Virginie, d'avoir accepté d'examiner, parmi l'ensemble de tes thèmes de recherche, un sujet qui touche à celui de ta thèse et pour lequel ton expertise sera grandement profitable.

Merci aux chercheurs et chercheuses qui ont accepté de collaborer avec moi. Thank you Fabian for all the time we spent together, DMET-wise but not only, and for making our meetings around the world possible. Merci Antoine, pour la vivacité et l'énergie avec lesquelles tu partages tes connaissances, pour ton esprit critique-constructif. Sur le volet pédagogique, je remercie grandement François, sans qui je n'aurais pas enseigné plus de la moitié de mes cours à l'École. La confiance que tu as mis en moi à cet endroit m'a permis de découvrir le plaisir immense de l'enseignement en équipe, comme en autonomie complète, et j'en tire une grande confiance. Merci à Éloïse et Solal, d'avoir partagé avec moi quelques mois de recherche (sinon une année), pour l'égalité de nos rapports face à l'inconnu, la complémentarité de nos idées (et de nos erreurs), et peut-être, surtout, l'amitié qui naquit de nos échanges et que j'espère voir fleurir au-delà de ce doctorat.

Merci à l'entièreté de l'équipe Matherials et du CERMICS, à Isabelle et Stéphanie pour leur travail formidable. Merci aux stagiaires, aux doctorants et post-doctorants pour l'ambiance si inattendue et si agréable qui règne entre nous, pour les amitiés que j'ai nouées avec certains d'entre vous. Merci aux plus proches d'entre eux, à Jean, Hélène, Mathias, Zoé, Laurent et Alicia, pour l'élargissement de nos liens et l'appui que j'ai trouvé en vous. Merci à Maxime et aux jumeaux Saa d'avoir été de formidables étudiants d'hier et pour leur amitié d'aujourd'hui. Merci aux autres de mes amis proches, Jean-Baptiste, Thomas, Frédéric, Charly, Baptiste, Guillaume, Lila, Leïla, à qui j'ai parfois imposé mes réflexions et qui auront eu la gentillesse de les écouter sans toujours les comprendre. Merci aux maraudeurs du mercredi soir, à cette association qui m'a donné beaucoup plus que ce que je lui ai apporté, à Jean-Jacques pour son amitié et sa folie rajeunissante, aux autres rencontres de la rue.

Merci enfin à ma famille, à mon père. Merci à mes piliers, Elena, ma mère et mon frère, pour tout.

# Contents

<b>1 An introduction to embedding methods in quantum mechanics</b>	<b>16</b>
1.1 Strongly correlated materials: motivations for the Hubbard model . . . . .	16
1.1.1 Motivation: high $T_c$ superconductivity . . . . .	16
1.1.2 Fermionic Hubbard model . . . . .	19
1.2 One-particle reduced quantities in quantum mechanics . . . . .	22
1.2.1 Second quantization, one-particle reduced density matrix . . . . .	22
1.2.2 Quantum one-body Green's functions . . . . .	24
1.3 Embedding methods . . . . .	29
1.3.1 Dynamical Mean-Field Theory . . . . .	29
1.3.2 "A Simple Alternative to DMFT": Density Matrix Embedding Theory. . . . .	31
1.3.3 Overview table and perspectives. . . . .	34
Bibliography . . . . .	36
<b>2 Some mathematical insights on DMET</b>	<b>43</b>
2.1 Introduction . . . . .	44
2.2 The DMET formalism . . . . .	45
2.2.1 The quantum many-body problem and its fragment decomposition . . . . .	45
2.2.2 The impurity high-level problem . . . . .	46
2.2.3 The global low-level problem . . . . .	48
2.2.4 The DMET problem . . . . .	48
2.3 Main results . . . . .	48
2.4 Numerical simulations . . . . .	51
2.4.1 $H_{10}$ ring . . . . .	51
2.4.2 $H_6$ model . . . . .	52
2.5 Impurity problems and high-level map . . . . .	56
2.5.1 Impurity Hamiltonians . . . . .	56
2.5.2 Domain of the high-level map . . . . .	57
2.6 $N$ -representability and low-level map . . . . .	57
2.7 Proofs . . . . .	58
2.7.1 Proof of Lemma 2.6 . . . . .	58
2.7.2 Proof of Proposition 2.7 . . . . .	59
2.7.3 Proof of Lemma 2.8 . . . . .	62
2.7.4 Proof of Lemma 2.10 . . . . .	63
2.7.5 Proof of Proposition 2.1 . . . . .	63
2.7.6 Proof of Theorem 2.4 . . . . .	67
2.7.7 Proof of Theorem 2.5 . . . . .	74
2.A Notation table . . . . .	79
2.B Analysis of the DMET bifurcation for $H_6^{4-}$ . . . . .	80
Bibliography . . . . .	82
<b>3 A mathematical analysis of IPT-DMFT.</b>	<b>87</b>
3.1 Introduction . . . . .	88
3.2 DMFT of the Hubbard model . . . . .	90
3.2.1 One-body Green's functions and the self-energy . . . . .	90
3.2.2 Hubbard model . . . . .	93
3.2.3 Anderson Impurity Model (AIM) . . . . .	94
3.2.4 Dynamical Mean-Field Theory (DMFT) . . . . .	96

3.2.5	A specific impurity solver : the Iterated Perturbation Theory (IPT) solver.	100
3.3	Main results . . . . .	104
3.3.1	Pick functions . . . . .	105
3.3.2	Functional setting: the Bath Update and IPT maps . . . . .	106
3.3.3	Existence and properties of IPT-DMFT solutions . . . . .	108
3.4	Proofs . . . . .	108
3.4.1	Proofs of the results in Section 3.2 . . . . .	108
3.4.2	Proof of Proposition 3.3.3 ( $-G, -\Sigma, -\Delta$ are Pick matrices) . . . . .	112
3.4.3	Proof of Proposition 3.3.5 (no finite-dimensional bath solution) . . . . .	112
3.4.4	Proof of Proposition 3.3.6 (Bath Update map) . . . . .	114
3.4.5	Proof of Proposition 3.3.8 (IPT map) . . . . .	115
3.4.6	Continuity of the IPT-DMFT map . . . . .	117
3.4.7	Proof of Theorem 3.3.9: existence of a fixed point . . . . .	118
3.4.8	Proof of Proposition 3.3.10 . . . . .	119
3.A	Uniqueness theorem for an interpolation problem . . . . .	120
3.A.1	Introduction and some general properties . . . . .	120
3.A.2	A uniqueness result for ACPs with a rational solution . . . . .	122
3.B	Paramagnetic IPT-DMFT equations . . . . .	124
	Bibliography . . . . .	125
<b>4</b>	<b>A mathematical analysis of the discretized IPT-DMFT equations.</b>	<b>129</b>
4.1	IPT-DMFT on the Matsubara's frequencies . . . . .	129
4.1.1	Analytic continuation . . . . .	130
4.1.2	Matsubara's formalism . . . . .	131
4.2	Existence of solutions to the discretized equations . . . . .	132
4.2.1	Main result . . . . .	132
4.2.2	Proof of Theorem 4.2.1 . . . . .	133
4.3	Iterative scheme and Mott transition . . . . .	135
4.3.1	Mott transition . . . . .	135
4.3.2	Linear convergence for small and large on-site repulsion . . . . .	137
4.3.3	Continuation method and metastable solution . . . . .	141
4.4	Uniqueness of the solution in perturbative regimes. . . . .	143
4.4.1	Main result . . . . .	143
4.4.2	Proof of Theorem 4.4.1 . . . . .	144
	Bibliography . . . . .	145



f

# Chapter 1

## An introduction to embedding methods in quantum mechanics

### Contents

---

<b>1.1 Strongly correlated materials: motivations for the Hubbard model . . . . .</b>	<b>16</b>
1.1.1 Motivation: high $T_c$ superconductivity . . . . .	16
1.1.2 Fermionic Hubbard model . . . . .	19
<b>1.2 One-particle reduced quantities in quantum mechanics . . . . .</b>	<b>22</b>
1.2.1 Second quantization, one-particle reduced density matrix . . . . .	22
1.2.2 Quantum one-body Green's functions . . . . .	24
<b>1.3 Embedding methods . . . . .</b>	<b>29</b>
1.3.1 Dynamical Mean-Field Theory . . . . .	29
1.3.2 “A Simple Alternative to DMFT”: Density Matrix Embedding Theory. . . . .	31
1.3.3 Overview table and perspectives. . . . .	34
<b>Bibliography . . . . .</b>	<b>36</b>

---

This thesis is devoted to the mathematical and numerical analysis of embedding methods in quantum mechanics. In this chapter, we introduce these methods and the context in which they emerged: the study of strongly correlated systems, for which a complete theory has not yet been established. We begin with a physical motivation, by introducing a concrete and prototypical example of strongly correlated material, namely some high critical temperature superconductors, to give the reader an idea of the stakes involved in research in this area of physics. We then present the Hubbard model, its various physical realizations and what is known about it analytically. This will motivate the introduction of reduced quantities, namely the one-body density matrix and one-body Green's functions, after a brief reminder of the second quantization. Special emphasis will be placed on quantum Green's functions, which are widely used in physics but little treated from a mathematical-physics point of view. Once these notions are defined, we finally introduce the two embedding methods that we deal with in this thesis, Dynamical Mean-Field Theory (DMFT) (based on one-body Green's functions) and Density Matrix Embedding Theory (DMET) (based on one-body density matrices), and describe the contributions of this thesis. We conclude this introduction with perspectives and what we consider to be interesting problems to discuss in the (near) future.

### 1.1 Strongly correlated materials: motivations for the Hubbard model

#### 1.1.1 Motivation: high $T_c$ superconductivity

**Introductory experiment** Let us begin with the description of an experiment that we can reproduce at École des Ponts: consider a normal magnet, placed on top of a button made out of a certain ceramic that has no magnetic properties at room temperature. These two are placed in a cryostat in which we pour liquid nitrogen (Figure 1.1a). The liquid boils instantly, and a few seconds after the evaporation slows down, the magnet lifts off the bottom and floats in a stable position above the ceramic (Figure



(a) Overview of the experimental setup: liquid nitrogen lies in the Dewar storage (blue), while the magnet (metallic) is placed on top of the ceramic button (black), the two later being placed in the cryostat (beige). The white fumes are due to the solidification of water vapor when it comes into contact with cold nitrogen vapor.



(b) A few seconds after pouring, the liquid nitrogen stops boiling, and the magnet lifts off the ceramic. The latter two are then removed from the cryostat to make the levitation easier to visualize. Note again the white fumes exhaling from the ceramic, due to the solidification of ambient water vapor near the cold ceramic.



(c) When the magnet levitates, it can be perturbed a little with the tip of a tweezers without causing it to fall: the levitation is stable, which means, according to Earnshaw's theorem, that the magnetic properties of the ceramic at a sufficiently low temperature are not compatible with paramagnetism/ferromagnetism.

Figure 1.1: Levitation of a magnet over a button of ceramics, cooled down with liquid nitrogen. Experiment carried out at École des Ponts. Credits: F. Chevoir and M. Lemaire (Navier) for the safety equipment, materials and liquid nitrogen, K. Chikhaoui (student) for the pictures.

1.1b). When the liquid nitrogen is completely evaporated, the system reheats and the magnet lands on the ceramic.

Let us try to explain the different mechanisms at work in this experiment:

- When we pour liquid nitrogen into the cryostat, it comes into contact with the system which is much warmer: at ambient pressure, liquid nitrogen is in equilibrium with its vapor at a temperature of  $T_{l-v} = 77 \text{ K}$  (-196 °C), while the cryostat and the button of ceramic are at room temperature (of the order of 300 K / 25 °C). Therefore, heat flows from the latter to liquid nitrogen, which boils: the liquid-gas phase transition is associated with a latent heat, so that the heat of the ceramic is absorbed by the change of the physical state of nitrogen. The temperature of liquid nitrogen being fixed by its equilibrium with its vapor, the ceramic knob eventually reaches the temperature  $T_{l-v}$ .
- As soon as the ceramic knob is cold enough, it exerts a force that lifts the magnet: in addition to gravity, the only force the magnet is subject to are magnetic forces, so that the ceramic creates a magnetic field. Since the two bodies are not moving one with respect to the other, and there is no electric field, we can exclude *induction* as the origin of this magnetic field. The most convincing explanation is therefore the following: at a sufficiently low temperature, the ceramic exhibits magnetic properties.

For most phenomena, magnetic systems can be classified according to their response to magnetic field intensity: a magnetic system is paramagnetic/ferromagnetic (resp. diamagnetic) if for a given magnetic field intensity  $\mathbf{H}$ , the magnetic induction  $\mathbf{B}$  is greater (resp. smaller) than what it would be in the vacuum [105, 26]. The described levitation is stable (one can even touch the magnet with the tip of a tweezers without making it fall, as in Figure 1.1c), which by Earnshaw's theorem [2] cannot be achieved with paramagnetism/ferromagnetism: at 77 K, the ceramic is diamagnetic.

Levitation with diamagnetic systems is not specific to this experiment: for example, one can levitate a thin sheet of pyrolytic graphite over a set of magnets, as shown in Figure 1.2. To explain the big difference with the previous experiment, we need to introduce the notion of magnetic susceptibility  $\mu$ : a homogeneous isotropic diamagnetic medium satisfies the linear constitutive relation

$$\mathbf{B} = \mu \mathbf{H},$$

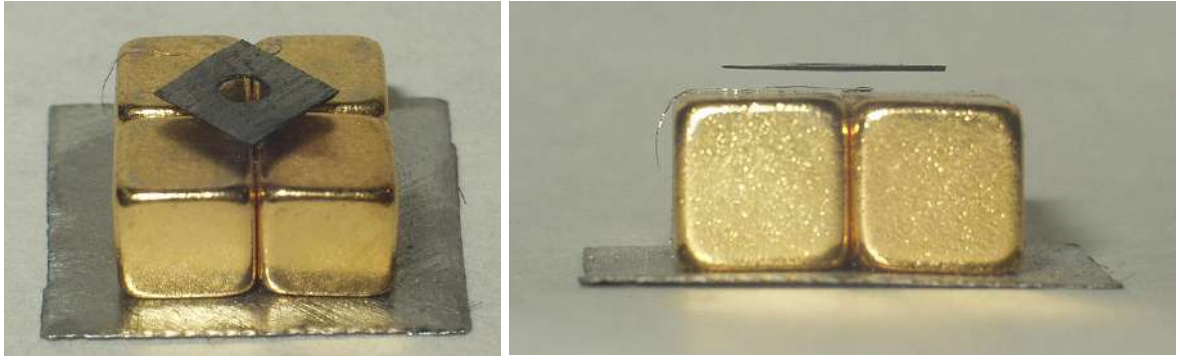


Figure 1.2: A thin sheet of pyrolytic graphite levitating over a set of magnets. Credits: Splarka - English Wikipedia, Own work, Public Domain.

where  $\mu$  is less than the magnetic susceptibility of vacuum  $\mu_0$ . For pyrolytic carbon,  $\mu$  differs from  $\mu_0$  by only a few tenth of a percent [37], while in our experiment, (most of) the medium has magnetic susceptibility  $\mu = 0$ : inside the ceramic, the magnetic induction is zero  $\mathbf{B} = 0$ <sup>1</sup>.

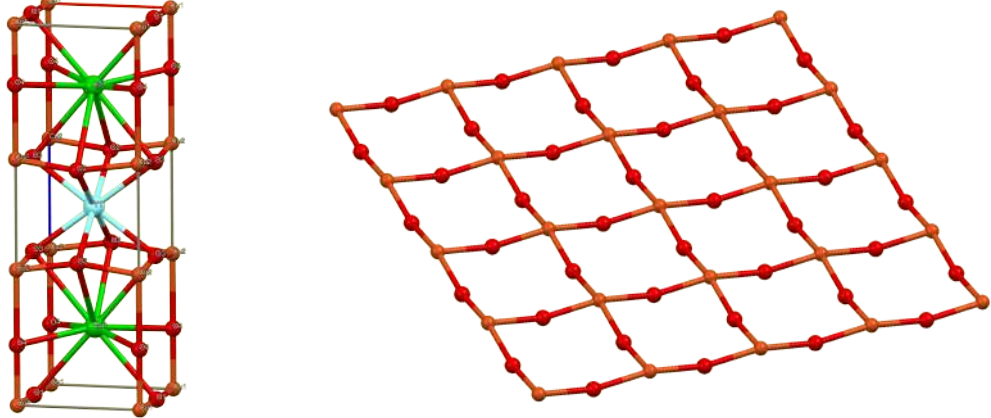
This effect, discovered in 1933 [33], is known as the Meissner effect: below a certain temperature, called the *critical temperature*  $T_c$ , some materials are perfectly diamagnetic (i.e.  $\mu = 0$ ). An other crucial and unrelated property of these materials is the absence of electrical resistivity below the critical temperature, as already discovered by K. Onnes in 1911 [87]: for this reason, they are referred to as *superconductors*. These two properties make superconductors attractive for industrial applications: they can be used in very-low friction bearings, magnetic sustained trains, generation of high-magnetic fields (for instance for Nuclear Magnetic Resonances, see the recent breakthrough [21]) and indeed lossless energy transport. At the time of writing, their usage is limited by the cost related to their refrigeration: in spite of a global research effort [20], no superconductor phase has yet been observed in ambient temperature and pressure conditions [38], and no general theory accounting for ambient critical temperature exists.

**Lack of a microscopic theory for cuprate-based superconductors:** Many attempts have been made to provide a microscopic theory of superconductivity. The most fundamental and generally accepted theory is the Bardeen-Cooper-Schrieffer (BCS) theory [9]. We will not detail its derivation nor its origins, and refer to [34, 35, 49] for a mathematical approach to this theory and how it relates to other models such as the Ginzburg-Landau theory. Suffice it to say that this theory is based on a phonon-mediated attractive interaction model for electrons, and is able to estimate the maximum critical temperature  $T_c$ , which is found to be of the order of  $20K$  [22], much colder than the temperature of liquid nitrogen. Therefore, the ceramic we have used in the experiment cannot be described by conventional superconductivity theory, and is called a *high- $T_c$*  superconductor.

A common classification of high- $T_c$  superconductors is based on their chemical composition. The ceramic presented in the experiment is a crystalline material with unit cell represented in Figure 1.3a, compound of yttrium, barium and copper oxide, and admits as chemical composition  $\text{YBa}_2\text{Cu}_3\text{O}_{7-\delta}$  where  $\delta \in [0, 1]$  is a doping parameter controlled experimentally during the synthesis [108, 106]: it belongs to the so-called group of *cuprates* high- $T_c$  superconductors, for whose discovery [10] the 1987 Nobel prize was awarded to J. Bednorz and K. Müller. A shared feature of the compounds of this family is the presence of  $\text{CuO}_2$  planes as illustrated in Figure 1.3b. These planes are considered to be the medium for the superconducting charge carriers, while the rest of the crystal controls the amount and presence of electrons in these planes (see [110] for a recent direct evidence).

As we will see in the next section, many models attempt to describe these materials. Contrarily to the BCS theory, a whole class of them try to explain the observed superconductivity in terms of electronic and magnetic effects on the copper ions of these planes [5, 6, 111] rather than in terms of coupling to the phonon modes of the ionic lattice. A prototypical example of this is presented below, and is referred to the Hubbard model.

<sup>1</sup>This is a bit oversimplified: with this particular shape, levitation would not be stable if the whole of the ceramic knob where perfectly diamagnetic. In practice, some localized regions called *vertices* remain in the conventional state while the bulk of the body is actually perfectly diamagnetic. The physics of these vertices is well described by the well-established Ginzburg-Landau model and we refer to [96] for an detailed discussion of this model. For the purposes of this experiment, the double image dipole model [53], which assumes the existence of vertices and the perfect diamagnetism of the bulk of the ceramic, is sufficient to explain the stability.



(a) Unit cell of  $\text{YBa}_2\text{Cu}_3\text{O}_7$       (b)  $\text{CuO}_2$  planes, characteristic to cuprate superconductors.

Figure 1.3: Unit cell of  $\text{YBa}_2\text{Cu}_3\text{O}_7$  (left) and  $\text{CuO}_2$  planes (right). Yttrium (electric blue) is sandwiched between two copper (orange-brown) oxide (red) squares, which in turn are sandwiched between two barium (green) elements. The (two parallel)  $\text{CuO}_2$  planes are obtained after replicating the unit cell along the two directions orthogonal to the Ba-Y-Ba axis. Credits: Ben Mills - Own work, Public Domain.

### 1.1.2 Fermionic Hubbard model

In this thesis, we will not introduce quantum physics in detail, and refer to [93, 23] for a general overview and [50, 63] for a first mathematical approach.

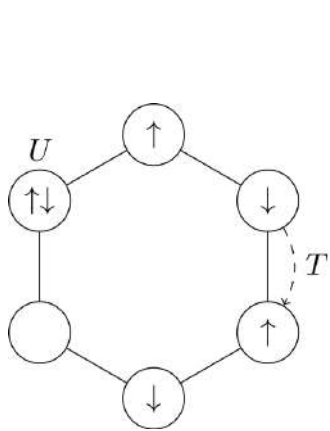
Originally introduced in chemistry to provide with a minimal model for interacting electrons in unsaturated conjugated hydrocarbons [89, 91], the Hubbard model erupted in condensed matter physics [52, 47, 57, 3] to report on magnetic properties of crystalline materials with narrow energy bands. From the perspective of magnetic materials (resp. unsaturated conjugated hydrocarbons), the Hubbard model can be seen as an extension of the tight-binding model [7, 59] (resp. the Hückel method [109]), the latter being much more founded mathematically [32, 95]. In this approach, the Hubbard model is most relevant for almost *flat* bands, where the velocity of single electrons is low enough for them to interact significantly.

This model describes particles evolving in a static medium (in the atomic picture, it focuses on valence electrons while ions are fixed as in the Born-Oppenheimer approximation [12]). As is the case for periodic tight-binding models, the spatial representation of electrons is reduced: to be more precise, the position of an electron is described by a finite collection of orbitals, which can be thought of as *localized*. For instance, assuming that electrons are restricted to moving on a torus  $[0, L]$ , the natural spatial one-particle space in the continuous approach,  $L^2([0, L], \mathbb{C})$ , is discretized using a set  $(\phi_i)_{i \in \Lambda}$  of  $L = |\Lambda|$  localized orbitals (for particles moving on  $\mathbb{R}$ , one can choose a finite set of exponentially localized Wannier functions [76], if such functions exist [88]). In any case, the spatial description of single electrons is described by a finite set  $\Lambda$  of what are commonly called *sites* and which we call *Hubbard vertices* in this presentation for reasons that will become clearer in the following. Taking into account the spin degrees of freedom, the one-particle space  $\mathcal{H}$  is therefore the  $2L$  dimensional space spanned by the basis  $\mathcal{B}_1$  given by

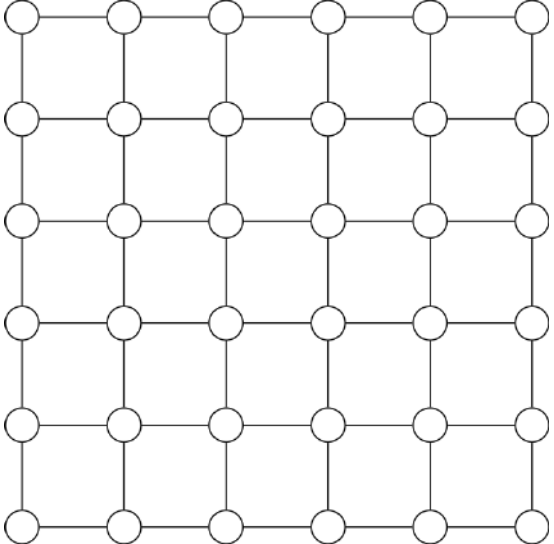
$$\mathcal{H} = \text{Span}(\mathcal{B}_1), \quad \mathcal{B}_1 = (\phi_i \otimes \sigma)_{i \in \Lambda, \sigma \in \{\uparrow, \downarrow\}} = \mathcal{B}_\uparrow \sqcup \mathcal{B}_\downarrow. \quad (1.1)$$

Now we will describe what the model aims at taking into account. This is encoded in the Hamiltonian, which is best expressed using second quantization techniques. We will recall this formalism in Section 1.2, and for now refer the unfamiliar reader to [51, 101, 86, 75] for a chemistry/physics orientated presentation of these notions, and [13], [14] for a mathematical overview about this formalism. Below are the effects included in the model.

- On the one hand, it aims to describe the tunneling effect that single electrons experience, just as in tight-binding models: electrons can jump from one site to an neighbouring one. To model this, we associate each allowed transition with an edge, forming the set  $E$  of *Hubbard edges*: the strength of the tunneling effect depends on the corresponding sites and is modeled by the *hopping matrix*  $T$ , which can be chosen real-valued in the absence of magnetic field  $T : E \rightarrow \mathbb{R}$ .



(a) The Pariser-Parr-Pople (PPP) model of benzene ( $\mathcal{G}_H = C_6$ , the 6-vertex cyclic graph).



(b) The square grid graph, used to model truncated square lattices.

Figure 1.4: Schematic of the two effects modeled by the Hubbard model (left), on the cyclic graph (left). The square-grid graph (right) is widely used to provide with 2d models of cuprates.

- On the other hand, it includes interactions between electrons. In the picture where the sites model local (in space) one-electron states, the model includes only the shortest (in range) interactions, namely when two electrons are on the same site: the strength of this interaction is governed by the *on-site repulsion*  $U : \Lambda \rightarrow \mathbb{R}$ .

Denoting by  $(\hat{a}_{i,\sigma}/\hat{a}_{i,\sigma}^\dagger)_{i \in \Lambda, \sigma \in \{\uparrow, \downarrow\}}$  the annihilation/creation operators associated to the one-particle states that span  $\mathcal{H}$  and satisfying the Canonical Anti-commutation Relations (see Section 1.2), the Hubbard Hamiltonian thus reads

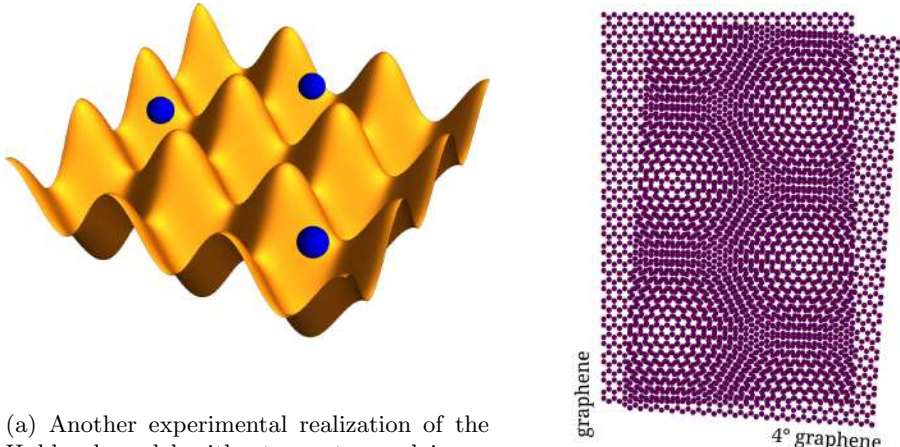
$$\hat{H}_H = \sum_{\{i,j\} \in E, \sigma \in \{\uparrow, \downarrow\}} T_{i,j} (\hat{a}_{i,\sigma}^\dagger \hat{a}_{j,\sigma} + \hat{a}_{j,\sigma}^\dagger \hat{a}_{i,\sigma}) + \sum_{i \in \Lambda} U_i \hat{n}_{i,\uparrow} \hat{n}_{i,\downarrow}, \quad \text{with } \hat{n}_{i,\sigma} = \hat{a}_{i,\sigma}^\dagger \hat{a}_{i,\sigma}$$

where the first term models the tunnel effect, and the second the local interaction. These two effects are shown schematically in Figure 1.4a, and the advantage of the graph formulation  $\mathcal{G}_H = (\Lambda, E)$  (which is not new [81, 82, 8]) lies in its generality, placing unsaturated molecules and truncated lattices with arbitrary hopping on the same ground. Another advantage of this formulation is that it makes the Dynamical Mean-Field Theory (DMFT) easier to express as we will see in Section 1.3.1.

To get a first insight into this model, let us have a look at two simplifying limits:

- When  $U = 0$ , the model reduces precisely to the aforementioned tight-binding model. Note that in this setting, the Hamiltonian describes a set of *non-interacting electrons*, which greatly reduces its complexity: all its properties can be derived from studying the one-particle Hamiltonian as in band theory [7, 63]. The matrix of the latter in the basis set  $\mathcal{B}_1$  even reduces to the block diagonal matrix  $\text{Adj}(\mathcal{G}_H, T) \oplus \text{Adj}(\mathcal{G}_H, T)$  where  $\text{Adj}(\mathcal{G}_H, T)$  is the adjacency matrix of the weighted graph  $(\mathcal{G}_H, T)$ , about which much is known for graphs representing common lattices. For example, eigenstates of the model designed with  $\mathcal{G}_H$  being the  $d$ -dimensional grid with periodic boundary conditions  $C_N^{\square d}$  are delocalized (in the picture where sites represent localized orbitals).
- If  $T = 0$ , the Hubbard Hamiltonian is already diagonal in the basis  $\mathcal{B}_1$ : the model reduces to a collection of idealized one-orbital atoms (in the atomic picture), whose energy is spin-independent and depends only on the doubly occupied sites. In this setting, the model describes a set of *non-interacting sites* (and strictly correlated electrons), and unlike the prior setting, eigenstates are localized (still in the picture where sites represent localized orbitals).

For generic fillings, the first limit describes a *metal*, while the second describes an *insulator*: as the on-site repulsion  $U$  increases, a metal-to-insulator phase transition is expected to occur. This



(a) Another experimental realization of the Hubbard model with atoms, trapped in an optical lattice. In this experiment, the “sites” correspond to optical wells, and the particles described are atoms rather than electrons. (b) An example of moire bilayer material, a low angle twisted bilayer graphene that can be described by Hubbard models.

Figure 1.5: Two others realizations of the Hubbard model: atoms in an optical lattice (left) and moire materials (right). Credits: Jpagett - Own work, CC BY-SA 4.0 (left), Ponor - Own work, CC BY-SA 4.0 (right)<sup>2</sup>.

interaction-driven phase transition is known as the Mott transition [85, 84, 6, 19, 30] and represents a first example of *strongly correlated effect*. Note also that both limits are incompatible with ferromagnetism/antiferromagnetism: however, spin-ordering is expected to appear in between. As was shown mathematically soon after its introduction in condensed matter physics (see the review [64] for a general discussion of mathematical results in this field), these phase transitions are strongly dependent on the graph involved: for instance, the seminal paper [65, 66] shows the absence of Mott transition for the ground state of the “1d chain” (the cyclic graph, as depicted in Figure 1.4a), while ferromagnetism is shown to occur in ground states of line graphs such as the kagome lattice [81, 82, 83].

When it comes to cuprates, several Hubbard models have been derived since the discovery of their superconducting phase: for example, it can be derived from a Wannier function approach as in [5, 6, 111] or as a specific low coupling limit of the Emery model [27, 28] (which was introduced as an “extended Hubbard model”, and is now referred to as a three-band Hubbard model [24, 54]), both being based on the square-grid graph (and its various next-nearest-neighbor extensions). More than 30 years after the first models were introduced, these derivations still form an active research area [72, 54], due to the very complexity of the associated Hubbard model. At the time of writing, we are not aware of any mathematical derivation of this model from first principles of quantum mechanics for *fermions* (see the unpublished [36] for a derivation related to the bosonic case), and this matter is far beyond the scope of this manuscript. It is rather a starting point for the derivation of other models, with for instance the derivation of the Heisenberg model in the  $U \rightarrow \infty$  limit [64, 3], or, for bosons, the derivation of the discrete non-linear Schrödinger equation as a mean-field limit [90]. The Hubbard model is also motivated by the study of optical lattices [29] and moire bilayer materials [107], the two being complementary tunable platforms to explore the different parameter regimes, shedding new light from experiments on strongly correlated effects.

In this context, *embedding methods* have emerged as new approximations to better understand strongly correlated systems. In this manuscript, we will present two related methods, the Dynamical Mean-Field Theory (DMFT) and a “simple alternative” to it [60], the Density Matrix Embedding Theory (DMET). The general idea of these two embedding schemes is to design approximations for reduced quantities, instead of wave-functions methods like (generalized) Hartree-Fock [8]. The first theory, DMFT, focuses on the quantum one-body Green’s function, while DMET aims to provide an approximation of the one-body reduced density matrix. In the next section, we will introduce these objects, and describe their properties, both from a physical and mathematical point of view. This will pave the way for the introduction of the embedding methods we are interested in.

<sup>2</sup><https://commons.wikimedia.org/w/index.php?curid=97679108>, and <https://commons.wikimedia.org/w/index.php?curid=91250759>

## 1.2 One-particle reduced quantities in quantum mechanics

In this section, we introduce the main quantities on which our embedding methods focus. After a reminder about second quantization, we introduce the well-known one-particle reduced density matrix  $\gamma_\Omega$ , and give some of its properties and uses. We then switch to the dynamical setting, by introducing quantum *equilibrium* one-body Green's functions. As already mentioned, these quantities are of general use in the physical community, much less in the mathematical one. In order to define them without difficulty, we restrict ourselves to the *fermionic* setting, where the annihilation/creation operators are bounded. We discuss their properties, and clarify the origin of their designation by focusing on the case of non-interacting Hamiltonians. We also introduce their Fourier transform in the appropriate sense, showing the link between different approaches and the relevance of Pick functions in this setting.

### 1.2.1 Second quantization, one-particle reduced density matrix

We place ourselves in a similar setting to that of [14], and we refer the reader to this reference for a general introduction. A pedagogical introduction can also be found in [8] and [102].

The setting is as follows: let the Hilbert space  $\mathcal{H}$  endowed with the sesquilinear inner product  $\langle \cdot, \cdot \rangle$  be the *one-particle space*. The *fermionic Fock space*  $\mathcal{F}$ , which describes statistical states with an arbitrary number of fermions, is defined as

$$\mathcal{F} = P_- (\tilde{\mathcal{F}}), \quad \tilde{\mathcal{F}} = \overline{\bigoplus_{n=0}^{+\infty} \mathcal{H}^{\otimes n}}, \quad \mathcal{H}^{\otimes n} = \bigotimes^n \mathcal{H}, \quad \mathcal{H}^{\otimes 0} = \mathbb{C},$$

where the closure is taken for the norm induced by the canonical Fock inner product inherited from  $\langle \cdot, \cdot \rangle$ , and the operator  $P_-$  is the projection defined on tensor products with for all  $n \in \mathbb{N}^*$ , for all  $\phi_1, \dots, \phi_n \in \mathcal{H}$ ,

$$P_-(\phi_1 \otimes \dots \otimes \phi_n) = \frac{1}{n!} \sum_{\sigma \in \mathfrak{S}_n} \epsilon(\sigma) \phi_{\sigma(1)} \otimes \dots \otimes \phi_{\sigma(n)},$$

where  $\mathfrak{S}_n$  is the set of permutations with  $n$  elements, and extended to  $\tilde{\mathcal{F}}$  by linearity and continuity. The creation/annihilation operators  $\hat{a}_\phi^\dagger / \hat{a}_\phi$  are then defined as follows: for all  $\phi \in \mathcal{H}$ , first define  $\tilde{a}_\phi^\dagger$  and  $\tilde{a}_\phi$  on finite linear combinations of tensor products with, for all  $n \in \mathbb{N}^*$ , for all  $\phi_1, \dots, \phi_n \in \mathcal{H}$ , for all  $\lambda \in \mathbb{C}$ ,

$$\begin{aligned} \tilde{a}_\phi^\dagger (\phi_1 \otimes \dots \otimes \phi_n) &= (\sqrt{n+1}) \phi \otimes \phi_1 \dots \otimes \phi_n, & \tilde{a}_\phi^\dagger \lambda &= \lambda \phi, \\ \tilde{a}_\phi (\phi_1 \otimes \dots \otimes \phi_n) &= (\sqrt{n} \langle \phi, \phi_1 \rangle) \phi_2 \dots \otimes \phi_n, & \tilde{a}_\phi \lambda &= 0. \end{aligned}$$

The fermionic creation/annihilation operators  $\hat{a}_\phi^\dagger, \hat{a}_\phi$  are then defined on linear combinations of tensor products by

$$\hat{a}_\phi^\dagger = P_- \tilde{a}_\phi^\dagger P_-, \quad \hat{a}_\phi = P_- \tilde{a}_\phi P_-$$

They satisfy the Canonical Anti-commutation Relations (CAR): for all  $\phi, \phi' \in \mathcal{H}$ , we have

$$\{\hat{a}_\phi, \hat{a}_{\phi'}\} = \{\hat{a}_\phi^\dagger, \hat{a}_{\phi'}^\dagger\} = 0, \quad \{\hat{a}_\phi, \hat{a}_{\phi'}^\dagger\} = \langle \phi, \phi' \rangle$$

where  $\{\cdot, \cdot\}$  stands for the anticommutator. Using the adjoint relation  $\hat{a}_\phi^\dagger = (\hat{a}_\phi)$  which holds for linear combinations of tensor products, it follows that the creation/annihilation operators  $\hat{a}_\phi^\dagger, \hat{a}_\phi$  are bounded, hence admit bounded extensions to  $\mathcal{F}$ , with

$$\|\hat{a}_\phi\| = \|\hat{a}_\phi^\dagger\| = \|\phi\| \tag{1.2}$$

Note also that  $\phi \mapsto \hat{a}_\phi^\dagger$  is linear, and that  $\phi \mapsto \hat{a}_\phi$  is anti-linear. They belong to the  $C^*$ -algebra  $B(\mathcal{F})$  of bounded operators on  $\mathcal{F}$ . A state  $\Omega$  is a linear functional on  $B(\mathcal{F})$ , that is *positive*, meaning it satisfies for all  $\hat{O} \in B(\mathcal{F})$ ,  $\Omega(\hat{O}^\dagger \hat{O}) \geq 0$ , and of norm 1, that is  $\sup\{|\Omega(\hat{O})|, \|\hat{O}\| = 1\} = 1$ . They are a generalization of quantum states to the statistical mechanics setting, and we will come back to this point later. For now, we define the *one-particle reduced density matrix* [102, Chapter 8].

**Definition 1.2.1** (One-particle reduced density matrix  $\gamma_\Omega$ ). *The one-particle reduced density matrix  $\gamma_\Omega$  associated to  $\Omega$  is the unique self-adjoint operator in  $B(\mathcal{H})$  represented by the sesquilinear form defined by for all  $\phi, \phi' \in \mathcal{H}$ ,*

$$\langle \phi, \gamma_\Omega \phi' \rangle = \Omega(\hat{a}_\phi^\dagger \hat{a}_\phi).$$

The operator  $\gamma_\Omega$  is positive because  $\Omega$  is also positive, self-adjoint by the fact that positivity of  $\Omega$  implies  $\Omega(\hat{O}^\dagger) = \overline{\Omega(\hat{O})}$  for all  $\hat{O} \in B(\mathcal{F})$ , and it satisfies  $0 \leq \gamma_\Omega \leq 1$  in the operator sense (this follows from (1.2) and the fact that states are of norm unity). At this point, we will provide examples to help the reader grasp its meaning. We will abbreviate it by *1-pdm* [8, 102] or *1-RDM* [17] indifferently in the following.

Suppose we want to describe a quantum system of  $N$  particles, with the wave function  $\Psi_N \in \mathcal{H}_N = P_-(\mathcal{H}^{\otimes N})$  such that  $\|\Psi\| = 1$ . In the formalism of second quantization, it is described by the vector state  $\Omega_{\Psi_N} : B(\mathcal{F}) \ni \hat{O} \mapsto \langle \Psi_N, \hat{O}\Psi_N \rangle$ . From this example, we see that states defined as linear forms provide with a generalization of the *average value of observables*. For such a state, the 1-pdm  $\gamma_\Psi$  is very useful to characterize the wave function from which it is defined: it is easy to show that the number of particles  $N$  is equal to the trace of  $\gamma_\Psi$  (which is trace-class in this setting):

$$\text{Tr}(\gamma_\Psi) = N.$$

Another crucial property in this setting is the following equivalence:  $\gamma_\Psi$  is a projector if and only if there exists  $\phi_1, \dots, \phi_N \in \mathcal{H}$  such that

$$\Psi = \hat{a}_{\phi_1}^\dagger \dots \hat{a}_{\phi_N}^\dagger |\emptyset\rangle, \quad (1.3)$$

where  $|\emptyset\rangle \in \mathbb{C}$ ,  $\| |\emptyset\rangle \| = 1$  represents the vacuum, and in this case  $\text{Ran}(\gamma_\Psi) = \text{Span}(\phi_i)_{i \in \llbracket 1, N \rrbracket}$ . Such a wave function is called the *Slater determinant* associated with the one-particle states  $\phi_1, \dots, \phi_N$  (also called spin-orbitals), and  $\text{Ran}(\gamma_\Psi)$  is the so-called *occupied spin-orbitals space*, while its orthogonal complement is the *virtual spin-orbitals space*. These states prove particularly useful for describing *non-interacting* fermions: given a one-particle Hamiltonian  $H^0 \in \mathcal{S}(\mathcal{H})$ , with domain  $D(H^0)$ , its *second quantization*  $d\Gamma(H^0)$  is defined [14] as the self-adjoint operator which, for all  $n \in \mathbb{N}^*$ , for all  $\phi_1, \dots, \phi_n \in D(H^0)$ , satisfies

$$d\Gamma(H^0)P_-(\phi_1 \otimes \dots \otimes \phi_n) = P_- \left( \sum_{i=1}^n \phi_1 \otimes \dots \otimes H^0 \phi_i \otimes \dots \otimes \phi_n \right).$$

This Hamiltonian models *non-interacting* fermions and therefore will be called a *non-interacting Hamiltonian*. In this context, an interesting problem in quantum physics is to determine the  $N$ -particle *ground state* of this Hamiltonian, which is a solution (if it exists) to the following optimization problem:

$$\inf \{ \Omega_\Psi(d\Gamma(H^0)), \quad \Psi \in \mathcal{H}_N \cap D(d\Gamma(H^0)), \quad \|\Psi\| = 1 \}. \quad (1.4)$$

Assuming that  $H^0$  is bounded from below, this problem is equivalent to the following one, which involves only 1-pdms  $\gamma_\Omega$  associated with Slater determinants,

$$\inf \{ \text{Tr}(\gamma_\Omega H^0), \quad \gamma_\Omega^2 = \gamma_\Omega, \quad \text{Ran}(\gamma_\Omega) \subset D(H^0), \quad \text{Tr}(\gamma_\Omega) = N \}.$$

This result is at the basis of the *Hartree-Fock theory*, which provides the ground state of a quantum system while imposing the latter to be a Slater determinant. We refer the interested reader to [51] for a general overview about this theory and its augmented versions. Its very great successes led to many generalizations that we will not cover here: in view of its application to the Hubbard model and superconductivity, let us only mention the Generalized Hartree-Fock theory [8] which is formulated using the generalized 1-pdm.

To make things even clearer, we give the expression of  $\gamma_\Psi$  when the one-particle space consists in the continuous setting  $\mathcal{H} = L^2(\mathbb{R}^d, \mathbb{C})$ , which represents spinless particles evolving in the  $d$ -dimensional space: for all  $\phi, \phi' \in \mathcal{H}$ , we have

$$\langle \phi, \gamma_\Psi \phi' \rangle = \int_{\mathbb{R}^d \times \mathbb{R}^d} \overline{\phi(r)} \gamma_\Psi(r, r') \phi'(r') dr dr', \quad \text{with } \gamma_\Psi(r, r') = N \int_{\mathbb{R}^{(N-1)d}} \overline{\Psi(r, \cdot)} \Psi(r', \cdot) \quad (1.5)$$

so that  $\gamma_\Psi$  is a kernel operator: the diagonal elements of the latter coincide with the *one-body density*, the key quantity in *Density Functional Theory* (DFT).

Vector states are included in the more general class of *normal states*  $\Omega : B(\mathcal{F}) \ni \hat{O} \mapsto \text{Tr}(\hat{\rho}\hat{O})$  where  $\hat{\rho}$  is the associated *density matrix*, a self-adjoint, positive operator satisfying the trace condition  $\text{Tr}(\hat{\rho}) = 1$ . In the previous case of a vector state,  $\hat{\rho}$  is the orthogonal projection on  $\Psi$ : this fact, in combination with Equation (1.5), is related to the denomination of the one-particle reduced density matrix: the latter can be seen as a partial trace of the density matrix.

Another typical example of normal state is a Gibbs state: for all chemical potential  $\mu \in \mathbb{R}$  and inverse temperature  $\beta \in \mathbb{R}_+^*$ , assuming  $e^{-\beta(\hat{H}-\mu\hat{N})}$  is trace-class where  $\hat{N} = d\Gamma(\mathbf{1})$  is the *number operator*, the density matrix reads

$$\hat{\rho} = \frac{1}{\text{Tr}(e^{-\beta(\hat{H}-\mu\hat{N})})} e^{-\beta(\hat{H}-\mu\hat{N})}.$$

In the setting of a non-interacting Hamiltonian  $d\Gamma(H^0)$ , the trace-class condition is equivalent to  $e^{-\beta H^0} \in \mathcal{S}(\mathcal{H})$  being trace-class as a *one-body* operator [14, Proposition 5.2.22], and in this case the 1-pdm is given by the well-known *Fermi-Dirac distribution*:

$$\gamma_\Omega = \frac{1}{1 + e^{\beta(H^0 - \mu)}}.$$

As we will see in Section 1.3.2, Density Matrix Embedding Theory is formulated in terms of 1-pdms  $\gamma_\Omega$  (and not density matrices  $\hat{\rho}$ !). We postpone its derivation below, and give for now a mathematical presentation of the objects Dynamical Mean-Field Theory is based on: quantum one-body Green's functions.

### 1.2.2 Quantum one-body Green's functions

In this section, we introduce quantum one-body Green's functions, a fundamental concept in condensed matter physics that has been used for more than half a century.

Their appearance in quantum mechanics is closely related to two other disciplines: quantum field theory on the one hand, in the generally accepted affiliation [55, 25] of Schwinger's ideas [99, 100, 74, 98] and from which it can be seen as an implementation of an elaborated technique in a simpler setting, and kinetic theory of fluids on the other hand, to which it owes the BBGKY hierarchy (see the series of papers by M. Born and H. Green [11], and T. Matsubara's remark about them [77] for this affiliation) and from which it appears merely as a quantum generalization of the classical notion of dynamical correlation.

In this manuscript, we introduce them from a mathematical perspective, with a presentation that resembles more the second point of view and fits better with the above presentation of the 1-pdm. This approach is actually not new, with for instance, the demonstration of the existence of their thermodynamic limit in [94] based on similar results obtained for the reduced density matrices in [44]. More recently, the properties of these objects for ground state has been studied in the infinite-dimensional setting of the GW approximation in [16], and in a finite dimensional setting for various applications, including DMFT, in [71]. Our presentation lies in between these two milestones, with a general presentation in the Hilbert space setting, using second quantization formalism, with applications in the finite dimensional setting when needed. In any case, we will consider *equilibrium* states, which encompass ground states and Gibbs states as we detail below. The aim of this section is also to clarify to what extent quantum Green's functions are indeed Green's functions in the sense of fundamental solutions to linear differential operators. Note also that we do not consider the anomalous setting [69], which is a generalization of Green's functions similar as the one that generalizes the 1-pdm in Generalized Hartree-Fock theory [8].

**Equilibrium states** We place ourselves in the same setting as in the previous section and refer to  $\hat{H} \in \mathcal{S}(\mathcal{F})$  for any self-adjoint operator on the Fock space. In this setting, the dynamics is governed by the strongly continuous one-parameter unitary group  $\{e^{-it\hat{H}}\}_{t \in \mathbb{R}}$ , defined by functional calculus [63]. For all bounded operator  $\hat{O} \in B(\mathcal{F})$ , we denote by  $\mathbb{H}(\hat{O}) : \mathbb{R} \rightarrow B(\mathcal{F})$  its *Heisenberg picture* defined by, for all  $t \in \mathbb{R}$ ,

$$\mathbb{H}(\hat{O})(t) = e^{it\hat{H}} \hat{O} e^{-it\hat{H}}$$

In layman's terms, the Heisenberg picture of an operator represents its evolution with time under the dynamics of  $\hat{H}$ . For the sake of simplicity, we consider only *equilibrium* states in this thesis, which are normal states with density matrix  $\hat{\rho}$  such that, for all  $t \in \mathbb{R}$ ,

$$[\hat{\rho}, e^{it\hat{H}}] = 0.$$

This assumption, if violated, leads to the much more sophisticated *out-of-equilibrium Green's functions*, about which we are not aware of any mathematical approach and that we do not cover in this document (see for instance the Schwinger-Keldysh formalism [58, 55, 48]). Our setting includes the cases of vector states with eigenvectors of  $\hat{H}$  (provided such vectors exist) and Gibbs state (provided the operator  $e^{-\beta(\hat{H}-\mu\hat{N})}$  is trace-class). We are now in position to introduce the particle and hole propagator which are specific correlations between evolved-in-time annihilation and creation operators.

**Definition 1.2.2** (Particle propagator). *Given  $\hat{H} \in \mathcal{S}(\mathcal{F})$  a self-adjoint operator and a corresponding equilibrium state  $\Omega$ , the particle propagator  $P_p : \mathbb{R} \rightarrow B(\mathcal{H})$  is the unique bounded-operator-valued map with, for all  $t \in \mathbb{R}$ ,  $P_p(t)$  being represented by the sesquilinear form defined by, for all  $\phi, \phi' \in \mathcal{H}$ ,*

$$\langle \phi, P_p(t)\phi' \rangle = \Omega(\mathbb{H}(\hat{a}_\phi)(t)\hat{a}_{\phi'}^\dagger).$$

*Similarly, the hole propagator  $P_h : \mathbb{R} \rightarrow B(\mathcal{H})$  is the unique bounded-operator-valued map with, for all  $t \in \mathbb{R}$ ,  $P_h(t)$  being represented by the sesquilinear map defined by, for all  $\phi, \phi' \in \mathcal{H}$ ,*

$$\langle \phi, P_h(t)\phi' \rangle = \Omega(\hat{a}_{\phi'}^\dagger \mathbb{H}(\hat{a}_\phi)(t)).$$

*In particular, we have  $\|P_p(t)\| \leq 1$ ,  $\|P_h(t)\| \leq 1$  for all  $t \in \mathbb{R}$ .*

The bounds can be proven similarly as for the bound on the 1-pdm. Note that, contrarily to the latter, the operators  $P_p(t), P_h(t)$  are not self-adjoint for generic values of  $t$ . Nevertheless, they satisfy the following adjoint relations: for all  $t \in \mathbb{R}$ ,

$$P_p(t)^\dagger = P_p(-t), \quad P_h(t)^\dagger = P_h(-t). \quad (1.6)$$

Note finally that our definition encompasses correlations between  $\mathbb{H}(\hat{a}_\phi)(t)$  and  $\mathbb{H}(\hat{a}_{\phi'}^\dagger)(t')$  for all  $t, t' \in \mathbb{R}$ : as expected from a physical intuition, these correlations only depend on time differences (equilibrium states are time-translation invariant), and one can prove using the cyclicity of the trace that

$$\Omega\left(\mathbb{H}(\hat{a}_\phi)(t)\mathbb{H}(\hat{a}_{\phi'}^\dagger)(t')\right) = \langle \phi, P_p(t-t')\phi' \rangle, \quad \Omega\left(\mathbb{H}(\hat{a}_{\phi'}^\dagger)(t)\mathbb{H}(\hat{a}_\phi)(t')\right) = \langle \phi, P_h(t'-t)\phi' \rangle.$$

Before we go any further, let us say a few words about their denomination. As for the 1-pdm, it originates from the setting of vector states  $\Omega_\Psi$  with  $N$  particles ( $\Psi \in \mathcal{H}_N$ ): for such a state, the particle propagator is given by

$$\langle \phi, P_p(t)\phi' \rangle = \langle \hat{a}_\phi^\dagger e^{-it\hat{H}} \Psi, e^{-it\hat{H}} \hat{a}_{\phi'}^\dagger \Psi \rangle,$$

and can be given the following interpretation: assuming that  $\hat{H}$  is particle conserving<sup>3</sup>, it provides a comparison between two states with  $N+1$  particles, one being the evolution at time  $t$  of  $\hat{a}_{\phi'}^\dagger \Psi$ , the other being  $\hat{a}_\phi^\dagger$  applied to the evolution at time  $t$  of  $\Psi$ . It therefore provides information about how added particles propagate in the system. Similarly, the hole propagator supply information about how holes (removing of particles) propagate in the system.

Finally, note that the 1-pdm is related to the two propagators by  $\gamma_\Omega = P_h(0) = 1 - P_p(0)$ . For arbitrary time, the relation is in general more complex, apart from the setting of *non-interacting Hamiltonians* which we present now. This setting will also motivate the definitions of Green's functions.

### Non-interacting Hamiltonians and Green's functions

The notion of non-interacting Hamiltonian has already been presented in the previous section: when it comes to dynamics, the physical intuition is that particles precisely evolve independently one from another. In mathematical terms, this is ensured by the following property: given a non-interacting Hamiltonian  $d\Gamma(H^0) \in \mathcal{S}(\mathcal{F})$  being the (self-adjoint) second quantization of the one-particle Hamiltonian  $H^0 \in \mathcal{S}(\mathcal{H})$ , the evolution operator reads, for all  $t \in \mathbb{R}$ ,

$$e^{-itd\Gamma(H^0)} = \Gamma(e^{-itH^0}) \quad (1.7)$$

where for all one-particle unitary operator  $U \in B(\mathcal{H})$ , its unitary second quantization  $\Gamma(U)$  is defined with for all  $n \in \mathbb{N}^*$ , for all  $\phi_1, \dots, \phi_n \in \mathcal{H}$ , for all  $\lambda \in \mathbb{C}$ ,

$$\Gamma(U)P_-(\phi_1 \otimes \dots \otimes \phi_n) = P_-(U\phi_1, \dots, U\phi_n), \quad \Gamma(U)\lambda = \lambda$$

The proof of (1.7), based on Stone's theorem [63], poses no problem and can be found in classical textbooks [14]. The dynamics is therefore dictated by a strongly continuous unitary operator group that takes a very simpler form, and we find as a direct consequence that for all  $\phi \in \mathcal{H}$ , for all  $t \in \mathbb{R}$ ,

$$\mathbb{H}(\hat{a}_\phi)(t) = \hat{a}_{e^{itH^0}\phi}. \quad (1.8)$$

In other words,  $B(\mathcal{F}) \ni \hat{O} \mapsto \mathbb{H}(\hat{O})(t)$  is the *Bogoliubov transform* [14] induced by the unitary  $e^{itH^0}$ . A consequence of this property is the well-known following property about propagators.

<sup>3</sup>Meaning that  $\hat{H}$  and  $\hat{N}$  commute, in the sense that  $[e^{it\hat{H}}, e^{is\hat{N}}] = 0$  for all  $t, s \in \mathbb{R}$  [63], which is the case for the molecular and Hubbard Hamiltonians.

**Proposition 1.2.3** (Particle and hole propagators of a non-interacting Hamiltonian). *Given a non-interacting Hamiltonian  $d\Gamma(H^0) \in \mathcal{S}(\mathcal{F})$  associated to the one-particle Hamiltonian  $H^0 \in \mathcal{S}(\mathcal{H})$ , the particle and hole propagators  $P_p, P_h$  associated to an equilibrium state  $\Omega$  read*

$$P_p(t) = e^{-itH^0}(1 - \gamma_\Omega), \quad P_h(t) = e^{-itH^0}\gamma_\Omega, \quad (1.9)$$

where  $\gamma_\Omega$  is the 1-pdm associated to  $\Omega$ . In particular, these propagators are continuous for the strong operator topology. Moreover, they satisfy the following differential equation on the domain of  $H^0$ , for all  $t \in \mathbb{R}$ ,

$$i \frac{dP}{dt} = H^0 P.$$

*Proof.* We give it for the particle propagator only, the other case being similar. The proof of Equation (1.9) is a direct consequence of (1.8): for all  $\phi, \phi' \in \mathcal{H}$ , for all  $t \in \mathbb{R}$ , we have

$$\langle \phi, P_p(t)\phi' \rangle = \Omega(\hat{a}_{e^{itH^0}\phi}\hat{a}_{\phi'}^\dagger) = \langle \phi, e^{-itH^0}P_p(0)\phi' \rangle = \langle \phi, e^{-itH^0}(1 - \gamma_\Omega)\phi' \rangle.$$

As for the continuity, it follows from the continuity of  $e^{itH^0}$ . Moreover, by definition of equilibrium states, the 1-pdm  $\gamma_\Omega$  and  $e^{itH^0}$  commute for all  $t \in \mathbb{R}$ : using Equation (1.8) and the cyclicity of the trace, we have for all  $\phi, \phi' \in \mathcal{H}$ , for all  $t \in \mathbb{R}$ ,

$$\langle \phi, e^{-itH^0}\gamma_\Omega e^{itH^0}\phi' \rangle = \Omega(\hat{a}_{e^{itH^0}\phi}\hat{a}_{e^{itH^0}\phi'}^\dagger) = \text{Tr}(e^{-itd\Gamma(H^0)}\hat{\rho}e^{itd\Gamma(H^0)}\hat{a}_\phi\hat{a}_{\phi'}^\dagger) = \langle \phi, \gamma_\Omega\phi' \rangle$$

using the commutation of  $\hat{\rho}$  with  $e^{-itd\Gamma(H^0)}$ . This implies that  $[\gamma_\Omega, H^0] = 0$  on the domain of  $H^0$ , so that finally, we have by Stone's theorem, for all  $\phi$  in the domain of  $H^0$

$$i \frac{dP_p}{dt}(t)\phi = (1 - \gamma_\Omega)e^{-itH^0}H^0\phi = H^0P_p(t)\phi$$

□

Note that stronger continuity is not expected to hold in the general case: for instance, the 1-pdm associated to the vacuum vector state is 0, so that the particle propagator is precisely  $e^{-itH^0}$ , which from Stone's theorem is known to be continuous for the norm topology if and only if  $H^0$  is bounded [50].

The above result gives a second insight about the denomination of the propagators: for a vector state  $\Psi$  being a Slater determinant of  $N$  eigenstates of  $H^0$ , the particle propagator describes how particle added to the virtual orbitals space evolve in time, while the hole propagator describes the evolution of particles in the occupied orbitals space. This fact shows how complementary these objects are, even in the non-interacting setting: the one-body time-ordered Green's function, which we introduce now, makes use of this property by combining them appropriately.

**Definition 1.2.4** (One-body time-ordered Green's function). *Given  $\hat{H} \in \mathcal{S}(\mathcal{F})$  a self-adjoint operator and a corresponding equilibrium state  $\Omega$ , the one-body time-ordered Green's function  $\tilde{G} : \mathbb{R} \rightarrow B(\mathcal{H})$  is the map defined by*

$$i\tilde{G} = \chi_{\mathbb{R}_+}P_p - \chi_{\mathbb{R}_-}P_h,$$

where  $\chi_A$  is the characteristic function of the set  $A \subset \mathbb{R}$ . For all  $t \in \mathbb{R}$ , we have  $\|\tilde{G}(t)\| \leq 1$ .

As we did for the propagators, let us say a few words about the terminology: “body” encompasses “particle” and “hole”, and “time-ordered” comes from the fact that, for all  $t \in \mathbb{R}$ , for all  $\phi, \phi' \in \mathcal{H}$ , we have

$$\langle \phi, i\tilde{G}(t)\phi' \rangle = \Omega\left(\mathcal{T}(\mathbb{H}(\hat{a}_\phi), \mathbb{H}(\hat{a}_{\phi'}^\dagger))(t, 0)\right), \quad (1.10)$$

where for all operator-valued functions  $\mathbb{R} \ni t \mapsto \hat{O}(t) \in B(\mathcal{F}), \mathbb{R} \ni t \mapsto \hat{O}'(t) \in B(\mathcal{F})$ , their fermionic time-ordered product  $\mathcal{T}(\hat{O}, \hat{O}')$  is the operator-valued function  $\mathbb{R}^2 \rightarrow B(\mathcal{F})$  defined as

$$\mathcal{T}(\hat{O}, \hat{O}')(t, t') = \begin{cases} \hat{O}(t)\hat{O}'(t') & \text{if } t \geq t', \\ -\hat{O}'(t')\hat{O}(t) & \text{otherwise.} \end{cases} \quad (1.11)$$

In a sense, the time-ordered Green's function encapsulates both the particle and hole propagators, making use of the redundancy induced by their adjoint relation (1.6). Finally, “Green's function” comes from the following statement, which holds true only in the *non-interacting* setting.

**Proposition 1.2.5** (Non-interacting one-body time-ordered Green's function). *For a non-interacting Hamiltonian  $d\Gamma(H^0)$ , with  $H^0 \in \mathcal{S}(\mathcal{H})$ , the one-body time-ordered Green's function satisfies the following differential equation in the distribution sense for all  $\phi$  in the domain of  $H^0$*

$$\left( i \frac{d}{dt} - H^0 \right) \tilde{G}\phi = \delta_0 \phi, \quad (1.12)$$

with the initial condition  $i\tilde{G}(0^+) = 1 - \gamma_\Omega$  in the strong operator topology.

*Proof.* The proof follows from Proposition 1.2.3, and the fact  $\tilde{G}$  has a jump in 0 which is given by

$$i\tilde{G}(0^+) - i\tilde{G}(0^-) = P_p(0^+) + P_h(0^-)^\dagger = 1 - \gamma_\Omega + P_h(0^+) = 1 \quad (1.13)$$

where all the limits are in the strong operator sense and where we have used the adjoint relation of  $P_h$ .  $\square$

Other one-body Green's functions are used, depending on the context in which they can be applied [45, 74, 56, 55, 73, 75]. Among them, there are the advanced (resp. retarded) Green's function  $\tilde{G}^A$  (resp.  $\tilde{G}^R$ ), given by

$$i\tilde{G}^A = -\chi_{\mathbb{R}_-}(P_h + P_p), \quad i\tilde{G}^R = \chi_{\mathbb{R}_+}(P_p + P_h). \quad (1.14)$$

In the non-interacting setting, they reduce to:

$$i\tilde{G}^A = -\chi_{\mathbb{R}_-} e^{-itH^0}, \quad i\tilde{G}^R = \chi_{\mathbb{R}_+} e^{-itH^0}. \quad (1.15)$$

Indeed, they also satisfy (1.12) in this setting, but with initial conditions

$$i\tilde{G}^A(0^+) = 0, \quad i\tilde{G}^R(0^+) = 1. \quad (1.16)$$

The particle (resp. hole) Green's function  $\tilde{G}^P$  (resp.  $\tilde{G}^H$ ) [16], defined by

$$\tilde{G}^P = \chi_{\mathbb{R}_+} P_p, \quad \tilde{G}^H = -\chi_{\mathbb{R}_-} P_h^\dagger \quad (1.17)$$

satisfy, still in the non-interacting setting, the differential equations

$$\left( i \frac{d}{dt} - H^0 \right) \tilde{G}^P = \delta_0(1 - \gamma_\Omega) \quad (1.18)$$

$$\left( i \frac{d}{dt} - H^0 \right) \tilde{G}^H = \delta_0 \gamma_\Omega \quad (1.19)$$

and therefore are not Green's functions even in the non-interacting setting. They merely serve as “building blocks that have to be combined” [75, p.107] to lead to  $\tilde{G}$ .

For reasons that will become clearer in the following, it proves useful to look at the Green's functions in the *Fourier* domain. For this purpose, the adequate notion is the one of Generalized Fourier Transform (GFT), already introduced by Titschmarsh in [104]: given  $\tilde{f} : \mathbb{R} \rightarrow B(\mathcal{H})$ , the associated GFT  $f$  is defined on the whole *upper half-plane*  $\mathbb{C}_+ = \{z \in \mathbb{C}, \Im(z) > 0\}$ , by for all  $z \in \mathbb{C}_+$ ,

$$f(z) = f_+(z) + f_-(\bar{z})^\dagger, \quad \text{with } \forall z \in \mathbb{C}_+, f_+(z) = \int_{\mathbb{R}_+} e^{izt} f(t) dt, \quad (1.20)$$

$$\text{and } \forall z \in \mathbb{C}_-, f_-(z) = \int_{\mathbb{R}_-^*} e^{izt} f(t) dt, \quad (1.21)$$

where  $\mathbb{C}_- = \{z \in \mathbb{C}, \Im(z) < 0\}$ , provided the integrals make sense for an appropriate operator topology. This approach has the advantage to circumvent any analytical continuation techniques and is particularly relevant in the non-interacting setting, as we state now. This result explains the  $i$  prefactor present in all our definitions of Green's functions.

**Proposition 1.2.6** (Non-interacting Green's functions are resolvents in the Fourier domain). *Given a non-interacting Hamiltonian  $H^0 \in \mathcal{S}(\mathcal{H})$ , the Generalized Fourier Transforms of the one-body time-ordered, advanced and retarded Green's function  $G : \mathbb{C}_+ \rightarrow B(\mathcal{H})$  of an equilibrium state  $\Omega$  are well-defined for the strong operator topology, coincide, and read for all  $z \in \mathbb{C}_+$ ,*

$$G(z) = (z - H^0)^{-1}. \quad (1.22)$$

*Namely, they are the resolvent of  $H^0$ , and are independent of the state  $\Omega$ . We call  $G^0$  the non-interacting Green's function.*

*Proof.* The proof is a consequence of [13, Proposition 3.1.6]: for all  $\phi \in \mathcal{H}$ , we have in the strong operator topology, for all  $z \in \mathbb{C}_+$ ,

$$\int_{\mathbb{R}_+} e^{izt} e^{-itH^0} dt = i(z - H^0)^{-1}, \quad (1.23)$$

and similarly, for all  $z \in \mathbb{C}_-$ ,

$$\int_{\mathbb{R}_-} e^{izt} e^{-itH^0} dt = -i(z - H^0)^{-1}. \quad (1.24)$$

It gives immediately the result for the GFT of  $\tilde{G}^R$ . For the advanced, we have, for all  $z \in \mathbb{C}_-$ ,  $G_-^A(z) = (z - H^0)^{-1}$  which gives the awaited result by reflection to  $\mathbb{C}_+$ . Finally, we find, for all  $z \in \mathbb{C}_+$ ,  $G_+(z) = (1 - \gamma_\Omega)(z - H^0)^{-1}$  and, for all  $z \in \mathbb{C}_-$ ,  $G_-(z) = \gamma_\Omega(z - H^0)^{-1}$  from which we conclude.  $\square$

This result is indeed of paramount importance, and holds only in the non-interacting setting. At this stage, let us introduce the imaginary part of an operator: for any bounded operator  $\hat{O} \in B(\mathcal{H})$ , it is defined as

$$\Im(\hat{O}) = \frac{1}{2i}(\hat{O} - \hat{O}^\dagger). \quad (1.25)$$

For the present case, the non-interacting Green's function satisfies  $\Im(G^0(z)) \leq 0$  for all  $z \in \mathbb{C}_+$ , and is indeed analytic on  $\mathbb{C}_+$ . Hence, it is the negative of an operator-valued *Pick function* [43]. This property also holds for the interacting Green's function, but we will not deal with the fully general case here. Let us only say that in the simpler case of *vector state*  $\Omega_\Psi$  with  $\Psi$  an eigenvector of  $\hat{H}$  (this setting is highly similar to the one of [16], to which the reader is referred to for more details), we have for all  $\phi, \phi' \in \mathcal{H}$ , for all  $t \in \mathbb{R}$ ,

$$\langle \phi, P_p(t)\phi' \rangle = \langle \Psi, \hat{a}_\phi e^{-it(\hat{H}-E_\Psi)} \hat{a}_{\phi'}^\dagger \Psi \rangle, \quad (1.26)$$

so that, using the same property as in the proof of Proposition 1.2.6 but for the strongly continuous one-parameter unitary group  $e^{it\hat{H}} \in B(\mathcal{F})$ , we have for all  $z \in \mathbb{C}_+$ ,

$$\langle \phi, G_+(z)\phi' \rangle = \langle \Psi, \hat{a}_\phi \left( z - (\hat{H} - E_\Psi) \right)^{-1} \hat{a}_{\phi'}^\dagger \Psi \rangle \quad (1.27)$$

where the GFT makes sense in the weak operator topology as in [16]. This shows in particular that we have for the GFT of the time-ordered Green's function

$$\langle \phi, \Im(G_+(z))\phi \rangle = \langle \hat{a}_\phi^\dagger \Psi, \Im\left(z - (\hat{H} - E_\Psi)\right)^{-1} \hat{a}_\phi^\dagger \Psi \rangle \leq 0. \quad (1.28)$$

Similarly,  $\Im(G_-(z)) \leq 0$  for all  $z \in \mathbb{C}_+$ ; this shows that the Generalized Fourier Transform of the time-ordered Green's function is well defined. In addition with the fact that it is analytic, it is therefore a negative of an operator-valued Pick function. We then have the following representation property [42]: there exists a bounded-operator-valued Borel measure  $A$  on  $\mathbb{R}$ , such that

$$G(z) = \int_{\mathbb{R}} \frac{1}{z - \varepsilon} dA(\varepsilon) \quad (1.29)$$

This measure is known as the *spectral function* in condensed matter physics and is full of physical interpretation. For instance, as we mention in Chapter 4, it allows to determine whether an interacting quantum system is a conductor or not, based on its low energy properties, and reveals (if they exist) the quasi-particles of the system. Moreover, it is theoretically measurable by Angle Resolved Photo Emission Spectroscopy (ARPES) experiments, and we refer to [75] for a discussion about this statement. Finally, the measure  $A$  takes a very simpler form in the finite-dimensional setting: as detailed in the next chapter, the Green's function can be theoretically calculated using the Källen-Lehmann representation: it reads, for all  $z \in \mathbb{C}_+$ , for all  $\phi, \phi' \in \mathcal{H}$ ,

$$\langle \phi, G(z)\phi' \rangle = \sum_{\psi, \psi' \in \mathcal{B}} \frac{\rho_\psi + \rho_{\psi'}}{z + (E_\psi - E_{\psi'})} \langle \psi, \hat{a}_\phi \psi' \rangle \langle \psi', \hat{a}_{\phi'}^\dagger \psi \rangle, \quad (1.30)$$

where  $\mathcal{B}$  is a joint eigenbasis of  $\hat{\rho}, \hat{H}$  with corresponding eigenvalues  $\rho_\psi, E_\psi$ . The spectral function therefore gives the one-particle excitation energies of the system.

This formula could let the reader think that for finite dimensional systems, meaning any computation, Green's function are easily computable as a sum of explicit terms. But this sum implies the prior diagonalization of a self-adjoint operator *in the Fock space*, whose dimension grows exponentially with the dimension of the one-particle Hilbert space, which is precisely the bottleneck of computations of quantum systems. The idea of *embedding methods* is precisely to *bypass* this step, in a manner that we detail in the next section.

## 1.3 Embedding methods

In this last section, we introduce the embedding methods we were interested in during the PhD. Since the mathematical analysis of these approximations is new, we had to give a detailed mathematically oriented presentation of these methods, in [17] (Chapter 2) for DMET and [18] (Chapter 3) for DMFT, so that we will not discuss all the details but rather give a general overview. We present them in the order in which they appeared chronologically: first DMFT, from the perspective of the sparsity pattern of the self-energy rather than that of path integrals and the “cavity method” [41], then DMET which was developed as a “simple alternative” to DMFT. In this order, we highlight the main similarities and differences between these two methods, comparing DMET with respect to DMFT, the symmetric comparison being given in Section 3.1. The interested reader will find very helpful resources in [71], Part VI and VII for DMFT (see in particular the original Euclidean field presentation of DMFT) and Part V for a discussion about a similar embedding of 1-RDM. Finally, we present some guidelines for future work on DMFT, which this thesis calls for.

### 1.3.1 Dynamical Mean-Field Theory

In its original formulation [40, 41], the principle of DMFT is to approximate the Green’s function of a Hubbard model using an Anderson Impurity Model (AIM), whose parameters are determined by a self-consistent condition. An AIM describes an impurity embedded in a medium, and for this reason, DMFT was also called “Local Impurity Self-consistent Approximation” (LISA) in its early days [41]. Before discussing its principle in more detail, let us say that the design of this approximation was motivated by previous studies of the “ $d = \infty$ ” Hubbard model [80], this model simplifying in this limit in a similar way as that of *classical spin systems*, for example the Ising model on the  $d$ -dimensional hypercubic lattice, as  $d$  goes to infinity. From this point of view, DMFT is a “mean-field” method in the sense of a classical-quantum analogy with mean-field methods applied to classical spin systems such as the Ising model, and it is “dynamical” due to the fact that Green’s functions are time-dependent functions [39].

**Anderson Impurity Model** The AIM [4] is a quantum model for magnetic impurities embedded in a set of conducting electrons living in a system that is called the “bath”. Originally formulated for a single-site impurity, it has been then extended to multiple sites to model impurity clusters and for the purpose of cluster DMFT. Its formulation is better expressed using the formalism of second quantization and is fully given in Section 3.2: briefly, it describes two subsystems, on the one hand the “impurity”, described by a Hubbard model and onto which electrons interact, and on the other hand a “bath” of non-interacting electrons, these two subsystems being coupled by the tunnel effect, meaning that electrons can jump from one to the other, in a similar way as in a tight-binding model. A crucial property of this model lies in the *locality* of the interactions between the electrons (they interact *only* on the impurity), which translates mathematically into the fact that the Hamiltonian reads

$$\hat{H}_{AI} = d\Gamma(H^0) + \hat{H}^I, \quad \text{with } \hat{H}^I \in \mathcal{A}\{\hat{a}_\phi^\dagger \hat{a}_{\phi'}, \phi, \phi' \in \mathcal{H}_{\text{imp}}\}, \quad (1.31)$$

where the latter is the impurity Gauge Invariant Canonical Anti-commutation Relations (GICAR) sub-algebra (see [97] for a self-contained presentation of these algebras). The consequence of this property is that the *self-energy*  $\Sigma$ , well defined for any equilibrium state of a finite dimensional quantum system as

$$\Sigma = (G^0)^{-1} - G^{-1} \quad (1.32)$$

is non-zero only on the impurity, meaning that in the orthogonal decomposition  $\mathcal{H} = \mathcal{H}_{\text{imp}} \oplus \mathcal{H}_{\text{bath}}$  of the one-particle space, it reads

$$\Sigma = \begin{pmatrix} \Sigma_{\text{imp}} & 0 \\ 0 & 0 \end{pmatrix}. \quad (1.33)$$

This property of the self-energy is known as its *sparsity pattern* [69] and Theorem 3.2.8, and lays the groundwork for DMFT. The main idea of this method, illustrated in Figure 1.6, is to use a partition  $\mathfrak{P}$  of the original set of Hubbard vertices  $\Lambda$ , and to “embed” each of the elements of this partition in a “bath”, thus defining a collection of Anderson Impurity Models. The “impurity” is defined by the subgraph induced by the DMFT partition  $\mathfrak{P}$ , while the baths, represented by their *hybridization function*  $\Delta_p$  are chosen so as to satisfy the following self-consistent equations for all  $p \in \mathfrak{P}$ ,

$$G_{\text{imp},p} = G_{\text{DMFT},p} \quad (1.34)$$

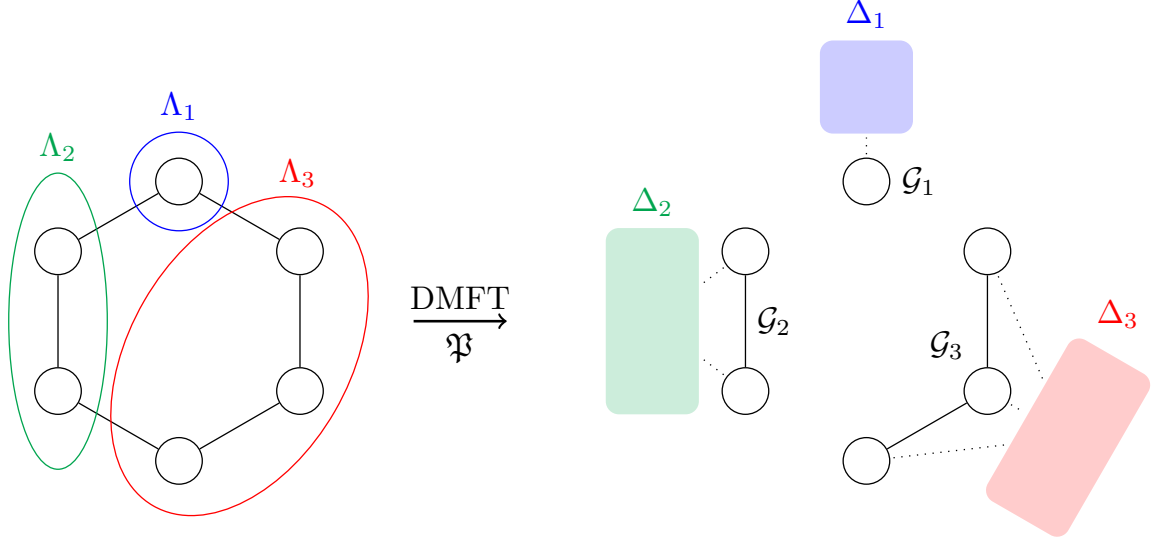


Figure 1.6: Principle of the DMFT approximation: after partitionning with  $\mathfrak{P}$ , define a collection of self-consistent AIMs

where  $G_{\text{DMFT}}$  is defined as

$$G_{\text{DMFT}} = (z - H_H^0 - \Sigma_{\text{DMFT}})^{-1} \quad (1.35)$$

where  $H_H^0$  is the one-particle Hamiltonian associated to the non-interacting part of the original Hubbard model, and  $\Sigma_{\text{DMFT}}$  is given by

$$\Sigma_{\text{DMFT}} = \bigoplus_{p \in \mathfrak{P}} \Sigma_{\text{imp}, p} \quad (1.36)$$

To close the loop, the last ingredient to be provided is an *impurity solver* which, for fixed impurity parameters, gives the self-energy  $\Sigma_{\text{imp}}$  of an AIM given a hybridization function  $\Delta$ : in our work, we were interested in the Iterated Perturbation Theory (IPT) version of this solver, which we present at length in Section 3.2.5 after introducing the formalism of Matsubara's Green's functions. Note that Equation (1.36) imposes self-consistency, and is the justification of the terminology of DMFT, each subgraph being treated as if its neighborhood hosted non-interacting electrons. Overall, we end up with the following equations

$$\forall z \in \mathbb{C}_+, \quad \Delta(z) = W (z - H_\perp^0 - \Sigma(z))^{-1} W^\dagger \quad (1.37)$$

$$\Sigma = \text{IPT}_\beta(U, \Delta). \quad (1.38)$$

**Contributions of this thesis** To our knowledge, the only mathematical contributions to the analysis of DMFT are found in [71, Part VII], where the authors show that the “DMFT loop” (corresponding to our Bath Update map) defined by (1.37) is a well-defined map between self-energies and hybridization functions of finite dimensional systems. In this thesis, we give in Chapter 3 a mathematical analysis of these equations, which discusses the existence of solutions to these equations as we describe below:

- After a lengthy introduction in which we detail the definition of the appropriate objects and the derivation of DMFT, we provide in Proposition 3.2.18 the counterpart of what is proven in [71], by showing that the IPT solver involved in Equation (1.38) is well defined for hybridization functions associated with finite dimensional baths, and returns a self-energy associated with a finite dimensional system structure. The proof of this statement relies on *analytic continuation* problems, which we introduce in Appendix 3.A.1, and for which we give a uniqueness result which, to the extent of our knowledge, is new.
- With the two equations being well-defined between hybridization functions and self-energies of finite-dimensional systems, we are in a position to study the existence of solutions to the IPT-DMFT equations: we prove in Proposition 3.3.5 that, apart from trivial limits for which DMFT admits a unique (and exact) solution as we present in Proposition 3.2.12, there is no solution associated with finite-dimensional baths. This result is well known in physics, and relies on the fact that, without

bath truncation, the dimension of the AIM’s baths increases with each iteration of the DMFT map. Note that this result depends on the impurity solver implied in the DMFT loop: it is also expected to hold for the theoretical (and exact) impurity solver, but not for less accurate solvers such as (static) Hartree-Fock theory which returns constant (in frequency) self-energies.

- The latter fact suggests to look for solutions in the closure of the set of hybridization functions and self-energies associated to finite dimensional systems: our approach is based on an extension using (negatives of) Pick functions, which are analytic maps from the upper half-plane  $\mathbb{C}_+$  with positive imaginary part. Using the Nevanlinna-Riesz measure associated with the latter, we reformulate the equations in terms of *matrix-valued positive measures*, and in this setting we show that both the Bath Update map (Proposition 3.3.6) and the IPT map (Proposition 3.3.8) are well defined for the appropriate spaces of measures, which encompass the finite-dimensional baths setting.
- This framework proves useful in Theorem 3.3.9, our main result, in which we show that the IPT-DMFT equations admit a solution. Our proof is based on a reformulation of the equations into a fixed-point problem, for which we use a Schauder(-Singbal) fixed-point theorem with the weak topology on the space of finite measures. As a by-product of the proof, we show that a solution of the DMFT equations admits moments up to any order in Proposition 3.3.10. This property implies that the Green’s function associated with a solution admits a spectral measure  $A$  with moments up to any order: from a physical point of view, this means that no global quasiparticle is predicted by DMFT, the presence of which being associated with a Lorentzian spectral function [75] that does not have moments of order higher than zero.

Since DMFT is a practical computational scheme, in Chapter 4 we also discuss the standard discretisation scheme used with the IPT solver, which is based on the restrictions of the hybridization function and the self-energy to the discrete set of Matsubara’s frequencies. The mathematical and numerical contributions of this analysis are presented below:

- After presenting how this algorithm can be used to gain insight into the Mott transition, we start by proving the existence of the solution of the discretized equations in Theorem 4.2.1: contrary to what is done in [18], our proof is not based on Pick functions, and the result we obtain is weaker, requiring assumptions on the parameters defining the model. Moreover, there is no guarantee that the obtained solution is compatible with a “physical” solution, and our theorem only ensures the solution satisfies a necessary condition for this to hold.
- We then provide a numerical exploration of the classical fixed-point algorithm associated with the discretized equations for the Hubbard dimer in Section 4.3. We start by showing evidence for a Mott transition at high-enough temperature using Pade approximants for analytic continuation, and show in this setting that linear convergence up to machine precision is observed for high temperature ( $\beta = 1$ ), independently of the value of the on-site repulsion  $U$  and for two very distinct initial guesses. However, for low temperature ( $\beta = 10$ ) and intermediate values of the on-site repulsion  $U$  we see a very different trend, where the convergence is not monotonous and sometimes leads to unphysical solutions (see Figure 6). Results for small and large on-site repulsion indicate that uniqueness should hold in this regime.
- These results suggest implementing a continuation method to explore the intermediate  $U$  region, starting from low/large values of  $U$ . Our simulations indicate that coexisting solutions for intermediate values of  $U$  are not observed, and merely correspond to “metastable” solutions that require many more iterations to reach convergence.
- We conclude this chapter by proving what is observed for small and large on-site repulsion in Theorem 4.4.1, namely that solution is unique in these regimes. Our proof is based on a simple estimate of the discretized DMFT map and on the Picard fixed-point theorem, and provides only with a uniqueness result in a neighborhood of the origin.

### 1.3.2 “A Simple Alternative to DMFT”: Density Matrix Embedding Theory.

As claimed in the seminal papers [60, 61], Density Matrix Embedding Theory (DMET) is inspired by the principles of DMFT, and aims to provide a “simple alternative” to the latter, both in the setting of quantum lattices [60] and molecular Hamiltonians [61]. These methods are both based on an approximation of a large interacting system by a collection of smaller, self-coherent subsystems, obtained after

the decomposition of the one-particle space. If a direct comparison of "simplicity" with DMFT is not a mathematical question, we can outline how the setting of DMET is simpler than that of DMFT before giving the details of its derivation: on the one hand, it focuses on the one-particle reduced density matrix (which we will abbreviate as 1-RDM and note  $D$  in this section, to be consistent with Chapter 2 and more generally with the chemistry literature, and not 1-pdm as we did in the previous Section) of a finite dimensional system, and on the other hand, the dimension of the bath is finite and fixed by the decomposition of the one-particle space.

As its name suggests, DMET provides an approximation to 1-RDM  $D$  of a quantum system in one of its ground states  $\Psi$ , with a given number of electrons  $N$  (generalizations to Gibbs states are emerging [103] but we do not discuss them here). For interacting electrons, such a vector is not expected to be a Slater determinant so the exact 1-RDM is not a projector (see the previous Section for a discussion about this property). Nevertheless, DMET approximates the exact 1-RDM with a projector, and is similar to the Hartree-Fock method in this respect. In other words, the approximate 1-RDM lies in the following set:

$$\mathcal{D} = \{D \in \mathcal{S}(\mathcal{H}), \quad D^2 = D, \text{Tr}(D) = N\}, \quad (1.39)$$

while a general 1-RDM of a  $N$  particle vector state lies in the convex hull of the former set:

$$\text{CH}(\mathcal{D}) = \{D \in \mathcal{S}(\mathcal{H}), \quad 0 \leq D \leq 1, \text{Tr}(D) = N\}. \quad (1.40)$$

Like DMFT, DMET is based on a "fragmentation" of the one-particle space: in DMFT, it is given by the partition  $\mathfrak{P}$  of the Hubbard vertices, while in DMET it is given by an orthogonal decomposition of  $\mathcal{H}$  into so-called "fragments"  $X_x$  which are *finite dimensional* ( $\dim(X_x) = L_x$ ): we assume that

$$\mathcal{H} = \bigoplus_{x=1}^{N_f} X_x \quad (1.41)$$

where  $N_f$  is the number of fragments. Note that such a decomposition can also be derived in DMFT, from a DMFT partition  $\mathfrak{P}$  and using the basis given in (1.1), showing the importance of localized orbitals in the development of this method. In our analysis [17], we have dealt with a finite number of fragments, making  $\mathcal{H}$  finite dimensional, which corresponds to the setting in which numerical simulations are carried out. Now for a given projector 1-RDM  $D \in \mathcal{D}$ , we define for each fragment  $X_x$  the associated "impurity space"  $W_{x,D} \subset \mathcal{H}$  as

$$W_{x,D} = X_x + D(X_x) = D(X_x) \oplus (1 - D)(X_x) \quad (1.42)$$

where the last sum is orthogonal. This space is of *finite* dimension  $\dim(W_{x,D}) \leq 2L_x$  and our assumption (A2) for the main theorems is that this equality holds for a specific non-interacting 1-RDM  $D^0$ , which we will specify later (impurity spaces are of maximal dimension): in the following we consider it holds for any  $D$ , which is true in the neighborhood of such a  $D^0$ . Since DMET is interested in the ground state of a given Hamiltonian  $\hat{H} \in \mathcal{S}(\mathcal{F})$ , it aims at giving an approximation to the following minimization problem

$$\inf_{\Psi \in \mathcal{H}^N, \|\Psi\|=1} \langle \Psi, \hat{H}\Psi \rangle \quad (1.43)$$

which we already discussed in the previous section. The search space for such a problem is of very high dimension, and the principle of DMET is to reduce it by "freezing" the degrees of freedom that are outside the impurity space. This is done as follows for each impurity space  $W_{x,D}$ :

- Start by defining the associated "core space"  $\mathcal{H}_{x,D}^{\text{core}}$  by decomposing in orthogonal subspaces  $\text{Ran}(D) = D(X_x) \oplus \mathcal{H}_{x,D}^{\text{core}}$ . As we mentioned previously when introducing 1-RDM, a 1-RDM is a projector if and only if it is associated with a Slater determinant  $\Psi_D = \hat{a}_{\phi_1}^\dagger \dots \hat{a}_{\phi_N}^\dagger |\emptyset\rangle$  of a set of  $\{\phi_i\}_{i \in [1,N]}$  spin-orbitals (see Equation (1.3)): in the following, the latter are chosen to be consistent with the previous decomposition, meaning  $D(X_x) = \text{Span}(\phi_i)_{i \in [1,L_x]}$  and  $\mathcal{H}_{x,D}^{\text{core}} = \text{Span}(\phi_i)_{i \in [L_x+1,N]}$ .
- Then similarly define the associated "virtual space"  $\mathcal{H}_{x,D}^{\text{virt}}$  by decomposing into orthogonal subspaces  $\text{Ran}(1 - D) = (1 - D)(X_x) \oplus \mathcal{H}_{x,D}^{\text{virt}}$  (note that the "virtual space" of DMET is not the virtual spin-orbitals space introduced in the previous section, which corresponds to  $\text{Ran}(1 - D)$ ), so that we end up with the following decomposition of the one-particle space  $\mathcal{H}$

$$\mathcal{H} = \underbrace{D(X_x) \oplus (1 - D)(X_x)}_{W_{x,D}} \oplus \underbrace{\mathcal{H}_{x,D}^{\text{core}} \oplus \mathcal{H}_{x,D}^{\text{virt}}}_{\mathcal{H}_{x,D}^{\text{env}}}. \quad (1.44)$$

- Now recall that the vector states  $\Omega_{\Psi_D}$  are normal states (in finite dimension, every state is a normal state), with the density matrix  $\hat{\rho}_D \in \mathcal{S}(\mathcal{F})$  being the orthogonal projector on  $\Psi_D$ : using the following isomorphism for the Fock space  $\mathcal{F}(\mathcal{H})$  associated to  $\mathcal{H}$  (see for instance [102, Problem 6.3], the Fock space operation being somehow an exponential for  $\oplus$  and  $\otimes$ ):

$$\mathcal{F}(\mathcal{H}) \simeq \mathcal{F}(W_{x,D}) \otimes \mathcal{F}(\mathcal{H}_{x,D}^{\text{env}}), \quad (1.45)$$

the density operator reads up to this isomorphism

$$\hat{\rho}_D = \hat{\rho}_{W_{x,D}} \otimes \hat{\rho}_{\mathcal{H}_{x,D}^{\text{env}}} \quad (1.46)$$

where  $\hat{\rho}_{W_{x,D}} \in \mathcal{S}(\mathcal{F}(W_{x,D}))$  (resp.  $\hat{\rho}_{\mathcal{H}_{x,D}^{\text{env}}} \in \mathcal{S}(\mathcal{F}(\mathcal{H}_{x,D}^{\text{env}}))$ ) is the orthogonal projection on the Slater Determinant state  $\Psi_{W_{x,D}}$  (resp.  $\Psi_{\mathcal{H}_{x,D}^{\text{env}}}$ ) associated with  $\{\phi_i\}_{i \in \llbracket 1, L_x \rrbracket} \subset D(X_x) \subset W_{x,D}$  (resp.  $\{\phi_i\}_{i \in \llbracket L_x+1, N \rrbracket} \subset \mathcal{H}_{x,D}^{\text{core}} \subset \mathcal{H}_{x,D}^{\text{env}}$ ).

- Writing  $\hat{\rho} = (\hat{\rho}_{W_{x,D}} \otimes \mathbf{1})(\mathbf{1} \otimes \hat{\rho}_{\mathcal{H}_{x,D}^{\text{env}}})$ , we end up with

$$\langle \Psi, \hat{H}\Psi \rangle = \text{Tr}((\hat{\rho}_{W_{x,D}} \otimes \mathbf{1})((\mathbf{1} \otimes \hat{\rho}_{\mathcal{H}_{x,D}^{\text{env}}})\hat{H})) = \text{Tr}(\hat{\rho}_{W_{x,D}}\hat{H}_{x,D}^{\text{imp}}) = \langle \Psi_{W_{x,D}}, \hat{H}_{x,D}^{\text{imp}}\Psi_{W_{x,D}} \rangle \quad (1.47)$$

where  $\hat{H}_{x,D}^{\text{imp}} = \text{Tr}_{\mathcal{F}(\mathcal{H}_{x,D}^{\text{env}})}((\mathbf{1} \otimes \hat{\rho}_{\mathcal{H}_{x,D}^{\text{env}}})\hat{H})$  is given by a partial trace on the environment Fock space  $\mathcal{F}(\mathcal{H}^{\text{env}})$  (see [92] for a discussion of the meaning of partial trace in quantum information) and is called the “impurity Hamiltonian”. Its expression for  $\hat{H} = d\Gamma(H^0) + \hat{H}^I$ , where  $\hat{H}^I$  is a two-body operator, is given in detail in [17, Proposition 7] and in part in [71, Part V, Section 5].

- With this formula, freezing the environment degrees of freedom means fixing  $\hat{H}_{x,D}^{\text{env}}$ , and optimizing on  $\Psi_{W_{x,D}}$  when looking at the ground state. Finally, for reasons that will become clearer when looking at the big picture, DMET considers the “grand canonical” impurity Hamiltonian  $\hat{H}_{x,D}^{\text{imp}} - \mu \hat{N}_x$ , where  $\hat{N}_x$  is the *fragment* (and not impurity !) number operator  $\hat{N}_x = d\Gamma(\Pi_x)$ ,  $\Pi_x$  being the orthogonal projector on  $X_x$ , and  $\mu$  is the chemical potential to be specified below. With all these considerations, we arrive at the *impurity problem* which reads as a grand canonical ground state minimization over  $\mathcal{F}(W_{x,D})$ :

$$\inf_{\Psi_x^{\text{imp}} \in \mathcal{F}(W_{x,D}), \|\Psi_x\|=1} \langle \Psi_x^{\text{imp}}, (\hat{H}_{x,D}^{\text{imp}} - \mu \hat{N}_x) \Psi_x^{\text{imp}} \rangle \quad (1.48)$$

Assuming that the above minimization problems have a unique solution for all  $x \in \llbracket 1, N_f \rrbracket$ , we denote by  $P_{\mu,x}(D)$  the 1-RDM of the solution to the  $x$ -th impurity problem. The high-level DMET map  $F^{\text{HL}}$  is then defined as

$$F^{\text{HL}}(D) = \sum_{x=1}^{N_f} \Pi_x P_{\mu,x}(D) \Pi_x \quad (1.49)$$

where  $\mu$  is chosen such as  $\text{Tr}(F^{\text{HL}}(D)) = N$ . This is the first part of the DMET iteration, and is called “high-level” because it requires high-level computations to solve the impurity problems (compared to cheap computations such as Hartree-Fock). In comparison with DMFT, this step corresponds to the *impurity solver*, but unlike our analysis of DMFT where we were interested in the IPT approximate solver, here we assume that the impurity problems can be solved exactly. Note that  $F^{\text{HL}}(D)$  is in

$$\mathcal{P} = \text{Bd}(\text{CH}(\mathcal{D})), \quad \text{with } \text{Bd}(\hat{O}) = \sum_{x=1}^{N_f} \Pi_x \hat{O} \Pi_x. \quad (1.50)$$

Now the second step, called the low-level step, is much shorter to express: it consists, for a given  $P \in \mathcal{P}$ , in finding the closest projector 1-RDM  $D \in \mathcal{D}$  that matches with the block diagonal entries, meaning satisfies  $\text{Bd}(D) = P$ . In our article, we studied the following low-level map:

$$F^{\text{LL}}(P) = \underset{D \in \mathcal{D}, \text{Bd}(D)=P}{\text{argmin}} \mathcal{E}^{\text{HF}}(D) \quad (1.51)$$

where  $\mathcal{E}^{\text{HF}}(D)$  is nothing but the (Hartree-Fock) energy  $\langle \Psi_D, \hat{H}\Psi_D \rangle$  where  $\Psi_D$  is the Slater determinant associated with  $D$ . Compared to DMFT, this step is the equivalent of the Bath update map, but

poses much more problems from a mathematical point of view: to be well defined, the above functional must admit a unique minimizer, over a set which raises representability issues [31]. Overall, the DMET equations consist of the following set of self-consistent equations:

$$D = F^{\text{LL}}(P) \in \mathcal{D} \quad (1.52)$$

$$P = F^{\text{HL}}(D) \in \mathcal{P}. \quad (1.53)$$

**Contributions of this thesis** To our knowledge, the very existence of a solution to the DMET equations was not proven mathematically. In Chapter 2, we partly answer this question by considering the weakly interacting regime: given a Hamiltonian  $\hat{H} = d\Gamma(H^0) + \hat{H}^I$  where  $\hat{H}^I$  is a two-body operator, we consider the family of Hamiltonians  $\hat{H}_\alpha$  where for all  $\alpha \in \mathbb{R}$ ,

$$\hat{H}_\alpha = d\Gamma(H^0) + \alpha \hat{H}^I. \quad (1.54)$$

The case  $\alpha = 0$  corresponds to the non-interacting setting, while the case  $\alpha = 1$  corresponds to the original one. Our study provides insights into the weakly interacting setting, meaning for  $\alpha$  in a neighborhood of 0. The first assumption (A1) is based on the one-particle Hamiltonian  $H^0$  and concerns the low-level solver: its eigenvalues (counted by multiplicity) satisfy  $\varepsilon_N < 0 < \varepsilon_{N+1}$ , so that it admits a unique  $N$ -particle ground state  $\Psi$  being a Slater determinant, with associated 1-RDM (defined by functional calculus) being

$$D^0 = \chi_{\mathbb{R}_-}(H^0). \quad (1.55)$$

The second assumption (A2) concerns the high-level solver in the non-interacting case: we assume that the impurities  $W_{x,D^0}$  are of maximal dimension. Under these two assumptions, we first show in Proposition 2.1 that for the non-interacting setting  $\alpha = 0$ , the 1-RDM  $D^0$ , together with its block diagonal counterpart  $P^0 = \text{Bd}(D^0)$  form a solution to the DMET equations. This is partly a justification for the claim that DMET “is exact in the non-interacting [...] limit” [60], and is the equivalent of Proposition 3.2.12 for DMFT. Note however that nothing ensures that this solution is the unique solution to the DMET equations, even in the non-interacting setting.

We then study the weakly interacting limit, where we need two additional assumptions: Assumption (A3) deals with representability issues near  $D^0$ , and expresses that the block-diagonal mapping  $\text{Bd}$  is surjective from the tangent plane  $\mathcal{T}_{D^0}\mathcal{D}$  of  $(D)$  at  $D^0$  to the tangent plane  $\mathcal{T}_{P^0}(\mathcal{P})$ . This assumption ensures the existence of projectors 1-RDM that coincide on the block diagonal entries for  $P$  in a neighborhood of  $P^0$ , and is motivated by the fact that in general, the sets  $\text{Bd}(\mathcal{D})$  and  $\mathcal{P}$  do not coincide, as we prove in Lemma 2.8. The last assumption (A4) is a bit more technical and concerns the invertibility of the response function associated with the high-level solver, and we refer the reader to Section 2.3 for a more detailed discussion of this. Under Assumptions (A1)-(A4), we are able to prove the following main theorems.

- We first prove in Theorem 2.4 that in the vicinity of  $\alpha = 0$ , there exists a unique solution  $(D_\alpha, P_\alpha)$  which lies in the neighborhood of  $(D^0, P^0)$ . We call this set of solutions the “physical branch”: both are real analytic in  $\alpha$  and reduce to  $(D^0, P^0)$  when  $\alpha = 0$ . The proof is based on the implicit function theorem.
- Subsequently, we prove in Theorem 2.5 that this branch provides an approximation to the exact 1-RDM to first order in  $\alpha$  in the weakly interacting regime.

We conclude the paper with numerical insights: we show numerically that exactness to higher order is not generally observed for the physical branch, and that our assumptions, if violated, can lead to multiple solutions.

### 1.3.3 Overview table and perspectives.

For the reader’s convenience, we sum up our presentation of the two embedding methods this thesis focuses on in the following table:

To conclude this introduction, we give below some guidelines for future work related to the mathematical description of DMFT. The first project, in the continuation of Chapters 3 and 4, could provide insights into the uniqueness of the solution of the (non-discretized) IPT-DMFT equations and an alternative discretization scheme to that of Chapter 4, based on optimal transport algorithms and free from analytic continuation techniques. The two others are more prospective and explore two facets of Green’s

	DMFT	DMET
General framework		
Equilibrium state	Gibbs state, $\hat{\rho} = e^{-\beta(\hat{H}-\mu\hat{N})}/Z$	Ground state, $\hat{\rho}$ projector onto $\Psi$
Reduced quantity	Green's function $G$ (Pick function)	1-RDM $D$ (self-adjoint)
Model of interest	Hubbard model ( $\mathcal{G}_H = (\Lambda, E), T, U$ )	Any finite dimensional
Decomposition of $\mathcal{H}$	DMFT partition $\mathfrak{P}$ of $\Lambda$	Any orthogonal decomposition $\oplus_x X_x$
Mean-field model	Collection of AIMs	Collection of $(W_{x,D}, \hat{H}_{x,D}^{\text{imp}})$
Bath dimension	Infinite (non-interacting)	Finite, $\dim(W_{x,D}) = 2 \dim(X_x)$
Impurity step	Impurity solver $\Delta \mapsto \Sigma$ (IPT here)	High-level solver $F^{\text{HL}} : D \mapsto P$
Self-consistency	Bath Update map $\Sigma \mapsto \Delta$	Low-level solver $F^{\text{LL}} : P \mapsto D$
Mathematical results on self-consistent equations in this thesis		
Existence	Global [18], conditional Chapter 4	Near $\alpha = 0$ , under (A1)-(A4)
Uniqueness	Trivial limits [18], locally Chapter 4	Near $\alpha = 0$ , locally
Exactness	Trivial limits [18]	First order in $\alpha$ , near $\alpha = 0$

Table 1.1: Overview table of the main features of DMFT and DMET from the perspective of this thesis.

functions theory: on the one hand, the very definition of the impurity solver of an Anderson Impurity Model, and on the other hand, the thermodynamic limit of the Green's functions for a “ $d = \infty$ ” Hubbard model.

Certainly, much remains to be done concerning the mathematical status of DMET: let us mention, for example, the study of the strictly correlated limit which has been initiated by some authors of [17], which would provide insights into the complementary limit than that of Chapter 2. However, the author of this manuscript is more interested in the problem of the mathematical description of DMFT, both from the point of view of the mathematical tools involved and of the progress it would bring to the understanding of Green's functions methods.

**Uniqueness, new numerical scheme** In Chapter 3, we prove the existence of solutions to the IPT-DMFT equations, and in Chapter 4 we prove for the discretized equations that a solution also exists, and is unique in some parameter regimes: the next point to be clarified is indeed the question of the uniqueness of the solution of the original IPT-DMFT equations. To answer this question, the arguments invoked for the discretized equations do not easily transfer to the original ones: as mentioned in the introduction of Chapter 4, the big difference is in the functional setting, where in Chapter 3 we require solutions to be “physical”, i.e. to be the Stieltjes transform of a positive measure. In order to conclude on uniqueness, estimates for measure distances must be found and at this stage, we have not yet given a satisfactory bound on the IPT map. A different approach might be to look at the moment problem associated with a solution [1], with a first insight from the formal  $\beta \rightarrow \infty$  limit, for which we have derived a recursive formula on the moments. An answer to this question of uniqueness would help to understand Mott transition as predicted by DMFT, whose order as a phase transition is directly related to the coexistence of solutions.

Another idea to investigate is the design of a new numerical scheme for the IPT-DMFT equations, that bypasses the analytic continuation. It is based on Proposition 3.2.18, which states that the analytic continuation problem posed by IPT for a discrete measure admits a unique solution in the set of (negatives) of Pick functions, which turns out to have a discrete Nevanlinna-Riesz measure. The support of the latter can be deduced from the set of roots of a given rational function, which can be searched in parallel and using classical root-finding algorithms, while the weights are given analytically. Moreover, it is easy to show that a similar property holds for the bath-update map. These statements suggest an “exact diagonalization” approach [15, 70, 78] to IPT as a fixed point algorithm on discrete measures. Indeed the bath dimension increases exponentially with the number of iterations, and this algorithm needs to be complemented with a bath truncation procedure [79] to avoid an explosion of the computation time along the iterations: in light of the proofs exposed in Chapter 3, we believe that this procedure may be advantageously done using discrete Kantorovich optimal transport algorithms.

**Well-posedness of the exact impurity solver** In this thesis, we have focused on the IPT approximation of the impurity solver in our study of DMFT. In fact, precise computations are based on more accurate solvers, and in order to provide mathematical insights about DMFT in this setting, the first step

is to study the *exact* impurity solver. For given impurity parameters  $\mathcal{G}_H, T, U$ , the latter is the map that gives the self-energy  $\Sigma$  of an Anderson Impurity Model for a given hybridization function  $\Delta$ . As shown in [69] and Theorem 3.2.8, this self-energy is sparse, and we would begin by showing its well-posedness. Further work would include a study of its regularity in terms of measure distances, as we did for IPT, and would lead to results on the existence of solutions to the “exact” DMFT equations. We believe that the setting of AIM is a good candidate for discussing the definition of Green’s functions for general equilibrium states, and this project could in the longer term contribute to the understanding of the Luttinger-Ward formalism [62, 67, 68], while paving the way for the study of Continuous Time Quantum Monte Carlo algorithms [46].

**Thermodynamic limits of DMFT (“ $d=\infty$ ” exactness)** Once the question of the uniqueness of the solution to the (IPT) DMFT equations is resolved, an interesting question is the existence and properties of thermodynamic limits of the solution, DMFT being designed to understand periodic materials. A particularly interesting topic would be to discuss the exactness of the solution of the DMFT equations in the “ $d = \infty$ ” limit [80], meaning for the nearest neighbor graph of the  $d$ -dimensional hypercubic lattice in the limit  $d \rightarrow \infty$ , and to discuss the scaling of the hopping matrix  $T$  and the on-site interaction  $U$  which lead to non-trivial limits.

## Bibliography

- [1] Naum I. Akhiezer. *The Classical Moment Problem and Some Related Questions in Analysis*. Society for Industrial and Applied Mathematics, Philadelphia, PA, 2020.
- [2] Grégoire Allaire and Jeffrey Rauch. Instability of dielectrics and conductors in electrostatic fields. *Archive for Rational Mechanics and Analysis*, 124:233–268, 2017.
- [3] Philip W. Anderson. New Approach to the Theory of Superexchange Interactions. *Physical Review*, 115(1):2–13, July 1959.
- [4] Philip W. Anderson. Localized Magnetic States in Metals. *Physical Review*, 124(1):41–53, 1961.
- [5] Philip W. Anderson. The Resonating Valence Bond State in La<sub>2</sub>CuO<sub>4</sub> and Superconductivity. *Science*, 235(4793):1196–1198, March 1987.
- [6] Philip W. Anderson. 50 Years of the Mott Phenomenon: Insulators, Magnets, Solids and Superconductors as Aspects of Strong-Repulsion Theory. In *A Career in Theoretical Physics*, pages 595–635. 1994.
- [7] N. W. Ashcroft and N. D. Mermin. *Solid State Physics*. Holt-Saunders, 1976.
- [8] Volker Bach, Elliott H. Lieb, and Jan Philip Solovej. Generalized Hartree-Fock theory and the Hubbard model. *Journal of Statistical Physics*, 76(1):3–89, July 1994.
- [9] J. Bardeen, L. N. Cooper, and J. R. Schrieffer. Theory of Superconductivity. *Physical Review*, 108(5):1175–1204, December 1957.
- [10] Johannes G. Bednorz and Karl A. Müller. Possible highTc superconductivity in the Ba-La-Cu-O system. *Zeitschrift für Physik B Condensed Matter*, 64(2):189–193, June 1986.
- [11] Max Born and Herbert S. Green. A General Kinetic Theory of Liquids. *Physics Today*, 3(10):35–37, October 1950.
- [12] Max Born and Robert Oppenheimer. Zur Quantentheorie der Moleküle. *Annalen der Physik*, 389(20):457–484, 1927.
- [13] Ola Bratteli and Derek William Robinson. *Operator algebras and quantum statistical mechanics 1. C\*-and W\*-Algebras. Symmetry Groups. Decomposition of States*. Theoretical and Mathematical Physics. Springer Berlin, Heidelberg, 2 edition, 1987.
- [14] Ola Bratteli and Derek William Robinson. *Operator algebras and quantum statistical mechanics 2. Equilibrium States. Models in Quantum Statistical Mechanics*. Theoretical and Mathematical Physics. Springer Berlin Heidelberg, 2 edition, 1997.

- [15] Michel Caffarel and Werner Krauth. Exact diagonalization approach to correlated fermions in infinite dimensions: Mott transition and superconductivity. *Physical Review Letters*, 72(10):1545–1548, 1994.
- [16] Eric Cancès, David Gontier, and Gabriel Stoltz. A mathematical analysis of the GW0 method for computing electronic excited energies of molecules. *Reviews in Mathematical Physics*, 28(04):1650008, 2016.
- [17] Éric Cancès, Fabian M. Faulstich, Alfred Kirsch, Eloïse Letournel, and Antoine Levitt. Some mathematical insights on Density Matrix Embedding Theory, 2023. arXiv:2305.16472.
- [18] Éric Cancès, Alfred Kirsch, and Solal Perrin-Roussel. A mathematical analysis of IPT-DMFT, June 2024. arXiv:2406.03384.
- [19] Massimo Capone. The Hubbard model and the Mott–Hubbard transition. 2023.
- [20] Davide Castelvecchi. Why superconductor research is in a ‘golden age’ — despite controversy. *Nature*, November 2023.
- [21] CEA. Première mondiale : le cerveau dévoilé comme jamais grâce à l’IRM le plus puissant au monde, April 2024.
- [22] Marvin L. Cohen and P. W. Anderson. Comments on the Maximum Superconducting Transition Temperature. *AIP Conference Proceedings*, 4(1):17–27, February 1972.
- [23] Claude Cohen-Tannoudji, Bernard Diu, and Franck Laloë. *Quantum Mechanics*. Wiley, 2nd edition, 2020.
- [24] Zhi-Hao Cui, Chong Sun, Ushnish Ray, Bo-Xiao Zheng, Qiming Sun, and Garnet Kin-Lic Chan. Ground-state phase diagram of the three-band Hubbard model from density matrix embedding theory. *Physical Review Research*, 2(4):043259, November 2020.
- [25] Eleftherios N. Economou. *Green’s Functions in Quantum Physics*, volume 7 of *Springer Series in Solid-State Sciences*. Springer, Berlin, Heidelberg, 2006.
- [26] Alan Elcrat and Piero Bassanini. Mathematical Theory of Electromagnetism. *SIMAI e-Lecture Notes*, 2(0):09001–09001.348, June 2009.
- [27] Victor J. Emery. Theory of high- T c superconductivity in oxides. *Physical Review Letters*, 58(26):2794–2797, June 1987.
- [28] Victor J. Emery and George Reiter. Mechanism for high-temperature superconductivity. *Physical Review B*, 38(7):4547–4556, September 1988.
- [29] Tilman Esslinger. Fermi-Hubbard Physics with Atoms in an Optical Lattice. *Annual Review of Condensed Matter Physics*, 1(Volume 1, 2010):129–152, August 2010.
- [30] Michele Fabrizio, Alexander O. Gogolin, and Alexander A. Nersesyan. From Band Insulator to Mott Insulator in One Dimension. *Physical Review Letters*, 83(10):2014–2017, September 1999.
- [31] Fabian M. Faulstich, Raehyun Kim, Zhi-Hao Cui, Zaiwen Wen, Garnet Kin-Lic Chan, and Lin Lin. Pure State v-Representability of Density Matrix Embedding Theory. *Journal of Chemical Theory and Computation*, 18(2):851–864, 2022.
- [32] Charles L. Fefferman, James P. Lee-Thorp, and Michael I. Weinstein. Honeycomb Schrödinger Operators in the Strong Binding Regime. *Communications on Pure and Applied Mathematics*, 71(6):1178–1270, June 2018.
- [33] A M Forrest. Meissner and Ochsenfeld revisited. *European Journal of Physics*, 4(2):117–120, April 1983.
- [34] Rupert L Frank, Christian Hainzl, Serguei Naboko, and Robert Seiringer. The critical temperature for the BCS equation at weak coupling. *The Journal of Geometric Analysis*, 17:559–567, 2007.

- [35] Rupert L. Frank, Christian Hainzl, Robert Seiringer, and Jan Philip Solovej. Microscopic derivation of Ginzburg-Landau theory. *Journal of the American Mathematical Society*, 25(3):667–713, September 2012.
- [36] Reika Fukushima and Andrea Sacchetti. Derivation of the Bose-Hubbard model in the multiscale limit, August 2012. arXiv:1208.5867 [math-ph].
- [37] N. Ganguli and Srinivasa Krishnan Karimannikam. Magnetic and other properties of the free electrons in graphite. *Proceedings of the Royal Society of London. Series A. Mathematical and Physical Sciences*, January 1941.
- [38] Dan Garisto. LK-99 isn't a superconductor — how science sleuths solved the mystery. *Nature*, 620(7975):705–706, August 2023.
- [39] Antoine Georges. Lectures at Collège de France. Fermions en interaction : Introduction à la théorie du champ moyen dynamique, 2018.
- [40] Antoine Georges and Gabriel Kotliar. Hubbard model in infinite dimensions. *Physical Review B*, 45(12):6479–6483, March 1992.
- [41] Antoine Georges, Gabriel Kotliar, Werner Krauth, and Marcelo J. Rozenberg. Dynamical mean-field theory of strongly correlated fermion systems and the limit of infinite dimensions. *Reviews of Modern Physics*, 68(1):13–125, January 1996.
- [42] Fritz Gesztesy, Nigel J. Kalton, Konstantin A. Makarov, and Eduard Tsekanovskii. Some Applications of Operator-valued Herglotz Functions. In *Operator Theory, System Theory and Related Topics*, pages 271–321. Birkhäuser Basel, Basel, 2001.
- [43] Fritz Gesztesy and Eduard Tsekanovskii. On Matrix-Valued Herglotz Functions. *Mathematische Nachrichten*, 218(1):61–138, 2000.
- [44] Jean Ginibre. Reduced Density Matrices of Quantum Gases. I. Limit of Infinite Volume. *Journal of Mathematical Physics*, 6(2):238–251, February 1965.
- [45] Lev Petrovich Gor'kov. Microscopic derivation of the Ginzburg-Landau equations in the theory of superconductivity. *Sov. Phys. JETP*, 9(6):1364–1367, 1959.
- [46] Emanuel Gull, Andrew J. Millis, Alexander I. Lichtenstein, Alexey N. Rubtsov, Matthias Troyer, and Philipp Werner. Continuous-time Monte Carlo methods for quantum impurity models. *Reviews of Modern Physics*, 83(2):349–404, 2011.
- [47] Martin C. Gutzwiller. Effect of Correlation on the Ferromagnetism of Transition Metals. *Physical Review Letters*, 10(5):159–162, March 1963.
- [48] Felix M. Haehl, R. Loganayagam, and Mukund Rangamani. Schwinger-Keldysh formalism. Part I: BRST symmetries and superspace. *Journal of High Energy Physics*, 2017(6):69, June 2017.
- [49] Christian Hainzl and Robert Seiringer. The Bardeen–Cooper–Schrieffer functional of superconductivity and its mathematical properties. *Journal of Mathematical Physics*, 57(2):021101, February 2016.
- [50] Brian C. Hall. *Quantum Theory for Mathematicians*, volume 267 of *Graduate Texts in Mathematics*. Springer, New York, NY, 2013.
- [51] Trygve Helgaker, Poul Jorgensen, and Jeppe Olsen. *Molecular electronic-structure theory*. John Wiley & Sons, 2013.
- [52] John Hubbard. Electron correlations in narrow energy bands. *Proceedings of the Royal Society of London. Series A. Mathematical and Physical Sciences*, 276(1365):238–257, 1963.
- [53] John R. Hull. Bulk Superconducting Magnets for Bearings and Levitation. In *Encyclopedia of Applied Physics*, pages 1–15. John Wiley & Sons, Ltd, 2016.
- [54] Shengtao Jiang, Douglas J. Scalapino, and Steven R. White. Density-matrix-renormalization-group-based downfolding of the three-band Hubbard model: the importance of density-assisted hopping. *Physical Review B*, 108(16):L16111, October 2023. arXiv:2303.00756 [cond-mat].

- [55] Leo P. Kadanoff and Gordon Baym. *Quantum Statistical Mechanics: Green's Function Methods in Equilibrium and Nonequilibrium Problems*. CRC Press, Boca Raton, 1962.
- [56] Leo P. Kadanoff and Paul C. Martin. Theory of Many-Particle Systems. II. Superconductivity. *Physical Review*, 124(3):670–697, November 1961.
- [57] Junjiro Kanamori. Electron Correlation and Ferromagnetism of Transition Metals. *Progress of Theoretical Physics*, 30(3):275–289, 1963.
- [58] Leonid V. Keldysh. Diagram technique for nonequilibrium processes. *Zh. Eksp. Teor. Fiz.*, 47:1515–1527, 1964.
- [59] Charles Kittel and Paul McEuen. *Introduction to solid state physics*. John Wiley & Sons, 2018.
- [60] Gerald Knizia and Garnet Kin-Lic Chan. Density Matrix Embedding: A Simple Alternative to Dynamical Mean-Field Theory. *Physical Review Letters*, 109(18):186404, November 2012.
- [61] Gerald Knizia and Garnet Kin-Lic Chan. Density Matrix Embedding: A Strong-Coupling Quantum Embedding Theory. *Journal of Chemical Theory and Computation*, 9(3):1428–1432, March 2013.
- [62] Evgeny Kozik, Michel Ferrero, and Antoine Georges. Nonexistence of the Luttinger-Ward Functional and Misleading Convergence of Skeleton Diagrammatic Series for Hubbard-Like Models. *Physical Review Letters*, 114(15):156402, April 2015.
- [63] Mathieu Lewin. *Théorie spectrale et mécanique quantique*, volume 87 of *Mathématiques et Applications*. Springer International Publishing, Cham, 2022.
- [64] Elliott H. Lieb. The Hubbard model: Some Rigorous Results and Open Problems. In *Condensed Matter Physics and Exactly Soluble Models: Selecta of Elliott H. Lieb*. Berlin, Heidelberg, 2004.
- [65] Elliott H. Lieb and F. Y. Wu. Absence of Mott Transition in an Exact Solution of the Short-Range, One-Band Model in One Dimension. *Physical Review Letters*, 20(25):1445–1448, June 1968.
- [66] Elliott H. Lieb and F.Y. Wu. The one-dimensional Hubbard model: a reminiscence. *Physica A: Statistical Mechanics and its Applications*, 321(1-2):1–27, April 2003.
- [67] Lin Lin and Michael Lindsey. Bold Feynman diagrams and the Luttinger-Ward formalism via Gibbs measures. Part I: Perturbative approach. *arXiv:1809.02900 [math-ph, physics:physics]*, September 2018. arXiv: 1809.02900.
- [68] Lin Lin and Michael Lindsey. Bold Feynman diagrams and the Luttinger-Ward formalism via Gibbs measures. Part II: Non-perturbative analysis. *arXiv:1809.02901 [math-ph, physics:physics]*, September 2018. arXiv: 1809.02901.
- [69] Lin Lin and Michael Lindsey. Sparsity Pattern of the Self-energy for Classical and Quantum Impurity Problems. *Annales Henri Poincaré*, 21(7):2219–2257, 2020.
- [70] Nan Lin, C. A. Marianetti, Andrew J. Millis, and David R. Reichman. Dynamical Mean-Field Theory for Quantum Chemistry. *Physical Review Letters*, 106(9):096402, March 2011. arXiv: 1010.3180.
- [71] Michael Lindsey. *The Quantum Many-Body Problem: Methods and Analysis*. PhD thesis, University of California, Berkeley, 2019.
- [72] A. Macridin, M. Jarrell, Th. Maier, and G. A. Sawatzky. Physics of cuprates with the two-band Hubbard model: The validity of the one-band Hubbard model. *Physical Review B*, 71(13):134527, April 2005.
- [73] Paul C. Martin. *Measurements and correlation functions*. CRC Press, 1968.
- [74] Paul C. Martin and Julian Schwinger. Theory of Many-Particle Systems. I. *Phys. Rev.*, 115(6):1342–1373, September 1959.
- [75] Richard M. Martin, Lucia Reining, and David M. Ceperley. *Interacting Electrons: Theory and Computational Approaches*. Cambridge University Press, Cambridge, 2016.

- [76] Nicola Marzari, Arash A. Mostofi, Jonathan R. Yates, Ivo Souza, and David Vanderbilt. Maximally localized Wannier functions: Theory and applications. *Reviews of Modern Physics*, 84(4):1419–1475, October 2012.
- [77] Takeo Matsubara. A New Approach to Quantum-Statistical Mechanics. *Progress of Theoretical Physics*, 14(4):351–378, October 1955.
- [78] Darya Medvedeva, Sergei Iskakov, Friedrich Krien, Vladimir V. Mazurenko, and Alexander I. Lichtenstein. Exact diagonalization solver for extended dynamical mean-field theory. *Physical Review B*, 96(23):235149, 2017.
- [79] Carlos Mejuto-Zaera, Leonardo Zepeda-Núñez, Michael Lindsey, Norm Tubman, Birgitta Whaley, and Lin Lin. Efficient hybridization fitting for dynamical mean-field theory via semi-definite relaxation. *Physical Review B*, 101(3):035143, January 2020.
- [80] Walter Metzner and Dieter Vollhardt. Correlated Lattice Fermions in  $d = \infty$  Dimensions. *Physical Review Letters*, 62(3):324–327, January 1989.
- [81] Andreas Mielke. Ferromagnetic ground states for the Hubbard model on line graphs. *Journal of Physics A: Mathematical and General*, 24(2):L73, January 1991.
- [82] Andreas Mielke. Exact ground states for the Hubbard model on the Kagome lattice. *Journal of Physics A: Mathematical and General*, 25(16):4335, August 1992.
- [83] Andreas Mielke. Ferromagnetism in the Hubbard model and Hund’s rule. *Physics Letters A*, 174(5):443–448, March 1993.
- [84] Niels F. Mott. Metal-Insulator Transition. *Reviews of Modern Physics*, 40(4):677–683, October 1968.
- [85] Niels F. Mott and R. Peierls. Discussion of the paper by de Boer and Verwey. *Proceedings of the Physical Society*, 49(4S):72, August 1937.
- [86] John W. Negele and Henri Orland. *Quantum Many-particle Systems*. CRC Press, Boca Raton, May 2019.
- [87] H. Kamerlingh Onnes. Further experiments with liquid helium. C. On the change of electric resistance of pure metals at very low temperatures etc. IV. The resistance of pure mercury at helium temperatures. Number 120b in Communication from the Physical Laboratory of Leiden. April 1911.
- [88] Gianluca Panati and Adriano Pisante. Bloch Bundles, Marzari-Vanderbilt Functional and Maximally Localized Wannier Functions. *Communications in Mathematical Physics*, 322(3):835–875, September 2013.
- [89] Rudolph Pariser and Robert G. Parr. A Semi-Empirical Theory of the Electronic Spectra and Electronic Structure of Complex Unsaturated Molecules. II. *The Journal of Chemical Physics*, 21(5):767–776, 1953.
- [90] E. Picari, A. Ponno, and L. Zanelli. Mean Field Derivation of DNLS from the Bose–Hubbard Model. *Annales Henri Poincaré*, 23(5):1525–1553, May 2022.
- [91] John A. Pople. Electron interaction in unsaturated hydrocarbons. *Transactions of the Faraday Society*, 49(0):1375–1385, 1953.
- [92] Renato Renner. Quantum Information Theory, Lecture Notes. 2013.
- [93] S.R.P.G. Ripka, J.P. Blaizot, and G. Ripka. *Quantum Theory of Finite Systems*. MIT Press, 1986.
- [94] David Ruelle. Analyticity of Green’s functions of dilute quantum gases. *Journal of Mathematical Physics*, 12(6):901–903, 1971.
- [95] Andrea Sacchetti. Derivation of the Tight-Binding Approximation for Time-Dependent Nonlinear Schrödinger Equations. *Annales Henri Poincaré*, 21(2):627–648, February 2020.

- [96] Etienne Sandier, Sylvia Serfaty, Haim Brezis, Antonio Ambrosetti, A. Bahri, Felix Browder, Luis Caffarelli, Lawrence C. Evans, Mariano Giaquinta, David Kinderlehrer, Sergiu Klainerman, Robert Kohn, P. L. Lions, Jean Mawhin, Louis Nirenberg, Lambertus Peletier, Paul Rabinowitz, and John Toland. *Vortices in the Magnetic Ginzburg-Landau Model*, volume 70 of *Progress in Nonlinear Differential Equations and Their Applications*. Birkhäuser, Boston, MA, 2007.
- [97] Ryosuke Sato. GICAR Algebras and Dynamics on Determinantal Point Processes: Discrete Orthogonal Polynomial Ensemble Case. *Communications in Mathematical Physics*, 405(5):115, May 2024.
- [98] Silvan S. Schweber. The sources of Schwinger's Green's functions. *Proceedings of the National Academy of Sciences*, 102(22):7783–7788, May 2005.
- [99] Julian Schwinger. On the Green's functions of quantized fields. I. *Proceedings of the National Academy of Sciences*, 37(7):452–455, July 1951.
- [100] Julian Schwinger. On the Green's functions of quantized fields. II. *Proceedings of the National Academy of Sciences*, 37(7):455–459, July 1951.
- [101] Isaiah Shavitt and Rodney J. Bartlett. *Many-Body Methods in Chemistry and Physics: MBPT and Coupled-Cluster Theory*. Cambridge Molecular Science. Cambridge University Press, Cambridge, 2009.
- [102] Jan Philip Solovej. Many Body Quantum Mechanics. Lecture notes. 2014.
- [103] Chong Sun, Ushnish Ray, Zhi-Hao Cui, Miles Stoudenmire, Michel Ferrero, and Garnet Kin-Lic Chan. Finite-temperature density matrix embedding theory. *Physical Review B*, 101(7):075131, February 2020.
- [104] E. C. Titchmarsh. *Introduction to the Theory of Fourier Integrals*. Clarendon Press, Oxford, 1948.
- [105] Chao-Cheng Wang. *Mathematical Principles of Mechanics and Electromagnetism*. Springer US, Boston, MA, 1979.
- [106] A. Williams, G. H. Kwei, R. B. Von Dreele, I. D. Raistrick, and D. L. Bish. Joint x-ray and neutron refinement of the structure of superconducting  $\text{YBa}_2\text{Cu}_3\text{O}_{7-x}$ : Precision structure, anisotropic thermal parameters, strain, and cation disorder. *Physical Review B*, 37(13):7960–7962, May 1988.
- [107] Fengcheng Wu, Timothy Lovorn, Emanuel Tutuc, and A. H. MacDonald. Hubbard Model Physics in Transition Metal Dichalcogenide Moiré Bands. *Physical Review Letters*, 121(2):026402, July 2018.
- [108] M. K. Wu, J. R. Ashburn, C. J. Torng, P. H. Hor, R. L. Meng, L. Gao, Z. J. Huang, Y. Q. Wang, and C. W. Chu. Superconductivity at 93 K in a new mixed-phase  $\text{Y}-\text{Ba}-\text{Cu}-\text{O}$  compound system at ambient pressure. *Physical Review Letters*, 58(9):908–910, March 1987.
- [109] Keith Yates. *Hückel molecular orbital theory*. Elsevier, 2012.
- [110] Yijun Yu, Liguo Ma, Peng Cai, Ruidan Zhong, Cun Ye, Jian Shen, G. D. Gu, Xian Hui Chen, and Yuanbo Zhang. High-temperature superconductivity in monolayer  $\text{Bi}_2\text{Sr}_2\text{Ca}\text{Cu}_2\text{O}_{8+\delta}$ . *Nature*, 575(7781):156–163, November 2019.
- [111] F. C. Zhang and T. M. Rice. Effective Hamiltonian for the superconducting Cu oxides. *Physical Review B*, 37(7):3759–3761, March 1988.



# Chapter 2

## Some mathematical insights on DMET

In this chapter, we provide a mathematical and numerical analysis of Density Matrix Embedding Theory (DMET) in the non-interacting limit. This part is joint work with Éric Cancès, Fabian Faulstich, Eloïse Letournel and Antoine Levitt, and as been submitted to Communications on Pure and Applied Mathematics (CPAM).

**Abstract** This article provides the first mathematical analysis of the Density Matrix Embedding Theory (DMET) method. We prove that, under certain assumptions, (i) the exact ground-state density matrix is a fixed-point of the DMET map for non-interacting systems, (ii) there exists a unique physical solution in the weakly-interacting regime, and (iii) DMET is exact at first order in the coupling parameter. We provide numerical simulations to support our results and comment on the physical meaning of the assumptions under which they hold true. We show that the violation of these assumptions may yield multiple solutions of the DMET equations. We moreover introduce and discuss a specific  $N$ -representability problem inherent to DMET.

### Contents

---

<b>2.1</b>	<b>Introduction</b>	44
<b>2.2</b>	<b>The DMET formalism</b>	45
2.2.1	The quantum many-body problem and its fragment decomposition	45
2.2.2	The impurity high-level problem	46
2.2.3	The global low-level problem	48
2.2.4	The DMET problem	48
<b>2.3</b>	<b>Main results</b>	48
<b>2.4</b>	<b>Numerical simulations</b>	51
2.4.1	$H_{10}$ ring	51
2.4.2	$H_6$ model	52
<b>2.5</b>	<b>Impurity problems and high-level map</b>	56
2.5.1	Impurity Hamiltonians	56
2.5.2	Domain of the high-level map	57
<b>2.6</b>	<b><math>N</math>-representability and low-level map</b>	57
<b>2.7</b>	<b>Proofs</b>	58
2.7.1	Proof of Lemma 2.6	58
2.7.2	Proof of Proposition 2.7	59
2.7.3	Proof of Lemma 2.8	62
2.7.4	Proof of Lemma 2.10	63
2.7.5	Proof of Proposition 2.1	63
2.7.6	Proof of Theorem 2.4	67
2.7.7	Proof of Theorem 2.5	74
<b>2.A</b>	<b>Notation table</b>	79
<b>2.B</b>	<b>Analysis of the DMET bifurcation for <math>H_6^{4-}</math></b>	80
	<b>Bibliography</b>	82

---

## 2.1 Introduction

Electronic structure theory is a powerful quantum mechanical framework for investigating the intricate behavior of electrons within molecules and crystals. At the core lies the interaction between particles, specifically the electron-electron and electron-nuclei interactions. Embracing the essential quantum physical effects, this theory is the foundation for *ab initio* quantum chemistry and materials science calculations performed by many researchers in chemistry and related fields, complementing and supplementing painstaking laboratory work. With its diverse applications in chemistry and materials science, electronic structure theory holds vast implications for the mathematical sciences. Integrating mathematical doctrines into this field leads to the development of precise and scalable numerical methods, enabling extensive *in silico* studies of chemistry for e.g. sustainable energy, green catalysis, and nanomaterials. The synergy between mathematics and electronic structure theory offers the potential for groundbreaking advancements in addressing these global challenges.

Within the realm of electronic structure theory, the treatment of *strongly correlated quantum systems* is a particularly challenging and long-standing challenge. Here, the application of high-accuracy quantum chemical methods that are able to capture the electronic correlation effects at chemical accuracy is inevitable. Unfortunately, the application of such high-accuracy methods is commonly stymied by a steep computational scaling with respect to the system's size. A potential remedy is provided by quantum embedding theories, i.e., a paradigm for bootstrapping the success of highly accurate solvers at small scales up to significantly larger scales by decomposing the original system into smaller fragments, where each fragment is then solved individually and from which, a solution to the whole system is then obtained [17, 20, 44]. Such approaches include dynamical mean-field theory [32, 15, 16, 26, 30], or variational embedding theory [27, 7, 22].

Subject of this article is a widely-used quantum embedding theory, namely, density matrix embedding theory (DMET) [23, 24, 51, 3, 56, 10, 48, 9]. The general idea of DMET is to partition the global quantum system into several quantum “impurities”, each impurity being treated accurately via a high-level theory (such as full configuration interaction (FCI) [25, 39, 52], coupled cluster theory [8], density matrix renormalization group (DMRG) [55], etc.). More precisely, the DMET methodology follows the procedure sketched out as: 1) fragment the system, 2) for each fragment, construct an interacting bath that describes the coupling between the fragment and the remaining system, thus giving rise to a so-called impurity problem, 3) solve an interacting problem for each impurity using a highly accurate method, 4) extract properties of the system, 5) perform step 2)–4) self-consistently in order to embed updated correlation effects back into the full system. Over the past years, a large variety of this general framework has been developed, including how the bath space is defined (including the choice of low-level theory) [13, 35, 36, 59], how the interacting cluster Hamiltonian is constructed and solved [38, 41, 29, 14, 43], and the choice of self-consistent requirements [57, 58, 12]. This variety of DMET flavors has been successfully applied to a wide range of systems such as Hubbard models [23, 3, 6, 65, 67, 66, 54, 46, 45], quantum spin models [11, 18, 42], and a number of strongly correlated molecular and periodic systems [24, 56, 9, 37, 2, 40, 19, 49, 64, 60, 63, 61, 62, 50, 31, 33, 34, 1]. Recently, the application of DMET variants on quantum computers has been explored [28, 53, 5].

In this article, we follow the computational procedure where the global information, at the level of the one-electron reduced density matrix (1-RDM), is made consistent between all the impurities with the help of a low-level Hartree-Fock (HF) type of theory. In the self-consistent-field DMET (SCF-DMET)<sup>1</sup>, this global information is then used to update the impurity problems in the next self-consistent iteration, until a consistency condition of the 1-RDM is satisfied between the high-level and low-level theories.

This article is organized as follows. In Section 2.2.1, we introduce the many-body quantum model under investigation and its fragment decomposition, and set up some notation used in the sequel. In Section 2.2.2, we present a mathematical formulation of the DMET impurity problem and introduce (formally) the high-level DMET map. The low-level DMET map and the DMET fixed point problem are defined (still formally) in Sections 2.2.3 and 2.2.4 respectively. In Section 2.3, we state our main results:

1. in Proposition 2.1, we show that for non-interacting systems, the exact ground-state density matrix is a fixed-point of the DMET map if (i) the system is gapped (Assumption (A1)), and (ii) the fragment decomposition satisfies a natural and rather mild condition (Assumption (A2)). Although this result is well-known in the physics and chemistry community, a complete mathematical proof was still missing;

---

<sup>1</sup>Throughout the paper, DMET refers to SCF-DMET. This is in contrast to one-shot DMET, in which the impurity problem is only solved once without self-consistent updates.

2. in Theorem 2.4, we prove that under two additional assumptions ((A3) and (A4)), the DMET fixed-point problem has a unique physical solution in the weakly-interacting regime, which is real-analytic in the coupling parameter  $\alpha$ . Assumption (A3) is related to some specific  $N$ -representability condition inherent to the DMET approach, while Assumption (A4) has a physical interpretation in terms of linear response theory;

3. in Theorem 2.5, we prove that in the weakly-interacting regime, DMET is exact at first order in  $\alpha$ .

The numerical simulations reported in Section 2.4 illustrate the above results and indicate that DMET does not seem to be exact at second order. Although, in the special case when there is only one site per fragment, Assumption (A4) is a consequence of Assumptions (A1)-(A3) (see Remark 2.3), the numerical simulations presented show that this is in general not the case. Further investigations using the  $H_6$ -model (vide infra) reveal the existence of a specific configuration  $(\Theta_3)$  for which only Assumption (A4) is not satisfied. In the vicinity of this configuration, DMET has at least two distinct solutions that arise from a transcritical bifurcation at  $\Theta_3$ . In Section 2.5, we formulate the impurity problem in more detail and discuss the domain of the high-level DMET map. In Section 2.6, we study the  $N$ -representability problem mentioned above and provide a simple criterion of local  $N$ -representability directly connected to Assumption (A3). In order to improve the readability of the paper, we postponed the technical proofs to Section 2.7. For the reader's convenience, the main notations used throughout this article are collected in Table 2.A.1 in Appendix 2.A.

## 2.2 The DMET formalism

### 2.2.1 The quantum many-body problem and its fragment decomposition

We consider a physical system with  $L$  quantum sites, with one orbital per site, occupied by  $1 \leq N < L$  electrons, and assume that magnetic effects (interaction with an external magnetic field, spin-orbit coupling, etc.) can be neglected. This allows us to work with real-valued wave-functions and density matrices. We set

$$\begin{aligned} \mathcal{H} &:= \mathbb{R}^L \quad (\text{one-particle state space}), \quad \mathcal{B}_{\text{at}} := \{e_\kappa\}_{\kappa \in \llbracket 1, L \rrbracket} \quad (\text{canonical basis of } \mathbb{R}^L), \\ \mathcal{H}_n &:= \bigwedge^n \mathcal{H} \quad (n\text{-particle state space}), \quad \text{Fock}(\mathcal{H}) := \bigoplus_{n=0}^L \mathcal{H}_n \quad (\text{real fermionic Fock space}). \end{aligned} \quad (2.1)$$

We denote by  $\hat{a}_\kappa$  and  $\hat{a}_\kappa^\dagger$  the generators of the (real) CAR algebra associated with the canonical basis of  $\mathcal{H}$ , i.e.

$$\hat{a}_\kappa := \hat{a}(e_\kappa) \quad \text{and} \quad \hat{a}_\kappa^\dagger = \hat{a}^\dagger(e_\kappa).$$

Recall that the maps

$$\mathbb{R}^L \ni f \mapsto \hat{a}^\dagger(f) \in \mathcal{L}(\text{Fock}(\mathcal{H})) \quad \text{and} \quad \mathbb{R}^L \ni f \mapsto \hat{a}(f) \in \mathcal{L}(\text{Fock}(\mathcal{H})),$$

are both linear in this setting since we work in a real Hilbert space framework. Here and below,  $\mathcal{L}(E)$  is the space of linear operators from the finite-dimensional vector space  $E$  to itself. We also define the number operator  $\hat{N}$  by

$$\hat{N} := \sum_{n=0}^L n \hat{\mathbf{1}}_{\mathcal{H}_n} = \sum_{\kappa=1}^L \hat{a}_\kappa^\dagger \hat{a}_\kappa \quad (\text{particle number operator}).$$

For each linear subspace  $E$  of  $\mathcal{H}$ , we denote the orthogonal projector on  $E$  by  $\Pi_E \in \mathcal{L}(\mathcal{H})$ . We assume that the Hamiltonian of the system in the second-quantized formulation reads

$$\hat{H} := \sum_{\kappa, \lambda=1}^L h_{\kappa\lambda} \hat{a}_\kappa^\dagger \hat{a}_\lambda + \frac{1}{2} \sum_{\kappa, \lambda, \nu, \xi=1}^L V_{\kappa\lambda\nu\xi} \hat{a}_\kappa^\dagger \hat{a}_\lambda^\dagger \hat{a}_\xi \hat{a}_\nu, \quad (2.2)$$

where the matrix  $h \in \mathbb{R}^{L \times L}$  and the 4th-order tensor  $V \in \mathbb{R}^{L \times L \times L \times L}$  satisfy the following symmetry properties:

$$h_{\kappa\lambda} = h_{\lambda\kappa} \quad \text{and} \quad V_{\kappa\lambda\nu\xi} = V_{\nu\lambda\kappa\xi} = V_{\kappa\xi\nu\lambda} = V_{\nu\xi\kappa\lambda}.$$

We denote by  $\mathcal{D}$  the Grassmannian of rank- $N$  orthogonal projectors in  $\mathbb{R}^L$ :

$$\mathcal{D} := \text{Gr}_{\mathbb{R}}(N, L) = \{D \in \mathbb{R}_{\text{sym}}^{L \times L} \mid D^2 = D, \text{Tr}(D) = N\}, \quad (2.3)$$

and by  $\text{CH}(\mathcal{D})$  the convex hull of  $\mathcal{D}$ , i.e.

$$\text{CH}(\mathcal{D}) = \{D \in \mathbb{R}_{\text{sym}}^{L \times L} \mid 0 \leq D \leq 1, \text{Tr}(D) = N\}. \quad (2.4)$$

Physically, the set  $\text{CH}(\mathcal{D})$  corresponds to the set of (real-valued, mixed-state)  $N$ -representable one-body density matrices with  $N$  electrons, and  $\mathcal{D}$  is the set of one-body density matrices generated by (real-valued) Slater determinants in  $\mathcal{H}_N$ .

We consider a fixed partition of the  $L$  sites into  $N_f$  non-overlapping fragments  $\{\mathcal{I}_x\}_{x \in [1, N_f]}$  of sizes  $\{L_x\}_{x \in [1, N_f]}$  such that  $L_x < N$  for all  $x$ . Up to reordering the sites, we can assume that the partition is the following:

$$[1, L] = \left\{ \underbrace{(1, \dots, L_1)}_{\mathcal{I}_1}, \underbrace{(1 + L_1, \dots, L_1 + L_2)}_{\mathcal{I}_2}, \dots, \underbrace{(1 + L_1 + \dots + L_{N_f-1}, \dots, L)}_{\mathcal{I}_{N_f}} \right\}. \quad (2.5)$$

This partition corresponds to a decomposition of the space into  $N_f$  fragment subspaces fulfilling

$$\mathcal{H} = X_1 \oplus \dots \oplus X_{N_f} \quad \text{with} \quad X_x := \text{Span}(e_\kappa, \kappa \in \mathcal{I}_x). \quad (2.6)$$

For  $M \in \mathbb{R}_{\text{sym}}^{L \times L}$ , we set

$$\text{Bd}(M) := \sum_{x=1}^{N_f} \Pi_x M \Pi_x, \quad (2.7)$$

where  $\Pi_x := \Pi_{X_x}$  is the orthogonal projector on  $X_x$ . The operator  $\text{Bd} \in \mathcal{L}(\mathbb{R}_{\text{sym}}^{L \times L})$  is the orthogonal projector onto the set of block-diagonal matrices for the partition (2.5) (endowed with the Frobenius inner product).

As we will see, a central intermediary in DMET is the diagonal blocks of the density matrix,  $P = \text{Bd}(D) \in \text{Bd}(\mathcal{D})$ . It is clear that these blocks must satisfy  $0 \leq P_x \leq 1$  and  $\sum_{x=1}^{N_f} \text{Tr}(P_x) = N$ . Conversely, it is easy to see that grouping these blocks together into a block-diagonal matrix produces a matrix in  $\text{CH}(\mathcal{D})$ ; therefore, we have

$$\begin{aligned} \mathcal{P} := \text{Bd}(\text{CH}(\mathcal{D})) = \left\{ P = \begin{pmatrix} P_1 & 0 & \dots & 0 \\ 0 & P_2 & \dots & 0 \\ \vdots & & \ddots & \vdots \\ 0 & 0 & \dots & P_{N_f} \end{pmatrix} \right. \\ \left. \text{s.t. } \forall 1 \leq x \leq N_f, P_x \in \mathbb{R}_{\text{sym}}^{L_x \times L_x}, 0 \leq P_x \leq 1, \sum_{x=1}^{N_f} \text{Tr}(P_x) = N \right\}. \end{aligned} \quad (2.8)$$

From a geometrical viewpoint,  $\mathcal{P}$  is a non-empty, compact, convex subset of an affine vector subspace of  $\mathbb{R}_{\text{sym}}^{L \times L}$  with base vector space

$$\mathcal{Y} := \left\{ Y = \begin{pmatrix} Y_1 & 0 & \dots & 0 \\ 0 & Y_2 & \dots & 0 \\ \vdots & & \ddots & \vdots \\ 0 & 0 & \dots & Y_{N_f} \end{pmatrix} \text{s.t. } \forall 1 \leq x \leq N_f, Y_x \in \mathbb{R}_{\text{sym}}^{L_x \times L_x}, \sum_{x=1}^{N_f} \text{Tr}(Y_x) = 0 \right\}. \quad (2.9)$$

The structure of the set  $\text{Bd}(\mathcal{D}) \subset \mathcal{P}$  is a more subtle issue that we will investigate in Section 2.6.

### 2.2.2 The impurity high-level problem

Given one of the spaces  $X_x$  and a one-body density matrix  $D \in \mathcal{D}$ , we set:

$$W_{x,D} := X_x + DX_x = DX_x \oplus (1 - D)X_x \quad (\text{$x$-th impurity subspace}). \quad (2.10)$$

We will assume in the following that

$$\dim(DX_x) = \dim((1 - D)X_x) = \dim(X_x) = L_x \quad (\text{maximal-rank assumption}), \quad (2.11)$$

so that  $\dim(W_{x,D}) = 2L_x$ . Decomposing  $\text{Ran}(D)$  and  $\text{Ker}(D)$  as

$$\text{Ran}(D) = DX_x \oplus \mathcal{H}_{x,D}^{\text{core}} \quad \text{and} \quad \text{Ker}(D) = (1 - D)X_x \oplus \mathcal{H}_{x,D}^{\text{virt}},$$

we obtain the following decomposition of  $\mathcal{H} = \mathbb{R}^L$ :

$$\mathcal{H} = W_{x,D} \oplus \underbrace{\mathcal{H}_{x,D}^{\text{core}} \oplus \mathcal{H}_{x,D}^{\text{virt}}}_{=: \mathcal{H}_{x,D}^{\text{env}}}.$$

Note that the space  $\mathcal{H}_{x,D}^{\text{core}}$  has dimension  $(N - L_x)$ . The matrix  $D$  can be seen as the one-body density matrix associated with the Slater determinant

$$\Psi_{N,D}^0 = \Psi_{x,D}^{0,\text{imp}} \wedge \Psi_{x,D}^{0,\text{core}} \quad \text{with} \quad \Psi_{x,D}^{0,\text{imp}} \in \bigwedge^{L_x} DX_x \quad \text{and} \quad \Psi_{x,D}^{0,\text{core}} \in \bigwedge^{(N-L_x)} \mathcal{H}_{x,D}^{\text{core}},$$

where  $\Psi_{x,D}^{0,\text{imp}}$  and  $\Psi_{x,D}^{0,\text{core}}$  are normalized. More precisely,  $\Psi_{N,D}^0$  is the Slater determinant built from an orthonormal basis of  $L_x$  orbitals in  $DX_x$  and an orthonormal basis of  $(N - L_x)$  orbitals in  $\mathcal{H}_{x,D}^{\text{core}}$ . The so-defined wave-function  $\Psi_{N,D}^0$  is unique up to an irrelevant sign.

We denote by  $\hat{N}_{X_x} \in \mathcal{L}(\text{Fock}(\mathcal{H}))$  the projection of the number operator onto the fragment Fock space  $\text{Fock}(X_x)$ . Solving the impurity problem aims at minimizing, for a given  $\mu \in \mathbb{R}$  which will be specified later, the thermodynamic potential

$$\langle \Psi | (\hat{H} - \mu \hat{N}_{X_x}) | \Psi \rangle \quad (2.12)$$

over the set of normalized trial states in  $\text{Fock}(\mathcal{H})$  of the form

$$\Psi = \Psi_{x,D}^{\text{imp}} \wedge \Psi_{x,D}^{0,\text{core}} \quad (2.13)$$

with  $\Psi_{x,D}^{0,\text{core}}$  fixed, and  $\Psi_{x,D}^{\text{imp}}$  in

$$\text{Fock}(W_{x,D}) := \bigoplus_{n=0}^{L_x} \bigwedge^n W_{x,D} \quad (\text{x-th impurity Fock space}).$$

The impurity Hamiltonian is the unique operator  $\hat{H}_{x,D}^{\text{imp}}$  on  $\text{Fock}(W_{x,D})$  such that

$$\forall \Psi_{x,D}^{\text{imp}} \in \text{Fock}(W_{x,D}), \quad \langle \Psi_{x,D}^{\text{imp}} | \hat{H}_{x,D}^{\text{imp}} | \Psi_{x,D}^{\text{imp}} \rangle = \langle \Psi_{x,D}^{\text{imp}} \wedge \Psi_{x,D}^{0,\text{core}} | \hat{H} | \Psi_{x,D}^{\text{imp}} \wedge \Psi_{x,D}^{0,\text{core}} \rangle. \quad (2.14)$$

For an explicit expression of  $\hat{H}_{x,D}^{\text{imp}}$ , see Proposition 2.7.

The impurity problem defined by (2.12)-(2.13) can then be reformulated as

$$\min_{\Psi_{x,D}^{\text{imp}} \in \text{Fock}(W_{x,D}), \|\Psi_{x,D}^{\text{imp}}\|=1} \langle \Psi_{x,D}^{\text{imp}} | \hat{H}_{x,D}^{\text{imp}} - \mu \hat{N}_{X_x} | \Psi_{x,D}^{\text{imp}} \rangle \quad (\text{impurity problem}). \quad (2.15)$$

In practice, this full-CI problem in the Fock space  $\text{Fock}(W_{x,D})$  is solved by an approximate correlated wave-function method such as CASSCF, CCSD or DMRG for example, but we assume in this analysis that it can be solved exactly.

If (2.15) has a non-degenerate ground state for all  $x$ , we denote the one-body ground-state density matrices by  $P_{\mu,x}(D)$ , seen as matrices in  $\mathbb{R}_{\text{sym}}^{L \times L}$ , and finally set

$$F_{\mu,x}^{\text{HL}}(D) := \Pi_{X_x} P_{\mu,x}(D) \Pi_{X_x}. \quad (2.16)$$

Let us remark incidentally that if the ground state of the impurity problem is degenerate, we can either consider  $F_{\mu,x}^{\text{HL}}(D)$  as a multivalued function or define them from finite-temperature versions of (2.15), which are strictly convex compact problems on the set of density operators on the Fock space, and therefore always have a unique minimizer. We will not proceed further in this direction and only consider here the case of impurity problems with non-degenerate ground states.

The combination of the  $N_f$  impurity problems introduced in (2.15) (see also (2.16)) gives rise to a high-level DMET map  $F^{\text{HL}}$

$$\mathcal{D} \ni D \mapsto F^{\text{HL}}(D) \in \mathcal{P} \quad (2.17)$$

formally defined by

$$F^{\text{HL}}(D) := \sum_{x=1}^{N_f} F_{\mu,x}^{\text{HL}}(D) \quad (\text{high-level map}) \quad (2.18)$$

with  $\mu \in \mathbb{R}$  chosen such that  $\text{Tr}(F^{\text{HL}}(D)) = N$ . The domain of  $F^{\text{HL}}$  and the regularity properties of this map will be studied in Section 2.5.

### 2.2.3 The global low-level problem

The low-level map is defined by

$$F^{\text{LL}}(P) := \underset{D \in \mathcal{D}, \text{Bd}(D)=P}{\operatorname{argmin}} \mathcal{E}^{\text{HF}}(D) \quad (\text{low-level map}), \quad (2.19)$$

where  $\mathcal{E}^{\text{HF}}$  is the Hartree-Fock (mean-field) energy functional of the trial density-matrix  $D$ . The latter reads

$$\mathcal{E}^{\text{HF}}(D) := \text{Tr}(hD) + \frac{1}{2}\text{Tr}(J(D)D) - \frac{1}{2}\text{Tr}(K(D)D), \quad (2.20)$$

where

$$[J(D)]_{\kappa\lambda} := \sum_{\nu,\xi=1}^L V_{\lambda\xi\kappa\nu} D_{\nu\xi} \quad \text{and} \quad [K(D)]_{\kappa\lambda} := \sum_{\nu,\xi=1}^L V_{\kappa\xi\nu\lambda} D_{\nu\xi}. \quad (2.21)$$

The existence and uniqueness of a minimizer to (2.19) will be discussed in Section 2.6.

### 2.2.4 The DMET problem

Finally, the full DMET map is formally defined as the self-consistent solution to the system

$$\begin{aligned} D &= F^{\text{LL}}(P) \in \mathcal{D}, \\ P &= F^{\text{HL}}(D) \in \mathcal{P}. \end{aligned}$$

In particular,  $D = F^{\text{LL}}(P)$  implies that  $P = \text{Bd}(D)$ . Equivalently, we can formulate the problem as

$$P = F^{\text{DMET}}(P) := F^{\text{HL}}(F^{\text{LL}}(P)).$$

Assuming that the solution to this fixed-point problem exists and is unique,  $P$  is expected to provide a good approximation of the diagonal blocks (in the decomposition (2.6) of  $\mathcal{H}$ ) of the ground-state one-body density matrix of the interacting system. The mathematical properties of this self-consistent loop will be studied in the next section, first for the non-interacting case, and second, for the interacting case in a perturbative regime.

## 2.3 Main results

We now embed the Hamiltonian  $H$  into the family of Hamiltonians

$$\hat{H}_\alpha := \sum_{\kappa,\lambda=1}^L h_{\kappa\lambda} \hat{a}_\kappa^\dagger \hat{a}_\lambda + \frac{\alpha}{2} \sum_{\kappa,\lambda,\nu,\xi=1}^L V_{\kappa\lambda\nu\xi} \hat{a}_\kappa^\dagger \hat{a}_\lambda^\dagger \hat{a}_\xi \hat{a}_\nu, \quad \alpha \in \mathbb{R}, \quad (2.22)$$

acting on  $\text{Fock}(\mathcal{H})$ . For  $\alpha = 0$ , we obtain the one-body Hamiltonian

$$\hat{H}_0 := \sum_{\kappa,\lambda=1}^L h_{\kappa\lambda} \hat{a}_\kappa^\dagger \hat{a}_\lambda \quad (2.23)$$

describing non-interacting particles, and we recover the original Hamiltonian  $\hat{H}$  for  $\alpha = 1$ . We denote by  $F_\alpha^{\text{HL}}$ ,  $F_\alpha^{\text{LL}}$ , and  $F_\alpha^{\text{DMET}}$  the high-level, low-level, and DMET maps constructed from  $\hat{H}_\alpha$ .

We first assume that the non-interacting problem is non-degenerate. Denoting by  $\varepsilon_n$  the  $n$ -th lowest eigenvalue of  $h$  (counting multiplicities), this condition reads

$$(\mathbf{A1}) \quad \varepsilon_N < 0 < \varepsilon_{N+1},$$

where without loss of generality we have chosen the Fermi level to be 0. Assumption (A1) indeed implies that the ground-state of  $\hat{H}_0$  in the  $N$ -particle sector of the Fock space is non-degenerate, and that the ground-state one-body density is the rank- $N$  orthogonal projector given by

$$D_0 = \mathbf{1}_{(-\infty, 0]}(h). \quad (2.24)$$

By perturbation theory, the ground state of  $\hat{H}_\alpha$  in the  $N$ -particle sector is non-degenerate for all  $\alpha \in (-\alpha_+, \alpha_+)$  for some  $0 < \alpha_+ \leq +\infty$ . We denote by  $D_\alpha^{\text{exact}}$  the corresponding ground-state one-body density matrix. As a consequence of analytic perturbation theory for hermitian matrices, the map  $(-\alpha_+, \alpha_+) \ni \alpha \mapsto D_\alpha^{\text{exact}} \in \mathbb{R}_{\text{sym}}^{L \times L}$  is real-analytic.

Second, we make the maximal-rank assumption:

$$(\mathbf{A2}) \quad \text{For all } 1 \leq x \leq N_f, \dim(D_0 X_x) = \dim((1 - D_0) X_x) = \dim(X_x) = L_x.$$

Assumption (A2) implies that the impurity problem (2.15) for  $\hat{H} = \hat{H}_0$  and  $D = D_0$  is well-defined for each  $x$  and each  $\mu$ . We emphasize however that this does not prejudge that the so-obtained  $N_f$  impurity problems are well-posed (i.e. have a unique ground-state) for a given value of  $\mu$ , nor *a fortiori* that  $D_0$  is in the domain of the high-level map  $F_0^{\text{HL}}$ . We will elaborate more on the meaning of Assumptions (A2) in Section 2.5.

DMET is then consistent in the non-interacting case:

**Proposition 2.1** ( $P_0 := \text{Bd}(D_0)$  is a fixed point of the DMET map for  $\alpha = 0$ ). *Under Assumptions (A1)-(A2),  $P_0 := \text{Bd}(D_0)$  is a fixed point of the non-interacting DMET iterative scheme, i.e.  $P_0$  is in the domain of  $F_0^{\text{LL}}$ ,  $D_0$  is in the domain of  $F_0^{\text{HL}}$ , and  $F_0^{\text{DMET}}(P_0) = P_0$ .*

**Remark 2.2.** *We formally define the high-level Hartree-Fock map*

$$F_{\text{MF}}^{\text{HL}} : \mathcal{D} \rightarrow \mathcal{P},$$

*as the high-level map constructed from the Hartree-Fock  $N$ -body Hamiltonian*

$$\hat{H}_D^{\text{HF}} := \sum_{\kappa, \lambda=1}^L [h^{\text{HF}}(D)]_{\kappa \lambda} \hat{a}_\kappa^\dagger \hat{a}_\lambda,$$

*where*

$$h^{\text{HF}}(D) = h + J(D) - K(D) \quad (2.25)$$

*is the one-particle mean-field (Fock) Hamiltonian. Using exactly the same arguments as in the proof of Proposition 2.1, we obtain that the low-level map  $F^{\text{LL}}$  satisfies the mean-field consistency property*

$$F^{\text{LL}}(F_{\text{HF}}^{\text{HL}}(D_*)) = D_*,$$

*for any Hartree-Fock ground state  $D_*$ . We will make use of this important observation in the proof of Theorem 2.4.*

We now study the DMET equations in the perturbative regime of  $\alpha$  small. In order to use perturbative techniques, we need to determine the space in which we seek  $P$ . Generically, at  $\alpha \neq 0$ , we expect  $P$  to be equal to the block diagonal of the one-body density matrix, which is not a projector. Therefore it is natural to seek  $P$  in  $\mathcal{P} = \text{Bd}(\text{CH}(\mathcal{D}))$ . However, in the DMET method,  $D$  is constrained to be a projector, and therefore  $P$  will necessarily belong to  $\text{Bd}(\mathcal{D})$ . We will study in Section 2.6 the relationship between the two sets  $\mathcal{P}$  and  $\text{Bd}(\mathcal{D})$  (the  $N$ -representability problem), and in particular show that, in the regime of interest to DMET (many relatively small fragments, so that  $L \gg \max_x L_x$ ), the two sets are (generically) locally the same. Therefore, it is natural to assume the local  $N$ -representability condition:

**(A3)** The linear map  $\text{Bd}$  is surjective from  $\mathcal{T}_{D_0}\mathcal{D}$  to  $\mathcal{Y}$ ,

where  $\mathcal{Y}$  is the vector subspace defined in (2.9). Indeed,  $\mathcal{P}$  is a (non-empty, compact, convex) subset of the affine space  $P_0 + \mathcal{Y}$  and Assumption (A2) implies that  $P_0 \in \overset{\circ}{\mathcal{P}}$ , where  $\overset{\circ}{\mathcal{P}}$  is the interior of  $\mathcal{P}$  in  $P_0 + \mathcal{Y}$ . Thus  $\mathcal{Y}$  can be identified with the tangent space at  $P_0$  to the manifold  $\overset{\circ}{\mathcal{P}}$ . By the local submersion theorem, this implies that any  $P$  in the neighborhood of  $P_0$  can be expressed as the block diagonal of a density matrix in the neighborhood of  $D_0$  in  $\mathcal{D}$ .

Our last assumption is concerned with the response properties of the impurity problems at the non-interacting level. Consider a self-adjoint perturbation  $Y \in \mathbb{R}_{\text{sym}}^{L \times L}$  of the one-particle Hamiltonian  $h$ , non-local but block-diagonal in the fragment decomposition, i.e. such that  $Y \in \mathbb{R}I_L + \mathcal{Y}$ , and denote by  $\widetilde{F}^{\text{HL}}_{h+Y}(D)$  the non-interacting high-level map obtained by replacing  $h$  with  $h + Y$  (so that  $\widetilde{F}^{\text{HL}}_h(D) = F_0^{\text{HL}}$ ). Formally, we have

$$\widetilde{F}^{\text{HL}}_{h+Y}(D_0) = P_0 + RY + o(\|Y\|), \quad (2.26)$$

with  $R : \mathbb{R}I_L + \mathcal{Y} \rightarrow \mathcal{Y}$  linear (the fact that  $RY \in \mathcal{Y}$  is due to particle-number conservation). The map  $R$  can be interpreted as a non-interacting static 4-point density-density linear response function for frozen impurity spaces. It follows from Assumption (A1) that constant perturbations do not modify the density matrix:  $R(I_L) = 0$ . Our fourth assumption reads:

**(A4)** the 4-point linear response function  $R : \mathcal{Y} \rightarrow \mathcal{Y}$  is invertible.

This condition is somewhat reminiscent of the Hohenberg-Kohn theorem from Density Functional Theory. Together with the local inversion theorem, it implies that, locally around  $h$ , in the non-interacting case and for frozen impurity spaces  $W_{x,D_0}$ , the high-level map defines a one-to-one correspondence between non-local fragment potentials (up to a constant shift) and fragment density matrices.

**Remark 2.3.** We will show in Section 2.7.6 that in the case when  $N_f = L$  (one site per fragment), it holds: under Assumptions (A1)-(A2),

$(A3)$  is satisfied  $\implies D_0$  is an irreducible matrix  $\iff (A4)$  is satisfied.

On the other hand, numerical simulations indicate that in the general case, Assumption (A4) is not a consequence of Assumptions (A1)-(A3).

We are now in position to state our main results.

**Theorem 2.4** (DMET is well-posed in the perturbative regime). Under assumptions (A1)-(A4), there exist  $0 < \tilde{\alpha}_+ \leq \alpha_+$ , and a neighborhood  $\Omega$  of  $D_0$  in  $\mathcal{D}$  such that for all  $\alpha \in (-\tilde{\alpha}_+, \tilde{\alpha}_+)$ , the fixed-point DMET problem

$$P_\alpha^{\text{DMET}} = F_\alpha^{\text{HL}}(D_\alpha^{\text{DMET}}), \quad D_\alpha^{\text{DMET}} = F_\alpha^{\text{LL}}(P_\alpha^{\text{DMET}})$$

has a unique solution  $(D_\alpha^{\text{DMET}}, P_\alpha^{\text{DMET}})$  with  $D_\alpha^{\text{DMET}} \in \Omega$  (otherwise stated, the DMET map for  $H_\alpha$  has a unique fixed point  $P_\alpha^{\text{DMET}}$  in the neighborhood of  $P_0$ ). In addition, the maps  $(-\tilde{\alpha}_+, \tilde{\alpha}_+) \ni \alpha \mapsto D_\alpha^{\text{DMET}} \in \mathbb{R}_{\text{sym}}^{L \times L}$  and  $(-\tilde{\alpha}_+, \tilde{\alpha}_+) \ni \alpha \mapsto P_\alpha^{\text{DMET}} \in \mathbb{R}_{\text{sym}}^{L \times L}$  are real-analytic and such that

$$D_0^{\text{DMET}} = D_0 = \mathbf{1}_{(-\infty, 0]}(h), \quad P_0^{\text{DMET}} = P_0 = \text{Bd}(D_0).$$

As is standard, the first-order perturbation of the exact density matrix is given by the Hartree-Fock method. DMET is able to reproduce this, and is therefore exact at first order:

**Theorem 2.5** (DMET is exact to first order). Under Assumptions (A1)-(A4) and with the notation of Theorem 2.4, it holds

$$D_\alpha^{\text{DMET}} = D_\alpha^{\text{exact}} + O(\alpha^2) = D_\alpha^{\text{HF}} + O(\alpha^2),$$

where  $D_\alpha^{\text{HF}}$  is the Hartree-Fock ground-state density matrix for  $\hat{H}_\alpha$ , which is unique for  $\alpha$  small enough.

The numerical simulations reported in the next section show that such exactness property is not expected to hold at second order.

In the weakly interacting regime, the solution  $D_\alpha^{\text{DMET}}$  to the DMET fixed-point problem is the only physical one because it is the only one laying in the vicinity of  $D_0$ , where the exact ground-state density matrix is known to be by analytic perturbation theory.

## 2.4 Numerical simulations

In this section, we perform numerical investigations of DMET for two distinct test systems: The first system is  $H_{10}$  in a circular geometry which serves as a benchmark where DMET has been previously recognized for its exceptional performance [24]. By studying this system, we aim to reaffirm the efficacy of DMET and numerically showcase that DMET is exact to first order in the non-interacting limit. However, to gain a comprehensive understanding of DMET’s limitations, we also explore a second system which is an  $H_6$  variant. This particular system allows us to numerically scrutinize the assumptions made in the analysis presented above. Through these numerical investigations, we aim to provide valuable insights into the mathematical structure of DMET, paving the way for further advancements and improvements in this promising computational approach. Throughout this section, we denote by  $\|\cdot\|_F$  the Frobenius norm on matrix spaces.

### 2.4.1 $H_{10}$ ring

We consider a circular arrangement of ten hydrogen atoms, with a nearest-neighbor distance of  $1.5 a_0$  between each pair of atoms (where  $a_0 \simeq 0.529 \text{ \AA}$  is the Bohr radius). The system is treated using the STO-6G basis set and is half-filled, i.e., containing ten electrons. We partition the system into five fragments, each consisting of two atoms, as shown in Figure 2.1.

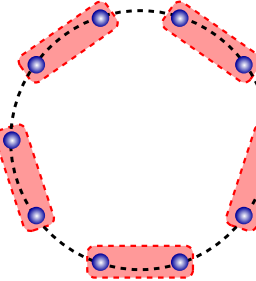


Figure 2.1: Depiction of the  $H_{10}$  system in circular geometry. The red-shaded areas show the chosen fragmentation.

In order to numerically confirm that DMET is exact to first order for this “well-behaved” system, we determine  $P_\alpha$  for  $\alpha \in [0, 1]$  and compute  $\|dP_\alpha/d\alpha\|_F$ . Figure 2.2 compares the DMET result with the exact diagonalization result (abbreviated FCI). We clearly see that DMET is indeed exact to first order for the considered system.

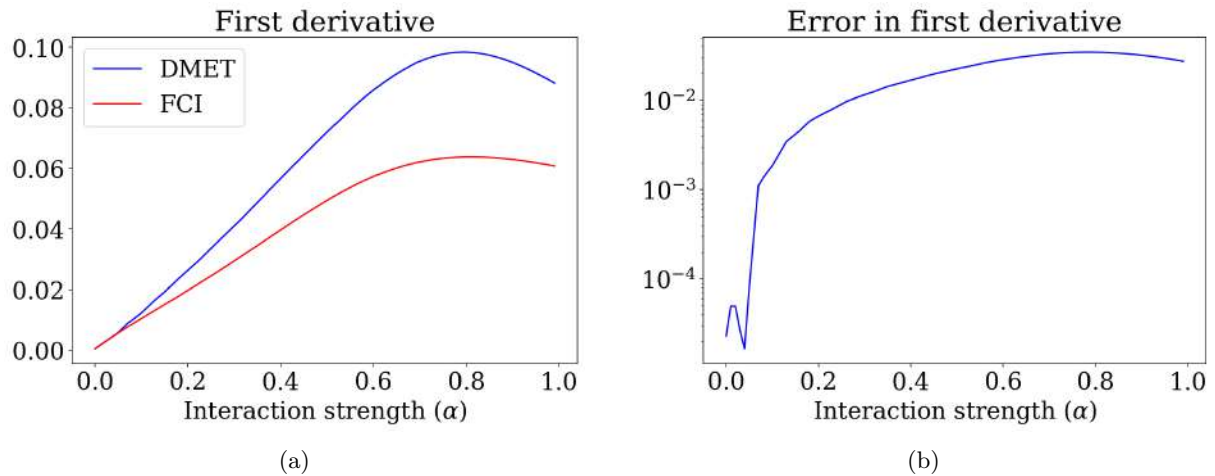


Figure 2.2: (a) Shows  $\|dP_\alpha/d\alpha\|_F$  for DMET and FCI, respectively (b) Shows the error on  $dP_\alpha/d\alpha$  between DMET and FCI, measured in Frobenius norm.

## 2.4.2 $H_6$ model

In this section, we will numerically investigate the assumptions required for the analysis presented in this article. To that end, we consider a non-interacting  $H_6^{4-}$  system, undergoing the following transition on a circular geometry: We begin by placing three hydrogen molecules in equilibrium geometry, i.e., bond length of  $1.4 a_0$ , equidistantly on a circle of radius  $3 a_0$ . We then dissociate each hydrogen molecule while maintaining a circular geometry. Specifically, we break each hydrogen molecule in such a way that the hydrogen atoms from neighboring molecules can form new molecules. We stop this transition at  $\Theta = \Theta_{\max}$ , when the hydrogen atoms from neighboring molecules form new hydrogen molecules in equilibrium geometry. We steer this transition with the angle  $\Theta$  that measures the displacement of the individual hydrogen atoms relative to their initial positions. The dissociation is done in a manner that maintains the circular arrangement of the hydrogen atoms throughout the process, see Figure 2.3 for a schematic depiction of this process and a depiction of  $\Theta$ . The system is partitioned into 3 fragments that correspond to the initial molecules. Note that the fragments remain unchanged during the transition process. In order to fulfill the  $N$ -representability condition (2.33) below (which is necessary for Assumption (A3) to be fulfilled), we dope the system with four additional electrons, i.e., 10 electrons in total. The system is discretized using the 6-31G basis set.

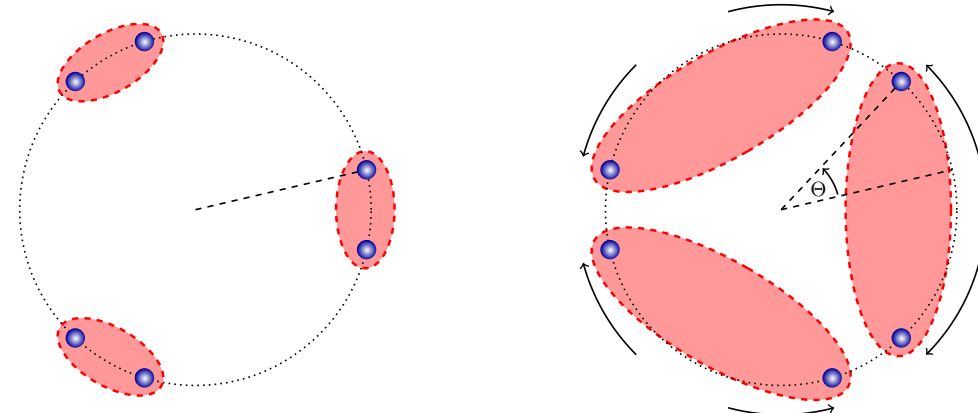


Figure 2.3: Schematic depiction of the considered  $H_6$  transition. The left panel shows the initial configuration for  $\Theta = 0$ ; the right panel shows the final configuration  $\Theta = \Theta_{\max}$ . The red-shaded areas depict the imposed fragmentation. The arrows indicate the transition of the hydrogen atoms for  $\Theta \in [0, \Theta_{\max}]$ .

In order to numerically depict Theorem 2.5, we compute  $P_\alpha$  and  $D_\alpha$  using a mean-field theory approach (HF), DMET, and the exact diagonalization (FCI), and compare these quantities for  $\alpha = 0$  as well as their first derivatives with respect to  $\alpha$ . Note that in the non-interacting limit, the mean-field theory is exact, which is reflected in our simulations. We indeed observe that  $\sup_\Theta \|P_0^{\text{HF}}(\Theta) - P_0^{\text{FCI}}(\Theta)\|_F$  and  $\sup_\Theta \|D_0^{\text{HF}}(\Theta) - D_0^{\text{FCI}}(\Theta)\|_F$  are equal to zero up to numerical accuracy, while  $\sup_\Theta \|P_0^{\text{DMET}}(\Theta) - P_0^{\text{FCI}}\|_F$ ,  $\sup_\Theta \|D_0^{\text{DMET}}(\Theta) - D_0^{\text{FCI}}(\Theta)\|_F$  are respectively of the order of  $10^{-13}$  and  $10^{-7}$  with the chosen convergence thresholds. Figure 2.4 shows the first-order exactness of DMET in the non-interacting limit for the  $H_6^{4-}$  model.

Our numerical investigations include an analysis of Assumptions (A1)-(A4). We present a check of Assumptions (A1) and (A2) in Figure 2.5. Assumption (A1) can be directly tested by calculating the HOMO-LUMO gap of the non-interacting Hamiltonian under consideration for each value of  $\Theta$ . Furthermore, Assumption (A2) can be tested by monitoring the behavior of the smallest and largest singular values of the matrix  $P_0$  as a function of the variable  $\Theta$  (see Lemma 2.6).

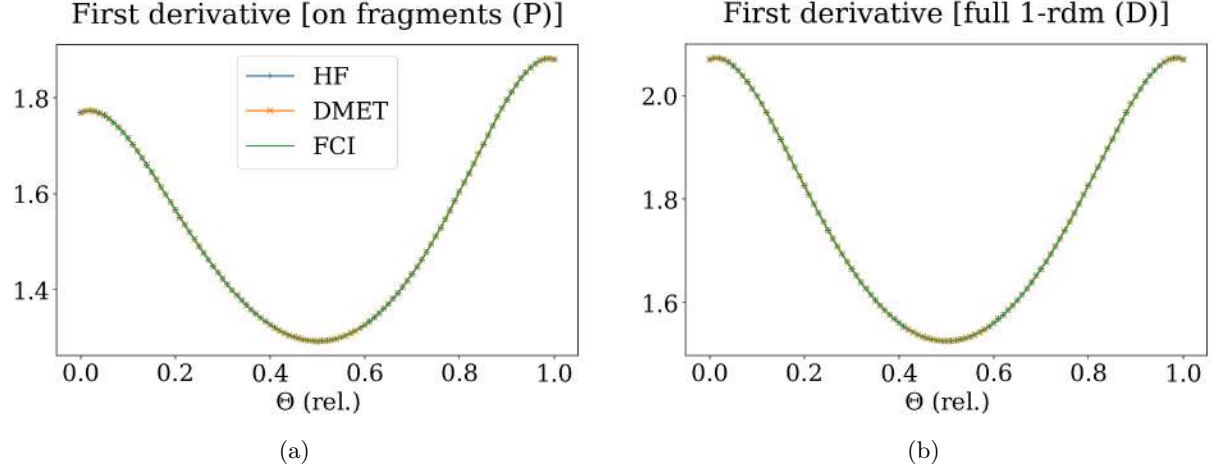


Figure 2.4: (a) Shows  $\|\partial_\alpha P_\alpha\|_{\alpha=0}\|_F$  for HF, DMET and FCI (b) Shows  $\|\partial_\alpha D_\alpha\|_{\alpha=0}\|_F$  for HF, DMET and FCI.

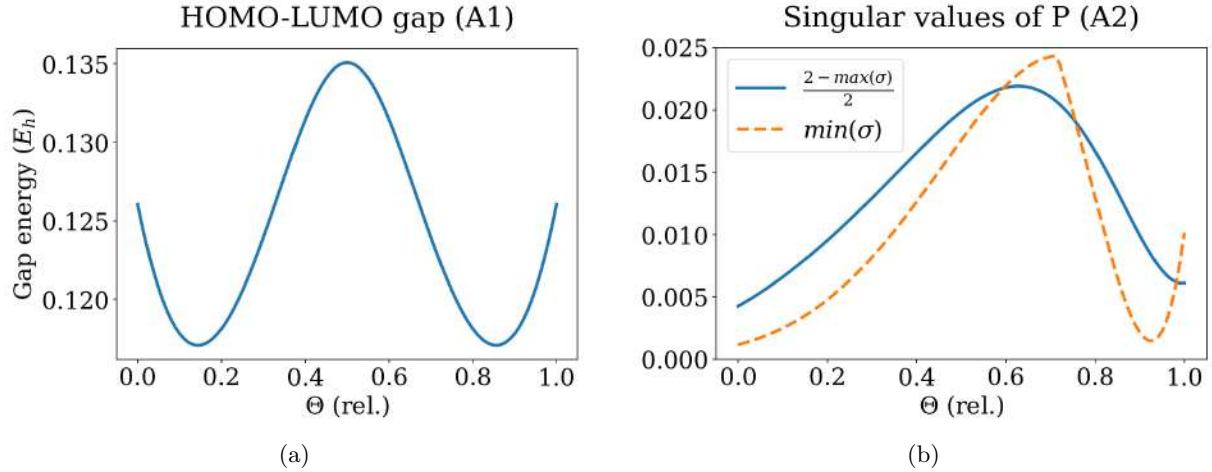


Figure 2.5: (a) Shows the HOMO-LUMO gap for the  $H_6$  model as a function of  $\Theta$  for  $\alpha = 0$ . (b) Shows the largest and smallest singular values of  $P$  for the  $H_6$  model as a function of  $\Theta$  for  $\alpha = 0$ .

The validity of assumptions (A3) and (A4) is tested in Figure 2.6 by monitoring the lowest eigenvalue of the operator  $S := (\text{Bd}|_{T_{D_0} \mathcal{D} \rightarrow \mathcal{Y}})^* \text{Bd}|_{T_{D_0} \mathcal{D} \rightarrow \mathcal{Y}}$  (which corresponds to (A3)), and the smallest singular value of the operator  $R|_{\mathcal{Y} \rightarrow \mathcal{Y}}$  (which corresponds to (A4)).

We see that Assumptions (A1) and (A2) are uniformly fulfilled over the whole range  $[0, \Theta_{\max}]$ . Assumption (A3) seems to be satisfied for all  $\Theta$  except two values  $\Theta_1 \simeq 0.885$  and  $\Theta_2 \simeq 0.957$ . Careful testing around  $\Theta_2$  shows that Assumption (A4) is additionally not satisfied at  $\Theta_3 \simeq 0.958$ , where all other assumptions are satisfied. This illustrates the fact that in the general case  $N_f < L$ , Assumption (A4) is independent of Assumptions (A1)-(A3) (see Remark 2.3).

Figure 2.7a shows the Frobenius norms of the second derivative of  $P_\alpha$  and  $D_\alpha$  at  $\alpha = 0$  for HF, DMET, and FCI. We see that the three methods give different results, and that the result in Theorem 2.5 is therefore optimal. We also observe that for DMET, the second derivatives become noisy in the range of  $\Theta$ 's where Assumptions (A3) and (A4) are poorly or not satisfied. This is probably due to conditioning issues or to the use of convergence thresholds not directly connected to the computed quantity of interest. The numerical analysis of DMET is left for future work.

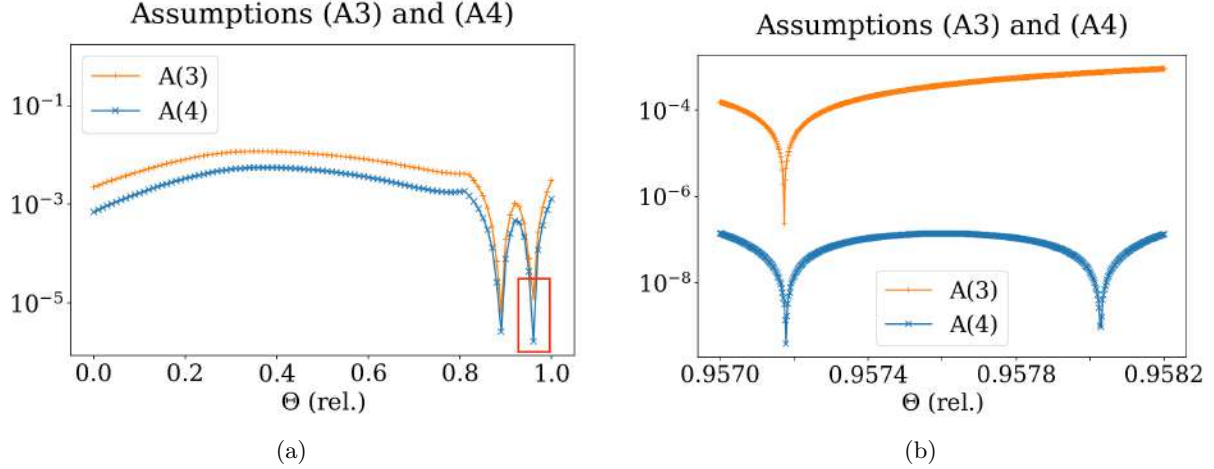


Figure 2.6: (a) The orange line shows the lowest eigenvalue of  $S := (\text{Bd}|_{T_{D_0}\mathcal{D} \rightarrow \mathcal{Y}})^* \text{Bd}|_{T_{D_0}\mathcal{D} \rightarrow \mathcal{Y}}$  for the  $H_6$  model as a function of  $\Theta$  for  $\alpha = 0$  (which corresponds to (A3)), and the blue line shows the smallest singular value  $\sigma_{\min}$  of  $R|_{\mathcal{Y} \rightarrow \mathcal{Y}}$  (which corresponds to (A4)). (b) Shows a zoomed version of (a) around the second (local) minimum.

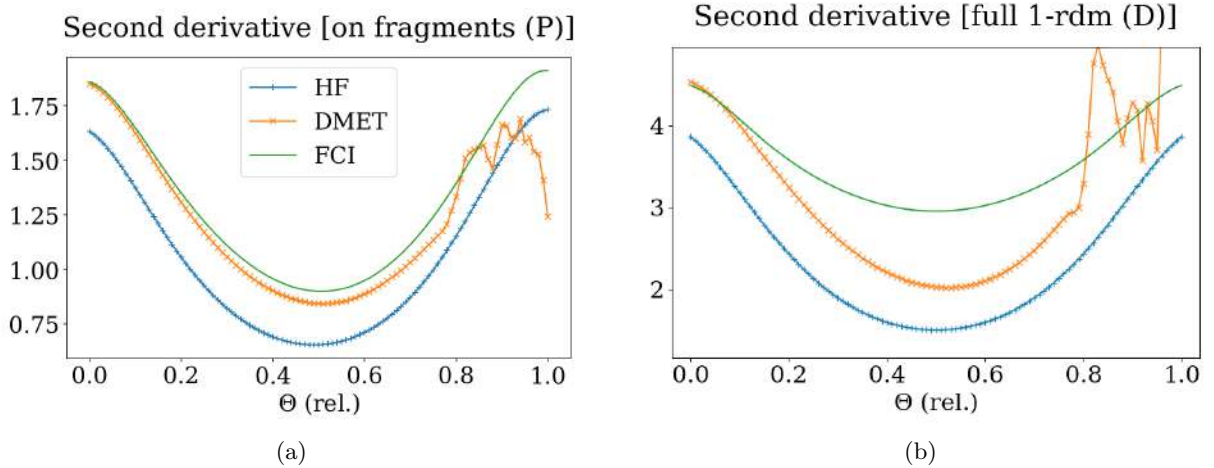


Figure 2.7: (a) shows  $\|\partial_\alpha^2 P_\alpha|_{\alpha=0}\|_F$  for HF, DMET and FCI (b) shows  $\|\partial_\alpha^2 D_\alpha|_{\alpha=0}\|_F$  for HF, DMET and FCI.

We now investigate more closely the violation of the hypotheses at  $\Theta_3$ , where  $R$  is not invertible, but (A3) is still satisfied. To that end, we compute the differential of  $F_0^{\text{DMET}}(P_0)$  at  $P_0$ , as a function of  $\Theta$ , and see that for  $\Theta$  close to  $\Theta_3$ ,  $F_0^{\text{DMET}}(P_0(\Theta))$  possesses a simple real eigenvalue which transitions from being positive (for  $\Theta < \Theta_3$ ) to being negative (for  $\Theta > \Theta_3$ ), with all other eigenvalues having negative real parts. As is standard, this type of eigenvalue crossing generically gives rise to a transcritical bifurcation [47]. This suggests the existence of another branch of solutions  $P_1(\Theta)$  of  $P = F_0^{\text{DMET}}(P)$ , which collides with  $P_0(\Theta)$  at  $\Theta = \Theta_3$ , and such that the largest eigenvalue of the differential of  $F_0^{\text{DMET}}$  at  $P_0$  has the opposite sign to that at  $P_1$ .

To find this branch of solutions, we employ a Newton algorithm on  $F_0^{\text{DMET}}$ . Since we are looking at small differences, this requires accurate computations of  $F_0^{\text{HL}}$  and  $F_0^{\text{LL}}$  as well as their differentials (without resorting to finite differences). The differential of  $F_0^{\text{HL}}$  is computed analytically by perturbation theory (taking into account the self-consistent Fermi level). For  $F_0^{\text{LL}}$ , we implemented a manifold Newton algorithm to compute an accurate solution of the problem defining the low-level solver. This is done by, starting from the point  $D_n$ , parametrizing  $D_{n+1}$  as  $D(X)$  with an unconstrained matrix  $X$  as in the proof of Lemma 2.10, and then performing a Newton step on the Lagrangian  $L(X, \Lambda)$  that corresponds to minimizing  $\mathcal{E}^{\text{HF}}(D(X))$  subject to  $\text{Bd}(D(X)) = P$ . From the Hessian of the Lagrangian one can also compute the differential of  $F_0^{\text{LL}}$ , and then ultimately of  $F_0^{\text{DMET}}$ .

To initialize the Newton algorithm on  $F_0^{\text{DMET}}$  at a given  $\Theta$  close to  $\Theta_3$ , we start from  $P_0$ , and

compute the eigenvector  $Y$  of  $dF_0^{\text{DMET}}$  associated with the eigenvalue that crosses zero. Then, we run a Newton algorithm started from  $P_0 + \alpha(\Theta - \Theta_3)Y$ , where  $\alpha$  is an empirically chosen parameter (its precise determination involves higher derivatives [47], which are cumbersome to compute). We observe the two branches  $P_0$  and  $P_1$  shown in Figure 2.8, confirming the transcritical bifurcation. Let us emphasize that this bifurcation is not due to symmetry breaking, as can be shown from a detailed analysis of the solutions  $P_0$  and  $P_1$  (see Appendix 2.B).

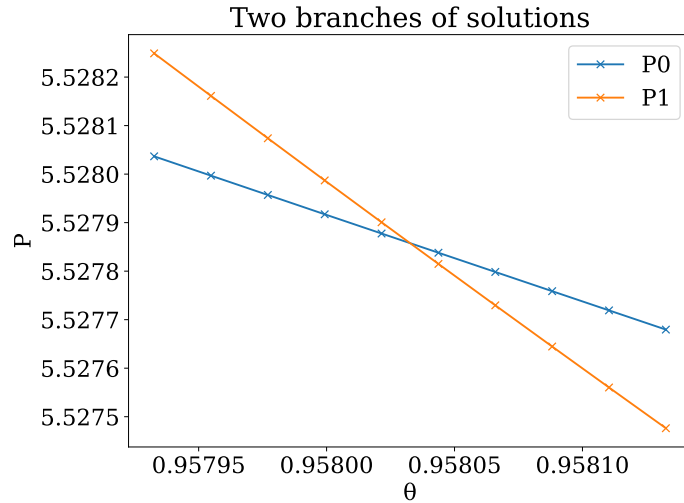


Figure 2.8: The two branches  $P_0$  and  $P_1$  (displayed are the scalars  $\sum_{ij} P_{ij}$ ) as functions of  $\Theta$  near  $\Theta = \Theta_3$ .

## 2.5 Impurity problems and high-level map

### 2.5.1 Impurity Hamiltonians

It follows from the considerations in Section 2.2.2 that if

$$\forall x \in \llbracket 1, N_f \rrbracket, \quad \dim(DX_x) = \dim((1 - D)X_x) = L_x.$$

the impurity problem is well-defined for each fragment since the maximal rank assumption (2.11) is satisfied for each  $X_x$ . The next lemma gives useful equivalent characterizations of these conditions.

Let us introduce the matrix

$$E_x := \text{mat}_{\mathcal{B}_{\text{at}}}(e_\kappa, \kappa \in \mathcal{I}_x) = \begin{pmatrix} 0_{L'_x \times L_x} \\ I_{L_x} \\ 0_{L''_x \times L_x} \end{pmatrix} \in \mathbb{R}^{L \times L_x} \quad \text{with} \quad \begin{cases} L'_x := \sum_{1 \leq x' < x} L_{x'} \\ L''_x := \sum_{x < x' \leq N_f} L_{x'} \end{cases} \quad (2.27)$$

representing the orbitals of fragment  $x \in \llbracket 1, N_f \rrbracket$ , whose range is  $X_x$ . We recall that  $\overset{\circ}{\mathcal{P}}$  denotes the interior of the set  $\mathcal{P} = \text{Bd}(\text{CH}(\mathcal{D}))$  in the affine space  $P_0 + \mathcal{Y}$ .

**Lemma 2.6** (Compatibility conditions). *Let  $D \in \mathcal{D}$ . The following assertions are equivalent:*

1.  $\text{Bd}(D) \in \overset{\circ}{\mathcal{P}}$ ;
2.  $\forall x \in \llbracket 1, N_f \rrbracket, \quad \dim(DX_x) = \dim((1 - D)X_x) = L_x$ ;
3.  $\forall x \in \llbracket 1, N_f \rrbracket, \quad 0 < E_x^T DE_x < 1$  (all the eigenvalues of  $E_x^T DE_x$  are in  $(0, 1)$ );
4.  $\forall x \in \llbracket 1, N_f \rrbracket, \quad E_x^T DE_x \in \text{GL}_{\mathbb{R}}(L_x) \quad \text{and} \quad E_x^T (1 - D)E_x \in \text{GL}_{\mathbb{R}}(L_x)$ .

If  $D$  satisfies these conditions, we say that it is compatible with the fragment decomposition.

It is easily seen that if  $D$  is compatible with the fragment decomposition, then the column vectors defined by the matrix

$$C^x(D) := \left( DE_x (E_x^T DE_x)^{-1/2} \left| (1 - D)E_x (E_x^T (1 - D)E_x)^{-1/2} \right. \right) \in \mathbb{R}^{L \times 2L_x} \quad (2.28)$$

form an orthonormal basis of the impurity one-particle state space  $W_{x,D}$  defined in (2.10). More precisely, the first  $L_x$  columns of  $C^x(D)$  form an orthonormal basis of  $DX_x$  and its last  $L_x$  columns form an orthonormal basis of  $(1 - D)X_x$ . Likewise, the column vectors of the matrix

$$\tilde{C}^x(D) := \left( E_x \left| (1 - \Pi_x)DE_x (E_x^T D(1 - \Pi_x)DE_x)^{-1/2} \right. \right) \in \mathbb{R}^{L \times 2L_x} \quad (2.29)$$

form an orthonormal basis of  $X_x \oplus (1 - \Pi_x)DX_x$ .

We denote by  $\hat{a}_j^x(D)$  and  $\hat{a}_j^x(D)^\dagger$ ,  $1 \leq j \leq 2L_x$  the annihilation and creation operators in the basis of the columns of  $C^x(D)$ :

$$\hat{a}_j^x(D) = \sum_{\kappa=1}^{L_x} (C^x(D))_{\kappa j} \hat{a}_\kappa, \quad \hat{a}_j^x(D)^\dagger = \sum_{\kappa=1}^{L_x} (C^x(D))_{\kappa j} \hat{a}_\kappa^\dagger.$$

These operators allow for an explicit form of the impurity Hamiltonian  $\hat{H}_{x,D}^{\text{imp}}$  as follows.

**Proposition 2.7** (Impurity Hamiltonian). *Let  $D \in \mathcal{D}$  be compatible with the fragment decomposition. The  $x$ -th impurity Hamiltonian  $\hat{H}_{x,D}^{\text{imp}}$  is the operator on  $\text{Fock}(W_{x,D})$  given by*

$$\begin{aligned} \hat{H}_{x,D}^{\text{imp}} &= E_x^{\text{env}}(D) + \sum_{i,j=1}^{2L_x} [C^x(D)^T (h + J(\mathfrak{D}^x(D)) - K(\mathfrak{D}^x(D))) C^x(D)]_{ij} \hat{a}_i(D)^\dagger \hat{a}_j(D) \\ &\quad + \frac{1}{2} \sum_{i,j,k,\ell=1}^{2L_x} [V^x(D)]_{ijkl} \hat{a}_i(D)^\dagger \hat{a}_j(D)^\dagger \hat{a}_\ell(D) \hat{a}_k(D), \end{aligned} \quad (2.30)$$

where

- the Coulomb and exchange matrices  $J(\mathfrak{D}^x(D)) \in \mathbb{R}^{L \times L}$  and  $K(\mathfrak{D}^x(D)) \in \mathbb{R}^{L \times L}$  for the  $x$ -th impurity are constructed from the density matrix

$$\mathfrak{D}^x(D) := D - DE_x(E_x^T DE_x)^{-1} E_x^T D \in \text{Gr}(N - L_x, L); \quad (2.31)$$

- the rank-4 tensor  $V^x(D)$  is given by

$$[V^x(D)]_{ijkl} := \sum_{\kappa, \lambda, \nu, \xi=1}^L V_{\kappa \lambda \nu \xi} [C^x(D)]_{\kappa i} [C^x(D)]_{\lambda j} [C^x(D)]_{\nu k} [C^x(D)]_{\xi l}; \quad (2.32)$$

- the value of the (irrelevant) constant  $E_x^{\text{env}}(D)$  is given in (2.39).

Note that the matrix  $\mathfrak{D}^x(D)$  is in fact the one-body density matrix associated with the Slater determinant  $\Psi_{x,D}^{0,\text{core}}$  (see Section 2.2.2).

### 2.5.2 Domain of the high-level map

A matrix  $D \in \mathcal{D}$  is in the domain of the high-level map  $F^{\text{HL}}$  formally defined in Section 2.2.3 if and only if

1.  $D$  is compatible with the fragment decomposition (see Lemma 2.6), in such a way that the impurity problem (2.15) is well defined for each  $x$ ;
2. the set

$$M_D := \left\{ \mu \in \mathbb{R} \mid \begin{array}{l} \forall x, \text{ the impurity problem (2.15) has a unique ground-state 1-RDM } P_{x,D,\mu}, \\ \text{and } \sum_{x=1}^{N_f} \text{Tr}(\Pi_x P_{x,D,\mu} \Pi_x) = N \end{array} \right\}$$

is non-empty;

3. the function

$$\mathcal{F}_D : M_D \ni \mu \mapsto \sum_{x=1}^{N_f} \Pi_x P_{x,D,\mu} \Pi_x \in \mathcal{P}$$

is a constant over  $M_D$ , which we denote by  $F^{\text{HL}}(D)$ .

In the proof of Theorem 2.4, we will study  $F_\alpha^{\text{HL}}$  in the non-interacting ( $\alpha = 0$ ) and weakly interacting ( $|\alpha|$  small) cases. We will see that in these regimes the domain of  $F_\alpha^{\text{HL}}$  contains a neighborhood of  $D_0$  in  $\mathcal{D}$ .

## 2.6 $N$ -representability and low-level map

In this section, we focus our study on the low level map defined in (2.19). Clearly, (2.19) has minimizers if and only if  $P \in \text{Bd}(\mathcal{D})$  (otherwise, the feasible set of the minimization problem is empty).

The next Lemma covers the extreme cases of minimal ( $N_f = 2$ ) and maximal ( $N_f = L$ ) numbers of fragments.

**Lemma 2.8** (Global  $N$ -representability).

1. If  $N_f = L$  (one site per fragment), then  $\text{Bd}(\mathcal{D}) = \text{Bd}(\text{CH}(\mathcal{D})) = \mathcal{P}$ .
2. If  $N_f = 2$  and  $L \geq 3$ , then  $\text{Bd}(\mathcal{D}) \subsetneq \text{Bd}(\text{CH}(\mathcal{D})) = \mathcal{P}$ . More precisely,

$$\text{Bd}(\mathcal{D}) = \{P \in \mathcal{P} \mid \forall 0 < n < 1, \dim(\text{Ker}(\Pi_1 P \Pi_1 - n)) = \dim(\text{Ker}(\Pi_2 P \Pi_2 - (1 - n)))\}.$$

Our analysis of the DMET method in the non-interacting and weakly perturbative settings relies on the following weaker  $N$ -representability result.

**Definition 2.9** (Local  $N$ -representability). Let  $D \in \mathcal{D}$  be compatible with the fragment decomposition. We say that the local  $N$ -representability condition is satisfied at  $D$  if the linear map  $\text{Bd}$  is surjective from  $T_D \mathcal{D}$  to  $\mathcal{Y}$ .

Note that Assumption (A3) can be rephrased as: the local  $N$ -representability condition is satisfied at  $D_0$ .

A necessary condition for the local  $N$ -representability condition to be satisfied at some  $D \in \text{Bd}^{-1} \mathring{\mathcal{P}}$  is that

$$N(L - N) = \dim(\mathcal{D}) = \dim(\mathbb{R}^{N_v \times N}) \geq \dim(\mathcal{Y}) = \sum_{x=1}^{N_f} \frac{L_x(L_x + 1)}{2} - 1. \quad (2.33)$$

If  $N_f = L$  (one site per fragment), the above condition reads  $N(L - N) \geq L - 1$ , and is therefore satisfied for any  $1 \leq N \leq L - 1$ , i.e. for any non-trivial case. On the other hand, if  $N_f = 2$  and  $L = 2L_1 = 2L_2$  (two fragments of identical sizes), the necessary condition reads  $N(L - N) \geq \frac{L(L+2)}{4} - 1$  and is never satisfied as soon as  $L \geq 3$ . This result is in agreement with the global  $N$ -representability results in Lemma 2.8. In usual DMET calculations, condition (2.33) is always satisfied, so that, generically,  $\mathcal{P}$  and  $\text{Bd}(\mathcal{D})$  coincide in the neighbourhood of  $P_0$ .

The next lemma provides a sufficient local  $N$ -representability criterion.

**Lemma 2.10** (A local  $N$ -representability criterion). Let  $D \in \mathcal{D}$  be compatible with the fragment decomposition (i.e.  $D \in \text{Bd}^{-1} \mathring{\mathcal{P}}$ ). The following assertions are equivalent:

1. the local  $N$ -representability condition is satisfied at  $D$ ;
2. the only matrices  $M \in \mathbb{R}_{\text{sym}}^{L \times L}$  commuting with both  $D$  and the matrices  $\Pi_x$  for all  $1 \leq x \leq N_f$  are of the form  $M = \lambda I_L$  for some  $\lambda \in \mathbb{R}$ ;
3. if  $\Phi \in \mathbb{R}^{L \times L}$  is an orthogonal matrix such that

$$D = \Phi \begin{pmatrix} I_N & 0 \\ 0 & 0 \end{pmatrix} \Phi^T, \quad (2.34)$$

then the linear map

$$\mathbb{R}^{(L-N) \times N} \ni X \mapsto \sum_{x=1}^{N_f} \Pi_x \Phi \begin{pmatrix} 0 & X^T \\ X & 0 \end{pmatrix} \Phi^T \Pi_x \in \mathcal{Y} \quad (2.35)$$

is surjective.

The third assertion of Lemma 2.10 gives a practical way to check the local  $N$ -representability criterion: it suffices to (i) diagonalize  $D$  in order to write it as in (2.34) (the columns of  $\Phi \in O(L)$  form an orthonormal basis of eigenvectors of  $D$ ), (ii) assemble the matrix of the linear map (2.35) in the canonical bases of  $\mathbb{R}^{(L-N) \times N}$  and  $\mathcal{Y}$ , and (iii) check whether the number of positive singular values of this matrix is equal to  $\dim(\mathcal{Y}) = \sum_{x=1}^{N_f} \frac{L_x(L_x + 1)}{2} - 1$ .

## 2.7 Proofs

### 2.7.1 Proof of Lemma 2.6

Let  $D \in \mathcal{D}$ .

2)  $\iff$  3). Assume that

$$\forall 1 \leq x \leq N_f, \quad \dim(DX_x) = \dim((1 - D)X_x) = L_x.$$

Since  $D^2 = D$ , we have for all  $y \in \mathbb{R}^{L_x}$ ,

$$y^T (E_x^T D E_x) y = y^T (E_x^T D^2 E_x) y = (D(E_x y))^T (D(E_x y)) = |D(E_x y)|^2, \quad (2.36)$$

and therefore,

$$0 \leq y^T (E_x^T D E_x) y = |D(E_x y)|^2 \leq |E_x y|^2 = |y|^2.$$

Thus  $0 \leq E_x^T DE_x \leq 1$  in the sense of hermitian matrices. Assume now that  $y^T (E_x^T DE_x) y = 0$ . Then,  $E_x y \in \text{Ker}(D)$ . But we also have  $E_x y \in X_x$ . Since  $\dim(DX_x) = L_x$ , this implies that  $y = 0$ . Thus  $0 < E_x^T DE_x$  in the sense of hermitian matrices. Likewise, we have  $E_x^T DE_x < 1$ . This proves that 2)  $\implies$  3). Conversely, if for all  $1 \leq x \leq N_f$ ,  $0 < E_x^T DE_x$ , we infer from (2.36) that  $D(E_x y) = 0$  implies  $y = 0$ , hence that  $\dim(DX_x) = L_x$ . Likewise,  $E_x^T DE_x < 1$  implies  $\dim((1 - D)X_x) = L_x$ . Therefore, 3)  $\implies$  2).

3)  $\iff$  4). Since  $0 < E_x^T DE_x$  is equivalent to  $E_x^T DE_x \in \text{GL}_{\mathbb{R}}(L_x)$  and  $E_x^T DE_x < 1$  is equivalent to  $E_x^T (1 - D)E_x \in \text{GL}_{\mathbb{R}}(L_x)$ , we conclude that 3)  $\iff$  4).

Lastly, it follows from the definition of  $\mathcal{P}$  that

$$P = \begin{pmatrix} P_1 & 0 & \cdots & 0 \\ 0 & P_2 & \cdots & 0 \\ \vdots & \ddots & \ddots & \vdots \\ 0 & 0 & \cdots & P_{N_f} \end{pmatrix} \in \overset{\circ}{\mathcal{P}} \iff (\forall 1 \leq x \leq N_f, 0 < P_x = E_x^T PE_x < 1). \quad (2.37)$$

This shows that 1)  $\iff$  3), which concludes the proof.

### 2.7.2 Proof of Proposition 2.7

Let  $D \in \mathcal{D}$  and  $1 \leq x \leq N_f$ . Let us first concatenate the matrix  $C^x(D) \in \mathbb{R}^{L \times 2L_x}$  introduced in (2.28) with a matrix  $C_{\text{env}}^x(D) \in \mathbb{R}^{L \times (L-2L_x)}$  in order to form an orthogonal matrix

$$\mathfrak{C}^x(D) = (C^x(D) | C_{\text{env}}^x(D)) \in O(L).$$

The column vectors of  $\mathfrak{C}^x(D)$  define an orthonormal basis of  $\mathcal{H} = \mathbb{R}^L$  adapted to the decomposition  $\mathcal{H} = W_{x,D} \oplus \mathcal{H}_{x,D}^{\text{env}}$ . The generators of the real CAR algebra associated with this basis are given by

$$\hat{a}_i^x(D) = \sum_{\kappa=1}^L \mathfrak{C}^x(D)_{\kappa i} \hat{a}_\kappa, \quad \hat{a}_i^x(D)^\dagger = \sum_{\kappa=1}^L \mathfrak{C}^x(D)_{\kappa i} \hat{a}_\kappa^\dagger,$$

so that the Hamiltonian

$$\hat{H} = \sum_{\kappa, \lambda=1}^L h_{\kappa \lambda} \hat{a}_\kappa^\dagger \hat{a}_\lambda + \frac{1}{2} \sum_{\kappa, \lambda, \nu, \xi=1}^L V_{\kappa \lambda \nu \xi} \hat{a}_\kappa^\dagger \hat{a}_\lambda^\dagger \hat{a}_\xi \hat{a}_\nu$$

can be rewritten as

$$\hat{H} = \sum_{i,j=1}^L [h^x(D)]_{ij} \hat{a}_i^x(D)^\dagger \hat{a}_j^x(D) + \frac{1}{2} \sum_{i,j,k,l=1}^L [V^x(D)]_{ijkl} \hat{a}_i^x(D)^\dagger \hat{a}_j^x(D)^\dagger \hat{a}_l^x(D) \hat{a}_k^x(D)$$

with

$$[h^x(D)]_{ij} := \sum_{\kappa, \lambda=1}^L h_{\kappa \lambda} \mathfrak{C}^x(D)_{\kappa i} \mathfrak{C}^x(D)_{\lambda j} \quad \text{i.e.} \quad h^x(D) = \mathfrak{C}^x(D)^T h \mathfrak{C}^x(D)$$

and

$$[V^x(D)]_{ijkl} := \sum_{\kappa, \lambda, \nu, \xi=1}^L V_{\kappa \lambda \nu \xi} \mathfrak{C}^x(D)_{\kappa i} \mathfrak{C}^x(D)_{\lambda j} \mathfrak{C}^x(D)_{\nu k} \mathfrak{C}^x(D)_{\xi l}.$$

Note that if  $1 \leq i, j, k, l \leq 2L_x$ ,

$$[h^x(D)]_{ij} = [C^x(D)^T h C^x(D)]_{ij} \quad \text{and} \quad [V^x(D)]_{ijkl} := \sum_{\kappa, \lambda, \nu, \xi=1}^L V_{\kappa \lambda \nu \xi} C^x(D)_{\kappa i} C^x(D)_{\lambda j} C^x(D)_{\nu k} C^x(D)_{\xi l},$$

in agreement with (2.32). Let  $\Psi \in \text{Fock}(\mathcal{H})$  be of the form

$$\Psi = \Psi_{x,D}^{\text{imp}} \wedge \Psi_{x,D}^{0,\text{core}} \quad \text{with} \quad \Psi_{x,D}^{\text{imp}} \in \text{Fock}(W_{x,D}) \quad \text{and} \quad \Psi_{x,D}^{0,\text{core}} \in \bigwedge^{(N-L_x)} \mathcal{H}_{x,D}^{\text{core}}.$$

We have

$$\begin{aligned} \langle \Psi | \hat{H} | \Psi \rangle &= \langle \Psi_{x,D}^{\text{imp}} \wedge \Psi_{x,D}^{0,\text{core}} | \sum_{i,j=1}^L [h^x(D)]_{ij} \hat{a}_i^x(D)^\dagger \hat{a}_j^x(D) \\ &\quad + \frac{1}{2} \sum_{i,j,k,l=1}^L [V^x(D)]_{ijkl} \hat{a}_i^x(D)^\dagger \hat{a}_j^x(D)^\dagger \hat{a}_l^x(D) \hat{a}_k^x(D) | \Psi_{x,D}^{\text{imp}} \wedge \Psi_{x,D}^{0,\text{core}} \rangle. \end{aligned}$$

The terms in the Hamiltonian which change the number of particles in the impurity space or the environment do not contribute. The terms which act only on the environment subspace yield a term proportional to  $\|\Psi_{x,D}^{\text{imp}}\|^2$ . Expanding the above expression, we thus obtain

$$\langle \Psi | \hat{H} | \Psi \rangle = a_1 + a_2 + a_3 + a_4 + a_5 + a_6 + a_7$$

with

$$\begin{aligned} a_1 &:= \sum_{i,j=1}^{2L_x} [h^x(D)]_{ij} \langle \Psi_{x,D}^{\text{imp}} \wedge \Psi_{x,D}^{0,\text{core}} | \hat{a}_i^x(D)^\dagger \hat{a}_j^x(D) | \Psi_{x,D}^{\text{imp}} \wedge \Psi_{x,D}^{0,\text{core}} \rangle \\ &= \sum_{i,j=1}^{2L_x} [h^x(D)]_{ij} \langle \Psi_{x,D}^{\text{imp}} | \hat{a}_i^x(D)^\dagger \hat{a}_j^x(D) | \Psi_{x,D}^{\text{imp}} \rangle \\ &= \sum_{i,j=1}^{2L_x} [C^x(D)^T h C^x(D)]_{ij} \langle \Psi_{x,D}^{\text{imp}} | \hat{a}_i^x(D)^\dagger \hat{a}_j^x(D) | \Psi_{x,D}^{\text{imp}} \rangle, \\ a_2 &:= \sum_{i,j=2L_x+1}^L [h^x(D)]_{ij} \langle \Psi_{x,D}^{\text{imp}} \wedge \Psi_{x,D}^{0,\text{core}} | \hat{a}_i^x(D)^\dagger \hat{a}_j^x(D) | \Psi_{x,D}^{\text{imp}} \wedge \Psi_{x,D}^{0,\text{core}} \rangle \\ &= \left( \sum_{i,j=2L_x+1}^L [h^x(D)]_{ij} \langle \Psi_{x,D}^{0,\text{core}} | \hat{a}_i^x(D)^\dagger \hat{a}_j^x(D) | \Psi_{x,D}^{0,\text{core}} \rangle \right) \|\Psi_{x,D}^{\text{imp}}\|^2, \\ a_3 &:= \sum_{i=2L_x+1}^L \sum_{j=1}^{2L_x} [h^x(D)]_{ij} \left( \underbrace{\langle \Psi_{x,D}^{\text{imp}} \wedge \Psi_{x,D}^{0,\text{core}} |}_{\substack{L_x \text{ part. in imp.} \\ (N-L_x) \text{ part. in env.}}} \underbrace{|\hat{a}_i^x(D)^\dagger \hat{a}_j^x(D)|}_{\substack{(L_x+1) \text{ part. in imp.} \\ (N-L_x-1) \text{ part. in env.}}} \langle \Psi_{x,D}^{\text{imp}} \wedge \Psi_{x,D}^{0,\text{core}} \rangle \right. \\ &\quad \left. = 0, \right. \\ a_4 &:= \sum_{i=1}^{2L_x} \sum_{j=2L_x+1}^L [h^x(D)]_{ij} \left( \underbrace{\langle \Psi_{x,D}^{\text{imp}} \wedge \Psi_{x,D}^{0,\text{core}} |}_{\substack{L_x \text{ part. in imp.} \\ (N-L_x) \text{ part. in env.}}} \underbrace{|\hat{a}_i^x(D)^\dagger \hat{a}_j^x(D)|}_{\substack{(L_x-1) \text{ part. in imp.} \\ (N-L_x+1) \text{ part. in env.}}} \langle \Psi_{x,D}^{\text{imp}} \wedge \Psi_{x,D}^{0,\text{core}} \rangle \right. \\ &\quad \left. = 0, \right. \\ a_5 &:= \frac{1}{2} \sum_{i,j,k,l=1}^{2L_x} [V^x(D)]_{ijkl} \langle \Psi_{x,D}^{\text{imp}} \wedge \Psi_{x,D}^{0,\text{core}} | \hat{a}_i^x(D)^\dagger \hat{a}_j^x(D)^\dagger \hat{a}_l^x(D) \hat{a}_k^x(D) | \Psi_{x,D}^{\text{imp}} \wedge \Psi_{x,D}^{0,\text{core}} \rangle \\ &= \frac{1}{2} \sum_{i,j,k,l=1}^{2L_x} [V^x(D)]_{ijkl} \langle \Psi_{x,D}^{\text{imp}} | \hat{a}_i^x(D)^\dagger \hat{a}_j^x(D)^\dagger \hat{a}_l^x(D) \hat{a}_k^x(D) | \Psi_{x,D}^{\text{imp}} \rangle, \\ a_6 &:= \frac{1}{2} \sum_{i,j,k,l=2L_x+1}^L [V^x(D)]_{ijkl} \langle \Psi_{x,D}^{\text{imp}} \wedge \Psi_{x,D}^{0,\text{core}} | \hat{a}_i^x(D)^\dagger \hat{a}_j^x(D)^\dagger \hat{a}_l^x(D) \hat{a}_k^x(D) | \Psi_{x,D}^{\text{imp}} \wedge \Psi_{x,D}^{0,\text{core}} \rangle \\ &= \left( \frac{1}{2} \sum_{i,j,k,l=2L_x+1}^L [V^x(D)]_{ijkl} \langle \Psi_{x,D}^{0,\text{core}} | \hat{a}_i^x(D)^\dagger \hat{a}_j^x(D)^\dagger \hat{a}_l^x(D) \hat{a}_k^x(D) | \Psi_{x,D}^{0,\text{core}} \rangle \right) \|\Psi_{x,D}^{\text{imp}}\|^2, \end{aligned}$$

$$\begin{aligned}
a_7 := & \frac{1}{2} \sum_{i,k=1}^{2L_x} \sum_{j,l=2L_x+1}^L ([V^x(D)]_{ijkl} - [V^x(D)]_{ijlk} - [V^x(D)]_{jikl} + [V^x(D)]_{jilk}) \\
& \times \underbrace{\langle \Psi_{x,D}^{\text{imp}} \wedge \Psi_{x,D}^{0,\text{core}} | \hat{a}_i^x(D)^\dagger \hat{a}_j^x(D)^\dagger \hat{a}_l^x(D) \hat{a}_k^x(D) | \Psi_{x,D}^{\text{imp}} \wedge \Psi_{x,D}^{0,\text{core}} \rangle}_{\langle \Psi_{x,D}^{\text{imp}} | \hat{a}_i^x(D)^\dagger \hat{a}_k^x(D) | \Psi_{x,D}^{\text{imp}} \rangle \langle \Psi_{x,D}^{0,\text{core}} | \hat{a}_j^x(D)^\dagger \hat{a}_l^x(D) | \Psi_{x,D}^{0,\text{core}} \rangle}.
\end{aligned}$$

Noticing that

$$\forall 2L_x + 1 \leq j, l \leq L, \quad \langle \Psi_{x,D}^{0,\text{core}} | \hat{a}_j^x(D)^\dagger \hat{a}_l^x(D) | \Psi_{x,D}^{0,\text{core}} \rangle = (\mathfrak{C}^x(D)^T D \mathfrak{C}^x(D))_{jl} \quad (2.38)$$

we get

$$\begin{aligned}
a_7 = & \frac{1}{2} \sum_{i,k=1}^{2L_x} \sum_{j,l=2L_x+1}^L ([V^x(D)]_{ijkl} - [V^x(D)]_{ijlk} - [V^x(D)]_{jikl} + [V^x(D)]_{jilk}) \\
& \times (\mathfrak{C}^x(D)^T D \mathfrak{C}^x(D))_{jl} \langle \Psi_{x,D}^{\text{imp}} | \hat{a}_i^x(D)^\dagger \hat{a}_k^x(D) | \Psi_{x,D}^{\text{imp}} \rangle \\
= & \sum_{i,j=1}^{2L_x} \left( \sum_{k,l=2L_x+1}^L ([V^x(D)]_{ikjl} - [V^x(D)]_{iklj} - [V^x(D)]_{kijl} + [V^x(D)]_{kilj}) (\mathfrak{C}^x(D)^T D \mathfrak{C}^x(D))_{kl} \right) \\
& \times \langle \Psi_{x,D}^{\text{imp}} | \hat{a}_i^x(D)^\dagger \hat{a}_j^x(D) | \Psi_{x,D}^{\text{imp}} \rangle.
\end{aligned}$$

It holds for all  $1 \leq i, j \leq 2L_x$ ,

$$\begin{aligned}
& \sum_{k,l=2L_x+1}^L [V^x(D)]_{ikjl} (\mathfrak{C}^x(D)^T D \mathfrak{C}^x(D))_{kl} \\
= & \sum_{k,l=2L_x+1}^L \sum_{\kappa,\lambda,\nu,\xi,\sigma,\tau=1}^L V_{\kappa\lambda\nu\xi} [\mathfrak{C}^x(D)]_{\kappa i} [\mathfrak{C}^x(D)]_{\lambda k} [\mathfrak{C}^x(D)]_{\nu j} [\mathfrak{C}^x(D)]_{\xi l} [\mathfrak{C}^x(D)]_{\sigma k} D_{\sigma\tau} [\mathfrak{C}^x(D)]_{\tau l} \\
= & \sum_{k,l=1}^{L-2L_x} \sum_{\kappa,\lambda,\nu,\xi,\sigma,\tau=1}^L V_{\kappa\lambda\nu\xi} [C^x(D)]_{\kappa i} [C_{\text{env}}^x(D)]_{\lambda k} [C^x(D)]_{\nu j} [C_{\text{env}}^x(D)]_{\xi l} [C_{\text{env}}^x(D)]_{\sigma k} D_{\sigma\tau} [C_{\text{env}}^x(D)]_{\tau l} \\
= & \sum_{\kappa,\nu=1}^L [C^x(D)]_{\kappa i} \left( \sum_{\lambda,\xi,\sigma,\tau=1}^L V_{\kappa\lambda\nu\xi} \left( \sum_{k=1}^{L-2L_x} [C_{\text{env}}^x(D)]_{\lambda k} [C_{\text{env}}^x(D)]_{\sigma k} \right) \right. \\
& \quad \left. \times D_{\sigma\tau} \left( \sum_{l=1}^{L-2L_x} [C_{\text{env}}^x(D)]_{\tau l} [C_{\text{env}}^x(D)]_{\xi l} \right) \right) [C^x(D)]_{\nu j} \\
= & \sum_{\kappa,\nu=1}^L [C^x(D)]_{\kappa i} \left( \sum_{\lambda,\xi,\sigma,\tau=1}^L V_{\kappa\lambda\nu\xi} (C_{\text{env}}^x(D) C_{\text{env}}^x(D)^T D C_{\text{env}}^x(D) C_{\text{env}}^x(D)^T)_{\lambda\xi} \right) [C^x(D)]_{\nu j} \\
= & [C^x(D)^T J(\tilde{\mathfrak{D}}^x(D)) C^x(D)]_{ij},
\end{aligned}$$

with, recalling that  $\mathfrak{C}^x(D) = (C^x(D) | C_{\text{env}}^x(D))$  is an orthogonal matrix,

$$\begin{aligned}
\tilde{\mathfrak{D}}^x(D) := & C_{\text{env}}^x(D) C_{\text{env}}^x(D)^T D C_{\text{env}}^x(D) C_{\text{env}}^x(D)^T \\
= & (1 - C^x(D) C^x(D)^T) D (1 - C^x(D) C^x(D)^T) \\
= & D - D E_x (E_x^T D E_x)^{-1} E_x^T D \\
= & \mathfrak{D}^x(D) \quad (\text{see (2.31)}).
\end{aligned}$$

Using similar arguments, we get

$$a_7 = \sum_{i,k=1}^{2L_x} [C^x(D)^T (J(\mathfrak{D}^x(D)) - K(\mathfrak{D}^x(D))) C^x(D)]_{ij} \langle \Psi_{x,D}^{\text{imp}} | \hat{a}_i^x(D)^\dagger \hat{a}_j^x(D) | \Psi_{x,D}^{\text{imp}} \rangle.$$

We finally obtain

$$\langle \Psi | \hat{H} | \Psi \rangle = \langle \Psi_{x,D}^{\text{imp}} | \hat{H}_{x,D}^{\text{imp}} | \Psi_{x,D}^{\text{imp}} \rangle,$$

where  $\hat{H}_{x,D}^{\text{imp}}$  is given by (2.30) with

$$\begin{aligned} E^{\text{env}}(D) &= \sum_{i,j=2L_x+1}^L [h^x(D)]_{ij} \langle \Psi_{x,D}^{0,\text{core}} | \hat{a}_i^x(D)^\dagger \hat{a}_j^x(D) | \Psi_{x,D}^{0,\text{core}} \rangle \\ &\quad + \frac{1}{2} \sum_{i,j,k,l=2L_x+1}^L [V^x(D)]_{ijkl} \langle \Psi_{x,D}^{0,\text{core}} | \hat{a}_i^x(D)^\dagger \hat{a}_j^x(D)^\dagger \hat{a}_l^x(D) \hat{a}_k^x(D) | \Psi_{x,D}^{0,\text{core}} \rangle. \end{aligned} \quad (2.39)$$

### 2.7.3 Proof of Lemma 2.8

The first assertion is a direct consequence of [21, Theorem 6].

We now prove the second assertion. Let

$$\mathcal{K} := \{P = (P_1, P_2) \in \mathbb{R}_{\text{sym}}^{L_1 \times L_1} \times \mathbb{R}_{\text{sym}}^{L_2 \times L_2} \mid \forall 0 < n < 1, \dim(\text{Ker}(P_1 - n)) = \dim(\text{Ker}(P_2 - (1 - n)))\}.$$

Let  $P = (P_1, P_2) \in \text{Bd}(\mathcal{D})$  and  $D \in \mathcal{D}$  be such that  $\text{Bd}(D) = P$ . Let  $U_1$  and  $U_2$  be two orthogonal matrices of sizes  $(L_1 \times L_1)$  and  $(L_2 \times L_2)$  respectively, and  $D_1 = \text{diag}(m_1, \dots, m_{L_1})$  and  $D_2 = \text{diag}(m'_1, \dots, m'_{L_2})$  two diagonal matrices with entries in the range  $[0, 1]$  ranked such that  $m_1 \geq \dots \geq m_{L_1}$  and  $m'_1 \leq \dots \leq m'_{L_2}$ , such that  $P_1 = U_1 D_1 U_1^T$  and  $P_2 = U_2 D_2 U_2^T$ . It holds

$$D = \begin{pmatrix} U_1 & 0 \\ 0 & U_2 \end{pmatrix} \begin{pmatrix} D_1 & C \\ C^T & D_2 \end{pmatrix} \begin{pmatrix} U_1^T & 0 \\ 0 & U_2^T \end{pmatrix} \quad \text{for some } C \in \mathbb{R}^{L_1 \times L_2}.$$

The condition  $D^2 = D$  reads

$$CC^T = D_1 - D_1^2, \quad C^T C = D_2 - D_2^2, \quad C - D_1 C - C D_2 = 0,$$

that is

$$\forall 1 \leq i \leq L_1, \quad \forall 1 \leq j \leq L_2, \quad \sum_{k=1}^{L_2} C_{ik}^2 = m_i - m_i^2, \quad \sum_{k=1}^{L_1} C_{kj}^2 = m'_j - m'^2_j, \quad (1 - m_i - m'_j)C_{ij} = 0.$$

This implies that  $C_{ij} = 0$  unless  $m'_j = 1 - m_j$  and that  $C_{ij} = 0$  whenever  $m_i = 0$  or 1, or  $m'_j = 0$  or 1. It follows that

$$\begin{aligned} & \begin{pmatrix} U_1^T & 0 \\ 0 & U_2^T \end{pmatrix} D \begin{pmatrix} U_1 & 0 \\ 0 & U_2 \end{pmatrix} \\ &= \left( \begin{array}{cc|cc} I_{r_1} & & & \\ & n_1 I_{d_1} & & C_1 \\ & & \ddots & \ddots \\ & & n_\ell I_{d_\ell} & C_\ell \\ \hline & & 0_{s_1} & \\ & C_1^T & 0_{s_2} & (1 - n_1)I_{d'_1} \\ & & & \ddots \\ & C_\ell^T & & (1 - n_\ell)I_{d'_\ell} \\ & & & I_{r_2} \end{array} \right), \end{aligned} \quad (2.40)$$

with  $0 < n_\ell < \dots < n_1 < 1$ . Using again the idempotency of  $D$ , we obtain the relations  $C_j C_j^T = n_j(1 - n_j)I_{d_j}$  and  $C_j^T C_j = n_j(1 - n_j)I_{d'_j}$ . Taking the trace leads to  $d_j = d'_j$ . Therefore,  $P \in \mathcal{K}$  so that  $\text{Bd}(\mathcal{D}) \subset \mathcal{K}$ .

Conversely, let  $P \in \mathcal{K}$  and  $U_1, U_2, D_1, D_2$  as before. Then  $U_1^T P_1 U_1$  and  $U_2^T P_2 U_2$  read as the diagonal blocks of the right-hand side of (2.40) with  $d_j = d'_j$  for all  $j$ . Setting  $C_j = \sqrt{n_j(1 - n_j)}I_{d_j}$ , the matrix  $D$  defined by (2.40) is in  $\mathcal{M}_{\mathcal{S}}$  and satisfies  $\text{Bd}(D) = P$ . Hence,  $P \in \text{Bd}(\mathcal{D})$  and therefore  $\mathcal{K} \subset \text{Bd}(\mathcal{D})$ .

### 2.7.4 Proof of Lemma 2.10

Let  $N_v := L - N$ . For  $X \in \mathbb{R}^{N_v \times N}$  such that  $\|X\| < 1/2$ , we set

$$f_\Phi(X) := \Phi \begin{pmatrix} \frac{1}{2}(I_N + (I_N - 4X^T X)^{1/2}) & X^T \\ X & \frac{1}{2}(I_{N_v} - (I_{N_v} - 4XX^T)^{1/2}) \end{pmatrix} \Phi^T,$$

$$g_\Phi(X) := \text{Bd}(f_\Phi(X)).$$

The map  $f_\Phi$  provides a local system of coordinates of  $\mathcal{D}$  in the vicinity of  $D$ . Therefore, the local  $N$ -representability condition is satisfied at  $D$  if and only if the map

$$d_0 g_\Phi : \mathbb{R}^{N_v \times N} \ni X \mapsto d_0 g_\Phi = \sum_{x=1}^{N_f} \Pi_x \Phi \begin{pmatrix} 0 & X^T \\ X & 0 \end{pmatrix} \Phi^T \Pi_x \in \mathcal{Y}$$

is surjective. This proves the equivalence between the first and third assertions of the lemma.

Writing  $\Phi$  as  $\Phi = (\Phi^{\text{occ}} | \Phi^{\text{virt}})$  with  $\Phi^{\text{occ}} \in \mathbb{R}^{L \times N}$  and  $\Phi^{\text{virt}} \in \mathbb{R}^{L \times N_v}$ , the adjoint of  $d_0 g_\Phi$  is given by

$$d_0 g_\Phi^* : \mathcal{Y} \ni Y \mapsto d_0 g_\Phi^*(Y) = 2\Phi^{\text{virt}}{}^T Y \Phi^{\text{occ}} \in \mathbb{R}^{N_v \times N}.$$

We therefore have for all  $Y \in \mathcal{Y}$ ,

$$(d_0 g_\Phi d_0 g_\Phi^*)Y = 2 \sum_{x=1}^{N_f} \Pi_x ((1-D)YD + DY(1-D)) \Pi_x, \quad (2.41)$$

and therefore

$$\begin{aligned} \|d_0 g_\Phi^*(Y)\|^2 &= \text{Tr}(Y(d_0 g_\Phi d_0 g_\Phi^*)(Y)) = 2\text{Tr}\left(Y \sum_{x=1}^{N_f} \Pi_x ((1-D)YD + DY(1-D)) \Pi_x\right) \\ &= 2\text{Tr}\left(\sum_{x=1}^{N_f} \Pi_x Y \Pi_x ((1-D)YD + DY(1-D))\right) \\ &= 2\text{Tr}(Y((1-D)YD + DY(1-D))) = 4\|(1-D)YD\|^2. \end{aligned}$$

Thus

$$\forall Y \in \mathcal{Y}, \quad \|d_0 g_\Phi^*(Y)\| = 2\|(1-D)YD\|.$$

The map  $d_0 g_\Phi$  is surjective if and only if its adjoint is injective. Thus the criterion is satisfied if and only if

$$\forall Y \in \mathcal{Y}, \quad (1-D)YD = 0 \quad \Rightarrow \quad Y = 0.$$

As  $D$  is an orthogonal projector,  $(1-D)YD = 0$  if and only if  $Y$  commutes with  $D$ . In addition, a matrix  $Y \in \mathbb{R}_{\text{sym}}^{L \times L}$  is in  $\mathcal{Y}$  if and only if (i) it commutes with all the  $\Pi_x$ 's, and (ii) its trace is equal to 0. Thus, the criterion is satisfied if and only if any zero trace matrix  $Y \in \mathbb{R}_{\text{sym}}^{L \times L}$  commuting with  $D$  and the  $\Pi_x$ 's is the null matrix. Lastly, this condition is equivalent to: any matrix  $Y \in \mathbb{R}_{\text{sym}}^{L \times L}$  commuting with  $D$  and the  $\Pi_x$ 's is of the form  $\lambda I_L$  for some  $\lambda \in \mathbb{R}$ . This completes the proof of the second statement.

### 2.7.5 Proof of Proposition 2.1

For  $\alpha = 0$ , the low-level map is formally given by

$$F_0^{\text{LL}}(P) = \underset{D \in \mathcal{D}, \text{Bd}(D)=P}{\text{argmin}} \text{Tr}(hD) \quad (\text{formal}). \quad (2.42)$$

Under Assumption (A1) (i.e.  $\varepsilon_N < 0 < \varepsilon_{N+1}$ ),  $D_0$  is the unique minimizer of

$$\underset{D \in \mathcal{D}}{\text{argmin}} \text{Tr}(hD).$$

Since  $\text{Bd}(D_0) = P_0$  (by definition of  $P_0$ ),  $D_0$  is the unique minimizer of (2.42) for  $P = P_0$ . Thus,  $P_0$  is in the domain of  $F_0^{\text{LL}}$  and  $F_0^{\text{LL}}(P_0) = D_0$ .

For  $\alpha = 0$ , the high-level map takes the simple formal expression

$$F_0^{\text{HL}}(D) = \sum_{x=1}^{N_f} \Pi_x C^x(D) \mathbf{1}_{(-\infty, 0]} (C^x(D)^T (h - \mu \Pi_x) C^x(D)) C^x(D)^T \Pi_x \quad (\text{formal}),$$

where  $C^x(D)$  is defined in (2.28) and  $\mu \in \mathbb{R}$  is such that

$$\sum_{x=1}^{N_f} \text{Tr} (\Pi_x C^x(D) \mathbf{1}_{(-\infty, 0]} (C^x(D)^T (h - \mu \Pi_x) C^x(D)) C^x(D)^T \Pi_x) = N.$$

Therefore, a matrix  $D \in \mathcal{D}$  is in the domain of  $F_0^{\text{HL}}$  if and only if

1. the set

$$M_D := \left\{ \mu \in \mathbb{R} \mid \sum_{x=1}^{N_f} \text{Tr} (\Pi_x C^x(D) \mathbf{1}_{(-\infty, 0]} (C^x(D)^T (h - \mu \Pi_x) C^x(D)) C^x(D)^T \Pi_x) = N \right\}$$

is non-empty;

2. the function

$$\mathcal{F}_D : M_D \ni \mu \mapsto \sum_{x=1}^{N_f} \Pi_x C^x(D) \mathbf{1}_{(-\infty, 0]} (C^x(D)^T (h - \mu \Pi_x) C^x(D)) C^x(D)^T \Pi_x \in \mathbb{R}_{\text{sym}}^{L \times L}$$

is constant over  $M_D$ . Its value is an element of  $\mathcal{P}$ , which we denote by  $F_0^{\text{HL}}(D)$ .

Let us prove that under Assumptions (A1) and (A2),  $D_0$  belongs to the domain of  $F_0^{\text{HL}}$  and  $F_0^{\text{HL}}(D_0) = P_0$ .

First, we observe that for each  $1 \leq x \leq N_f$ , the space  $W_{x,0} := X_x + D_0 X_x$  is  $D_0$ -invariant since  $D_0$  is a projector. The linear operator  $D_0$  on  $\mathbb{R}^L$  therefore has a block-diagonal operator representation in the decomposition  $W_{x,0} \oplus W_{x,0}^\perp$  of  $\mathcal{H} = \mathbb{R}^L$ :

$$D_0 \equiv \begin{pmatrix} D_0^x & 0 \\ 0 & \widetilde{D}_0^x \end{pmatrix} \quad (\text{in the decomposition } \mathcal{H} = W_{x,0} \oplus W_{x,0}^\perp),$$

where  $D_0^x$  and  $\widetilde{D}_0^x$  are both orthogonal projectors. The corresponding representation of  $h$  is not necessarily block-diagonal:

$$h \equiv \begin{pmatrix} h^x & h_{\text{OD}}^x \\ h_{\text{OD}}^x & h^x \end{pmatrix} \quad (\text{in the decomposition } \mathcal{H} = W_{x,0} \oplus W_{x,0}^\perp).$$

Let us now focus on the operator  $h^x$ . To lighten the notation, we set

$$D_{0,x} := E_x^T D_0 E_x.$$

We infer from Assumption (A2) and Lemma 2.6 that  $\dim(D_0 X_x) = \dim((1 - D_0) X_x) = L_x$  and

$$C_0^x := C^x(D_0) = \left( D_0 E_x D_{0,x}^{-1/2} | (1 - D_0) E_x (1 - D_{0,x})^{-1/2} \right)$$

forms an orthonormal basis of  $W_{x,0}$ . In this basis, the operator  $h^x$  is represented by the matrix

$$\mathfrak{h}^x := C_0^{x,T} h C_0^x = \begin{pmatrix} \mathfrak{h}_-^x & 0 \\ 0 & \mathfrak{h}_+^x \end{pmatrix}, \quad (2.43)$$

with

$$\mathfrak{h}_-^x := D_{0,x}^{-1/2} E_x^T D_0 h D_0 E_x D_{0,x}^{-1/2}, \quad (2.44)$$

$$\mathfrak{h}_+^x := (1 - D_{0,x})^{-1/2} E_x^T (1 - D_0) h (1 - D_0) E_x (1 - D_{0,x})^{-1/2}. \quad (2.45)$$

The zeros in the off-diagonal blocks of  $\mathfrak{h}^x$  come from the fact that  $D_0 h(1 - D_0) = (1 - D_0)hD_0 = 0$  since  $h$  and  $D_0$  commute. In addition, we have

$$\varepsilon_1 D_0 \leq D_0 h D_0 = \sum_{i=1}^N \varepsilon_i \phi_i \phi_i^T \leq \varepsilon_N D_0, \quad (2.46)$$

$$\varepsilon_{N+1}(1 - D_0) \leq (1 - D_0)h(1 - D_0) = \sum_{a=N+1}^L \varepsilon_a \phi_a \phi_a^T \leq \varepsilon_L(1 - D_0). \quad (2.47)$$

Combining (2.44) and (2.46) on the one hand, and (2.45) and (2.47) on the other hand, we obtain

$$\varepsilon_1 I_{L_x} \leq \mathfrak{h}_-^x \leq \varepsilon_N I_{L_x} \quad \text{and} \quad \varepsilon_{N+1} I_{L_x} \leq \mathfrak{h}_+^x \leq \varepsilon_L I_{L_x}. \quad (2.48)$$

We therefore have

$$\mathbf{1}_{(-\infty, 0]}(\mathfrak{h}^x) = \mathbf{1}_{(-\infty, 0]}(\mathfrak{h}^x) = \begin{pmatrix} I_{L_x} & 0 \\ 0 & 0 \end{pmatrix}, \quad \mathbf{1}_{[0, \infty)}(\mathfrak{h}^x) = \mathbf{1}_{(0, \infty)}(\mathfrak{h}^x) = \begin{pmatrix} 0 & 0 \\ 0 & I_{L_x} \end{pmatrix}, \quad (2.49)$$

and thus

$$\begin{aligned} \sum_{r=1}^{N_f} \Pi_x C_0^x \mathbf{1}_{(-\infty, 0]}(\mathfrak{h}^x) C_0^{xT} \Pi_x &= \sum_{r=1}^{N_f} \Pi_x C_0^x \begin{pmatrix} I_{L_x} & 0 \\ 0 & 0 \end{pmatrix} C_0^{xT} \Pi_x \\ &= \sum_{r=1}^{N_f} (E_x E_x^T) D_0 E_x D_{0,x}^{-1} E_x^T D_0 (E_x E_x^T) \\ &= \sum_{r=1}^{N_f} \Pi_x D_0 \Pi_x = \text{Bd}(D_0) = P_0. \end{aligned}$$

As  $\text{Tr}(P_0) = N$ , we have  $0 \in M_{D_0}$  and  $\mathcal{F}_{D_0}(0) = P_0$ . Let us now show that  $M_{D_0} = \{0\}$ . It holds

$$\Pi_x \equiv \begin{pmatrix} \Pi_x^x & 0 \\ 0 & 0 \end{pmatrix} \quad (\text{in the decomposition } \mathcal{H} = W_{x,0} \oplus W_{x,0}^\perp),$$

and in the basis defined of  $W_{x,0}$  defined by  $C_0^x$ , the orthogonal projector  $\Pi_x^x$  is represented by the matrix

$$\mathfrak{p}^x := C_0^{xT} \Pi_x C_0^x = \begin{pmatrix} D_{0,x} & D_{0,x}^{1/2} (1 - D_{0,x})^{1/2} \\ (1 - D_{0,x})^{1/2} D_{0,x}^{1/2} & (1 - D_{0,x}) \end{pmatrix}. \quad (2.50)$$

We therefore have in particular  $\mathfrak{p}^{x^2} = \mathfrak{p}^x = \mathfrak{p}^{xT}$ . Consider the function

$$\begin{aligned} \mathbb{R} \ni \mu \mapsto \zeta(\mu) &:= \sum_{x=1}^{N_f} \text{Tr} \left( \Pi_x C_x^0 \mathbf{1}_{(-\infty, 0]} \left( C_x^{0T} (h - \mu \Pi_x) C_x^0 \right) C_x^{0T} \Pi_x \right) \\ &= \sum_{x=1}^{N_f} \text{Tr} \left( \mathfrak{p}^x \mathbf{1}_{(-\infty, 0]} (\mathfrak{h}^x - \mu \mathfrak{p}^x) \right) \\ &= \sum_{x=1}^{N_f} \text{Tr} \left( \mathfrak{p}^x \mathbf{1}_{(-\infty, 0]} (\mathfrak{h}^x - \mu \mathfrak{p}^x) \mathfrak{p}^x \right) \geq 0. \end{aligned}$$

We already know that  $\zeta(0) = N$ . We see from (2.48) that 0 is not in the spectrum of  $\mathfrak{h}$  for all  $x$ . By a simple continuity argument, we obtain that for  $|\mu|$  small enough, 0 is not in the spectrum of  $\mathfrak{h}^x - \mu \mathfrak{p}^x$  for all  $x$ . We therefore have

$$\zeta(\mu) = \sum_{x=1}^{N_f} \frac{1}{2\pi i} \oint_{\mathcal{C}} \text{Tr} \left( \mathfrak{p}^x (z - (\mathfrak{h}^x - \mu \mathfrak{p}^x))^{-1} \right) dz \quad (\text{for } |\mu| \text{ small enough}), \quad (2.51)$$

where  $\mathcal{C}$  is e.g. a circle in the complex plane, centered on the negative real axis, containing 0 and of large enough radius. It follows that  $\zeta$  is analytic in the vicinity of 0 and that

$$\zeta'(0) = - \sum_{x=1}^{N_f} \frac{1}{2\pi i} \oint_{\mathcal{C}} \text{Tr} \left( \mathfrak{p}^x (z - \mathfrak{h}^x)^{-1} \mathfrak{p}^x (z - \mathfrak{h}^x)^{-1} \right) dz = \sum_{x=1}^{N_f} \langle \mathfrak{p}^x, \mathfrak{L}_x^+ \mathfrak{p}^x \rangle, \quad (2.52)$$

where  $\mathfrak{L}_x^+$  is the linear operator on  $\mathbb{R}_{\text{sym}}^{2L_x \times 2L_x}$  defined by

$$\forall M \in \mathbb{R}_{\text{sym}}^{2L_x \times 2L_x}, \quad \mathfrak{L}_x^+ M = -\frac{1}{2\pi i} \oint_{\mathcal{C}} (z - \mathfrak{h}^x)^{-1} M (z - \mathfrak{h}^x)^{-1} dz, \quad (2.53)$$

which can alternatively be defined by the linear response formula

$$\mathbf{1}_{(-\infty, 0]}(\mathfrak{h}^x + M) = \mathbf{1}_{(-\infty, 0]}(\mathfrak{h}^x) - \mathfrak{L}_x^+ M + o(\|M\|). \quad (2.54)$$

Let us diagonalize the real symmetric matrix  $\mathfrak{h}^x$  as

$$\mathfrak{h}^x = \sum_{n=1}^{2L_x} \tilde{\varepsilon}_{x,n} \tilde{\phi}_{x,n} \tilde{\phi}_{x,n}^T \quad \text{with} \quad \tilde{\varepsilon}_{x,1} \leq \dots \leq \tilde{\varepsilon}_{x,2L_x}, \quad \tilde{\phi}_{x,m}^T \tilde{\phi}_{x,n} = \delta_{mn},$$

with (using (2.48))

$$\forall 1 \leq i \leq L_x, \quad \forall L_x \leq a \leq 2L_x, \quad \tilde{\varepsilon}_{x,i} \leq \varepsilon_N < 0 < \varepsilon_{N+1} \leq \tilde{\varepsilon}_{x,a}.$$

Using Cauchy residue formula, we get

$$\forall M = \begin{pmatrix} M^{--} & M^{+-} \\ M^{+-} & M_{++} \end{pmatrix} \in \mathbb{R}_{\text{sym}}^{2L_x \times 2L_x}, \quad \mathfrak{L}_x^+ M = \begin{pmatrix} 0 & N(M^{+-})^T \\ N(M^{+-}) & 0 \end{pmatrix} \quad (2.55)$$

with

$$\forall 1 \leq m, n \leq L_x, \quad [N(M^{+-})]_{mn} = \frac{[M^{+-}]_{mn}}{\tilde{\varepsilon}_{x,m+L_x} - \tilde{\varepsilon}_{x,n}}. \quad (2.56)$$

The operator  $\mathfrak{L}_x^+$  is self-adjoint and positive. Denoting by  $\gamma := \varepsilon_{N+1} - \varepsilon_N > 0$  the HOMO-LUMO gap, we have

$$\forall M = \begin{pmatrix} M^{--} & M^{-+} \\ M^{+-} & M_{++} \end{pmatrix} \in \mathbb{R}_{\text{sym}}^{2L_x \times 2L_x}, \quad \langle M, \mathfrak{L}_x^+ M \rangle \geq 2\gamma^{-1} \|M^{-+}\|^2. \quad (2.57)$$

Indeed, we have

$$\begin{aligned} \langle M, \mathfrak{L}_x^+ M \rangle &= 2 \sum_{x=1}^{N_f} \sum_{i=1}^{L_x} \sum_{a=L_x+1}^{2L_x} \frac{|\tilde{\phi}_{x,i}^T M \tilde{\phi}_{x,a}|^2}{\tilde{\varepsilon}_{x,a} - \tilde{\varepsilon}_{x,i}} \geq 2\gamma^{-1} \sum_{x=1}^{N_f} \sum_{i=1}^{L_x} \sum_{a=L_x+1}^{2L_x} |\tilde{\phi}_{x,i}^T M \tilde{\phi}_{x,a}|^2 \\ &= 2\gamma^{-1} \|\mathbf{1}_{(-\infty, 0)}(\mathfrak{h}^x) M \mathbf{1}_{(0, +\infty)}(\mathfrak{h}^x)\|^2 = 2\gamma^{-1} \|M^{-+}\|^2. \end{aligned}$$

Let

$$\mathcal{J}_0 := \left\{ \mu \in \mathbb{R} \mid \prod_{x=1}^{N_f} \det(\mathfrak{h}^x - \mu \mathfrak{p}^x) = 0 \right\}.$$

Since  $\mu \mapsto \det(\mathfrak{h}^x - \mu \mathfrak{p}^x)$  is a polynomial of degree  $L_x$ , the set  $\mathcal{J}_0$  contains at most  $L$  elements. By similar arguments as above, the function  $\zeta$  is real-analytic and non-decreasing on each connected components of  $\mathbb{R} \setminus \mathcal{J}_0$ . At each  $\mu_0 \in \mathcal{J}_0$ , the jump of  $\zeta$  is given by

$$\zeta(\mu_0 + 0) - \zeta(\mu_0 - 0) = \sum_{x=1}^{N_f} \text{Tr}(\mathfrak{p}^x \mathbf{1}_{\{0\}} (\mathfrak{h}^x - \mu_0 \mathfrak{p}^x) \mathfrak{p}^x) \geq 0.$$

The function  $\zeta$  is therefore nondecreasing on  $\mathbb{R}$ . As a consequence, the set  $M_{D_0}$  is an interval  $I_{D_0}$  containing 0. Using (2.50), (2.52) and (2.57), we get

$$\zeta'(0) \geq 2\gamma^{-1} \sum_{x=1}^{N_f} \|D_{0,x}^{1/2} (1 - D_{0,x})^{1/2}\|^2 = 2\gamma^{-1} \sum_{x=1}^{N_f} \text{Tr}(D_{0,x} (1 - D_{0,x})) > 0,$$

since, in view of Lemma 2.6, all the eigenvalues of the symmetric matrix  $D_{0,x} (1 - D_{0,x})$  are positive. Thus  $M_{D_0} = \{0\}$ . This proves that  $D_0$  is in the domain of  $F_0^{\text{HL}}$  and that  $F_0^{\text{HL}}(D_0) = P_0$ .

Combining this result with the previously established relation  $F_0^{\text{LL}}(P_0) = D_0$ , we obtain that  $P_0$  is a fixed point of the DMET map for  $\alpha = 0$ .

### 2.7.6 Proof of Theorem 2.4

We endow  $\mathcal{D}$  with the Riemannian metric induced by the Frobenius inner product on  $\mathbb{R}_{\text{sym}}^{L \times L}$ . For  $\eta > 0$ , we set

$$\omega_\eta := \{P \in \mathcal{P} \mid \|P - P_0\| < \eta\} \quad \text{and} \quad \Omega_\eta := \{D \in \mathcal{D} \mid \|D - D_0\| < \eta\}.$$

#### Low-level map in the perturbative regime

Let us introduce the maps

$$\begin{aligned} g : \mathcal{D} &\rightarrow \mathcal{Y} & \text{s.t. } \forall D \in \mathcal{D}, \quad g(D) := \text{Bd}(D) - P_0, \\ a : \mathcal{D} &\rightarrow \mathbb{R} & \text{s.t. } \forall D \in \mathcal{D}, \quad a(D) := \text{Tr}(hD), \\ b : \mathcal{D} &\rightarrow \mathbb{R} & \text{s.t. } \forall D \in \mathcal{D}, \quad b(D) := \frac{1}{2} \text{Tr}((J(D) - K(D))D), \\ E : \mathbb{R} \times \mathcal{D} &\rightarrow \mathbb{R} & \text{s.t. } \forall (\alpha, D) \in \mathbb{R} \times \mathcal{D}, \quad E(\alpha, D) := \mathcal{E}_\alpha^{\text{HF}}(D) = a(D) + \alpha b(D). \end{aligned}$$

Since the maps  $\text{Bd}, J, K : \mathbb{R}_{\text{sym}}^{L \times L} \rightarrow \mathbb{R}_{\text{sym}}^{L \times L}$  are linear, the maps  $g, a, b$  and  $E$  are real-analytic. With this notation, we have

$$(\text{Assumption (A3)}) \iff (B := d_{D_0}g = \text{Bd} : T_{D_0}\mathcal{D} \rightarrow \mathcal{Y} \text{ surjective}).$$

**Lemma 2.11** (Low-level map in the perturbative regime). *Under Assumptions (A1)-(A3), there exists  $\alpha_{\text{LL}} > 0$  and  $0 < \eta_{\text{LL}} < \frac{1}{2}$  such that*

1.  $\omega_{\eta_{\text{LL}}} \subset \text{Dom}(F_\alpha^{\text{LL}})$  for all  $\alpha \in (-\alpha_{\text{LL}}, \alpha_{\text{LL}})$ ;
2. the function  $(\alpha, P) \mapsto F_\alpha^{\text{LL}}(P)$  is real-analytic on  $(-\alpha_{\text{LL}}, \alpha_{\text{LL}}) \times \omega_{\eta_{\text{LL}}}^\mathcal{Y}$ .

*Proof.* The first assertion means that for all  $(\alpha, P) \in (-\alpha_{\text{LL}}, \alpha_{\text{LL}}) \times \omega_{\eta_{\text{LL}}}$ , the problem

$$\min_{D \in \mathcal{D} \mid \text{Bd}(D)=P} \mathcal{E}_\alpha^{\text{HF}}(D) = \min_{D \in \mathcal{D} \mid g(D)=P-P_0} E(\alpha, D) \quad (2.58)$$

has a unique minimizer, which we denote by  $F_\alpha^{\text{LL}}(P)$ .

Using Lemma 2.10 and the submersion theorem, we deduce from Assumptions (A2)-(A3) that there exists  $\eta > 0$  and  $C \in \mathbb{R}_+$  such that for all  $P \in \omega_\eta$ , the set  $\text{Bd}^{-1}(P)$  is nonempty and there exists  $D_P \in \text{Bd}^{-1}(P)$  such that  $\|D_P - D_0\| \leq C\|P - P_0\|$ . Let  $D_{\alpha,P}$  be a minimizer of  $\mathcal{E}_\alpha^{\text{HF}}$  on  $\text{Bd}^{-1}(P)$ . Such a minimizer exists since  $\mathcal{E}_\alpha^{\text{HF}}$  is continuous on  $\mathcal{D}$  and  $\text{Bd}^{-1}(P)$  is a nonempty compact subset of  $\mathcal{D}$ , and satisfies the optimality conditions

$$\nabla_{\mathcal{D}} E(\alpha, D_{\alpha,P}) + d_{D_{\alpha,P}} g^* \Lambda_{\alpha,P} = 0, \quad g(D_{\alpha,P}) = P - P_0, \quad (2.59)$$

where  $\nabla_{\mathcal{D}} E(\alpha, D_{\alpha,P}) \in T_{D_{\alpha,P}}\mathcal{D}$  is the gradient at  $D_{\alpha,P}$  of the function  $\mathcal{D} \ni D \mapsto E(\alpha, D) \in \mathbb{R}$  for the Riemannian metric induced with the Frobenius inner product, and  $\Lambda_{\alpha,P} \in \mathcal{Y}$  the Lagrange multiplier of the constraint  $g(D_{\alpha,P}) = P - P_0$ .

Denoting by

$$C_{\text{nl}} := \frac{1}{2} \max_{D \in \mathcal{D}} |\text{Tr}((J(D) - K(D))D)|,$$

we have

$$\mathcal{E}_\alpha^{\text{HF}}(D_{\alpha,P}) \leq \mathcal{E}_\alpha^{\text{HF}}(D_P) \leq \mathcal{E}_0^{\text{HF}}(D_P) + \alpha C_{\text{nl}} \leq \mathcal{E}_0^{\text{HF}}(D_0) + \|h\| \|P - P_0\| + \alpha C_{\text{nl}}. \quad (2.60)$$

To obtain a lower bound of  $\mathcal{E}_\alpha^{\text{HF}}(D_{\alpha,P})$ , we use that

$$\forall D \in \mathcal{D}, \quad \mathcal{E}_0^{\text{HF}}(D) = \text{Tr}(hD) \geq \mathcal{E}_0^{\text{HF}}(D_0) + \frac{\gamma}{2} \|D - D_0\|^2.$$

This inequality is classical, but we recall its proof for the sake of completeness. For  $M \in \mathbb{R}_{\text{sym}}^{L \times L}$  we set

$$M^{--} := D_0 M D_0, \quad M^{-+} := D_0 M (1 - D_0), \quad M^{+-} := (1 - D_0) M D_0, \quad M^{++} := (1 - D_0) M (1 - D_0).$$

Let  $D \in \mathcal{D}$  and  $Q := D - D_0$ . Since  $D_0 = \mathbf{1}_{(-\infty, 0]}(h)$ , we have

$$h^{-+} = h^{+-} = 0, \quad h^{--} \leq \varepsilon_N, \quad h^{++} \geq \varepsilon_{N+1}, \quad Q^{++} \geq 0, \quad Q^{--} \leq 0,$$

and we deduce from the fact that both  $D$  and  $D_0$  are rank- $N$  orthogonal projectors that

$$Q^2 = Q^{++} - Q^{--} \quad \text{and} \quad \text{Tr}(Q^{++}) + \text{Tr}(Q^{--}) = 0.$$

Combining all the above properties, we obtain

$$\begin{aligned} \forall D \in \mathcal{D}, \quad a(D) &= \text{Tr}(hD) \\ &= \text{Tr}(hD_0) + \text{Tr}(h(D - D_0)) \\ &= a(D_0) + \text{Tr}(h^{++}Q^{++}) + \text{Tr}(h^{--}Q^{--}) \\ &\geq a(D_0) + \varepsilon_{N+1}\text{Tr}(Q^{++}) + \varepsilon_N\text{Tr}(Q^{--}) \\ &= a(D_0) + \frac{\gamma}{2}\text{Tr}(Q^{++} - Q^{--}) \\ &= a(D_0) + \frac{\gamma}{2}\|D - D_0\|^2. \end{aligned} \tag{2.61}$$

As  $\mathcal{E}_0^{\text{HF}}(D) = a(D)$ , this implies that

$$\mathcal{E}_\alpha^{\text{HF}}(D_{\alpha,P}) \geq \mathcal{E}_0^{\text{HF}}(D_{\alpha,P}) - \alpha C_{\text{nl}} \geq \mathcal{E}_0^{\text{HF}}(D_0) + \frac{\gamma}{2}\|D_{\alpha,P} - D_0\|^2 - \alpha C_{\text{nl}}.$$

Combining this result with (2.60), we obtain

$$\|D_{\alpha,P} - D_0\|^2 \leq 2\gamma^{-1}(2\alpha C_{\text{nl}} + \|h\|P - P_0\|).$$

This implies in particular that for  $|\alpha|$  and  $\|P - P_0\|$  small enough, any minimizer  $D_{\alpha,P}$  of (2.58) is close to  $D_0$ . To conclude, it suffices to prove that for  $|\alpha|$  and  $\|P - P_0\|$  small enough, (2.59) has a unique critical point close to  $D_0$ . This leads us to introduce the function

$$\Theta : (\mathbb{R} \times \mathcal{P}) \times (\mathcal{D} \times \mathcal{Y}) \ni ((\alpha, P), (D, \Lambda)) \mapsto \Theta((\alpha, P), (D, \Lambda)) \in T_D \mathcal{D} \times \mathcal{Y}$$

defined by

$$\Theta((\alpha, P), (D, \Lambda)) := (\nabla_{\mathcal{D}} E(\alpha, D) + (d_D g)^* \Lambda, g(D) - (P - P_0)).$$

As  $D_0$  is the unique minimizer of  $D \mapsto E(0, D)$  on  $\mathcal{D}$  and  $P_0 = \text{Bd}(D_0)$ , we have  $\nabla_{\mathcal{D}} E(0, D_0) = 0$  and  $g(D_0) = 0$ , so that

$$\Theta((0, P_0), (D_0, 0)) = (0, 0).$$

In addition, denoting by

$$A := D_{\mathcal{D}}^2 a(D_0) : T_{D_0} \mathcal{D} \rightarrow T_{D_0} \mathcal{D} \tag{2.62}$$

the Hessian at  $D_0$  of the function  $a$  for the Riemannian metric induced by the Frobenius inner product, we have

$$\forall (Q, \Lambda) \in T_{D_0} \mathcal{D} \times \mathcal{Y}, \quad [d_{D,\Lambda} \Theta((0, P_0), (D_0, 0))] \begin{pmatrix} Q \\ \Lambda \end{pmatrix} = \begin{pmatrix} A & B^* \\ B & 0 \end{pmatrix} \begin{pmatrix} Q \\ \Lambda \end{pmatrix},$$

where we recall that  $B := d_{D_0} g$ . In view of (2.61), we have

$$\forall Q \in T_{D_0} \mathcal{D}, \quad \langle Q, AQ \rangle \geq \gamma \|Q\|^2. \tag{2.63}$$

Since  $A$  is coercive and  $B : T_{D_0} \mathcal{D} \rightarrow \mathcal{Y}$  is surjective, it follows from the Schur complement formula that the map

$$d_{D,\Lambda} \Theta((0, P_0), (D_0, 0)) : T_{D_0} \mathcal{D} \times \mathcal{Y} \rightarrow T_{D_0} \mathcal{D} \times \mathcal{Y}$$

is invertible. It follows from the real-analytic implicit function theorem on manifolds that there exists  $\alpha_{\text{LL}} > 0$ ,  $\eta > 0$  and  $\eta > 0$ , such that for all  $(\alpha, P) \in (-\alpha_{\text{LL}}, \alpha_{\text{LL}}) \times \omega_\eta$ , (2.59) has a unique solution  $(D_{\alpha,P}, \Lambda_{\alpha,P})$  with  $D_{\alpha,P} \in \omega_\eta$  and the map  $(\alpha, P) \mapsto D_{\alpha,P}$  is real-analytic on  $(-\alpha_{\text{LL}}, \alpha_{\text{LL}}) \times \omega_\eta$ .  $\square$

### High-level map in the perturbative regime

The following result states that the high-level map  $(\alpha, D) \mapsto F_\alpha^{\text{HL}}(D)$  is well-defined and real-analytic on a neighborhood of  $(0, D_0)$ .

**Lemma 2.12** (High-level map in the perturbative regime). *Under Assumptions (A1)-(A2), there exists  $\alpha_{\text{HL}} > 0$  and  $0 < \eta_{\text{HL}} < \frac{1}{2}$  such that*

1.  $\Omega_{\eta_{\text{HL}}} \subset \text{Dom}(F_\alpha^{\text{HL}})$  for all  $\alpha \in (-\alpha_{\text{HL}}, \alpha_{\text{HL}})$ ;
2. the function  $(\alpha, D) \mapsto F_\alpha^{\text{HL}}(D)$  is real-analytic on  $(-\alpha_{\text{HL}}, \alpha_{\text{HL}}) \times \Omega_{\eta_{\text{HL}}}$ .

*Proof.* For  $D \in \mathcal{D}$  compatible with the fragment decomposition, we set

$$[\tilde{h}_x(D)]_{\kappa\lambda} := \left[ \tilde{C}^x(D)^T h \tilde{C}^x(D) \right]_{\kappa\lambda} = \sum_{\kappa'\lambda'=1}^L [\tilde{C}^x(D)]_{\kappa,\kappa'} [\tilde{C}^x(D)]_{\lambda,\lambda'} h_{\kappa'\lambda'}, \quad (2.64)$$

$$[\tilde{V}_x(D)]_{\kappa\lambda\nu\xi} := \sum_{\kappa'\lambda'\nu'\xi'=1}^L [\tilde{C}^x(D)]_{\kappa,\kappa'} [\tilde{C}^x(D)]_{\lambda,\lambda'} [\tilde{C}^x(D)]_{\nu,\nu'} [\tilde{C}^x(D)]_{\xi,\xi'} V_{\kappa'\lambda'\nu'\xi'}, \quad (2.65)$$

where  $\tilde{C}^x(D)$  is defined in Lemma 2.6. Denoting by  $c_\kappa, c_\kappa^\dagger$ ,  $1 \leq \kappa \leq 2L_x$  the generators of the CAR algebra on  $\text{Fock}(\mathbb{R}^{2L_x})$  associated with the canonical basis of  $\mathbb{R}^{2L_x}$ , the high-level map can be formally written as

$$F_\alpha^{\text{HL}}(D) = \sum_{x=1}^{N_f} \sum_{\kappa,\lambda=1}^{L_x} e_{L'_x+\kappa} \text{Tr}_{\text{Fock}(\mathbb{R}^{2N_x})} (\Gamma_{\alpha,x,D,\mu} c_\kappa^\dagger c_\lambda) e_{L'_x+\lambda}^T \quad (\text{formal}), \quad (2.66)$$

where  $\Gamma_{\alpha,x,D,\mu} \in \mathcal{L}(\text{Fock}(\mathbb{R}^{2L_x}))$  is the ground-state (many-body) density matrix associated with the grand-canonical impurity Hamiltonian

$$\tilde{H}_{\alpha,x,D,\mu}^{\text{imp}} := \sum_{\kappa,\lambda=1}^{2L_x} [\tilde{h}_x(D)]_{\kappa\lambda} c_\kappa^\dagger c_\lambda + \alpha \sum_{\kappa,\lambda,\nu,\xi=1}^{2L_x} [\tilde{V}_x(D)]_{\kappa\lambda\nu\xi} c_\kappa^\dagger c_\lambda^\dagger c_\xi c_\nu - \mu \sum_{\kappa=1}^{L_x} c_\kappa^\dagger c_\kappa,$$

the parameter  $\mu \in \mathbb{R}$  being chosen such that

$$\sum_{x=1}^{N_f} \sum_{\kappa,\lambda=1}^{L_x} \text{Tr}_{\text{Fock}(\mathbb{R}^{2N_x})} (\Gamma_{\alpha,x,D,\mu} c_\kappa^\dagger c_\lambda) = N.$$

The results established in the proof of Proposition 2.1 can be rephrased as follows: under Assumptions (A1)-(A2),

1. the impurity Hamiltonian  $\tilde{H}_{0,x,D_0,0}^{\text{imp}}$  has a non-degenerate ground-state for each  $x$  and that it holds

$$\sum_{x=1}^{N_f} \sum_{\kappa,\lambda=1}^{L_x} \text{Tr}_{\text{Fock}(\mathbb{R}^{2N_x})} (\Gamma_{0,x,D_0,0} c_\kappa^\dagger c_\lambda) = N;$$

2. the function

$$\mathbb{R} \ni \mu \mapsto \sum_{x=1}^{N_f} \sum_{\kappa,\lambda=1}^{L_x} \text{Tr}_{\text{Fock}(\mathbb{R}^{2N_x})} (\Gamma_{0,x,D_0,\mu} c_\kappa^\dagger c_\lambda) \in \mathbb{R}$$

is non-decreasing, real-analytic in the neighborhood of  $\mu = 0$ , and its derivative at  $\mu = 0$  is positive.

Since the maps

$$\mathcal{D} \ni D \mapsto [\tilde{h}_x(D)]_{\kappa\lambda} \in \mathbb{R} \quad \text{and} \quad \mathcal{D} \ni D \mapsto [\tilde{V}_x(D)]_{\kappa\lambda\nu\xi} \in \mathbb{R}$$

are real-analytic in the neighborhood of  $D_0$ , we deduce from Kato's analytic perturbation theory and the implicit function theorem that there exists  $\alpha_{\text{HL}} > 0$ ,  $\eta_{\text{HL}} > 0$ , and  $\mu_{\text{HL}} > 0$  such that

1. for each  $(\alpha, D, \mu) \in (-\alpha_{\text{HL}}, \alpha_{\text{HL}}) \times \Omega_{\eta_{\text{HL}}} \times (-\mu_{\text{HL}}, \mu_{\text{HL}})$ , the impurity Hamiltonian  $H_{\alpha,x,D,\mu}^{\text{imp}}$  has a non-degenerate ground-state for each  $x$ ; we denote by  $\Gamma_{\alpha,x,D,\mu(\alpha,X)}$  the corresponding ground-state many-body density matrix;
2. for each  $(\alpha, D) \in (-\alpha_{\text{HL}}, \alpha_{\text{HL}}) \times \Omega_{\eta_{\text{HL}}}$ , there exists a unique  $\mu(\alpha, D) \in (-\mu_{\text{HL}}, \mu_{\text{HL}})$  such that

$$\sum_{x=1}^{N_f} \sum_{\kappa,\lambda=1}^{L_x} \text{Tr}_{\text{Fock}(\mathbb{R}^{2N_x})} (\Gamma_{\alpha,x,D,\mu(\alpha,D)} c_\kappa^\dagger c_\lambda) = N;$$

3. the maps  $(\alpha, D) \mapsto \mu(\alpha, D)$ ,  $(\alpha, D) \mapsto \Gamma_{\alpha, x, D, \mu(\alpha, D)}$ , and

$$(\alpha, D) \mapsto F_\alpha^{\text{HL}}(D) := \left( \sum_{x=1}^{N_f} \sum_{\kappa, \lambda=1}^{L_x} e_{L'_x + \kappa} \text{Tr}_{\text{Fock}(\mathbb{R}^{2N_x})} (\Gamma_{\alpha, x, D, \mu(\alpha, D)} c_\kappa^\dagger c_\lambda) e_{L'_x + \lambda}^T \right)$$

are real-analytic on  $(-\alpha_{\text{HL}}, \alpha_{\text{HL}}) \times \Omega_{\eta_{\text{HL}}}$ .

This proves the two assertions of Lemma 2.12.  $\square$

### Existence, uniqueness, and analyticity

We infer from Lemma 2.11 and Lemma 2.12 that there exist  $\alpha_{\text{DMET}} > 0$  and  $\eta_{\text{DMET}} > 0$  such that the function

$$(-\alpha_{\text{DMET}}, \alpha_{\text{DMET}}) \times \omega_{\eta_{\text{DMET}}} \ni \alpha, P \mapsto \Phi(\alpha, P) := F_\alpha^{\text{DMET}}(P) - P := F_\alpha^{\text{HL}}(F_\alpha^{\text{LL}}(P)) - P \in \mathcal{Y}$$

is well-defined and real-analytic, and we know from Proposition 2.1 that

$$\Phi(0, P_0) = 0.$$

To complete the proof of Theorem 2.4, we have to check that the function  $\Phi$  satisfies all the hypotheses of the implicit function theorem, namely that

$$d_P \Phi(0, P_0) = (d_{D_0} F_0^{\text{HL}})(d_{P_0} F_0^{\text{LL}}) - I_{\mathcal{Y}} : \mathcal{Y} \rightarrow \mathcal{Y} \quad (2.67)$$

is invertible.

Let us first compute  $d_{P_0} F_0^{\text{LL}} : \mathcal{Y} \rightarrow T_{D_0} \mathcal{D}$ . Differentiating the equality

$$\forall P \in \omega_\eta, \quad \Theta((0, P), (F_0^{\text{LL}}(P), \Lambda_{0, P})) = (0, 0),$$

we obtain that the derivatives at  $P_0$  of the functions  $\omega_\eta \ni P \mapsto F_0^{\text{LL}}(P) \in \mathcal{D}$  and  $\omega_\eta \ni P \mapsto \lambda(P) := \Lambda_{0, P} \in \mathcal{Y}$  are characterized by the relation

$$\forall Y \in \mathcal{Y}, \quad \underbrace{[d_P \Theta((0, P_0), (D_0, 0))] Y}_{=(0, -Y)} + \underbrace{[d_{(D, \Lambda)} \Theta((0, P_0), (D_0, 0))] ((d_{P_0} F_0^{\text{LL}}) Y, (d_{P_0} \lambda) Y)}_{=A[(d_{P_0} F_0^{\text{LL}}) Y] + B^*(d_{P_0} \lambda) Y, B[(d_{P_0} F_0^{\text{LL}}) Y]} = 0,$$

from which we infer that

$$d_{P_0} F_0^{\text{LL}} = A^{-1} B^* (B A^{-1} B^*)^{-1}. \quad (2.68)$$

Let us now compute  $d_{D_0} F_0^{\text{HL}} : T_{D_0} \mathcal{D} \rightarrow \mathcal{Y}$ . We have

$$\forall D \in \Omega_{\eta_{\text{HL}}}, \quad F_0^{\text{HL}}(D) = \sum_{x=1}^{N_f} \Pi_x C^x(D) \mathbf{1}_{(-\infty, 0]} (C^x(D)^T (h - \mu(0, D) \Pi_x) C^x(D)) C^x(D)^T \Pi_x,$$

where the function

$$\mathcal{D} \ni D \mapsto C^x(D) = \underbrace{(D E_x (E_x^T D E_x)^{-1/2})}_{C_-^x(D)} \underbrace{|(1 - D) E_x (E_x^T (1 - D) E_x)^{-1/2}|}_{C_+^x(D)} \in \mathbb{R}^{L \times (2L_x)}$$

has been introduced in (2.28). Setting as previously  $C_0^x := C^x(D_0)$ , and denoting by  $M(Q) := [d_{D_0} C^x](Q)$  and  $\ell(Q) := [d_D \mu(0, D_0)](Q)$ , we get

$$\begin{aligned} d_{D_0} F^{\text{HL}}(Q) &= \sum_{x=1}^{N_f} \Pi_x \left( M(Q) \mathbf{1}_{(-\infty, 0]} (\mathfrak{h}^x) C_0^{xT} + C_0^x \mathbf{1}_{(-\infty, 0]} (\mathfrak{h}^x) M(Q)^T \right) \Pi_x \\ &\quad - \sum_{x=1}^{N_f} \Pi_x C_0^x \mathfrak{L}_x^+ \left( M(Q)^T h C_0^x + C_0^{xT} h M(Q) - \ell(Q) \mathfrak{p}^x \right) C_0^{xT} \Pi_x. \end{aligned}$$

Using (2.49), we obtain

$$\begin{aligned} M(Q) \mathbf{1}_{(-\infty, 0]} (\mathfrak{h}^x) C_0^{xT} + C_0^x \mathbf{1}_{(-\infty, 0]} (\mathfrak{h}^x) M(Q)^T &= [d_{D_0} C_-^x(Q)] [C_-^x(D_0)]^T + C_-^x(D_0) [d_{D_0} C_-^x(Q)]^T \\ &= d_{D_0} [C_-^x C_-^{xT}](Q). \end{aligned}$$

This implies that

$$\Pi_x \left( M(Q) \mathbf{1}_{(-\infty, 0]}(\mathfrak{h}^x) C_0^{xT} + C_0^x \mathbf{1}_{(-\infty, 0]}(\mathfrak{h}^x) M(Q)^T \right) \Pi_x = d_{D_0} [\Pi_x C_-^x C_-^{xT} \Pi_x](Q).$$

Since

$$\Pi_x C_-^x (D) C_-^x (D)^T \Pi_x = (E_x E_x^T) (DE_x (E_x^T DE_x)^{-1/2}) ((E_x^T DE_x)^{-1/2} E_x^T D) (E_x E_x^T) = \Pi_x D \Pi_x,$$

we get  $d_{D_0} [\Pi_x C_-^x C_-^{xT} \Pi_x](Q) = \Pi_x Q \Pi_x$  and therefore

$$\sum_{x=1}^{N_f} \Pi_x \left( M(Q) \mathbf{1}_{(-\infty, 0]}(\mathfrak{h}^x) C_0^{xT} + C_0^x \mathbf{1}_{(-\infty, 0]}(\mathfrak{h}^x) M(Q)^T \right) \Pi_x = \text{Bd}(Q) = BQ.$$

Next, observing that for all  $Q \in T_{D_0} \mathcal{D}$ ,

$$\begin{aligned} d_{D_0} C_-^x(Q) &= D_0 E_x S_-(Q) + Q E_x (E_x^T D_0 E_x)^{-1/2}, \\ d_{D_0} C_+^x(Q) &= (1 - D_0) E_x S_+(Q) - Q E_x (E_x^T (1 - D_0) E_x)^{-1/2}, \end{aligned}$$

with  $Q \mapsto S_\pm(Q) \in \mathbb{R}^{L_x \times L_x}$  linear and

$$Q = D_0 Q (1 - D_0) + (1 - D_0) Q D_0, \quad (2.69)$$

we obtain that

$$M(Q)^T h C_0^x + C_0^{xT} h M(Q) = \begin{pmatrix} * & N(Q)^T \\ N(Q) & * \end{pmatrix}$$

with

$$\begin{aligned} N(Q) &:= (E_x^T (1 - D_0) E_x)^{-1/2} E_x^T ((1 - D_0) h Q - Q h D_0) E_x (E_x^T D_0 E_x)^{-1/2} \\ &= (E_x^T (1 - D_0) E_x)^{-1/2} E_x^T (1 - D_0) [h, Q] D_0 E_x (E_x^T D_0 E_x)^{-1/2}. \end{aligned}$$

We thus have

$$M(Q)^T h C_0^x + C_0^{xT} h M(Q) = \begin{pmatrix} * & 0 \\ 0 & * \end{pmatrix} - C_0^{xT} [D_0, [h, Q]] C_0^x,$$

which implies, using (2.55),

$$\mathfrak{L}_x^+ \left( M(Q)^T h C_0^x + C_0^{xT} h M(Q) - \ell(Q) \mathfrak{p}^x \right) = \mathfrak{L}_x^+ \left( -C_0^{xT} [D_0, [h, Q]] C_0^x - \ell(Q) \mathfrak{p}^x \right).$$

We therefore obtain

$$d_{D_0} F_0^{\text{HL}} = B + L,$$

with  $L : T_{D_0} \mathcal{D} \rightarrow \mathcal{Y}$  given by

$$\forall Q \in T_{D_0} \mathcal{D}, \quad LQ := \sum_{x=1}^{N_f} \Pi_x C_0^x \mathfrak{L}_x^+ \left( C_0^{xT} [D_0, [h, Q]] C_0^x + \ell(Q) \mathfrak{p}^x \right) C_0^{xT} \Pi_x. \quad (2.70)$$

Combining with (2.68), and setting

$$R := LA^{-1}B^* : \mathcal{Y} \rightarrow \mathcal{Y}, \quad (2.71)$$

we obtain

$$d_P \Phi(0, P_0) = (B + L)(A^{-1}B^*(BA^{-1}B^*)^{-1}) - I_{\mathcal{Y}} = R(BA^{-1}B^*)^{-1}.$$

To conclude, we just have to show that the map  $R$  rigorously defined by (2.71) actually coincides with the 4-point response function formally defined by (2.26) (the latter is bijective by Assumption (A4)). We have for all  $Q \in T_{D_0} \mathcal{D}$  and  $Y \in \mathcal{Y}$ ,

$$\begin{aligned} \langle Q, B^* Y \rangle_{T_{D_0} \mathcal{D}} &= \langle BQ, Y \rangle_{\mathcal{Y}} = \text{Tr}((BQ)Y) \\ &= \text{Tr} \left( \left( \sum_{x=1}^{N_f} \Pi_x Q \Pi_x \right) Y \right) = \sum_{x=1}^{N_f} \text{Tr}(\Pi_x Q \Pi_x Y) = \sum_{x=1}^{N_f} \text{Tr}(Q \Pi_x Y \Pi_x) \\ &= \text{Tr} \left( Q \left( \sum_{x=1}^{N_f} \Pi_x Y \Pi_x \right) \right) = \text{Tr}(QY) = \text{Tr}(Q \underbrace{(D_0 Y (1 - D_0) + (1 - D_0) Y D_0)}_{\in T_{D_0} \mathcal{D}}) \\ &= \langle Q, D_0 Y (1 - D_0) + (1 - D_0) Y D_0 \rangle_{T_{D_0} \mathcal{D}}. \end{aligned}$$

Therefore

$$Y \in \mathcal{Y}, \quad B^*Y = D_0Y(1 - D_0) + (1 - D_0)YD_0. \quad (2.72)$$

By a classical calculation (see e.g. [4, Section 2.2]), we have

$$\forall Q \in \mathcal{Y}, \quad AQ = -[D_0, [h, Q]]. \quad (2.73)$$

It is also easily checked that

$$C_0^{xT}(B^*Y)C_0^x = C_0^{xT}(D_0Y(1 - D_0) + (1 - D_0)YD_0)C_0^x = \begin{pmatrix} * & 0 \\ 0 & * \end{pmatrix} + C_0^{xT}YC_0^x. \quad (2.74)$$

Putting together (2.55) and (2.70)-(2.74) yields

$$RY = \sum_{x=1}^{N_f} \Pi_x C_0^x \mathfrak{L}_x^+ \left( C_0^{xT} \left( Y - \tilde{\ell}(Y)\Pi_x \right) C_0^x \right) C_0^{xT} \Pi_x, \quad (2.75)$$

where

$$\tilde{\ell}(Y) := \ell(A^{-1}B^*Y) = \text{Tr}(GY) \quad \text{with} \quad G := \sum_{x=1}^{N_f} C_0^x \mathfrak{L}_x^+ (\mathfrak{p}^x) C_0^{xT} \in \mathbb{R}_{\text{sym}}^{L \times L}. \quad (2.76)$$

Using the notation introduced in (2.26), we have

$$\widetilde{F}^{\text{HL}}_{h+Y}(D_0) = \sum_{x=1}^{N_f} \Pi_x C_0^x \mathbf{1}_{(-\infty, 0]} \left( C_0^{xT} (h + Y - \mu_Y \Pi_x) C_0^x \right) C_0^{xT} \Pi_x,$$

where  $\mu_Y \in \mathbb{R}$  is chosen such that  $\text{Tr}(\widetilde{F}^{\text{HL}}_{h+Y}(D_0)) = N$ . Using similar perturbation argument as in Section 2.7.6, one can check that  $\widetilde{F}^{\text{HL}}_{h+Y}(D_0)$  is well-defined for  $Y \in \mathcal{Y}$  small enough, and that

$$\begin{aligned} \widetilde{F}^{\text{HL}}_{h+Y}(D_0) &= \sum_{x=1}^{N_f} \Pi_x C_0^x \mathbf{1}_{(-\infty, 0]} \left( \mathfrak{h}^x + (C_0^{xT} (Y - \mu_Y \Pi_x) C_0^x) \right) C_0^{xT} \Pi_x \\ &= \widetilde{F}^{\text{HL}}_h(D_0) + \sum_{x=1}^{N_f} \Pi_x C_0^x \mathfrak{L}_x^+ \left( C_0^{xT} (Y + \mu_Y \Pi_x) C_0^x \right) C_0^{xT} \Pi_x + o(\|Y\|), \end{aligned}$$

with  $\mu_Y = \tilde{\ell}(Y)$  by particle conservation. This shows that the map  $R$  defined by (2.75)-(2.76) actually coincides with the 4-point response function in Assumption (A4).

### About Assumptions (A3) and (A4) in the one-site-per-fragment setting

Let us show that when  $N_f = L$ , we have under Assumptions (A1)-(A2),

(A3) are satisfied  $\implies D_0$  is an irreducible matrix  $\iff$  (A4) is satisfied.

Throughout this section, we assume that (A1)-(A2) are fulfilled.

Let us first show that (A3) implies that  $D_0$  is irreducible. We deduce from the second assertion of Lemma 2.10 that (A3) is satisfied if and only if the only matrices in  $\mathbb{R}_{\text{sym}}^{L \times L}$  which commute with  $D_0$  and all the  $\Pi_x$ 's are the multiples of the identity matrix. When  $N_f = L$ , the matrices in  $\mathbb{R}_{\text{sym}}^{L \times L}$  which commute with all the  $\Pi_x$  are the diagonal matrices. The diagonal matrices  $\Lambda = \text{diag}(\lambda_1, \dots, \lambda_L)$  which commute with  $D_0$  are the ones for which

$$\forall 1 \leq i, j \leq L, \quad \lambda_i [D_0]_{ij} = [D_0]_{ij} \lambda_j.$$

If  $D_0$  was reducible, then one could find a permutation matrix  $P \in O(L)$  such that  $PD_0P^{-1}$  is a  $2 \times 2$  block-diagonal matrix. The matrix  $P \text{diag}(1, \dots, 1, 2, \dots, 2)P^{-1}$ , where the numbers of entries 1 and 2 match the sizes of the blocks of  $PD_0P^{-1}$ , would then be a diagonal matrix which commutes with  $D_0$  and is not proportional to the identity matrix. We reach a contradiction. Thus, (A3) implies that  $D_0$  is irreducible.

Let us now show the equivalence

$$D_0 \text{ is an irreducible matrix} \iff (\text{A4}) \text{ is satisfied.}$$

We have for all  $Y \in \mathcal{Y}$ ,

$$\begin{aligned} \|RY\|^2 &= \text{Tr}((RY)(RY)) \\ &= \sum_{x,x'=1}^{N_f} \text{Tr} \left( \Pi_x C_0^x \mathfrak{L}_x^+ \left( C_0^{xT} \left( Y - \tilde{\ell}(Y) \Pi_x \right) C_0^x \right) C_0^{xT} \Pi_x \Pi_{x'} C_0^{x'} \mathfrak{L}_{x'}^+ \left( C_0^{x'T} \left( Y - \tilde{\ell}(Y) \Pi_{x'} \right) C_0^{x'} \right) C_0^{x'T} \Pi_{x'} \right) \\ &= \sum_{x=1}^{N_f} \text{Tr} \left( \Pi_x C_0^x \mathfrak{L}_x^+ \left( C_0^{xT} \left( Y - \tilde{\ell}(Y) \Pi_x \right) C_0^x \right) C_0^{xT} \Pi_x C_0^x \mathfrak{L}_x^+ \left( C_0^{xT} \left( Y - \tilde{\ell}(Y) \Pi_x \right) C_0^x \right) C_0^{xT} \Pi_x \right) \\ &= \sum_{x=1}^{N_f} \text{Tr} \left( \mathfrak{p}_x \mathfrak{L}_x^+ \left( C_0^{xT} \left( Y - \tilde{\ell}(Y) \Pi_x \right) C_0^x \right) \mathfrak{p}_x \mathfrak{L}_x^+ \left( C_0^{xT} \left( Y - \tilde{\ell}(Y) \Pi_x \right) C_0^x \right) \right) \\ &= \sum_{x=1}^{N_f} \|\mathfrak{p}_x \mathfrak{L}_x^+ \left( C_0^{xT} \left( Y - \tilde{\ell}(Y) \Pi_x \right) C_0^x \right) \mathfrak{p}_x\|^2. \end{aligned}$$

Using (2.50) and (2.55)-(2.56), we obtain after straightforward algebraic manipulations that

$$\begin{aligned} (RY = 0) &\iff \left( \forall 1 \leq x \leq N_f, \mathfrak{p}_x \mathfrak{L}_x^+ \left( C_0^{xT} \left( Y - \tilde{\ell}(Y) \Pi_x \right) C_0^x \right) \mathfrak{p}_x = 0 \right) \\ &\iff \left( \forall 1 \leq x \leq N_f, (1 - D_{0,x})^{1/2} \tilde{N}_x(Y) D_{0,x}^{1/2} + D_{0,x}^{1/2} \tilde{N}_x(Y)^T (1 - D_{0,x})^{1/2} = 0 \right), \end{aligned}$$

with

$$\tilde{N}_x(Y) := N \left( (1 - D_{0,x})^{-1/2} E_x^T (1 - D_0) Y D_0 E_x D_{0,x}^{-1/2} - \tilde{\ell}(Y) D_{0,x}^{1/2} (1 - D_{0,x})^{1/2} \right).$$

In the case when  $N_f = L$ , we have  $L_x = 1$  for all  $x$ , and thus,  $D_{0,x}$  and  $\tilde{N}(Y)$  are scalar quantities. We then have in this special case by assumption (A2),

$$(RY = 0) \iff (\forall 1 \leq x \leq N_f, \tilde{N}_x(Y) = 0) \iff (My = \tilde{\ell}(Y)z),$$

where  $y = (Y_{11}, \dots, Y_{LL})^T \in \mathbb{R}^L$ ,  $z = (D_{0,1}(1 - D_{0,1}), \dots, D_{0,L}(1 - D_{0,L}))^T \in \mathbb{R}^L$ , and  $M \in \mathbb{R}_{\text{sym}}^{L \times L}$  is the matrix with entries

$$M_{xx} = [D_0]_{xx} - [D_0]_{xx}^2, \quad M_{xx'} = -[D_0]_{xx'}^2 \text{ if } x \neq x'.$$

Still by Assumption (A2),  $\sum_{x=1}^{N_f} z_x > 0$ , and therefore using the fact that  $D_0$  is an orthogonal projector (hence that  $\sum_{x=1}^{N_f} [D_0]_{x,x}^2 = [D_0]_{xx}^2 = [D_0]_{xx}$ ), we get

$$(My = \tilde{\ell}(Y)z) \implies \left( \tilde{\ell}(Y) = \frac{\sum_{x,x'=1}^{N_f} M_{x,x'} y_{x'}}{\sum_{x=1}^{N_f} z_x} = \frac{\sum_{x=1}^{N_f} [D_0]_{x,x} y_x - \sum_{x,x'=1}^{N_f} [D_0]_{x,x'}^2 y_{x'}}{\sum_{x=1}^{N_f} z_x} = 0 \right).$$

Therefore,

$$(RY = 0) \iff (My = 0).$$

The matrix  $M$  is hermitian, diagonal dominant with positive diagonal elements and non-positive off-diagonal elements, and such that

$$\forall 1 \leq x \leq N_f, \quad M_{xx} = - \sum_{x' \neq x} M_{xx'}.$$

Therefore the kernel of  $M$  is reduced to  $\mathbb{R}(1, \dots, 1)^T$  if and only if  $M$  is irreducible. Besides, we see from the expressions of the coefficients of  $M$  and Assumption (A2) that  $M$  is irreducible if and only if  $D_0$  is irreducible. We conclude that  $R$  is injective, hence bijective, if and only if  $D_0$  is irreducible.

### 2.7.7 Proof of Theorem 2.5

#### Perturbation expansion in the Fock space

This calculation is classical in the physics and chemistry literature, but we report it here for the sake of completeness. Consider a family of Hamiltonians  $(\widehat{H}_\alpha)_{\alpha \in \mathbb{R}}$  of the form

$$\widehat{H}_\alpha := \widehat{H}_0 + \alpha(\widehat{W}_1 + \widehat{W}_2)$$

on the real Fock space  $\text{Fock}(\mathbb{R}^{N_b})$  where

$$\widehat{H}_0 := \sum_{m,n=1}^{N_b} [h_0]_{mn} c_m^\dagger c_n \quad \text{and} \quad \widehat{W}_1 := \sum_{m,n=1}^{N_b} [W_1]_{mn} c_m^\dagger c_n$$

are one-body Hamiltonians and

$$\widehat{W}_2 := \frac{1}{2} \sum_{m,n,p,q=1}^{N_b} [W_2]_{mnpq} c_m^\dagger c_n^\dagger c_q c_p$$

is a two-body Hamiltonian.

Let us provisionally assume that  $h_0$  is diagonal, and more precisely that

$$h_0 = \text{diag}(\varepsilon_1^0, \dots, \varepsilon_{N_b}^0) \quad \text{with} \quad \varepsilon_1^0 \leq \dots \leq \varepsilon_{\mathcal{N}}^0 < 0 < \varepsilon_{\mathcal{N}+1}^0 \leq \dots \varepsilon_{N_b}^0.$$

This amounts to working in a molecular orbital basis set of the unperturbed one-body Hamiltonian  $h_0$  and assuming that the Fermi level  $\epsilon_F$  for having  $\mathcal{N}$  particles in the ground state can be chosen equal to zero. The ground state  $\Psi_0$  of  $\widehat{H}_0$  in the  $\mathcal{N}$ -particle sector then is unique and so is the one of  $\widehat{H}_\alpha$  for  $\alpha$  small by perturbation theory. We have

$$\Psi_0 = \frac{1}{\sqrt{\mathcal{N}!}} c_\mathcal{N}^\dagger \cdots c_1^\dagger |0\rangle, \quad E_0 := \langle \Psi_0 | \widehat{H}_0 | \Psi_0 \rangle = \sum_{i=1}^{\mathcal{N}} \varepsilon_i^0.$$

Denoting by  $d(\alpha)$  the ground-state one-body reduced density matrix of  $\widehat{H}_\alpha$ , the map  $\alpha \mapsto d(\alpha)$  is real-analytic in the neighborhood of 0 and

$$d(\alpha) = d_0 + \alpha d_1 + O(\alpha^2) \quad \text{with} \quad d_0 := \begin{pmatrix} I_{\mathcal{N}} & 0 \\ 0 & 0 \end{pmatrix}.$$

In addition, we have

$$[d_1]_{mn} = \langle \Psi_1 | c_m^\dagger c_n | \Psi_0 \rangle + \langle \Psi_0 | c_m^\dagger c_n | \Psi_1 \rangle,$$

where  $\Psi_1$  is the first-order perturbation of the ground-state wave-function  $\Psi_0$ , solution to

$$(\widehat{H}_0 - E_0) \Psi_1 = -\Pi_{\Psi_0^\perp} ((\widehat{W}_1 + \widehat{W}_2) \Psi_0), \quad \Psi_1 \in \Psi_0^\perp.$$

For  $1 \leq i_1 < \dots < i_r \leq \mathcal{N}$  (occupied orbitals) and  $m+1 \leq a_1 < \dots < a_r \leq N_b$  (virtual orbitals), we set

$$\Phi_0^0 := \Psi_0 \quad \text{and} \quad \Phi_{i_1 \dots i_r}^{a_1 \dots a_r} = c_{a_r}^\dagger \cdots c_{a_1}^\dagger c_{i_1} \cdots c_{i_r} \Phi_0^0.$$

The  $\Phi_{i_1 \dots i_r}^{a_1 \dots a_r}$ 's ( $0 \leq r \leq \min(\mathcal{N}, N_b - \mathcal{N})$ ,  $1 \leq i_1 < \dots < i_r \leq \mathcal{N}$ ,  $a_1 < \dots < a_r \leq N_b$ , form an orthonormal basis of eigenfunctions of the restriction of  $\widehat{H}_0$  to the  $\mathcal{N}$ -particle sector and it holds

$$\widehat{H}_0 \Phi_{i_1 \dots i_r}^{a_1 \dots a_r} = E_{i_1 \dots i_r}^{a_1 \dots a_r} \Phi_{i_1 \dots i_r}^{a_1 \dots a_r} \quad \text{with} \quad E_{i_1 \dots i_r}^{a_1 \dots a_r} = E_0 + \sum_{s=1}^r \varepsilon_{a_s} - \sum_{s=1}^r \varepsilon_{i_s}.$$

We thus obtain the sum-over-state formula

$$\Psi_1 = - \sum_{1 \leq r \leq \min(\mathcal{N}, N_b - \mathcal{N})} \sum_{1 \leq i_1 < \dots < i_r \leq \mathcal{N}} \sum_{\mathcal{N}+1 \leq a_1 < \dots < a_r \leq N_b} \frac{\langle \Phi_{i_1 \dots i_r}^{a_1 \dots a_r} | \widehat{W}_1 + \widehat{W}_2 | \Phi_0^0 \rangle}{E_{i_1 \dots i_r}^{a_1 \dots a_r} - E_0} \Phi_{i_1 \dots i_r}^{a_1 \dots a_r},$$

yielding

$$[d_1]_{mn} = - \sum_{1 \leq r \leq \min(\mathcal{N}, N_b - \mathcal{N})} \sum_{1 \leq i_1 < \dots < i_r \leq \mathcal{N}} \sum_{\mathcal{N}+1 \leq a_1 < \dots < a_r \leq N_b} \frac{\langle \Phi_{i_1 \dots i_r}^{a_1 \dots a_r} | \widehat{W}_1 + \widehat{W}_2 | \Phi_0^0 \rangle}{E_{i_1 \dots i_r}^{a_1 \dots a_r} - E_0} \\ \times (\langle \Phi_{i_1 \dots i_r}^{a_1 \dots a_r} | c_m^\dagger c_n | \Phi_0^0 \rangle + \langle \Phi_0^0 | c_m^\dagger c_n | \Phi_{i_1 \dots i_r}^{a_1 \dots a_r} \rangle).$$

Since  $\langle \Phi_{i_1 \dots i_r}^{a_1 \dots a_r} | a_m^\dagger a_n | \Phi_0^0 \rangle = 0$  if  $r \geq 2$ , and

$$\langle \Phi_i^a | c_m^\dagger c_n | \Phi_0^0 \rangle = \delta_{n,i} \delta_{m,a}, \\ \langle \Phi_i^a | c_m^\dagger c_n^\dagger c_q c_p | \Phi_0^0 \rangle = -\delta_{m,q} \delta_{n,i} \delta_{p,a} \delta_{q \leq \mathcal{N}} + \delta_{m,p} \delta_{n,i} \delta_{q,a} \delta_{p \leq \mathcal{N}} + \delta_{m,i} \delta_{n,q} \delta_{p,a} \delta_{q \leq \mathcal{N}} - \delta_{m,i} \delta_{n,p} \delta_{q,a} \delta_{p \leq \mathcal{N}},$$

this expression reduces to

$$[d_1]_{mn} = - \sum_{i=1}^N \sum_{a=\mathcal{N}+1}^{N_b} \frac{\langle \Phi_i^a | \widehat{W}_1 + \widehat{W}_2 | \Phi_0^0 \rangle}{\varepsilon_a^0 - \varepsilon_i^0} (\delta_{n=i} \delta_{m=a} + \delta_{m=i} \delta_{n=a}).$$

We obtain that  $d_1$  is of the form

$$d_1 = \begin{pmatrix} 0 & d_1^{+-} \\ d_1^{+-T} & 0 \end{pmatrix} \quad \text{with} \quad \forall 1 \leq i \leq \mathcal{N} < \mathcal{N}+1 \leq a \leq N_b, \quad [d_1]_{ai} = \frac{\langle \Phi_i^a | \widehat{W}_1 + \widehat{W}_2 | \Phi_0^0 \rangle}{\varepsilon_a^0 - \varepsilon_i^0}.$$

Finally, we have

$$[d_1]_{ai} = \sum_{m,n=1}^{N_b} [W_1]_{mn} \frac{\langle \Phi_i^a | c_m^\dagger c_n | \Phi_0^0 \rangle}{\varepsilon_a^0 - \varepsilon_i^0} + \sum_{m,n,p,q=1}^{N_b} [W_2]_{mnpq} \frac{\langle \Phi_i^a | c_m^\dagger c_n^\dagger c_q c_p | \Phi_0^0 \rangle}{\varepsilon_a^0 - \varepsilon_i^0} \\ = \frac{[W_1 + J_{W_2}(d_0) - K_{W_2}(d_0)]_{ai}}{\varepsilon_a^0 - \varepsilon_i^0},$$

where the direct and exchange operators are respectively given by

$$[J_{W_2}(d)]_{mn} := \sum_{p,q=1}^{N_b} [W_2]_{npqm} d_{pq} \quad \text{and} \quad [K_{W_2}(d)]_{mn} := \sum_{p,q=1}^{N_b} [W_2]_{npqm} d_{pq}.$$

Introducing the linear response operator  $\mathfrak{L}_{h_0}^+$  such that

$$\mathbf{1}_{(-\infty, \epsilon_F]}(h_0 + W) = \underbrace{\mathbf{1}_{(-\infty, \epsilon_F]}(h_0 + W)}_{=d_0} - \mathfrak{L}_{h_0}^+ W + O(\|W\|),$$

we finally obtain

$$d_1 = -\mathfrak{L}_{h_0}^+ (W_1 + J_{W_2}(d_0) - K_{W_2}(d_0)), \quad (2.77)$$

this formula remaining valid in the general case when  $h_0$  is not *a priori* diagonal and  $\epsilon_F$  not *a priori* equal to zero.

### Perturbation expansion of the DMET ground-state

Under Assumption (A1), the Hartree-Fock problem

$$\operatorname{argmin}_{D \in \mathcal{D}} \mathcal{E}_\alpha^{\text{HF}}(D)$$

has a unique minimizer  $D^{\text{HF}}(\alpha)$  for  $\alpha$  small enough and the map  $\alpha \mapsto D^{\text{HF}}(\alpha)$  is real-analytic in the neighborhood of 0. This results from a straightforward application of nonlinear perturbation theory, which we do not detail here for the sake of brevity. We set  $P^{\text{HF}}(\alpha) := \text{Bd}(D^{\text{HF}}(\alpha))$ , and

$$D_1^{\text{exact}} := \frac{dD^{\text{exact}}}{d\alpha}(0), \quad D_1^{\text{HF}} := \frac{dD^{\text{HF}}}{d\alpha}(0), \quad D_1^{\text{DMET}} := \frac{dD^{\text{DMET}}}{d\alpha}(0), \\ P_1^{\text{exact}} := \frac{dP^{\text{exact}}}{d\alpha}(0), \quad P_1^{\text{HF}} := \frac{dP^{\text{HF}}}{d\alpha}(0), \quad P_1^{\text{DMET}} := \frac{dP^{\text{DMET}}}{d\alpha}(0).$$

We are going to prove that the above first three matrices on the one hand, and the last three ones on the other hand are equal in  $T_{D_0}\mathcal{D}$  and  $\mathcal{Y}$  respectively.

First, we deduce from (2.77) applied with  $N_b = L$ ,  $\epsilon_F = 0$ ,  $h_0 = h$ ,  $W_1 = 0$ ,  $W_2 = v$ , that

$$D_1^{\text{exact}} = -\mathfrak{L}_h^+ (J(D_0) - K(D_0)),$$

where  $J$  and  $K$  are the direct and exchange operators for the two-body interaction potential  $\hat{V}$  introduced in (2.21).

Next, by differentiating the self-consistent equation

$$D^{\text{HF}}(\alpha) = \mathbf{1}_{(-\infty, 0]} (h^{\text{MF}}(\alpha, D^{\text{HF}}(\alpha))),$$

where

$$h^{\text{MF}}(\alpha, D) = h + \alpha (J(D) - K(D))$$

is the Fock Hamiltonian for the interaction parameter  $\alpha$ , we get

$$D_1^{\text{HF}} = -\mathfrak{L}_h^+ (J(D_0) - K(D_0)).$$

Hence

$$D_1^{\text{HF}} = D_1^{\text{exact}} \quad \text{and} \quad P_1^{\text{HF}} = \text{Bd}(D_1^{\text{HF}}) = \text{Bd}(D_1^{\text{exact}}) = P_1^{\text{exact}}.$$

Let us now show that  $P_1^{\text{DMET}} = P_1^{\text{HF}}$ . For convenience, we will use the following notation

$$\begin{aligned} F^{\text{LL}}(\alpha, P) &:= F_\alpha^{\text{LL}}(P), \quad F^{\text{HL}}(\alpha, D) = F_\alpha^{\text{HL}}(D), \\ F_{\text{HF}}^{\text{HL}}(\alpha, D) &:= \sum_{x=1}^{N_f} \Pi_x C^x(D) \mathbf{1}_{(-\infty, 0]} (C^x(D)^T (h^{\text{MF}}(\alpha, D) - \mu^{\text{HF}}(\alpha, D) \Pi_x) C^x(D)) C^x(D)^T \Pi_x, \end{aligned}$$

where  $\mu^{\text{HF}}(\alpha, D) \in \mathbb{R}$  is the Lagrange parameter of the charge conservation constraint. The map  $F_{\text{HF}}^{\text{HL}}(\alpha, D)$  is the high-level Hartree-Fock map for the interacting parameter  $\alpha$ , introduced in Remark 2.2 for  $\alpha = 1$ .

We know from Theorem 2.4 that for all  $\alpha$  small enough

$$F^{\text{HL}}(\alpha, F^{\text{LL}}(\alpha, P^{\text{DMET}}(\alpha))) = P^{\text{DMET}}(\alpha).$$

Taking the derivative at  $\alpha = 0$ , we get

$$\partial_\alpha F^{\text{HL}}(0, D_0) + \partial_D F^{\text{HL}}(0, D_0) (\partial_\alpha F^{\text{LL}}(0, P_0) + \partial_P F^{\text{LL}}(0, P_0) P_1^{\text{DMET}}) = P_1^{\text{DMET}}. \quad (2.78)$$

The same arguments as in the proof of Proposition 2.1 allow one to show that for all  $\alpha$  small enough

$$F_{\text{HF}}^{\text{HL}}(\alpha, F^{\text{LL}}(\alpha, P^{\text{HF}}(\alpha))) = P^{\text{HF}}(\alpha),$$

yielding

$$\partial_\alpha F_{\text{HF}}^{\text{HL}}(0, D_0) + \partial_D F_{\text{HF}}^{\text{HL}}(0, D_0) (\partial_\alpha F^{\text{LL}}(0, P_0) + \partial_P F^{\text{LL}}(0, P_0) P_1^{\text{HF}}) = P_1^{\text{HF}}. \quad (2.79)$$

Since  $F_{\text{HF}}^{\text{HL}}(0, D) = F^{\text{HL}}(0, D)$  for all  $D$  in the neighborhood of  $D_0$ , we have

$$\partial_P F_{\text{HF}}^{\text{HL}}(0, D_0) = \partial_P F^{\text{HL}}(0, D_0).$$

Using (2.67) and the invertibility of  $d_P \Phi(0, P_0)$  established in Section 2.7.6, we obtain

$$P_1^{\text{DMET}} = -(d_P \Phi(0, P_0))^{-1} (\partial_\alpha F^{\text{HL}}(0, D_0) + \partial_D F^{\text{HL}}(0, D_0) \partial_\alpha F^{\text{LL}}(0, P_0)), \quad (2.80)$$

$$P_1^{\text{HF}} = -(d_P \Phi(0, P_0))^{-1} (\partial_\alpha F_{\text{HF}}^{\text{HL}}(0, D_0) + \partial_D F_{\text{HF}}^{\text{HL}}(0, D_0) \partial_\alpha F^{\text{LL}}(0, P_0)). \quad (2.81)$$

Let us show that  $\partial_\alpha F^{\text{HL}}(0, D_0) = \partial_\alpha F_{\text{HF}}^{\text{HL}}(0, D_0)$ . On the one hand, we have

$$F_{\text{HF}}^{\text{HL}}(\alpha, D_0) = \sum_{x=1}^{N_f} \Pi_x C_0^x \mathbf{1}_{(-\infty, 0]} (C_0^{xT} (h + \alpha (J(D_0) - K(D_0)) - \mu_{\text{HF}}(\alpha, D_0) \Pi_x) C_0^x) C_0^{xT} \Pi_x,$$

and therefore

$$\partial_\alpha F_{\text{HF}}^{\text{HL}}(0, D_0) = - \sum_{x=1}^{N_f} \Pi_x C_0^x \mathfrak{L}_x^+ \left( C_0^{xT} (J(D_0) - K(D_0)) C_0^x - \partial \mu_{\text{HF}}(0, D_0) \mathfrak{p}^x \right) C_0^{xT} \Pi_x. \quad (2.82)$$

On the other hand, we have

$$F^{\text{HL}}(\alpha, D_0) = \sum_{x=1}^{N_f} \Pi_x C_0^x D_{x, D_0}^{\text{imp}}(\alpha) C_0^{xT} \Pi_x,$$

where  $D_{x, D_0}^{\text{imp}}(\alpha)$  is the ground-state one-body reduced density matrix in the basis of  $Y_{x, D_0}$  defined by  $C_0^x$  of the impurity Hamiltonian (see Proposition 2.7)

$$\begin{aligned} \hat{H}_{x, D_0}^{\text{imp}}(\alpha) &= \sum_{i,j=1}^{2L_x} \left[ C_0^{xT} (h + \alpha(J(\mathfrak{D}^x(D_0)) - K(\mathfrak{D}^x(D_0)))) C_0^x \right]_{ij} \hat{a}_i(D_0)^\dagger \hat{a}_j(D_0) \\ &\quad + \frac{\alpha}{2} \sum_{i,j,k,\ell=1}^{2L_x} [V^x(D_0)]_{ijkl} \hat{a}_i(D_0)^\dagger \hat{a}_j(D_0)^\dagger \hat{a}_\ell(D_0) \hat{a}_k(D_0) \\ &\quad - \mu(\alpha) \sum_{i,j=1}^{2L_x} \left[ C_0^{xT} \Pi_x C_0^x \right]_{ij} \hat{a}_i(D_0)^\dagger \hat{a}_j(D_0), \end{aligned}$$

where  $\mu(\alpha)$  is the Lagrange multiplier of the charge neutrality constraint and where we have discarded the irrelevant constant  $E_x^{\text{env}}(D_0)$ . Using the notation introduced in (2.43), this Hamiltonian can be rewritten as

$$\begin{aligned} \hat{H}_{x, D_0}^{\text{imp}}(\alpha) &= \sum_{i,j=1}^{2L_x} [\mathfrak{h}^x]_{ij} \hat{a}_i(D_0)^\dagger \hat{a}_j(D_0) \\ &\quad + \alpha \left( \sum_{i,j=1}^{2L_x} \left[ C_0^{xT} (J(\mathfrak{D}^x(D_0)) - K(\mathfrak{D}^x(D_0))) C_0^x \right]_{ij} \hat{a}_i(D_0)^\dagger \hat{a}_j(D_0) \right. \\ &\quad \left. + \frac{1}{2} \sum_{i,j,k,\ell=1}^{2L_x} [V^x(D_0)]_{ijkl} \hat{a}_i(D_0)^\dagger \hat{a}_j(D_0)^\dagger \hat{a}_\ell(D_0) \hat{a}_k(D_0) \right) \\ &\quad - \mu(\alpha) \sum_{i,j=1}^{2L_x} \left[ C_0^{xT} \Pi_x C_0^x \right]_{ij} \hat{a}_i(D_0)^\dagger \hat{a}_j(D_0). \end{aligned}$$

We have

$$D_{x, D_0}^{\text{imp}}(0) = \begin{pmatrix} I_{L_x} & 0 \\ 0 & 0 \end{pmatrix}.$$

Since  $\mu(0) = 0$  and  $\alpha \mapsto \mu(\alpha)$  is real-analytic, we can easily adapt the analysis done in the previous section to the case when

$$N_b = 2L_x, \quad h_0 = \mathfrak{h}^x, \quad W_1 = C_0^{xT} (J(\mathfrak{D}^x(D_0)) - K(\mathfrak{D}^x(D_0)) - \mu'(0) \Pi_x) C_0^x, \quad W_2 = V^x(D_0),$$

and infer that

$$\begin{aligned} D_{x, D_0}^{\text{imp}}(\alpha) &= D_{x, D_0}^{\text{imp}}(0) - \mathfrak{L}_x^+ \left( C_0^{xT} (J(\mathfrak{D}^x(D_0)) - K(\mathfrak{D}^x(D_0)) - \mu'(0) \Pi_x) C_0^x \right. \\ &\quad \left. + J_{V^x(D_0)}(D_{x, D_0}^{\text{imp}}(0)) - K_{V^x(D_0)}(D_{x, D_0}^{\text{imp}}(0)) \right) + O(\alpha^2), \end{aligned}$$

where  $\mathfrak{L}_x^+$  is the linear response operator introduced in (2.54). Observing that

$$C_0^{xT} (J(\mathfrak{D}^x(D_0)) - K(\mathfrak{D}^x(D_0))) C_0^x + J_{V^x(D_0)}(D_{x, D_0}^{\text{imp}}(0)) - K_{V^x(D_0)}(D_{x, D_0}^{\text{imp}}(0)) = C_0^{xT} (J(D_0) - K(D_0)) C_0^x,$$

we obtain that

$$\partial_\alpha F^{\text{HL}}(0, D_0) = - \sum_{x=1}^{N_f} \Pi_x C_0^x \mathfrak{L}_x^+ \left( C_0^{xT} (J(D_0) - K(D_0)) C_0^x - \mu'(0) \mathfrak{p}^x \right) C_0^{xT} \Pi_x. \quad (2.83)$$

Since the roles of the scalars  $\partial_\alpha \mu(0, D_0)$  in (2.82) and  $\mu'(0)$  in (2.83) are simply to ensure charge neutrality, these two scalars are the same. It follows that  $\partial_\alpha F_{\text{HF}}^{\text{HL}}(0, D_0) = \partial_\alpha F^{\text{HL}}(0, D_0)$ , which allows us to deduce from (2.80)-(2.81) that  $P_1^{\text{DMET}} = P_1^{\text{HF}}$ . Finally, we obtain that  $D_1^{\text{DMET}} = D_1^{\text{HF}}$  by differentiating the relations

$$D^{\text{DMET}}(\alpha) = F^{\text{LL}}(\alpha, P^{\text{DMET}}(\alpha)) \quad \text{and} \quad D^{\text{HF}}(\alpha) = F^{\text{LL}}(\alpha, P^{\text{HF}}(\alpha)),$$

and using the fact that  $P_1^{\text{DMET}} = P_1^{\text{HF}}$ .

## Acknowledgements

This project has received funding from the European Research Council (ERC) under the European Union's Horizon 2020 research and innovation programm (grant agreement EMC2 No 810367) and from the Simons Targeted Grant Award No. 896630. Moreover, it was partially supported by the Air Force Office of Scientific Research under the award number FA9550-18-1-0095 and by the Simons Targeted Grants in Mathematics and Physical Sciences on Moiré Materials Magic (F.M.F.). The authors thank Emmanuel Fromager, Lin Lin, and Solal Perrin-Roussel for useful discussions and comments. Part of this work was done during the IPAM program *Advancing quantum mechanics with mathematics and statistics*.

# Appendices

## 2.A Notation table

The following table collects the main notations in use in this article.

Symbol	Meaning	See Eq.
$\text{Fock}(E)$	Fermionic Fock space associated with the one-particle state space $E \subset \mathcal{H}$	
$\mathcal{H} = \mathbb{R}^L$	One-particle state space of the whole system, $L$ its dimension	(2.1)
$\mathcal{B}_{\text{at}} = (e_\kappa)_{1 \leq \kappa \leq L}$	Canonical basis of $\mathcal{H}$	(2.1)
$\hat{H}$	Hamiltonian of the whole system (op. on $\text{Fock}(\mathcal{H})$ )	(2.2)
$\hat{H}_0$	Non-interacting Hamiltonian of the whole system	(2.23)
$\hat{H}_\alpha$	Hamiltonian of the whole system for coupling parameter $\alpha$	(2.22)
$N$	Number of electrons in the system	
$\mathcal{D}$	Set of 1-RDMs associated with $N$ -particles Slater states (Grassmann manifold $\text{Gr}(N, L)$ )	(2.3)
$\text{CH}(\mathcal{D})$	Convex hull of $\mathcal{D}$ (set of mixed-state 1-RDMs with $N$ particles)	(2.4)
$D_0$	$N$ -particle round-state 1-RDM of $\hat{H}_0$	(2.24)
$D_\alpha^{\text{exact}}$	$N$ -particle ground-state 1-RDM of $\hat{H}_\alpha$	
$D_\alpha^{\text{HF}}$	Hartree-Fock $N$ -particle ground state 1-RDM of $\hat{H}_\alpha$	
$\mathcal{E}^{\text{HF}}$	Hartree-Fock energy functional	(2.20)
$J$ and $K$	Coulomb and exchange energy functionals	(2.21)
$h^{\text{HF}}(D)$	Mean-field (Fock) Hamiltonian (op. on $\mathcal{H}$ )	(2.25)
$N_f$	Number of fragments	
$L_x$	Number of sites in fragment $x$	
$X_x$	$x$ -th fragment subspace, $X_x = \text{Span}(e_\kappa, \kappa \in \mathcal{I}_x) \subset \mathcal{H}$	(2.6)
$\Pi_x$	Orthogonal projector on $X_x$ (op. on $\mathbb{R}_{\text{sym}}^{L \times L}$ )	
$E_x$	Matrix of the $L_x$ orbitals of fragment $x$ ( $E_x \in \mathbb{R}^{L \times L_x}$ )	(2.27)
$\text{Bd}$	Projector defined by $\text{Bd}(M) = \sum_{x=1}^{N_f} \Pi_{X_x} M \Pi_{X_x}$ (op. on $\mathbb{R}_{\text{sym}}^{L \times L}$ )	(2.7)
$\mathcal{P}$	Convex set of block-diagonal matrices with eigenvalues in $[0, 1]$	(2.8)
$\mathcal{Y}$	Space of traceless block-diagonal matrices $\mathcal{Y} \subset \mathbb{R}_{\text{sym}}^{L \times L}$	(2.9)
$W_{x,D}$	$x$ -th impurity space, subspace of $\mathcal{H}$ , $W_{x,D} = X_x + D X_x \subset \mathcal{H}$	(2.10)
$C^x(D), \tilde{C}^x(D)$	Matrices in $\mathbb{R}^{L \times 2L_x}$ defining orthonormal bases of $W_{x,D}$	(2.28), (2.29)
$\hat{H}_{x,D}^{\text{imp}}$	$x$ -th impurity Hamiltonian (op. on $\text{Fock}(W_{x,D})$ )	(2.14), (2.30)
$R$	4-point DMET linear response function (op. on $\mathcal{Y}$ )	(2.26), (2.75)
$F^{\text{LL}}, \text{ resp. } F_\alpha^{\text{LL}}$	Low-level map for $\hat{H}$ , resp. $\hat{H}_\alpha$	(2.19)
$F^{\text{HL}}, \text{ resp. } F_\alpha^{\text{HL}}$	High-level map for $\hat{H}$ , resp. $\hat{H}_\alpha$	(2.18), (2.66)
$\mu$	DMET global chemical potential	

Table 2.A.1: Collection of the main notations used in the paper.

## 2.B Analysis of the DMET bifurcation for $\text{H}_6^{4-}$

We shall finally proceed with the analysis of the DMET solutions along the two bifurcation paths for  $\text{H}_6^{4-}$  around  $\Theta_3$  (see Section 2.4.2). To begin with, we calculate the molecular orbitals at  $\Theta_3$ . The molecular orbital energies exhibit two-fold degeneracies resulting from the fact that the  $E'$  and  $E''$  are irreducible representations of the  $\text{H}_6^{4-}$  symmetry point group ( $D_{3h}$ ) are two-dimensional. For a visual representation of the molecular orbital energies and their corresponding molecular orbitals, see Fig. 2.B.1a and Fig. 2.B.1b.

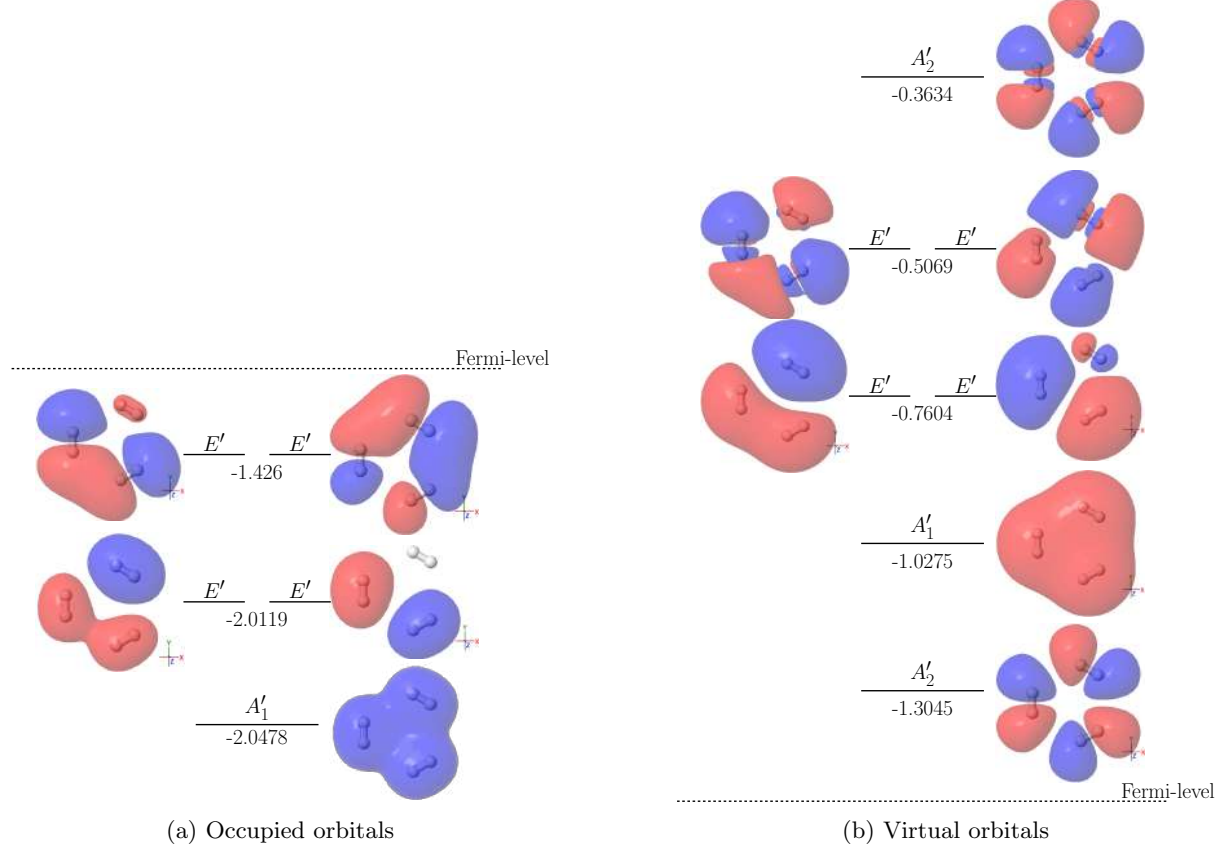


Figure 2.B.1: Depiction of the molecular orbitals, their irreducible representation with respect to the  $D_{3h}$  point group symmetry and molecular energies. The left panel shows the occupied molecular orbitals and the right panel shows the virtual molecular orbitals.

For the two solutions on the respective bifurcation branches,  $P_0$  and  $P_1$ , we compute

$$P_0(\Theta) - P_1(\Theta) = (\Theta - \Theta_3) \begin{bmatrix} 0 & Q_{+-} \\ Q_{-+} & 0 \end{bmatrix} + o(\Theta - \Theta_3), \quad (2.84)$$

where  $Q_{-+} = Q_{+-}^\top \in \mathbb{R}^{7 \times 5}$ . From the matrix  $Q_{-+}$  we deduce “excitation” patterns that give physical insight into the different branches. The numerical values of  $Q_{-+}$  are given by

$$Q_{-+} = \begin{bmatrix} 0 & 0 & 0 & 0 & 0 \\ -0.0004 & 0 & 0 & 0 & 0 \\ 0 & 0.0001 & 0 & 0.0002 & 0 \\ 0 & 0 & -0.0001 & 0 & -0.0002 \\ 0 & 0.0001 & 0 & 0.0001 & 0 \\ 0 & 0 & -0.0001 & 0 & -0.0001 \\ 0 & 0 & 0 & 0 & 0 \end{bmatrix} \quad (2.85)$$

Upon inspecting  $Q_{-+}$ , we observe the following “excitation” pattern: The first molecular orbital ( $A_1'$  symmetry) is rotated in the direction of the seventh molecular orbital ( $A_1'$  symmetry), while the 4-dimensional space generated by the second to fifth molecular orbitals ( $E'$  symmetry) is tilted according

to directions which are linear combinations of the eighth to eleventh molecular orbitals ( $E'$  symmetry). We summarize this “excitation” pattern in Fig. 2.B.2

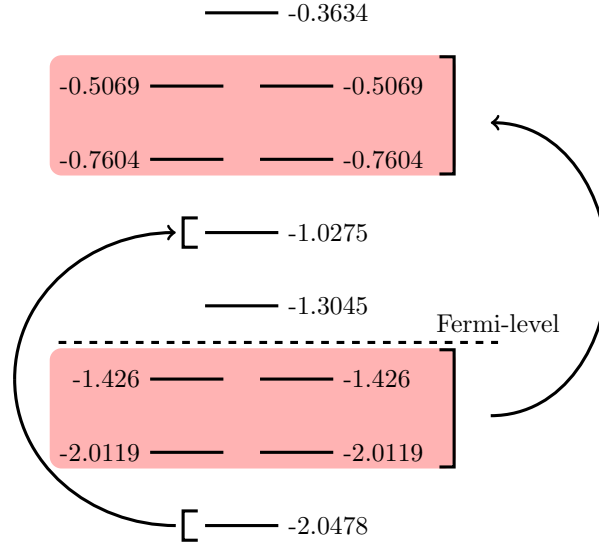


Figure 2.B.2: Molecular energies and “excitation” patterns concluded from  $Q_{-+}$

We see that the pair of degenerate occupied orbitals are excited into the pair of degenerate virtual orbitals. This block of excitations is highlighted by the red shaded area in Fig. 2.B.2 . A more detailed depiction of the excitations between the red-shaded areas is given in Fig. 2.B.3.

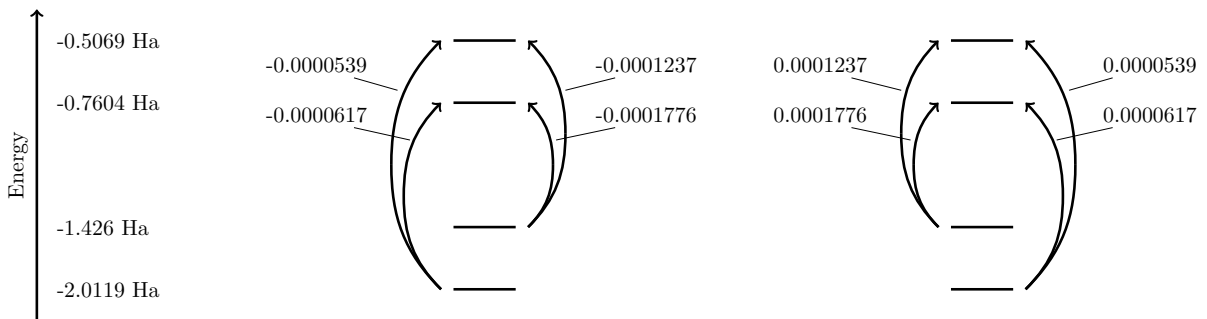


Figure 2.B.3: Excitation patterns concluded from  $Q_{-+}$  for symmetric and anti-symmetric molecular orbitals respectively.

This shows that the excitations remain in the respective symmetry sectors, i.e., the symmetric/anti-symmetric molecular orbitals are excited into the set of the symmetric/anti-symmetric molecular orbitals.

To further understand the structure that underlies these excitations we compute the singular value decomposition of  $Q_{-+} = U\Sigma V^\top$ . This yields insights into excitations of the form:

$$\bar{U} = \begin{bmatrix} 0 \\ U \end{bmatrix} \xrightarrow{\Sigma} \begin{bmatrix} V \\ 0 \end{bmatrix} = \bar{V}, \quad (2.86)$$

where  $\bar{U}$  and  $\bar{V}$  describe the natural excitation orbitals and  $\Sigma$  describes the excitation amplitudes. For the given  $Q_{-+}$  we find the singular values

$$0.0003866, 0.0002313, 0.0002313, 0, 0.$$

This unveils a twofold degeneracy in excitation, implying that a two-dimensional subspace of natural excitation orbitals undergoes excitation into another two-dimensional orbital space. We may moreover depict the different natural orbitals by plotting iso-surfaces in Fig. 2.B.4. The top row of orbitals in Fig. 2.B.4 corresponds to the natural orbitals defined via  $\bar{U}$ , and the second row of orbitals is defined through  $\bar{V}$ . Note that we only depict those orbitals that are involved in non-zero orbital excitations, i.e., non-zero singular values of  $\Sigma$ .

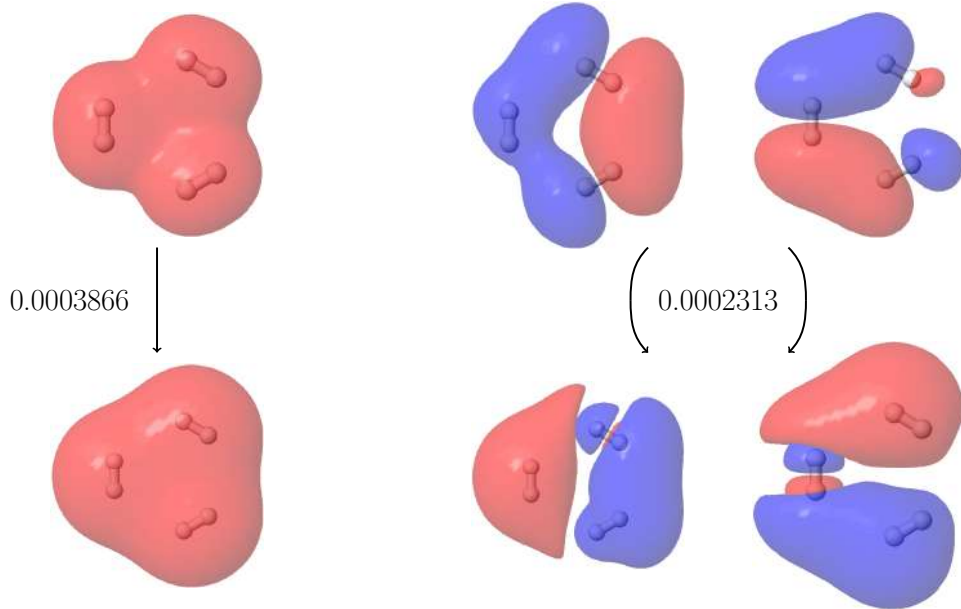


Figure 2.B.4: Schematic depiction of the excitation between the natural excitation orbitals. The excitations are labeled by the excitation amplitudes.

## Bibliography

- [1] Yuhang Ai, Qiming Sun, and Hong Jiang. Efficient multiconfigurational quantum chemistry approach to single-ion magnets based on density matrix embedding theory. *The Journal of Physical Chemistry Letters*, 13(45):10627–10634, 2022.
- [2] Ireneusz W Bulik, Weibing Chen, and Gustavo E Scuseria. Electron correlation in solids via density embedding theory. *The Journal of chemical physics*, 141(5):054113, 2014.
- [3] Ireneusz W Bulik, Gustavo E Scuseria, and Jorge Dukelsky. Density matrix embedding from broken symmetry lattice mean fields. *Phys. Rev. B*, 89(3):035140, 2014.
- [4] Éric Cancès, Gaspard Kemlin, and Antoine Levitt. Convergence analysis of direct minimization and self-consistent iterations. *SIAM Journal on Matrix Analysis and Applications*, 42(1):243–274, 2021.
- [5] Changsu Cao, Jinzhao Sun, Xiao Yuan, Han-Shi Hu, Hung Q Pham, and Dingshun Lv. Ab initio quantum simulation of strongly correlated materials with quantum embedding. *arXiv:2209.03202*, 2022.

- [6] Qiaoni Chen, George H Booth, Sandeep Sharma, Gerald Knizia, and Garnet Kin-Lic Chan. Intermediate and spin-liquid phase of the half-filled honeycomb Hubbard model. *Phys. Rev. B*, 89(16):165134, 2014.
- [7] Yian Chen, Yuehaw Khoo, and Michael Lindsey. Multiscale semidefinite programming approach to positioning problems with pairwise structure. *arXiv:2012.10046*, 2020.
- [8] J. Čížek. On the correlation problem in atomic and molecular systems. Calculation of wavefunction components in Ursell-type expansion using quantum-field theoretical methods. *J. Chem. Phys.*, 45:4256, 1966.
- [9] Zhi-Hao Cui, Chong Sun, Ushnish Ray, Bo-Xiao Zheng, Qiming Sun, and Garnet Kin-Lic Chan. Ground-state phase diagram of the three-band Hubbard model from density matrix embedding theory. *Physical Review Research*, 2(4):043259, 2020.
- [10] Zhi-Hao Cui, Tianyu Zhu, and Garnet Kin-Lic Chan. Efficient implementation of ab initio quantum embedding in periodic systems: Density matrix embedding theory. *J. Chem. Theory Comput.*, 16:119–129, 2020.
- [11] Zhuo Fan and Quan-lin Jie. Cluster density matrix embedding theory for quantum spin systems. *Phys. Rev. B*, 91(19):195118, 2015.
- [12] Fabian M Faulstich, Raehyun Kim, Zhi-Hao Cui, Zaiwen Wen, Garnet Kin-Lic Chan, and Lin Lin. Pure state v-representability of density matrix embedding theory. *Journal of Chemical Theory and Computation*, 18(2):851–864, 2022.
- [13] Edoardo Fertitta and George H Booth. Rigorous wave function embedding with dynamical fluctuations. *Physical Review B*, 98(23):235132, 2018.
- [14] Martin Ganahl, Markus Aichhorn, Hans Gerd Evertz, Patrik Thunström, Karsten Held, and Frank Verstraete. Efficient dmft impurity solver using real-time dynamics with matrix product states. *Physical Review B*, 92(15):155132, 2015.
- [15] Antoine Georges, Gabriel Kotliar, Werner Krauth, and Marcelo J Rozenberg. Dynamical mean-field theory of strongly correlated fermion systems and the limit of infinite dimensions. *Reviews of Modern Physics*, 68(1):13, 1996.
- [16] Antoine Georges and Werner Krauth. Numerical solution of the  $d=\infty$  Hubbard model: Evidence for a Mott transition. *Physical review letters*, 69(8):1240, 1992.
- [17] Mark S Gordon, Dmitri G Fedorov, Spencer R Pruitt, and Lyudmila V Slipchenko. Fragmentation methods: A route to accurate calculations on large systems. *Chemical reviews*, 112(1):632–672, 2012.
- [18] Klaas Gunst, Sebastian Wouters, Stijn De Baerdemacker, and Dimitri Van Neck. Block product density matrix embedding theory for strongly correlated spin systems. *Phys. Rev. B*, 95(19):195127, 2017.
- [19] Matthew R Hermes and Laura Gagliardi. Multiconfigurational self-consistent field theory with density matrix embedding: The localized active space self-consistent field method. *Journal of chemical theory and computation*, 15(2):972–986, 2019.
- [20] Leighton O Jones, Martín A Mosquera, George C Schatz, and Mark A Ratner. Embedding methods for quantum chemistry: Applications from materials to life sciences. *Journal of the American Chemical Society*, 142(7):3281–3295, 2020.
- [21] Richard V. Kadison. The Pythagorean theorem: I. The finite case. *Proceedings of the National Academy of Sciences*, 99(7):4178–4184, 2002.
- [22] Yuehaw Khoo and Michael Lindsey. Scalable semidefinite programming approach to variational embedding for quantum many-body problems. *arXiv:2106.02682*, 2021.
- [23] Gerald Knizia and Garnet Kin-Lic Chan. Density matrix embedding: A simple alternative to dynamical mean-field theory. *Phys. Rev. Lett.*, 109(18):186404, 2012.

- [24] Gerald Knizia and Garnet Kin-Lic Chan. Density matrix embedding: A strong-coupling quantum embedding theory. *J. Chem. Theory Comput.*, 9(3):1428–1432, 2013.
- [25] Peter J Knowles and Nicholas C Handy. A new determinant-based full configuration interaction method. *Chem. Phys. Lett.*, 111(4-5):315–321, 1984.
- [26] Gabriel Kotliar, Sergej Y Savrasov, Kristjan Haule, Viktor S Oudovenko, O Parcollet, and CA Marianetti. Electronic structure calculations with dynamical mean-field theory. *Reviews of Modern Physics*, 78(3):865, 2006.
- [27] Lin Lin and Michael Lindsey. Variational embedding for quantum many-body problems. *Communications on Pure and Applied Mathematics*, 75(9):2033–2068, 2022.
- [28] Yuan Liu, Oinam R Meitei, Zachary E Chin, Arkopal Dutt, Max Tao, Troy Van Voorhis, and Isaac L Chuang. Bootstrap embedding on a quantum computer. *arXiv:2301.01457*, 2023.
- [29] Y Lu, X Cao, P Hansmann, and MW Haverkort. Natural-orbital impurity solver and projection approach for Green’s functions. *Physical Review B*, 100(11):115134, 2019.
- [30] Thomas Maier, Mark Jarrell, Thomas Pruschke, and Matthias H Hettler. Quantum cluster theories. *Reviews of Modern Physics*, 77(3):1027, 2005.
- [31] Oinam Romesh Meitei and Troy Van Voorhis. Periodic bootstrap embedding. *arXiv:2301.06153*, 2023.
- [32] Walter Metzner and Dieter Vollhardt. Correlated lattice fermions in  $d=\infty$  dimensions. *Physical review letters*, 62(3):324, 1989.
- [33] Abhishek Mitra, Matthew R Hermes, Minsik Cho, Valay Agarawal, and Laura Gagliardi. Periodic density matrix embedding for co adsorption on the MgO (001) surface. *The Journal of Physical Chemistry Letters*, 13(32):7483–7489, 2022.
- [34] Abhishek Mitra, Hung Q Pham, Riddhish Pandharkar, Matthew R Hermes, and Laura Gagliardi. Excited states of crystalline point defects with multireference density matrix embedding theory. *The Journal of Physical Chemistry Letters*, 12(48):11688–11694, 2021.
- [35] Max Nusspickel and George H Booth. Efficient compression of the environment of an open quantum system. *Physical Review B*, 102(16):165107, 2020.
- [36] Max Nusspickel and George H Booth. Frequency-dependent and algebraic bath states for a dynamical mean-field theory with compact support. *Physical Review B*, 101(4):045126, 2020.
- [37] Max Nusspickel and George H Booth. Systematic improbability in quantum embedding for real materials. *Physical Review X*, 12(1):011046, 2022.
- [38] Max Nusspickel, Basil Ibrahim, and George H Booth. On the effective reconstruction of expectation values from ab initio quantum embedding. *arXiv:2210.14561*, 2022.
- [39] Jeppe Olsen, Poul Jørgensen, and Jack Simons. Passing the one-billion limit in full configuration-interaction (FCI) calculations. *Chem. Phys. Lett.*, 169(6):463–472, 1990.
- [40] Hung Q Pham, Varinia Bernales, and Laura Gagliardi. Can density matrix embedding theory with the complete activate space self-consistent field solver describe single and double bond breaking in molecular systems? *Journal of chemical theory and computation*, 14(4):1960–1968, 2018.
- [41] Michael Potthoff. Two-site dynamical mean-field theory. *Physical Review B*, 64(16):165114, 2001.
- [42] Nathan Ricke, Matthew Welborn, Hong-Zhou Ye, and Troy Van Voorhis. Performance of bootstrap embedding for long-range interactions and 2d systems. *Molecular Physics*, 115(17-18):2242–2253, 2017.
- [43] Charles JC Scott and George H Booth. Extending density matrix embedding: A static two-particle theory. *Physical Review B*, 104(24):245114, 2021.

- [44] Sajanthan Sekaran, Matthieu Saubanère, and Emmanuel Fromager. Local potential functional embedding theory: A self-consistent flavor of density functional theory for lattices without density functionals. *Computation*, 10(3):45, 2022.
- [45] Bruno Senjean. Projected site-occupation embedding theory. *Physical Review B*, 100(3):035136, 2019.
- [46] Bruno Senjean, Naoki Nakatani, Masahisa Tsuchiizu, and Emmanuel Fromager. Site-occupation embedding theory using Bethe ansatz local density approximations. *Physical Review B*, 97(23):235105, 2018.
- [47] Steven H Strogatz. *Nonlinear dynamics and chaos with student solutions manual: With applications to physics, biology, chemistry, and engineering*. CRC press, 2018.
- [48] Chong Sun, Ushnish Ray, Zhi-Hao Cui, Miles Stoudenmire, Michel Ferrero, and Garnet Kin-Lic Chan. Finite-temperature density matrix embedding theory. *Physical Review B*, 101(7):075131, 2020.
- [49] Henry K Tran, Troy Van Voorhis, and Alex JW Thom. Using scf metadynamics to extend density matrix embedding theory to excited states. *The Journal of chemical physics*, 151(3):034112, 2019.
- [50] Henry K Tran, Hong-Zhou Ye, and Troy Van Voorhis. Bootstrap embedding with an unrestricted mean-field bath. *The Journal of Chemical Physics*, 153(21):214101, 2020.
- [51] Takashi Tsuchimochi, Matthew Welborn, and Troy Van Voorhis. Density matrix embedding in an antisymmetrized geminal power bath. *J. Chem. Phys.*, 143(2):024107, 2015.
- [52] Konstantinos D Vogiatzis, Dongxia Ma, Jeppe Olsen, Laura Gagliardi, and Wibe A de Jong. Pushing configuration-interaction to the limit: Towards massively parallel mcsce calculations. *J. Chem. Phys.*, 147(18):184111, 2017.
- [53] Christian Vorwerk, Nan Sheng, Marco Govoni, Benchen Huang, and Giulia Galli. Quantum embedding theories to simulate condensed systems on quantum computers. *Nature Computational Science*, 2(7):424–432, 2022.
- [54] Matthew Welborn, Takashi Tsuchimochi, and Troy Van Voorhis. Bootstrap embedding: An internally consistent fragment-based method. *J. Chem. Phys.*, 145(7):074102, 2016.
- [55] Steven R. White. Density matrix formulation for quantum renormalization groups. *Phys. Rev. Lett.*, 69(19):2863–2866, November 1992.
- [56] Sebastian Wouters, Carlos A Jiménez-Hoyos, Qiming Sun, and Garnet K-L Chan. A practical guide to density matrix embedding theory in quantum chemistry. *Journal of chemical theory and computation*, 12(6):2706–2719, 2016.
- [57] Xiaojie Wu, Zhi-Hao Cui, Yu Tong, Michael Lindsey, Garnet Kin-Lic Chan, and Lin Lin. Projected density matrix embedding theory with applications to the two-dimensional Hubbard model. *The Journal of Chemical Physics*, 151(6):064108, 2019.
- [58] Xiaojie Wu, Michael Lindsey, Tiangang Zhou, Yu Tong, and Lin Lin. Enhancing robustness and efficiency of density matrix embedding theory via semidefinite programming and local correlation potential fitting. *Physical Review B*, 102(8):085123, 2020.
- [59] Saad Yalouz, Sajanthan Sekaran, Emmanuel Fromager, and Matthieu Saubanère. Quantum embedding of multi-orbital fragments using the block-Householder transformation. *The Journal of Chemical Physics*, 157(21):214112, 2022.
- [60] Hong-Zhou Ye, Nathan D Ricke, Henry K Tran, and Troy Van Voorhis. Bootstrap embedding for molecules. *Journal of chemical theory and computation*, 15(8):4497–4506, 2019.
- [61] Hong-Zhou Ye, Henry K Tran, and Troy Van Voorhis. Bootstrap embedding for large molecular systems. *Journal of Chemical Theory and Computation*, 16(8):5035–5046, 2020.
- [62] Hong-Zhou Ye, Henry K Tran, and Troy Van Voorhis. Accurate electronic excitation energies in full-valence active space via bootstrap embedding. *Journal of Chemical Theory and Computation*, 17(6):3335–3347, 2021.

- [63] Hong-Zhou Ye and Troy Van Voorhis. Atom-based bootstrap embedding for molecules. *The journal of physical chemistry letters*, 10(20):6368–6374, 2019.
- [64] Hong-Zhou Ye, Matthew Welborn, Nathan D Ricke, and Troy Van Voorhis. Incremental embedding: A density matrix embedding scheme for molecules. *J. Chem. Phys.*, 149(19):194108, 2018.
- [65] Bo-Xiao Zheng and Garnet Kin-Lic Chan. Ground-state phase diagram of the square lattice Hubbard model from density matrix embedding theory. *Phys. Rev. B*, 93(3):035126, 2016.
- [66] Bo-Xiao Zheng, Chia-Min Chung, Philippe Corboz, Georg Ehlers, Ming-Pu Qin, Reinhart M Noack, Hao Shi, Steven R White, Shiwei Zhang, and Garnet Kin-Lic Chan. Stripe order in the underdoped region of the two-dimensional Hubbard model. *Science*, 358(6367):1155–1160, 2017.
- [67] Bo-Xiao Zheng, Joshua S Kretchmer, Hao Shi, Shiwei Zhang, and Garnet Kin-Lic Chan. Cluster size convergence of the density matrix embedding theory and its dynamical cluster formulation: A study with an auxiliary-field quantum Monte Carlo solver. *Phys. Rev. B*, 95(4):045103, 2017.

# Chapter 3

## A mathematical analysis of IPT-DMFT.

In this chapter, we provide a mathematical and numerical analysis of the IPT-DMFT equations. This part is joint work with Éric Cancès, Solal Perrin-Roussel.

**Abstract** We provide a mathematical analysis of the Dynamical Mean-Field Theory (DMFT), a celebrated representative of a class of approximations in quantum mechanics known as *embedding methods*. We start by a pedagogical and self-contained mathematical formulation of the DMFT equations for the finite Hubbard model. After recalling the definition and properties of one-body time-ordered Green's functions and self-energies, and the mathematical structure of the Hubbard and Anderson impurity models, we describe a specific *impurity solver*, namely the Iterated Perturbation Theory (IPT) solver, which can be conveniently formulated using Matsubara's Green's functions. Within this framework, we prove under certain assumptions that the DMFT equations admit a solution for any set of physical parameters. Moreover, we establish some properties of the solution(s).

### Contents

---

<b>3.1</b>	<b>Introduction</b>	<b>88</b>
<b>3.2</b>	<b>DMFT of the Hubbard model</b>	<b>90</b>
3.2.1	One-body Green's functions and the self-energy	90
3.2.2	Hubbard model	93
3.2.3	Anderson Impurity Model (AIM)	94
3.2.4	Dynamical Mean-Field Theory (DMFT)	96
3.2.5	A specific impurity solver : the Iterated Perturbation Theory (IPT) solver.	100
<b>3.3</b>	<b>Main results</b>	<b>104</b>
3.3.1	Pick functions	105
3.3.2	Functional setting: the Bath Update and IPT maps	106
3.3.3	Existence and properties of IPT-DMFT solutions	108
<b>3.4</b>	<b>Proofs</b>	<b>108</b>
3.4.1	Proofs of the results in Section 3.2	108
3.4.2	Proof of Proposition 3.3.3 ( $-G, -\Sigma, -\Delta$ are Pick matrices)	112
3.4.3	Proof of Proposition 3.3.5 (no finite-dimensional bath solution)	112
3.4.4	Proof of Proposition 3.3.6 (Bath Update map)	114
3.4.5	Proof of Proposition 3.3.8 (IPT map)	115
3.4.6	Continuity of the IPT-DMFT map	117
3.4.7	Proof of Theorem 3.3.9: existence of a fixed point	118
3.4.8	Proof of Proposition 3.3.10	119
<b>3.A</b>	<b>Uniqueness theorem for an interpolation problem</b>	<b>120</b>
3.A.1	Introduction and some general properties	120
3.A.2	A uniqueness result for ACPs with a rational solution	122
<b>3.B</b>	<b>Paramagnetic IPT-DMFT equations</b>	<b>124</b>
	<b>Bibliography</b>	<b>125</b>

---

### 3.1 Introduction

The Dynamical Mean-Field Theory (DMFT) is an approximation method for the fermionic quantum many-body problem. It was introduced by Georges and Kotliar in 1992 and first applied to the case of the Hubbard model [51, 22]. It has since been extended to other settings [59] and coupled with Density Functional Theory (DFT) within the so-called DFT+DMFT method [27]. The latter is one of the reference methods for first-principle computations of electronic structures of strongly correlated materials. DMFT belongs to the class of quantum embedding methods, and has since been joined by many other methods such as Density-Matrix Embedding Theory (DMET) [32], Rotationally-Invariant Slave Boson (RISB) method [35], Energy-weighted DMET [18], Quantum Embedding Theory [42], and related methods.

At the time of writing, the mathematical analysis of quantum embedding methods is very limited. The rigorous results we are aware of are those on DMFT contained in Lindsey's PhD thesis [41], the ones on DMET recently obtained by the first two authors and their collaborators [14], and a few others with a numerically oriented approach such as [16, 66].

The purpose of this article is to establish a rigorous mathematical formulation of the DMFT equations and to prove, in particular, the existence of a solution to the DMFT equations for the Hubbard model within the Iterated Perturbation Theory (IPT) approximation [22]. This relies on the extension of some results from [41, Part VII] and is based upon a reformulation of the DMFT equations as a fixed-point problem in the space of probability measures on the real line.

In the language of linear algebra, solving the fermionic quantum many-body problem consists in computing some spectral properties of a Hermitian matrix  $\hat{H} \in \mathbb{C}^{M \times M}$ , the Hamiltonian of the system, such as its ground-state energy (i.e. its lowest eigenvalue), or the partition function

$$Z_{\beta, \epsilon_F} := \exp\left(-\beta(\hat{H} - \epsilon_F \hat{N})\right),$$

where  $\beta = \frac{1}{k_B T}$  is the inverse temperature,  $\epsilon_F \in \mathbb{R}$  is the chemical potential, and  $\hat{N}$  is the number operator, as well as derivatives of  $Z_{\beta, \epsilon_F}$  with respect to  $\beta$ ,  $\epsilon_F$  or parameters of  $\hat{H}$ .

The difficulty is that the size  $M$  of the matrix  $\hat{H}$  can be huge (up to  $10^{30}$  or more in some applications). Fortunately, the Hamiltonian  $\hat{H}$  has specific properties, allowing one to use tailored methods. Indeed, in most applications,  $\hat{H}$  is the matrix of a Hamiltonian operator acting on a fermionic Fock space  $\mathcal{F}$ , containing only one- and two-body terms, and satisfying symmetry properties (particle number conservation, spin, and possibly space, isospin, or time-reversal symmetries). Identifying the one-body state space  $\mathcal{H}$  with  $\mathbb{C}^{2L}$ , it holds  $M = 2^{2L}$  and

$$\mathcal{F} = \bigoplus_{N=0}^L \mathcal{H}_N,$$

where the  $N$ -particle sector  $\mathcal{H}_N = \bigwedge^N \mathcal{H}$  of the Fock space is of dimension  $\binom{2L}{N}$ . In this decomposition,

$\hat{N}$  is a block diagonal operator, the block corresponding to  $\mathcal{H}_N$  being equal to  $N$  times the identity matrix. If  $\hat{H}$  is particle-number conserving, then it is also block-diagonal in this decomposition (equivalently  $\hat{H}$  and  $\hat{N}$  commute). If it only contains one- and two-body terms, then  $\hat{H}$  has a compact representation in the second quantization formalism involving a Hermitian matrix  $H^0 \in \mathbb{C}^{2L \times 2L}$  and a fourth-order tensor  $V \in \mathbb{C}^{2L \times 2L \times 2L \times 2L}$ . Spin, space, isospin, or time-reversal symmetries allow one to further reduce the complexity of the representation of  $\hat{H}$  and refine its block diagonal structure. Still, solving the quantum many-body problem remains extremely challenging.

Quantum embedding methods can be seen as domain decomposition methods in the Fock space, using a partition of the  $L$  "sites" (also called orbitals) of the model into  $P$  non-overlapping clusters  $(\Lambda_p)_{1 \leq p \leq P}$  of cardinalities  $L_p := |\Lambda_p|$ . Without loss of generality, we can assume that the first cluster consists of the first  $L_1$  orbitals, the second cluster of the next  $L_2$  orbitals, and so on. To each cluster is associated an impurity model, a quantum many-body problem set on the  $L_p$  sites of the cluster, as well as on virtual sites called bath orbitals. In DMET, the number of bath orbitals is exactly equal to  $L_p$  so that the impurity quantum many-body problem is of size  $M_p := 2^{4L_p}$ . In practice, DMET impurity problems are solved either by brute-force diagonalization (full CI) if  $L_p$  is not too large, or by low-rank tensor methods (e.g. Density Matrix Renormalization Group, DMRG [64]). In DMFT, the impurity problem can be much larger, but the impurity Hamiltonian has the relatively simple form of an Anderson Impurity Model

(AIM): within each of the  $P$  impurity models, bath orbitals do not contribute to two-body interactions, and only interact with cluster orbitals via one-body interactions. It can be shown that the AIM associated with the  $p$ -th cluster can be completely described by the restriction of  $\hat{H}$  to the  $p$ -th cluster's orbitals and a hybridization function  $\Delta_p : \mathbb{C} \setminus \mathbb{R} \rightarrow \mathbb{C}^{L_p \times L_p}$ . AIMs are usually solved in practice either by a quantum Monte Carlo method [52], or by an approximate solver such as the IPT (Iterative Perturbation Theory) solver [22] considered in this article. The IPT solver was introduced in the seminal paper [68], and is still used to study very challenging systems such as moiré heterobilayers [60].

Quantum embedding methods are self-consistent theories: the  $P$  impurity problems are coupled through a mean-field defined on the whole quantum system with  $L$  orbitals.

In DMET, the role of the mean-field is played by an approximation  $D \in \mathbb{C}^{2L \times 2L}$  of the ground-state one-body density matrix (1-RDM) of the system. The matrix  $D$  allows one to define an impurity problem for each cluster, and the self-consistent condition is that for each cluster  $p$ , the diagonal block of  $D$  corresponding to this cluster agrees with the restriction of the exact ground-state 1-RDM of the  $p$ -th impurity problem to the cluster  $p$ . It is expected that at self-consistency the diagonal blocks of  $D$  corresponding to the cluster decomposition are good approximations of the diagonal blocks of the exact ground-state 1-RDM of the whole system [14].

In DMFT, the role of the mean-field is played by an approximation  $G$  of the exact one-body Green's function [43] associated with some equilibrium state, usually the ground-state of  $\hat{H}$  in the  $N$ -particle sector, or a canonical or grand-canonical thermodynamical equilibrium state. One-body Green's functions can be represented by analytic functions  $G : \mathbb{C} \setminus \mathbb{R} \rightarrow \mathbb{C}^{2L \times 2L}$  and are thus computationally tractable objects for values of  $L$  up to a few thousands. The function  $G$  is a particular holomorphic extension of the Fourier transform of the time-ordered Green's function. Loosely speaking, the latter is an equilibrium time-correlation function obtained by creating (resp. annihilating) a particle at time  $t_0 = 0$  (resp. at  $t < 0$ ), letting the system evolve from  $t_0$  to  $t$  (resp. from  $t$  to  $t_0$ ), and annihilating the extra particle (resp. restoring the missing particle) at time  $t$  (resp. at time  $t_0$ ). The exact one-body Green's function contains a lot of valuable information about the quantum system under investigation. In particular, the 1-RDM of the equilibrium state, hence the expectation value of any one-body observable, can be easily extracted from it. The same holds true for the average energy, thanks to Galitski-Migdal's formula [24, 43]. Also, the poles of the analytic continuation of  $G$  to the real-axis correspond to the one-particle excitation energies measured in photoemission and inverse-photoemission spectroscopies [69]. Remarkably, the exact Green's function  $G^0$  of a non-interacting system, i.e. of a many-body Hamiltonian which is the second quantization of a one-body hamiltonian  $d\Gamma(H^0)$  is simply the resolvent of  $H^0$ :  $G^0(z) = (z - H^0)^{-1}$ , whatever the reference equilibrium state. The self-energy of an interacting system with Hamiltonian  $\hat{H} = d\Gamma(H^0) + \hat{H}^I$ , where  $\hat{H}^I$  accounts for the two-body interactions, is the function  $\Sigma : \mathbb{C} \setminus \mathbb{R} \rightarrow \mathbb{C}^{2L \times 2L}$  defined by

$$\Sigma(z) = G^0(z)^{-1} - G(z)^{-1} \quad \text{or equivalently} \quad G(z) = (z - H^0 - \Sigma(z))^{-1}. \quad (3.1)$$

DMFT consists in

- approximating the exact self-energy of the whole system by a block diagonal self-energy  $\Sigma = \text{block-diag}(\Sigma_1, \dots, \Sigma_P)$ , with  $\Sigma_p : \mathbb{C} \setminus \mathbb{R} \rightarrow \mathbb{C}^{2L_p \times 2L_p}$  compatible with the cluster decomposition. This condition is sometimes called the DMFT approximation;
- imposing the self-consistent conditions that for each cluster
  - the self-energy  $\Sigma_p$  agrees with the restriction to the cluster of the exact self-energy of the associated AIM.
  - the restriction to the cluster of the approximate Green's function of the whole system agrees with the restriction to the cluster of the exact Green's function of the AIM. This condition is often referred to as the self-consistent condition.

In practice, the DMFT equations are solved by fixed-point iterations. The input of iteration  $n$  is a collection of  $P$  hybridization functions  $(\Delta_p^{(n)})_{1 \leq p \leq P}$ . At step 1, the  $P$  AIM problems with hybridization functions  $\Delta_p^{(n)}$  are solved in parallel, in order to compute  $P$  cluster self-energies  $\Sigma_p^{(n)}$ , yielding an approximation  $\Sigma^{(n)} = \text{block-diag}(\Sigma_1^{(n)}, \dots, \Sigma_P^{(n)})$  of the self-energy of the whole system. At step 2, the above two self-consistent conditions are combined yielding a new set  $(\Delta_p^{(n+1)})_{1 \leq p \leq P}$  of hybridization functions. The DMFT iteration scheme can therefore be sketched as

$$\Delta^{(n)} := (\Delta_p^{(n)})_{1 \leq p \leq P} \xrightarrow{f^{\text{AIM}}} \Sigma^{(n)} := (\Sigma_p^{(n)})_{1 \leq p \leq P} \xrightarrow{f^{\text{SC}}} \Delta^{(n+1)} := (\Delta_p^{(n+1)})_{1 \leq p \leq P},$$

or written in the more compact form

$$\Delta^{(n+1)} = f^{\text{DMFT}}(\Delta^{(n)}). \quad (3.2)$$

Of course, this basic self-consistent loop can be stabilized and accelerated using e.g. damping and Anderson-Pulay extrapolation methods. In this article, we forego an in-depth analysis of the iterative scheme and its convergence, opting instead to direct our attention towards a fundamental inquiry: the existence of solutions within the DMFT equations. Specifically, we address the question of the existence of a fixed-point of the DMFT map  $f^{\text{DMFT}}$ , a critical aspect which, to our knowledge remains unestablished in the current literature.

This article is organized as follows. In Section 3.2, we provide a mathematical introduction to DMFT for the Hubbard model aimed at being accessible to readers unfamiliar with this theory. The Hubbard model provides insights into the behavior of electrons in strongly correlated systems. Its integration within the DMFT framework offers a powerful tool for understanding the interplay between electron-electron interactions in finite structures (truncation of a lattice for instance), shedding light on phenomena such as metal-insulator transitions and high-temperature superconductivity. We recall the basics of second quantization formalism, the formulation of the Hubbard and Anderson impurity models, the definitions of one-body Green's functions, self-energies, and hybridization functions, and the precise formulation of the DMFT equations. In Section 3.3, we state our main results. They are based on the observation that the key mathematical objects involved in DMFT (exact and approximate one-body Green's functions and self-energies, hybridization functions) are all negatives of Pick functions. Recall that scalar Pick functions are analytic functions from the open upper-half plane to the closed upper-half plane [45], [49]. An interesting property of scalar Pick functions, which we use extensively in our analysis, is that any Pick function admits an integral representation involving a positive Borel measure on  $\mathbb{R}$ , called its Nevanlinna-Riesz measure [45]. Analogous properties hold true for matrix-valued Pick functions [23]. For the Hubbard model with a finite number of sites, the exact Green's function and self-energy can be extended to meromorphic functions on  $\mathbb{C}$  with finite numbers of poles, and are therefore represented by discrete Nevanlinna-Riesz measures with finite support. We then focus on the paramagnetic single-site translation invariant IPT-DMFT approximation of the Hubbard model, for which  $P = L$  and  $L_1 = \dots = L_P = 1$ . We show that these equations have no solutions in the class of (negatives of) Pick functions with discrete Nevanlinna-Riesz measures of finite support, but do have solutions in the set of (negatives of) Pick functions. More precisely, equation (3.2) has a translation invariant fixed point  $(\Delta, \dots, \Delta)$ ,  $\Delta$  being the negative of a Pick function whose Nevanlinna-Riesz measure has the form  $c\nu$ , where  $c \in \mathbb{R}_+$  is a fixed constant only depending on the matrix  $H^0$ , and  $\nu$  a Borel probability measure on  $\mathbb{R}$ . To obtain the latter result, we show that the IPT-DMFT iteration map  $f^{\text{DMFT}}$  in (3.2) can be rewritten as a map  $F^{\text{DMFT}} : \mathcal{P}(\mathbb{R}) \rightarrow \mathcal{P}(\mathbb{R})$ , which is continuous for the weak topology. We conclude by checking that the Schauder-Singbal's fixed-point theorem [57] can be applied to this setting.

## 3.2 DMFT of the Hubbard model

We provide in this section a mathematical description of the models and quantities of interest involved in Dynamical Mean-Field Theory (DMFT) for the Hubbard model. We first recall the definitions of one-body Green's functions and the self-energy. We then introduce the Hubbard model and the Anderson Impurity Model (AIM). Next, we derive the DMFT equations and finally present the Iterated Perturbation Theory (IPT) solver, which is the approximate impurity solver considered in this work.

### 3.2.1 One-body Green's functions and the self-energy

One-body Green's functions are key objects in DMFT. To avoid technicalities, we will define Green's functions in a finite-dimensional setting and assume that the one-body state space is a finite-dimensional Hilbert space  $(\mathcal{H}, \langle \cdot, \cdot \rangle)$ ,  $\dim(\mathcal{H}) = 2L \in \mathbb{N}^*$ . We refer to e.g. [13] for a mathematical introduction to Green's functions in an infinite-dimensional setting. The associated Fock space

$$\mathcal{F} = \bigoplus_{n=0}^{2L} \bigwedge^n \mathcal{H},$$

where the  $n$ -particle sector  $\bigwedge^n \mathcal{H}$  is the anti-symmetrized tensor product of  $n$  copies of  $\mathcal{H}$ , is then of dimension  $2^{2L}$ . Given a one-particle state  $\phi \in \mathcal{H}$ , we denote by  $\hat{a}_\phi$  (resp.  $\hat{a}_\phi^\dagger$ ) the usual annihilation

(resp. creation) operator defined on  $\mathcal{F}$  (see e.g. [12]), which satisfy the Canonical Anti-commutation Relations (CAR):

$$\forall \phi, \phi' \in \mathcal{H}, \quad \{\hat{a}_\phi, \hat{a}_{\phi'}\} = \{\hat{a}_\phi^\dagger, \hat{a}_{\phi'}^\dagger\} = 0, \quad \{\hat{a}_\phi, \hat{a}_{\phi'}^\dagger\} = \langle \phi, \phi' \rangle$$

where  $\{\hat{O}, \hat{O}'\} = \hat{O}\hat{O}' + \hat{O}'\hat{O}$  is the anti-commutator of the two operators  $\hat{O}, \hat{O}' \in \mathcal{L}(\mathcal{F})$ .

**Equilibrium states.** A *state*  $\Omega$  is a linear form on the set of operators  $\mathcal{L}(\mathcal{F})$ , which is positive ( $\Omega(\hat{O}^\dagger \hat{O}) \geq 0$ ) and normalized (i.e.  $\sup\{|\Omega(\hat{O})|, \|\hat{O}\| = 1\} = 1$ ). In the finite-dimensional case, any state  $\Omega$  can be represented by a unique self-adjoint operator  $\hat{\rho} \in \mathcal{S}(\mathcal{F})$  such that for all  $\hat{O} \in \mathcal{L}(\mathcal{F})$ ,  $\Omega(\hat{O}) = \text{Tr}(\hat{\rho}\hat{O})$ . The operator  $\hat{\rho}$  is positive and satisfies  $\text{Tr}(\hat{\rho}) = 1$ . It is called the *density operator* associated to the state  $\Omega$ . For an isolated quantum system described by a time-independent Hamiltonian  $\hat{H} \in \mathcal{S}(\mathcal{F})$ , an equilibrium state corresponds to a stationary solution to the quantum Liouville equation

$$i \frac{d\hat{\rho}}{dt}(t) = [\hat{H}, \hat{\rho}(t)],$$

where  $[\hat{O}, \hat{O}'] = \hat{O}\hat{O}' - \hat{O}'\hat{O}$  is the commutator of  $\hat{O}, \hat{O}' \in \mathcal{L}(\mathcal{F})$ . It follows that a state is an equilibrium state if and only if its density  $\hat{\rho}$  commutes with the Hamiltonian  $\hat{H}$ , namely  $[\hat{H}, \hat{\rho}] = 0$ . Important examples of equilibrium states are thermal and osmotic equilibrium states known as Gibbs states, as well as ground and excited states of  $\hat{H}$  with a prescribed number of particles (for particle-number conserving Hamiltonians).

**One-body Green's functions.** The *one-body time-ordered Green's functions* are then defined as follows:

**Definition 3.2.1** (One-body time-ordered Green's function). *Given a Hamiltonian  $\hat{H} \in \mathcal{S}(\mathcal{F})$  and an associated equilibrium state  $\Omega$ , one defines the  $\mathcal{L}(\mathcal{H})$ -valued function  $\tilde{G} : \mathbb{R} \rightarrow \mathcal{L}(\mathcal{H})$ , known as one-body time-ordered Green's function, so that  $i\tilde{G}(t)$  is the operator represented by the sesquilinear form*

$$\langle \phi, (i\tilde{G}(t))\phi' \rangle = \chi_{\mathbb{R}_+}(t) \Omega(\mathbb{H}(\hat{a}_\phi)(t)\hat{a}_{\phi'}^\dagger) - \chi_{\mathbb{R}_-^*}(t) \Omega(\hat{a}_{\phi'}^\dagger \mathbb{H}(\hat{a}_\phi)(t)) \quad (3.3)$$

where for all  $\hat{O} \in \mathcal{L}(\mathcal{F}), \mathbb{H}(\hat{O}) : \mathbb{R} \ni t \mapsto e^{it\hat{H}}\hat{O}e^{-it\hat{H}}$  is the Heisenberg picture of  $\hat{O}$  and  $\chi_A$  is the characteristic function of the set  $A$ .

Let us comment on the terminology. First, the term “body” encompasses “particle” and “hole”: the first term of the right hand side of (3.3) can be interpreted as describing the propagation from  $t_0 = 0$  to  $t > 0$  of a particle added to the system at  $t_0 = 0$ , while the second term can be interpreted as the propagation from  $t < 0$  to  $t_0 = 0$  of a hole created at  $t < 0$ . Second, it is “time-ordered”: the r.h.s. of (3.3) can be rewritten as

$$\Omega \left( \mathcal{T} \left( \mathbb{H}(\hat{a}_\phi), \mathbb{H}(\hat{a}_{\phi'}^\dagger) \right) (t, 0) \right)$$

where for all operators-valued functions  $\mathbb{R} \ni t \mapsto \hat{O}(t) \in \mathcal{L}(\mathcal{F}), \mathbb{R} \ni t \mapsto \hat{O}'(t) \in \mathcal{L}(\mathcal{F})$ , the fermionic *time-ordered product*  $\mathcal{T}(\hat{O}, \hat{O}')$  is the operator-valued function  $\mathbb{R}^2 \rightarrow \mathcal{L}(\mathcal{F})$  defined as

$$\mathcal{T}(\hat{O}, \hat{O}')(t, t') = \begin{cases} \hat{O}(t)\hat{O}'(t') & \text{if } t \geq t' \\ -\hat{O}'(t')\hat{O}(t) & \text{otherwise,} \end{cases}$$

where the minus sign is specific to the fermionic case. Up to a sign, it is the product of the operators applied in the order of increasing time.

The  $i$  prefactor in the left hand side of (3.3) is a convention that facilitates the expression of the results to come, especially Proposition 3.2.3.

Finally, note that  $\tilde{G}$  is real-analytic on  $(-\infty, 0) \cup (0, +\infty)$  with a  $-i\mathbf{1}$  jump at  $t = 0$  due to the CAR.

As  $\mathcal{F}$  is finite-dimensional, the Green's function can be expanded in a joint orthonormal eigenbasis  $\mathcal{B}$  of  $\hat{\rho}$  and  $\hat{H}$ , leading to the Källén-Lehmann (KL) representation [34, 36]

$$\forall \phi, \phi' \in \mathcal{H}, \quad \langle \phi, i\tilde{G}(t)\phi' \rangle = \sum_{\psi, \psi' \in \mathcal{B}} e^{it(E_\psi - E_{\psi'})} \langle \psi, \hat{a}_\phi \psi' \rangle \langle \psi', \hat{a}_{\phi'}^\dagger \psi \rangle \left( \rho_\psi \chi_{\mathbb{R}_+}(t) - \rho_{\psi'} \chi_{\mathbb{R}_-^*}(t) \right), \quad (3.4)$$

where  $\forall \psi \in \mathcal{B}, \hat{H}\psi = E_\psi \psi$  (with  $E_\psi \in \mathbb{R}$ ) and  $\hat{\rho}\psi = \rho_\psi \psi$  (with  $\rho_\psi \in \mathbb{R}_+$ ,  $\sum_{\psi \in \mathcal{B}} \rho_\psi = 1$ ).

Other types of Green's functions are encountered in the physics literature, notably retarded/advanced Green's functions. These objects encode the same information on the spectral properties of  $\hat{H}$  as the time-ordered Green's function, but this information is stored in a different way. A suitable way to highlight this information is to consider specific holomorphic extensions to the complex plane of the time-Fourier transform of these Green's functions [43, 13]. In the case of the time-ordered one-body Green's function, the suitable holomorphic extension is provided by the generalized Fourier transform introduced by Titchmarsh [61].

**Definition 3.2.2** (Generalized Fourier Transform (GFT)). *The Generalized Fourier Transform (GFT) of the one-body time-ordered Green's function  $\tilde{G}$  is the analytic function on the upper-half plane  $G : \mathbb{C}_+ \rightarrow \mathcal{L}(\mathcal{H})$ , also called a (one-body) Green's function, defined by*

$$\forall z \in \mathbb{C}_+, G(z) = G_+(z) + G_-(\bar{z})^\dagger \quad (3.5)$$

with

$$\begin{aligned} \forall z \in \mathbb{C}_+ := \{z \in \mathbb{C} \mid \Im(z) > 0\}, \quad G_+(z) &= \int_{\mathbb{R}_+} e^{izt} \tilde{G}(t) dt, \\ \forall z \in \mathbb{C}_- := \{z \in \mathbb{C} \mid \Im(z) < 0\}, \quad G_-(z) &= \int_{\mathbb{R}_-} e^{izt} \tilde{G}(t) dt. \end{aligned}$$

Note that the Green's function  $G$  can be extended to  $\mathbb{C} \setminus \mathbb{R}$  by reflection, namely by setting

$$\forall z \in \mathbb{C}_-, \quad G(z) = G(\bar{z})^\dagger. \quad (3.6)$$

By construction,  $G(z)$  is analytic on  $\mathbb{C}_+$ . In addition, it follows from the KL representation (3.4) that

$$\forall z \in \mathbb{C}_+, \quad \forall \phi, \phi' \in \mathcal{H}, \quad \langle \phi, G(z) \phi' \rangle = \sum_{\psi, \psi' \in \mathcal{B}} \frac{\rho_\psi + \rho_{\psi'}}{z + (E_\psi - E_{\psi'})} \langle \psi, \hat{a}_\phi \psi' \rangle \langle \psi', \hat{a}_{\phi'}^\dagger \psi \rangle. \quad (3.7)$$

An important observation is that

$$\forall z \in \mathbb{C}_+, \quad \forall \phi \in \mathcal{H} \setminus \{0\}, \quad \Im(\langle \phi, G(z) \phi \rangle) = -\Im(z) \sum_{\psi, \psi' \in \mathcal{B}} \frac{\rho_{\psi'} + \rho_\psi}{|z + (E_\psi - E_{\psi'})|^2} |\langle \psi, \hat{a}_\phi \psi' \rangle|^2 < 0, \quad (3.8)$$

which shows in particular that  $G(z)$  is invertible for all  $z \in \mathbb{C}_+$ .

Up to now, we have not specified the Hamiltonian  $\hat{H}$ ; in the sequel, we will assume that it is of the form

$$\hat{H} = d\Gamma(H^0) + \hat{H}^I, \quad H^0 \in \mathcal{S}(\mathcal{H}), \quad \hat{H}^I \in \mathcal{S}(\mathcal{F}) \quad (3.9)$$

where  $d\Gamma(H^0)$  is the second quantization of the one-particle Hamiltonian  $H^0 \in \mathcal{S}(\mathcal{H})$  (see e.g. [12]) and  $\hat{H}^I \in \mathcal{S}(\mathcal{F})$  some interaction Hamiltonian. We say that  $\hat{H}$  is *non-interacting* if  $\hat{H}^I = 0$ .

Depending on the formalism of interest, one can consider the grand canonical Hamiltonian  $\hat{H}' = \hat{H} - \epsilon_F \hat{N}$  without loss of generality.

The following is an essential property of the Green's function, to which it owes its name: the Green's function of a non-interacting system in an equilibrium state is the resolvent of the one-particle Hamiltonian.

**Proposition 3.2.3** (Non-interacting Green's function). *Let  $H^0 \in \mathcal{S}(\mathcal{H})$  be a one-particle Hamiltonian and  $\Omega$  an equilibrium state of the non-interacting Hamiltonian  $d\Gamma(H^0)$ . The Green's function  $G^0$  of  $d\Gamma(H^0)$  associated to  $\Omega$  is the resolvent of  $H^0$ :*

$$\forall z \in \mathbb{C}_+, \quad G^0(z) = (z - H^0)^{-1}. \quad (3.10)$$

In particular,  $G^0$  is independent of  $\Omega$ .

The proof of this classical result is recalled in Section 3.4.1. It is a consequence of the fact that the one-body Green's function  $\tilde{G}^0$  of the non-interacting Hamiltonian  $d\Gamma(H^0)$  is solution to the equation

$$\left( i \frac{d}{dt} - H^0 \right) \tilde{G} = \delta \mathbf{1} \quad \text{in } \mathcal{D}'(\mathbb{R}; \mathcal{L}(\mathcal{H})) \quad (3.11)$$

so that the time-ordered Green's function  $\tilde{G}^0$  is indeed a Green's function of the linear differential operator  $i \frac{d}{dt} - H^0$ . The various avatars of the Green's function (retarded/advanced) also satisfy this equation in  $\mathcal{D}'(\mathbb{R}^*; \mathcal{L}(\mathcal{H}))$ , but with different boundary conditions at infinity and jumps at  $t = 0$ . The properties (3.10)-(3.11) hold *only* for non-interacting Hamiltonians.

**Self-energy.** For interacting systems, the general relation between the Hamiltonian and the Green's function is more involved: the discrepancy with the non-interacting case is characterized by the *self-energy*.

**Definition 3.2.4** (Self-energy). *The self-energy  $\Sigma : \mathbb{C}_+ \rightarrow \mathcal{L}(\mathcal{H})$  of an Hamiltonian  $\hat{H}$  of the form (3.9) associated to an equilibrium state  $\Omega$  of  $\hat{H}$  is defined by*

$$\forall z \in \mathbb{C}_+, \quad \Sigma(z) = G^0(z)^{-1} - G(z)^{-1}, \quad (3.12)$$

where the non-interacting Green's function  $G^0$  is the Green's function of any equilibrium state of  $d\Gamma(H^0)$ .

Recall that  $G^0(z)^{-1} = z - H^0$  (3.10) and that  $G(z)$  is invertible in view of (3.8). Let us emphasize that the definition of the self-energy only depends on  $H$ ,  $H^0$ , and the considered equilibrium state  $\Omega$  of  $\hat{H}$ , since  $G^0$  is independent of the equilibrium state associated to  $d\Gamma(H^0)$ .

Using again (3.10) and the definition of the self-energy, the Green's function  $G$  can be rewritten as

$$\forall z \in \mathbb{C}_+, \quad G(z) = (z - (H^0 + \Sigma(z)))^{-1}$$

so that, for a given complex frequency  $z$ ,  $H^0 + \Sigma(z)$  can be considered as an *effective one-particle Hamiltonian* (compare with (3.10)): the self-energy is thus the extra term to be added to  $H^0$  to obtain a representation of the interacting system of particles in terms of a system of non-interacting ones. The frequency dependence of  $\Sigma$  comes from the fact that particles do interact in the original system.

### 3.2.2 Hubbard model

Originally introduced in quantum chemistry [48, 50], the Hubbard model [31, 29, 26] is an idealized model that minimally describes *interacting electrons* in a molecule or a crystalline material. From the mathematical physics' perspective, it is a prototypical example of short-range fermionic lattice system, and its mathematical study has been pioneered soon after its introduction in [38, 39], triggering an extensive study of its ground-states properties [37]. More recently, the discovery of cuprate-based high-temperature superconductors [8, 67], exhibiting a *layered structure*, shed new light on the *square lattice* Hubbard model, for which much remains to be discovered [37]. Since then, *approximation methods* have been derived for this model such as *generalized Hartree-Fock* [6], and Dynamical Mean-Field Theory [22].

In this article, we restrict ourselves to *finite-dimensional* Hubbard models, i.e. to Hubbard models defined on *finite graphs*. The reason for this is threefold. First, we stick to the case of finite-dimensional state spaces, for which all the objects involved in the mathematical formulation of DMFT are well-defined. Second, *graph theory* provides a suitable formalism to describe on the same footing different physical settings, ranging from molecular systems to truncated lattices, and with arbitrary hopping parameters (nearest neighbours, next nearest neighbors, ...). Third, this is precisely the language in which DMFT can be formulated concisely, as described in Section 3.2.4.

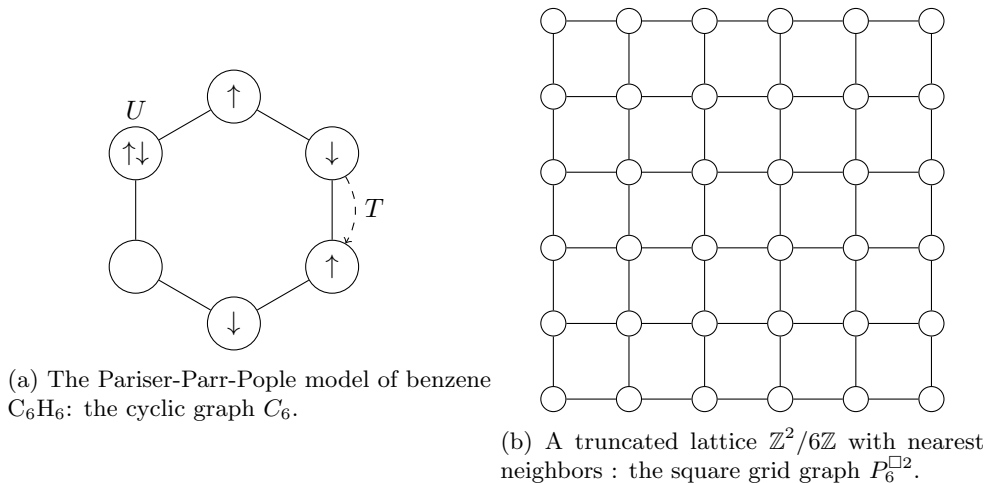


Figure 1: The Hubbard model for different graphs

Consider now a finite undirected graph  $\mathcal{G}_H = (\Lambda, E)$  that describes the “sites”  $\Lambda$  hosting electrons, as depicted in Figure 1. The state space of a site is the vector space spanned by the orthonormal vectors  $|\emptyset\rangle$

(empty site),  $|\uparrow\rangle$  (site occupied by one spin-up electron),  $|\downarrow\rangle$  (site occupied by one spin-down electron), and  $|\uparrow\downarrow\rangle$  (doubly-occupied site). Note that  $|\uparrow\downarrow\rangle$  is a shorthand notation for the two-electron singlet state  $2^{-1/2}(|\uparrow\rangle\otimes|\downarrow\rangle - |\downarrow\rangle\otimes|\uparrow\rangle)$ . In chemistry language, to each site is associated a single orbital (and thus two spin-orbitals); in physics, this setting is referred to as the *one-band* Hubbard model. Since the sites are distinguishable, the state space of the full system is the tensor product of the state space of each site. It is therefore of dimension  $4^{|\Lambda|} = 2^{2L}$  where  $L = |\Lambda|$  is the number of sites.

Let us now specify the Hamiltonian. In the Hubbard model, electrons can jump from one site to any other neighboring site. This models the tunnel effect, whose intensity is described by the *hopping matrix*  $T$ , as for tight-binding Hamiltonians. Electrons repel each other due to (screened) Coulomb interaction. The simplicity of the Hubbard model lies in the *range* of this interaction, which is the shortest possible: it is only effective for two electrons occupying the same site, and if the site  $i$  is doubly occupied, the energy of the system is increased by an *on-site repulsion*  $U_i$ .

More precisely, a finite-dimensional Hubbard model can be defined as follow.

**Definition 3.2.5** (Hubbard model of a finite graph). *Given a finite graph  $\mathcal{G}_H = (\Lambda, E)$ , a hopping matrix  $T : E \rightarrow \mathbb{R}$ , and an on-site repulsion  $U : \Lambda \rightarrow \mathbb{R}$ , the Hubbard Fock Space  $\mathcal{F}_H$  is defined as*

$$\mathcal{F}_H = \bigotimes_{i \in \Lambda} \mathcal{F}_1, \quad \mathcal{F}_1 = \text{Span}(|\emptyset\rangle, |\uparrow\rangle, |\downarrow\rangle, |\uparrow\downarrow\rangle)$$

and the Hubbard Hamiltonian  $\hat{H}_H \in \mathcal{S}(\mathcal{F}_H)$  as

$$\hat{H}_H = \sum_{\{i,j\} \in E, \sigma \in \{\uparrow, \downarrow\}} T_{i,j} \left( \hat{a}_{i,\sigma}^\dagger \hat{a}_{j,\sigma} + \hat{a}_{j,\sigma}^\dagger \hat{a}_{i,\sigma} \right) + \sum_{i \in \Lambda} U_i \hat{n}_{i,\uparrow} \hat{n}_{i,\downarrow}$$

where the usual annihilation and creation operators  $\hat{a}_{i,\sigma}$  and  $\hat{a}_{i,\sigma}^\dagger$  of an electron on site  $j$  with spin  $\sigma$  satisfy the CAR

$$\forall i, j \in \Lambda, \quad \sigma \in \{\uparrow, \downarrow\}, \quad \{\hat{a}_{i,\sigma}, \hat{a}_{j,\sigma'}\} = \{\hat{a}_{i,\sigma}^\dagger, \hat{a}_{j,\sigma'}^\dagger\} = 0, \quad \{\hat{a}_{i,\sigma}, \hat{a}_{j,\sigma'}^\dagger\} = \delta_{i,j} \delta_{\sigma,\sigma'}, \quad (3.13)$$

and the site number operators  $\hat{n}_{i,\sigma}$  are defined by  $\hat{n}_{i,\sigma} = \hat{a}_{i,\sigma}^\dagger \hat{a}_{i,\sigma}$ .

In this paper, we do not consider external magnetic field, so that we can assume without loss of generality that the hopping matrix  $T$  is real-valued [37]. For standard Coulomb interaction, the on-site repulsion  $U$  is positive, but we do not need to make this assumption here.

**Remark 3.2.6.** *The Hubbard Hamiltonian  $\hat{H}_H$  is particle-number and spin conserving, i.e. it commutes with the number operator  $\hat{N}_H = \sum_{i \in \Lambda} (\hat{n}_{i,\uparrow} + \hat{n}_{i,\downarrow})$  and the spin operators. In particular, it commutes with the z-component  $\hat{S}_H^z = \frac{1}{2} \sum_{i \in \Lambda} (\hat{n}_{i,\uparrow} - \hat{n}_{i,\downarrow})$  of the spin operator. This property will be used later to make the IPT-DMFT model spin-independent.*

### 3.2.3 Anderson Impurity Model (AIM)

**Impurity models** Impurity models are models in which an “impurity” is coupled to a “bath” in such a way that particles in the bath do not interact, and the coupling Hamiltonian between the impurity and the bath only involves one-body terms. Otherwise stated, the one-particle state space and the Fock space of the total system can be decomposed as

$$\mathcal{H}_{\text{IM}} = \mathcal{H}_{\text{imp}} \oplus \mathcal{H}_{\text{bath}} \quad \text{and} \quad \mathcal{F}_{\text{IM}} = \mathcal{F}_{\text{imp}} \otimes \mathcal{F}_{\text{bath}}, \quad (3.14)$$

and its Hamiltonian as

$$\hat{H}_{\text{IM}} = \hat{H}_{\text{imp}} \otimes 1_{\text{bath}} + 1_{\text{imp}} \otimes \hat{H}_{\text{bath}} + \hat{H}_{\text{coupling}}, \quad (3.15)$$

with

$$\hat{H}_{\text{imp}} = d\Gamma(H_{\text{imp}}^0) + \hat{H}_{\text{imp}}^I, \quad \hat{H}_{\text{bath}} = d\Gamma(H_{\text{bath}}^0), \quad \hat{H}_{\text{coupling}} = d\Gamma(H_{\text{coupling}}^0), \quad (3.16)$$

and  $H_{\text{coupling}}^0$  can be decomposed according to (3.14) as

$$H_{\text{coupling}}^0 = \begin{pmatrix} 0 & V \\ V^\dagger & 0 \end{pmatrix}.$$

Reshuffling the terms, we also have

$$\hat{H}_{\text{IM}} = d\Gamma(H_{\text{IM}}^0) + \hat{H}_{\text{imp}}^I \otimes 1_{\text{bath}}, \quad \text{with} \quad H_{\text{IM}}^0 = \begin{pmatrix} H_{\text{imp}}^0 & V \\ V^\dagger & H_{\text{bath}}^0 \end{pmatrix}. \quad (3.17)$$

As will be seen below, a key step of the DMFT iteration loop is to compute the restriction of the Green's function  $G_{\text{IM}}$  of an impurity model to the impurity space  $\mathcal{H}_{\text{imp}}$ . This is in general a difficult task. On the other hand, computing the restriction of the *non-interacting* Green's function can easily be done using a Schur complement technique. This leads to the concept of hybridization function, which, as announced in the introduction, is of paramount importance in the mathematical formulation of DMFT.

**Definition 3.2.7** (Hybridization function  $\Delta$  of an impurity model). *Given an impurity model of the form (3.14)-(3.17), its hybridization function  $\Delta : \mathbb{C}_+ \rightarrow \mathcal{L}(\mathcal{H}_{\text{imp}})$  is defined by*

$$\forall z \in \mathbb{C}_+, \quad \Delta(z) = V(z - H_{\text{bath}}^0)^{-1} V^\dagger. \quad (3.18)$$

Using this definition and Proposition 3.2.3, the non-interacting Green's function of the impurity model is then given in the decomposition (3.14) by

$$G^0(z) = (z - H_{\text{IM}}^0)^{-1} = \begin{pmatrix} (z - H_{\text{imp}}^0 - \Delta(z))^{-1} & * \\ * & * \end{pmatrix}.$$

The hybridization function  $\Delta$  thus plays a role analogous to the self-energy  $\Sigma$ . The equation

$$(G^0(z))_{\text{imp}} = (z - (H_{\text{imp}}^0 + \Delta(z)))^{-1}$$

means that  $H_{\text{imp}}^0 + \Delta(z)$  can be considered as an *effective one-particle impurity Hamiltonian*: the hybridization function is the extra term to be added to  $H_{\text{imp}}^0$  so that, in the non-interacting case, a particle in the whole system can be regarded as a particle localized on the impurity. In the time domain, the hybridization function describes the phenomenon of a particle localized on the impurity, jumping into the bath, and jumping back to the impurity, hence the name *hybridization*.

The most important result in this section is the following.

**Theorem 3.2.8** ( $\Sigma$  sparsity pattern of an impurity model). *Given an impurity model of the form (3.14)-(3.17), the self-energy  $\Sigma_{\text{IM}} : \mathbb{C}_+ \rightarrow \mathcal{H}_{\text{IM}}$  associated to any equilibrium state of  $\hat{H}_{\text{IM}}$  reads in the decomposition (3.14)*

$$\forall z \in \mathbb{C}_+, \quad \Sigma_{\text{IM}}(z) = \begin{pmatrix} \Sigma_{\text{imp}}(z) & 0 \\ 0 & 0 \end{pmatrix}. \quad (3.19)$$

In practical DMFT computations and as mentioned already in [19], the self-energy  $\Sigma$  of an impurity problem depends solely on the hybridization function  $\Delta$  and on the impurity Hamiltonian defined by  $H_{\text{imp}}^0$  and  $\hat{H}^I$ , via a quantum action defined by path integrals [25, eq. 9]. In this article, we focus on the IPT approximation (see section 3.2.5), which makes this dependence almost explicit, and postpone the study of the exact impurity solver in a more general framework to future works.

**Anderson Impurity Model** The original Anderson impurity model (AIM) [4] is a specific impurity model in which the impurity consists of a single-site Hubbard model. It was introduced by Anderson back in 1961 to explain the low-temperature behavior of the conductivity of metallic alloys with dilute magnetic impurities, later called the *Kondo effect* [33, 54]. The AIM was then extended to multiple-site Hubbard impurities. Figure 2 provides a graphical illustration of an AIM model with a 4-site Hubbard impurity and 5 bath orbitals ( $\dim(\mathcal{H}_{\text{imp}}) = 8$ ,  $\dim(\mathcal{H}_{\text{bath}}) = 10$ ). Without loss of generality, we can indeed identify the bath space  $\mathcal{H}_{\text{bath}}$  with  $\mathbb{C}^{2B}$  and assume that  $H_{\text{bath}}^0 = \text{diag}(\epsilon_1, \epsilon_1, \dots, \epsilon_B, \epsilon_B)$ . In this picture, the canonical basis of  $\mathbb{C}^{2B}$  corresponds to an orthonormal basis of bath spin-orbitals with energies  $\epsilon_1, \epsilon_1, \dots, \epsilon_B, \epsilon_B$ . The matrix  $V$  models jumps from the bath to the impurity, while the matrix  $V^\dagger$  models jumps from the impurity to the bath. The coupling terms  $V_{i,j}$  are also assumed to be real-valued due to the absence of magnetic field.

In the seminal paper [4], the *electronic bath* was thought as the set of *conducting electrons*, for instance described by a tight-binding model on a (truncated) lattice.

**Remark 3.2.9.** *As for the Hubbard model, the  $z$ -component of the total spin operator  $\hat{S}_{AI}^z = \hat{S}_H^z + \sum_{k=1}^B \hat{n}_{k,\uparrow} - \hat{n}_{k,\downarrow}$ , the total number operator  $\hat{N}_{AI} = \hat{N}_H + \sum_{k=1}^B \hat{n}_{k,\uparrow} + \hat{n}_{k,\downarrow}$  and the Anderson Impurity Hamiltonian  $\hat{H}_{AI}$  pairwise commute.*

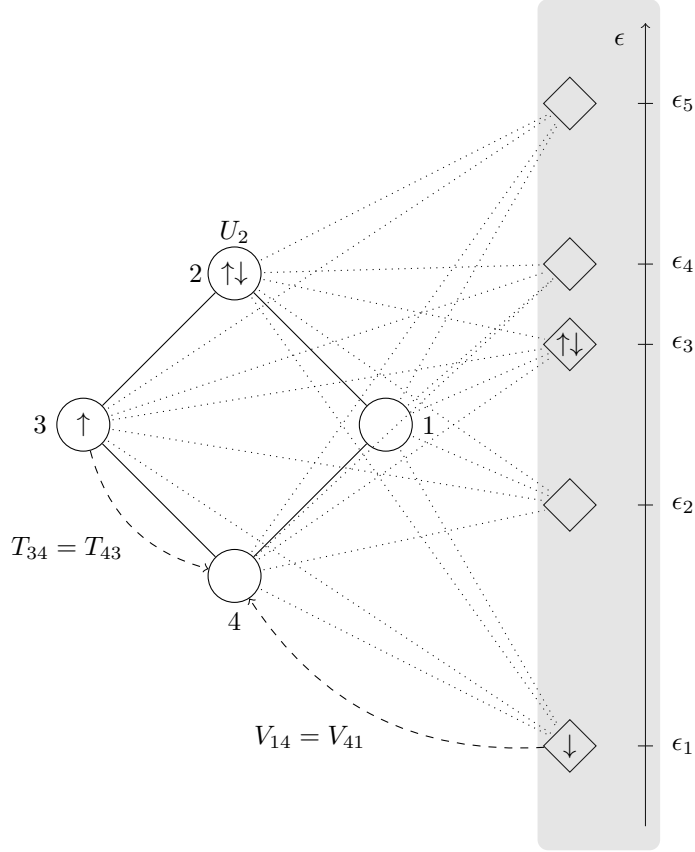


Figure 2: The Anderson Impurity Model of an impurity ( $\mathcal{G}_H = C_4, T, U$ ) and a *bath* ( $B = 5, \epsilon, V$ ) in a 6 electrons state.

### 3.2.4 Dynamical Mean-Field Theory (DMFT)

Consider a Hubbard model defined by  $(\mathcal{G}_H, T, U)$  in one of its equilibrium states  $\Omega$ . The purpose of DMFT is to provide an *approximation* of the corresponding Green's function  $G$ , and more precisely on some blocks of this Green's function.

To do so, DMFT uses a self-consistent mapping between the Hubbard model  $(\mathcal{G}_H, T, U)$  and a collection of Anderson Impurity Models associated to a partition  $\mathfrak{P}$  of the vertices of the Hubbard graph  $\mathcal{G}_H$ . The process, illustrated in Figure 3, is the following.

1. Choose a partition  $\mathfrak{P} = \{\Lambda_p, p \in \llbracket 1, P \rrbracket\}$  of the  $L$  sites of the Hubbard model into  $P$  impurities  $\Lambda_1, \dots, \Lambda_P$ ,  $\sqcup_{p=1}^P \Lambda_p = \Lambda$ , and consider for all  $p \in \llbracket 1, P \rrbracket$  the *induced subgraphs*  $\mathcal{G}_p = (\Lambda_p, E_p)$  with  $E_p = \{\{i, j\} \in E; i, j \in \Lambda_p\}$ . This partition leads to the canonical orthogonal decomposition

$$\mathcal{H}_H = \bigoplus_{p=1}^P \mathcal{H}_p, \quad \dim(\mathcal{H}_p) = 2|\Lambda_p| = 2L_p, \quad (3.20)$$

from which follows the decomposition of the Fock space

$$\mathcal{F}_H = \bigotimes_{p=1}^P \mathcal{F}_p, \quad \dim \mathcal{F}_p = 4^{L_p}. \quad (3.21)$$

The decomposition (3.20) of the one-particle state space of the original Hubbard model gives rise to block-operator representations of the exact Green's function and self-energy (for the state  $\Omega$ ) of the original Hubbard model

$$G(z) = \begin{pmatrix} G_1(z) & * & \cdots & * \\ * & G_2(z) & \cdots & * \\ \vdots & \vdots & \ddots & \vdots \\ * & * & \cdots & G_P(z) \end{pmatrix}, \quad \Sigma(z) = \begin{pmatrix} \Sigma_1(z) & * & \cdots & * \\ * & \Sigma_2(z) & \cdots & * \\ \vdots & \vdots & \ddots & \vdots \\ * & * & \cdots & \Sigma_P(z) \end{pmatrix};$$

2. The decomposition (3.20) also leads to a block-operator representation of the one-body Hamiltonian corresponding to the non-interacting part of the Hubbard Hamiltonian

$$H_{\text{H}}^0 = \begin{pmatrix} H_1^0 & * & \cdots & * \\ * & H_2^0 & \cdots & * \\ \vdots & \vdots & \ddots & \vdots \\ * & * & \cdots & H_P^0 \end{pmatrix},$$

where the diagonal block  $H_p^0$  is constructed from the *induced hopping matrices*  $T_p = T|_{E_p}$ ,  $1 \leq p \leq P$ . Due to the locality of the interactions in the Hubbard model, the interaction term is “block-diagonal” in the decomposition (3.21). It is represented by the *induced on-site repulsion*  $U_p = U|_{\Lambda_p}$ , and it reads  $\hat{H}^I = \bigoplus_{p=1}^P \hat{H}_p^I$ , with  $\hat{H}_p^I = \sum_{i \in \Lambda_p} U_i \hat{n}_{i,\uparrow} \hat{n}_{i,\downarrow}$ ;

3. The AIM associated to the  $p$ -th impurity is defined by (i) the impurity state space  $\mathcal{H}_{\text{imp},p} := \mathcal{H}_p$ , (ii) the impurity Hamiltonian defined by the induced Hubbard model  $(\mathcal{G}_p, T_p, U_p)$ , (iii) some bath state space  $\mathcal{H}_{\text{bath},p}$ , bath one-body Hamiltonian  $H_{\text{bath},p}^0$  and coupling one-body Hamiltonian  $H_{\text{coupling},p}^0 = \begin{pmatrix} 0 & V_p^\dagger \\ V_p & 0 \end{pmatrix}$  to be specified. From each of these  $P$  AIMs, one can compute the Green’s functions and self-energies

$$G_{\text{AI},p}(z) = \begin{pmatrix} G_{\text{imp},p}(z) & * \\ * & * \end{pmatrix}, \quad \Sigma_{\text{AI},p}(z) = \begin{pmatrix} \Sigma_{\text{imp},p}(z) & 0 \\ 0 & 0 \end{pmatrix},$$

for AIM equilibrium states  $\Omega_p$  of the same nature as  $\Omega$  (see Remark 3.2.10 below for a comment on this important point).

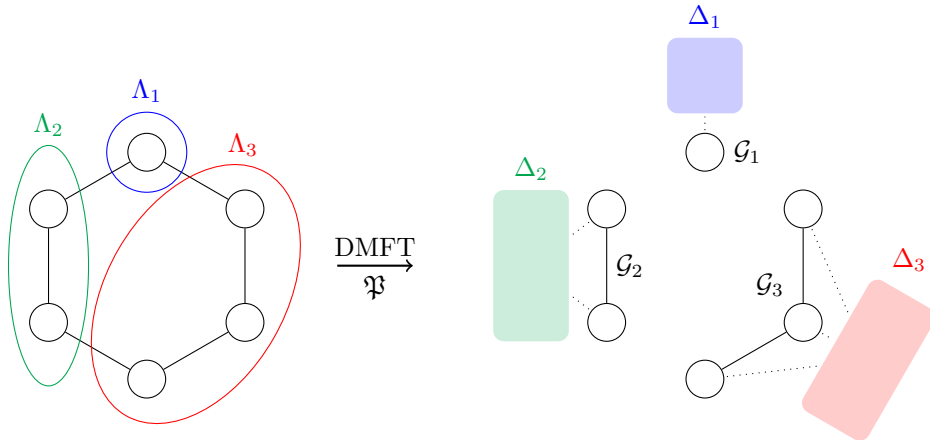


Figure 3: A partition  $\mathfrak{P} = \Lambda_1 \sqcup \Lambda_2 \sqcup \Lambda_3$  of the 6 vertices of the  $C_6$  graph, and the 3 induced graphs  $\mathcal{G}_1, \mathcal{G}_2, \mathcal{G}_3$ : the impurities of the corresponding AIMs are defined using the original Hubbard model, while the bath and the impurity-bath coupling are specified by the DMFT approximation.

DMFT aims at computing approximations of the diagonal-blocks  $G_1(z), \dots, G_P(z)$  of the exact Green’s function  $G(z)$ . Ideally, the baths should be adjusted in such a way that  $G_{\text{imp},p} = G_p$ , but of course this is not possible since the functions  $G_p$  are unknown. To make DMFT a practical tool, the idea is to introduce approximate Green’s functions and self-energies of the form

$$G_{\text{DMFT}}(z) = \begin{pmatrix} G_{\text{DMFT},1}(z) & * & \cdots & * \\ * & G_{\text{DMFT},2}(z) & \cdots & * \\ \vdots & \vdots & \ddots & \vdots \\ * & * & \cdots & G_{\text{DMFT},P}(z) \end{pmatrix}, \quad (3.22)$$

$$\Sigma_{\text{DMFT}}(z) = \begin{pmatrix} \Sigma_{\text{DMFT},1}(z) & 0 & \cdots & 0 \\ 0 & \Sigma_{\text{DMFT},1}(z) & \cdots & 0 \\ \vdots & \vdots & \ddots & \vdots \\ 0 & 0 & \cdots & \Sigma_{\text{DMFT},P}(z) \end{pmatrix}, \quad (3.23)$$

related by

$$G_{\text{DMFT}}(z) = ((G_{\text{DMFT}}^0)^{-1}(z) - \Sigma_{\text{DMFT}}(z))^{-1},$$

$$G_{\text{DMFT}}^0(z) = (z - H_{\text{H}}^0)^{-1},$$

and to choose the baths in such a way that

$$\forall 1 \leq p \leq P, \quad G_{\text{DMFT},p}(z) = G_{\text{imp},p}(z), \quad (3.24)$$

$$\Sigma_{\text{DMFT},p}(z) = \Sigma_{\text{imp},p}(z). \quad (3.25)$$

Of course, it is not clear whether a collection of baths that satisfies the above conditions exists, and this article partially answers this question.

Note that the DMFT Green's function  $G_{\text{DMFT}}(z)$  is *not*, a priori, the Green's function of some interacting quantum many-body problem which could be defined as in Section 3.2.1. Instead, it is defined from an approximate self-energy  $\Sigma_{\text{DMFT}}(z)$ . Equations (3.23) and (3.25) indicate that, in the DMFT approximation, each impurity interacts with its neighborhood as if the former were an impurity and the latter a bath, in accordance with Theorem 3.2.8, hence the name of *mean-field*. This mean-field is *dynamical* because it is frequency dependent, in contrast with static mean-field theory such as in Hartree-Fock or Density-Matrix Embedding Theory (DMET).

**Remark 3.2.10.** *In the above sketch of the DMFT framework, we did not specify the states  $(\Omega_p)_{p \in [1,P]}$  of the associated AIMs from which the self-energies  $(\Sigma_{\text{imp},p})_{p \in [1,P]}$  are computed. In [22], it is implicitly stated that, for a Hubbard model in the Gibbs state  $\Omega_{\text{H},\beta,\epsilon_F}$  as defined below in Section 3.2.5, the AIM's equilibrium states  $\Omega_p$  are defined to be Gibbs states as well  $\Omega_p = \Omega_{\text{AIM},\beta,\epsilon'_F}$ , with the same temperature as that of the Gibbs state of the whole system, but with a priori different chemical potential  $\epsilon'_F$ . The latter is to be chosen to satisfy appropriate filling conditions. We will address this question in a future work and simply assume here that the  $\epsilon'_F = \epsilon_F$ . Moreover, when working with the IPT solver, the chemical potential is fixed by the on-site interaction, as detailed in Section 3.2.5.*

Our analysis is based on a reformulation of conditions (3.24)-(3.25) using the hybridization functions  $(\Delta_p(z))_{1 \leq p \leq P}$  of the  $P$  impurity problems as the main variables. As mentioned previously, knowing  $\Delta_p$  as well as  $T_p$ ,  $U_p$  and  $\Omega_p$ , suffices in principle to compute  $\Sigma_{\text{imp},p}$ . In practice, this is done by using an approximate impurity solver. A particular example of such a solver will be presented in Section 3.2.5. Conversely, knowing  $(\Sigma_{\text{imp},p})_{1 \leq p \leq P}$  and  $T$  suffices to characterize the unique set  $(\Delta_p(z))_{1 \leq p \leq P}$  for which (3.24)-(3.25) hold true. Indeed, by denoting

$$\mathcal{H}_{\bar{p}} := \bigoplus_{p \neq q=1}^P \mathcal{H}_q,$$

$$\Sigma_{\text{DMFT},\bar{p}}(z) = \begin{pmatrix} \Sigma_{\text{DMFT},1}(z) & \cdots & 0 & \cdots & 0 \\ \vdots & \ddots & \vdots & & \\ 0 & \cdots & \Sigma_{\text{DMFT},p-1}(z) & 0 & \\ 0 & \cdots & 0 & \Sigma_{\text{DMFT},p+1}(z) & \cdots & 0 \\ \vdots & \ddots & \vdots & \vdots & & \\ 0 & \cdots & 0 & 0 & \cdots & \Sigma_{\text{DMFT},P}(z) \end{pmatrix},$$

and using the Schur complement formula, we have on the one hand

$$G_{\text{DMFT},p}(z) = \left( (z - (H_{\text{H}}^0 + \Sigma_{\text{DMFT}}(z)))^{-1} \right)_p$$

$$= \left( z - (H_p^0 + \Sigma_{\text{DMFT},p}(z)) - W_p (z - (H_{\bar{p}}^0 + \Sigma_{\text{DMFT},\bar{p}}(z)))^{-1} W_p^\dagger \right)^{-1}, \quad (3.26)$$

where

$$\begin{pmatrix} H_p^0 & W_p \\ W_p^\dagger & H_{\bar{p}}^0 \end{pmatrix} \text{ and } \begin{pmatrix} z - (H_p^0 + \Sigma_{\text{DFMT},p}(z)) & -W_p \\ -W_p^\dagger & z - (H_{\bar{p}}^0 + \Sigma_{\text{DFMT},\bar{p}}(z)) \end{pmatrix} \quad (3.27)$$

are the block-representations of  $H_{\text{H}}^0$  and  $(z - (H_{\text{H}}^0 + \Sigma_{\text{DMFT}}(z)))$ , respectively, in the decomposition  $\mathcal{H} = \mathcal{H}_p \oplus \mathcal{H}_{\bar{p}}$ . Note that  $H_p^0 \in \mathcal{L}(\mathcal{H}_p)$ ,  $W_p \in \mathcal{L}(\mathcal{H}_{\bar{p}}; \mathcal{H}_p)$ , and  $H_{\bar{p}}^0, \Sigma_{\text{DFMT},\bar{p}}(z) \in \mathcal{L}(\mathcal{H}_{\bar{p}})$ . On the other hand, using again the Schur complement formula, we have

$$G_{\text{AI},p}(z) = (G_{\text{AI},p}^0(z)^{-1} - \Sigma_{\text{AI},p}(z))^{-1} = (z - H_{\text{AI},p}^0 - \Sigma_{\text{AI},p}(z))^{-1}$$

$$= \begin{pmatrix} z - H_p^0 - \Sigma_{\text{imp},p}(z) & -V_p \\ -V_p^\dagger & z - H_{\text{bath},p}^0 \end{pmatrix}^{-1} = \begin{pmatrix} (z - H_p^0 - \Sigma_{\text{imp},p}(z) - \Delta_p(z))^{-1} & * \\ * & * \end{pmatrix},$$

so that

$$G_{\text{imp},p}(z) = (z - H_p^0 - \Sigma_{\text{imp},p}(z) - \Delta_p(z))^{-1}. \quad (3.28)$$

Conditions (3.24)-(3.25), together with (3.26)-(3.28) yield the self-consistent condition

$$\forall 1 \leq p \leq P, \quad \Delta_p(z) = W_p \left( z - H_p^0 - \bigoplus_{q=1, q \neq p}^P \Sigma_{\text{imp},q}(z) \right)^{-1} W_p^\dagger. \quad (3.29)$$

Note that the matrices  $W_p$ ,  $H_p^0$  depend only on the hopping matrix  $T$  through

$$[W_p]_{i\sigma, j\sigma'} = \begin{cases} T_{i,j} & \text{if } i \in \Lambda_p, j \in \Lambda \setminus \Lambda_p, \{i, j\} \in E, \sigma = \sigma', \\ 0 & \text{otherwise,} \end{cases}$$

$$[H_p^0]_{i\sigma, j\sigma'} = \begin{cases} T_{i,j} & \text{if } i, j \in \Lambda \setminus \Lambda_p, \{i, j\} \in E, \sigma = \sigma', \\ 0 & \text{otherwise,} \end{cases}$$

where  $i, j \in \Lambda$  denote site indices and  $\sigma, \sigma' \in \{\uparrow, \downarrow\}$  spin indices.

**Remark 3.2.11.** This formulation of DMFT agrees with the original one [21, 22] in the translation-invariant setting where

$$\forall p \in [\![1, P]\!], \quad \mathcal{H}_p = \mathcal{H}_1, \quad H_p^0 = H_1^0, \quad W_p = W_1, \quad H_{\bar{p}}^0 = H_1^0, \quad U_p = U_1. \quad (3.30)$$

In this setting, we can consider translation-invariant solutions to the DMFT equations, for which

$$\forall p \in [\![1, P]\!], \quad \forall z \in \mathbb{C}_+, \quad \Sigma_{\text{imp},p}(z) = \Sigma_{\text{imp}}(z), \quad \Delta_p(z) = \Delta(z),$$

where  $\Sigma_{\text{imp}}(z)$  and  $\Delta(z)$  are related by the translation-invariant self-consistent condition

$$\Delta(z) = W_1 \left( z - H_1^0 - \bigoplus_{q=2}^P \Sigma_{\text{imp}}(z) \right)^{-1} W_1^\dagger. \quad (3.31)$$

This setting is sketched in Figure 4. When  $\mathfrak{P}$  is a partition into singletons (single-site DMFT), condition (3.30) is equivalent to the fact that  $U$  is constant and  $(\mathcal{G}_H, T)$  is vertex-transitive, namely that for all  $\lambda_1, \lambda_2 \in \Lambda$ , there exists a graph isomorphism  $\tau : \Lambda \rightarrow \Lambda$  such that

$$\tau(\lambda_1) = \lambda_2, \quad \forall \lambda, \lambda' \in \Lambda, \quad T_{\tau(\lambda), \tau(\lambda')} = T_{\lambda, \lambda'}$$

In particular, the graph Cartesian product  $C_N^{\square d}$  of  $d$  copies of the  $N$ -cycle, which is the nearest neighbor graph of a truncation of the  $d$ -dimensional square lattice, with constant hopping and on-site repulsion, and artificial periodic boundary conditions (supercell method), is vertex-transitive due to the translation invariance of the corresponding lattice. This setting was the one considered in the first DMFT computations [22]. Due to translation invariance, a single impurity problem has to be solved at each iteration. Recall that the impurity solver is the computational bottleneck in DMFT.

The DMFT self-consistent equations (3.29), combined with an exact impurity solver, give the exact Green's function of the original Hubbard model in the following trivial limits.

**Proposition 3.2.12** (Exactness of DMFT in some trivial limits). Consider a Hubbard model  $(\mathcal{G}_H, T, U)$  in a Gibbs state  $\Omega_{\beta, \epsilon_F}$ . The self-consistent DMFT equations (3.29), combined with an exact impurity solver, admit a unique solution in each of the following two settings:

1. non-interacting particles. If the on-site repulsion term is equal to zero ( $U_i = 0$  for all  $i \in \Lambda$ ), then this solution is given by

$$\forall p \in [\![1, P]\!], \quad \forall z \in \mathbb{C}_+, \quad \Sigma_{\text{imp},p}(z) = 0,$$

$$\Delta_p(z) = W_p (z - H_{\bar{p}}^0)^{-1} W_p^\dagger; \quad (3.32)$$

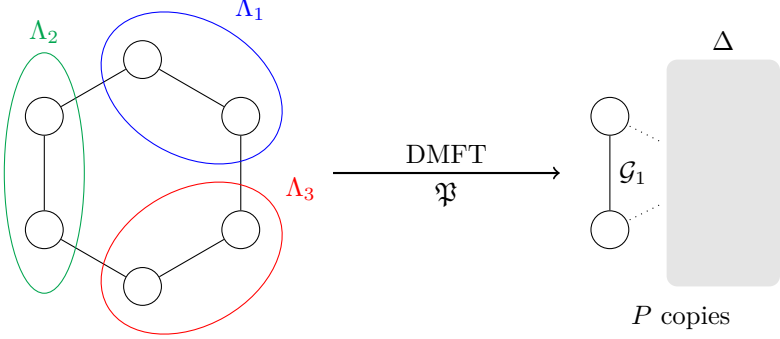


Figure 4: Translation-invariant DMFT formalism.

2. disconnected graphs and atomic limit. If the partition  $\mathfrak{P}$  of  $\mathcal{G}_H$  is such that  $\mathcal{G}_H = \bigoplus_{p=1}^P \mathcal{G}_p$  (meaning  $E_H = \sqcup_{p=1}^P E_p$ ), that is if the partition decomposes the original Hubbard model  $(\mathcal{G}_H, T, U)$  into  $P$  independent Hubbard models  $(\mathcal{G}_p, T_p, U_p)$ , or if the hopping matrix  $T$  vanishes, then this solution is given by

$$\begin{aligned} \forall p \in \llbracket 1, P \rrbracket, \quad \forall z \in \mathbb{C}_+, \quad \Sigma_{\text{imp},p}(z) &= \Sigma_p(z), \\ \Delta_p(z) &= 0, \end{aligned} \tag{3.33}$$

where  $\Sigma_p$  is the exact self-energy associated to the  $p$ -th Hubbard model in the associated Gibbs State  $\Omega_{\beta, \epsilon_F}^p$ .

In both settings, DMFT is exact in the sense that

$$\forall z \in \mathbb{C}_+, \quad G_{\text{DMFT}}(z) = G(z).$$

The purpose of DMFT [21] is to build an approximation that complies with these two limiting cases. Another limiting case in which DMFT is claimed to be exact is in the “infinite dimension” limit [44, 22]. We leave the mathematical investigation of this limit to future works.

We deduce from (3.32)-(3.33) that in the trivial limits considered in Proposition 3.2.12, the hybridization functions  $\Delta_p(z)$  are either identically zero, or have a finite number of poles, so that the corresponding baths can be chosen finite dimensional.

Anticipating on the following, we prove in Proposition 3.3.5 that, when coupled to the Iterated Perturbation Theory (IPT) impurity solver, the translation-invariant self-consistent equation (3.31) has no solution with a finite number of poles. This motivates the functional setting described in Section 3.3.

### 3.2.5 A specific impurity solver : the Iterated Perturbation Theory (IPT) solver.

To define properly the IPT solver, we need first to introduce *Matsubara’s* formalism, and more precisely *Matsubara’s Green’s function*  $\tilde{G}^M$ .

#### Matsubara’s Green’s functions

Matsubara’s Green’s functions are defined only for *Gibbs states*  $\Omega_{\beta, \epsilon_F}$  at a given inverse temperature  $\beta$  and chemical potential  $\epsilon_F$ . These functions have been more extensively studied mathematically than time-ordered Green’s functions [11, 12]. In this section, we recall their definition and prove an analytic continuation result that will be useful for our analysis. The setup remains the same as the one introduced in Section 3.2.1.

**Definition 3.2.13** (Gibbs’s state and Matsubara’s time-ordered Green’s function). *Given a particle-number conserving Hamiltonian  $\hat{H} \in \mathcal{S}(\mathcal{F})$ , that is  $[\hat{H}, \hat{N}] = 0$ , the Gibbs state  $\Omega_{\beta, \epsilon_F}$  at inverse temperature  $\beta \in \mathbb{R}_+^*$  and chemical potential  $\epsilon_F \in \mathbb{R}$  is defined through its density operator by*

$$\hat{\rho} = \frac{1}{Z_{\beta, \epsilon_F}} e^{-\beta(\hat{H} - \epsilon_F \hat{N})}, \quad Z_{\beta, \epsilon_F} = \text{Tr} \left( e^{-\beta(\hat{H} - \epsilon_F \hat{N})} \right).$$

The Matsubara's Green's function  $\tilde{G}^M$  is defined as the  $\mathcal{L}(\mathcal{H})$ -valued map  $\tilde{G}^M : [-\beta, \beta] \rightarrow \mathcal{L}(\mathcal{H})$  represented by the sesquilinear form verifying for all  $\phi, \phi' \in \mathcal{H}$ ,

$$\forall \tau \in [-\beta, \beta], \quad \langle \phi, -\tilde{G}^M(\tau)\phi' \rangle = \chi_{\mathbb{R}_+}(\tau) \Omega_{\beta, \epsilon_F} \left( \mathbb{M}(\hat{a}_\phi)(\tau) \hat{a}_{\phi'}^\dagger \right) - \chi_{\mathbb{R}_-}(\tau) \Omega_{\beta, \epsilon_F} \left( \hat{a}_{\phi'}^\dagger \mathbb{M}(\hat{a}_\phi)(\tau) \right), \quad (3.34)$$

where for all  $\hat{O} \in \mathcal{L}(\mathcal{F})$ ,

$$\mathbb{M}(\hat{O}) : [-\beta, \beta] \ni \tau \mapsto e^{\tau(\hat{H} - \epsilon_F \hat{N})} \hat{O} e^{-\tau(\hat{H} - \epsilon_F \hat{N})}$$

is the Matsubara picture of  $\hat{O}$ .

Recall that in our setting, any operator is trace-class since  $\mathcal{F}$  is finite dimensional, hence  $Z_{\beta, \epsilon_F}$  is always finite.

As it is the case for the time-ordered Green's function  $\tilde{G}$ , one can recast equation (3.34) using the time-ordered product :

$$\forall \phi, \phi' \in \mathcal{H}, \forall \tau \in [-\beta, \beta], \quad \langle \phi, -\tilde{G}^M(\tau)\phi' \rangle = \Omega_{\beta, \epsilon_F} \left( \mathcal{T} \left( \mathbb{M}(\hat{a}_\phi), \mathbb{M}(\hat{a}_{\phi'}^\dagger) \right) (\tau, 0) \right).$$

Note that the negative sign in the definition of  $\tilde{G}^M$  must be consistent with the  $i$  prefactor in the definition of  $\tilde{G}$  for Theorem 3.2.15 below to hold. Considering the grand canonical Hamiltonian  $\hat{H}' = \hat{H} - \epsilon_F \hat{N}$  as the Hamiltonian from which the Green's function  $\tilde{G}$  is defined, the Matsubara formalism involves the following formal connection (known as *Wick rotation* [65]):

$$\tau \leftrightarrow it$$

or, in other words, working with  $t \leftrightarrow -i\tau$  where  $\tau$  is real. Hence, the term *imaginary-time* Green's function [43].

Contrary to the Heisenberg picture  $\hat{O} \mapsto \mathbb{H}(\hat{O})$ , the Matsubara picture does not consist in a family of  $C^*$ -morphisms: one has for all  $\tau \in [-\beta, \beta]$ ,

$$\left( \mathbb{M}(\hat{O})(\tau) \right)^\dagger = \mathbb{M}(\hat{O}^\dagger)(-\tau).$$

A consequence of this property is that the Matsubara's Green's function is Hermitian:

$$\left( \tilde{G}^M(\tau) \right)^\dagger = \tilde{G}^M(\tau).$$

Note moreover that Gibbs states are *Kubo-Martin-Schwinger (KMS)* states [12], meaning that they satisfy the following property:

$$\forall \hat{O}, \hat{O}' \in \mathcal{L}(\mathcal{F}), \forall \tau \in [-\beta, 0], \quad \Omega_{\beta, \epsilon_F}(\mathbb{M}(\hat{O})(\tau + \beta)\hat{O}') = \Omega_{\beta, \epsilon_F}(\hat{O}'\mathbb{M}(\hat{O})(\tau)).$$

This implies that  $\tilde{G}^M$  is  $\beta$ -anti-periodic, i.e.

$$\forall \tau \in [-\beta, 0], \quad \tilde{G}^M(\tau + \beta) = -\tilde{G}^M(\tau).$$

As for the time-ordered Green's function, the Matsubara's Green's function has a Källén-Lehmann's representation: given an orthonormal basis  $\mathcal{B}$  of  $\mathcal{F}$  which jointly diagonalizes  $\hat{H}$  and  $\hat{N}$  ( $\forall \psi \in \mathcal{B}, \hat{H}\psi = E_\psi \psi, \hat{N}\psi = N_\psi \psi$ ), we have for all  $\tau \in [0, \beta]$ )

$$\begin{aligned} \langle \phi, -\tilde{G}^M(\tau)\phi' \rangle &= \sum_{\psi, \psi' \in \mathcal{B}} e^{\tau((E_\psi - \epsilon_F N_\psi) - (E_{\psi'} - \epsilon_F N_{\psi'}))} \langle \psi, \hat{a}_\phi \psi' \rangle \langle \psi', \hat{a}_{\phi'}^\dagger \psi \rangle e^{-\beta(E_\psi - \epsilon_F N_\psi)} \\ &= \sum_{\psi, \psi' \in \mathcal{B}} e^{\tau(E_\psi - E_{\psi'} + \epsilon_F)} \langle \psi, \hat{a}_\phi \psi' \rangle \langle \psi', \hat{a}_{\phi'}^\dagger \psi \rangle e^{-\beta(E_\psi - \epsilon_F N_\psi)}, \end{aligned}$$

as  $N_{\psi'} = N_\psi + 1$  whenever  $\langle \psi', \hat{a}_{\phi'}^\dagger \psi \rangle \neq 0$ .

Similarly to the time-ordered Green's function  $\tilde{G}$ , it is convenient to work with a Fourier representation of the Matsubara Green's function  $\tilde{G}^M$ . Since the latter is defined only on  $[-\beta, \beta]$ , it is quite natural to extend  $\tilde{G}^M$  to the real-line by periodicity and introduce the associated Fourier series with coefficients defined by

$$\forall n \in \mathbb{Z}, \quad \frac{1}{2} \int_{-\beta}^{\beta} \tilde{G}^M(\tau) e^{in\frac{\pi}{\beta}\tau} d\tau.$$

Due to the  $\beta$ -anti-periodicity of  $\tilde{G}^M$ , the even Fourier coefficients vanish and it holds

$$\frac{1}{2} \int_{-\beta}^{\beta} \tilde{G}^M(\tau) e^{in\frac{\pi}{\beta}\tau} d\tau = \begin{cases} \int_0^{\beta} \tilde{G}^M(\tau) e^{in\frac{\pi}{\beta}\tau} d\tau & \text{if } n \text{ is odd,} \\ 0 & \text{otherwise.} \end{cases}$$

**Definition 3.2.14** (Matsubara's Fourier series and frequencies). *The Matsubara's Fourier coefficients  $(G_n^M)_{n \in \mathbb{Z}}$  are defined by*

$$\forall n \in \mathbb{Z}, \quad G_n^M = \int_0^\beta \tilde{G}^M(\tau) e^{i\omega_n \tau} d\tau$$

where  $\omega_n = (2n + 1)\frac{\pi}{\beta}$  is the  $n$ -th Matsubara's frequency.

We thus have

$$\forall \tau \in [-\beta, \beta], \quad \tilde{G}^M(\tau) = \frac{1}{\beta} \sum_{n \in \mathbb{Z}} e^{-i\omega_n \tau} G_n^M.$$

The very reason these coefficients are useful in Green's functions methods lies in the following theorem.

**Theorem 3.2.15** (Matsubara's Fourier coefficients analytic continuation). *Let  $\hat{H} \in \mathcal{S}(\mathcal{F})$  be a particle-number-conserving Hamiltonian,  $\Omega_{\beta, \epsilon_F}$  the associated Gibbs state, and  $G : \mathbb{C}_+ \rightarrow \mathcal{L}(\mathcal{H})$  the Generalized Fourier Transform of the associated time-ordered Green's function  $\tilde{G}$  defined from the grand canonical Hamiltonian  $\hat{H}' = \hat{H} - \epsilon_F \hat{N}$ . Then  $G$  is the only analytic matrix-valued function such that*

$$\forall z \in \mathbb{C}_+, \quad \Im(G(z)) := \frac{G(z) - G(z)^\dagger}{2i} \leq 0, \quad \text{and} \tag{3.35}$$

$$\forall n \in \mathbb{N}, \quad G(i\omega_n) = G_n^M. \tag{3.36}$$

Note that, since  $\omega_{-n} = -\omega_{n-1}$  and  $\tilde{G}^M$  is Hermitian, it holds

$$\forall n \in \mathbb{N}^*, \quad (G_{n-1}^M)^\dagger = G_{-n}^M,$$

so that (3.36) actually holds for all  $n \in \mathbb{Z}$ , with the extension of  $G$  to  $\mathbb{C}_-$  defined as in (3.6).

**Remark 3.2.16.** *The requirement that  $G$  is analytic and verifies (3.35) is crucial for uniqueness: for instance, for each  $m \in 2\mathbb{Z} + 1$ , the function*

$$\mathbb{C}_+ \ni z \mapsto \frac{1 - e^{m\beta z}}{2} G(z) \in \mathcal{L}(\mathcal{H})$$

also satisfies (3.36) and is analytic, but its imaginary part is not negative semi-definite.

Theorem 3.2.15 is extensively used for practical computations: it is sufficient to run the computations for the Matsubara frequencies and then perform an analytic continuation [17].

Note that Theorem 3.2.15 works in particular for non-interacting Hamiltonians, which leads to the following definition.

**Definition 3.2.17** (Matsubara's self-energy). *The Matsubara's self-energy Fourier coefficients  $(\Sigma_n^M)_{n \in \mathbb{Z}}$  are defined by*

$$\forall n \in \mathbb{Z}, \quad \Sigma_n^M = i\omega_n + \epsilon_F - H^0 - (G_n^M)^{-1}.$$

In fact, the self-energy  $\Sigma : \mathbb{C}_+ \rightarrow \mathcal{L}(\mathcal{H})$  defined in (3.12) is the only analytic function with negative imaginary part such that

$$\forall n \in \mathbb{N}, \quad \Sigma(i\omega_n) = \Sigma_n^M.$$

This follows from Proposition 3.3.3 and Theorem 3.A.8. One can define the *Matsubara's self-energy*  $\tilde{\Sigma}^M(\tau)$  by Fourier summation formula as in Definition 3.2.14, but this function will not play any role in what follows.

With all these definitions in place, we can now introduce the final ingredient of the model under investigation, namely the paramagnetic single-site translation-invariant Iterated Perturbation Theory (IPT).

## IPT approximation

In this article, we will not discuss the derivation nor the validity of the Iterative Perturbation Theory (IPT) approximation and refer the interested reader to [5]. As in the review paper [22], we only consider *single-site* and *translation-invariant* DMFT. This seems to be a setting in which the usual IPT approximation is generally considered as valid in the physics literature, while constructing an IPT-like approximation for multi-site DMFT is still an active field of research [5]. In the former case,  $\mathfrak{P}$  is a partition of the  $L$  sites into  $P = L$  singletons and the on-site repulsion  $U$  is constant as exposed in remark 3.2.11. Also, we will focus on the paramagnetic case [51]. In other words, we will assume that there is no spin-symmetry breaking, so that the spin components can be factored out as detailed in Appendix 3.B. In the single-site translation invariant paramagnetic IPT-DMFT approximation considered in the sequel, we thus have  $P = L$  and for  $z \in \mathbb{C}_+$ ,

$$H_{\text{H}}^0, G^{DMFT}(z), \Sigma^{DMFT}(z) \in \mathbb{C}^{P \times P}.$$

Recall that in translation invariant DMFT, we restrict ourselves to translation invariant solutions to the DMFT equations, so that we consider only one hybridization function  $\Delta$  and self-energy  $\Sigma$ , with for all  $z \in \mathbb{C}_+$ ,

$$\Delta(z), \Sigma(z) \in \mathbb{C},$$

and we use the following notations

$$W^\dagger := W_p^\dagger \in \mathbb{C}^{P-1}, \quad H_\perp^0 := H_{\overline{P}}^0 \in \mathbb{C}^{(P-1) \times (P-1)}.$$

Moreover, we stick to the *half-filled* setting [22], for which the chemical potential  $\epsilon_F$  of the Anderson Impurity Model is set to  $U/2$ . The Hamiltonians of interest are then on the one-hand the grand canonical Hubbard Hamiltonian  $\hat{H}_H - \epsilon_F \hat{N}_H$ , and on the other hand the "impurity" grand canonical Hamiltonian  $\hat{H}_{AI} - \epsilon_F \hat{N}_{\text{imp}}$  where  $\hat{N}_{\text{imp}}$  is the impurity number operator, complying with [22, eq. 14].

The IPT solver is based on a second order *perturbation expansion* of the Matsubara's self-energy Fourier coefficients  $\Sigma_{\text{imp},n}^M$  of the single-site impurity problem in the parameter  $U$ : the Matsubara's self-energy Fourier coefficients of the impurity problem is approximated by

$$\forall n \in \mathbb{N}, \quad \Sigma_{\text{imp},n}^M \approx \Sigma_{\text{imp},n}^{M,IPT} := \frac{U}{2} + U^2 \int_0^\beta e^{i\omega_n \tau} \left( \tilde{G}_{\text{imp}}^{M,0}(\tau) \right)^3 d\tau,$$

where  $\tilde{G}_{\text{imp}}^{M,0}$  is the restriction to  $\mathcal{H}_{\text{imp}}$  of the Matsubara's Green's function of the non-interacting Hamiltonian  $H_{\text{AI}}^0$ . The Fourier coefficients of  $\tilde{G}_{\text{imp}}^{M,0}$  are given by

$$G_{\text{imp},n}^{M,0} = \left( (G_{\text{imp}}^0(i\omega_n))^{-1} - \epsilon_F \right)^{-1} = (i\omega_n - H_{\text{imp}}^0 - \Delta(i\omega_n))^{-1} = (i\omega_n - \Delta(i\omega_n))^{-1},$$

since  $H_{\text{imp}}^0 = 0$  and where the first equality is a consequence of a shift to enforce particle-hole symmetry [22, p.50]. Finally, noticing that

$$\Delta(z) = W (z + \epsilon_F - H_\perp^0 + \Sigma(z))^{-1} W^\dagger = W (z - H_\perp^0 - (\Sigma(z) - \epsilon_F))^{-1} W^\dagger, \quad (3.37)$$

we make the change of variable  $\Sigma \leftarrow \Sigma - \epsilon_F$  and we thus have, due to the filling condition,

$$\Sigma_{\text{imp},n}^{M,IPT} = U^2 \int_0^\beta e^{i\omega_n \tau} \left( \frac{1}{\beta} \sum_{n' \in \mathbb{Z}} (i\omega_{n'} - \Delta(i\omega_{n'}))^{-1} e^{-i\omega_{n'} \tau} \right)^3 d\tau. \quad (3.38)$$

The IPT approximation therefore provides an explicit expression of the Matsubara Fourier coefficients of the impurity self-energy  $\Sigma_{\text{imp}}$  as a function of  $U$  and  $\Delta$ . To reconstruct  $\Sigma_{\text{imp}}^{IPT}(z)$  from these Fourier coefficients, we have to solve an Analytical Continuation Problem. The following result shows that, in the case of finite-dimensional baths, this problem has a unique solution, which can be computed (almost) explicitly. Our results are similar to computations already obtained in [30, eq. 4].

**Proposition 3.2.18** (IPT solver for finite-dimensional baths). *Let  $U \in \mathbb{R}$ ,  $\Delta : \mathbb{C}_+ \rightarrow \mathbb{C}$  of the form*

$$\forall z \in \mathbb{C}_+, \quad \Delta(z) = \sum_{k=1}^K \frac{a_k}{z - \varepsilon_k}, \quad \text{with } \varepsilon_1 < \varepsilon_2 < \dots < \varepsilon_K \text{ and } a_k > 0 \text{ for all } 1 \leq k \leq K, \quad (3.39)$$

and  $(\Sigma_{\text{imp},n})_{n \in \mathbb{N}}$  defined by

$$\forall n \in \mathbb{N}, \quad \Sigma_{\text{imp},n} = U^2 \int_0^\beta e^{i\omega_n \tau} \left( \frac{1}{\beta} \sum_{n' \in \mathbb{Z}} (i\omega_{n'} - \Delta(i\omega_{n'}))^{-1} e^{-i\omega_{n'} \tau} \right)^3 d\tau.$$

Then, the Analytical Continuation Problem (ACP)

$$\begin{cases} \Sigma_{\text{imp}} : \mathbb{C}_+ \rightarrow \overline{\mathbb{C}_+} \\ \Sigma_{\text{imp}} \text{ is analytic} \\ \forall n \in \mathbb{N}, \quad \Sigma_{\text{imp}}(i\omega_n) = \Sigma_{\text{imp},n} \end{cases} \quad (3.40)$$

has a unique solution, which is given by

$$\forall z \in \mathbb{C}_+, \quad \Sigma_{\text{imp}}^{IPT}(z) = U^2 \sum_{k_1, k_2, k_3=1}^{K+1} \frac{a'_{k_1, k_2, k_3}}{z - (\varepsilon'_{k_1} + \varepsilon'_{k_2} + \varepsilon'_{k_3})}, \quad (3.41)$$

where  $\varepsilon'_1 < \varepsilon'_2 < \dots < \varepsilon'_{K+1}$  are the  $(K+1)$  real roots of the equation

$$\varepsilon - \Delta(\varepsilon) = 0,$$

which satisfy the interlacing relation

$$\varepsilon'_1 < \varepsilon_1 < \varepsilon'_2 < \varepsilon_2 < \dots < \varepsilon_K < \varepsilon'_{K+1},$$

and for all  $k_1, k_2, k_3 \in \llbracket 1, K+1 \rrbracket$ ,  $a_{k_1, k_2, k_3}$  is defined by

$$a'_{k_1, k_2, k_3} = \frac{1 + e^{-\beta(\varepsilon'_{k_1} + \varepsilon'_{k_2} + \varepsilon'_{k_3})}}{(1 + e^{-\beta\varepsilon'_{k_1}})(1 + e^{-\beta\varepsilon'_{k_2}})(1 + e^{-\beta\varepsilon'_{k_3}})} \prod_{i=1}^3 (1 - \Delta'(\varepsilon'_{k_i}))^{-1} > 0. \quad (3.42)$$

We denote by

$$\Sigma_{\text{imp}}^{IPT} = \text{IPT}_\beta(U, \Delta)$$

the output of this solver. At this time, this solver is defined only for finite baths, that is for hybridization functions that are rational functions of the form (3.39). We will see later (in Proposition 3.3.8) that this map can be extended by (weak) continuity to the space of all physically admissible hybridization functions. We thus finally obtain the system of translation invariant paramagnetic single-site IPT-DMFT equations

$$\forall z \in \mathbb{C}_+, \quad \Delta(z) = W(z - H_\perp^0 - \Sigma(z))^{-1} W^\dagger \quad (3.43)$$

$$\Sigma = \text{IPT}_\beta(U, \Delta), \quad (3.44)$$

where the on-site interaction energies  $U \in \mathbb{R}$ , the inverse temperature  $\beta > 0$ , the vector  $W^\dagger \in \mathbb{C}^{P-1}$  and the matrix  $H_\perp^0 \in \mathbb{C}^{(P-1) \times (P-1)}$  obtained from the hopping matrix  $T$  are the parameters of the model, and where  $\Delta : \mathbb{C}_+ \rightarrow \mathbb{C}$  and  $\Sigma : \mathbb{C}_+ \rightarrow \mathbb{C}$  are the unknowns.

In the remainder of this article, our main focus will be the existence of solutions to the above equations.

### 3.3 Main results

Let us introduce and recall some useful notation. We denote by

$$\mathbb{C}_+ := \{z \in \mathbb{C} \mid \Im(z) > 0\}$$

the complex open upper-half plane, that is the set of complex numbers with positive imaginary part. For a matrix  $M \in \mathbb{C}^{n \times n}$ ,  $n \geq 1$ , the imaginary part of  $M$  is defined by

$$\Im(M) = \frac{M - M^\dagger}{2i}.$$

The set of Hermitian matrices of size  $n$  is denoted by  $\mathcal{S}_n(\mathbb{C})$ , and the set of positive-semidefinite matrices by  $\mathcal{S}_n^+(\mathbb{C})$ . The notation  $M \geq 0$  (resp.  $M > 0$ ) means that the matrix  $M$  is positive semidefinite (resp. positive definite). In the following, we will also deal with measure and probability theory. The set of finite signed Borel measures on  $\mathbb{R}$  is denoted by  $\mathcal{M}(\mathbb{R})$ . The subset  $\mathcal{M}_+(\mathbb{R}) \subset \mathcal{M}(\mathbb{R})$  is the set of finite positive Borel measures on  $\mathbb{R}$ , and finally, the subset  $\mathcal{P}(\mathbb{R}) \subset \mathcal{M}_+(\mathbb{R})$  denotes the set of Borel probability measures on  $\mathbb{R}$ .

For a positive Borel measure  $\mu$  on  $\mathbb{R}$ , we say that  $\mu$  has a finite moment of order  $k \in \mathbb{N}$  if  $\int_{\mathbb{R}} |\varepsilon|^k d\mu(\varepsilon) < \infty$ . In this case, we denote by  $m_k(\mu) = \int_{\mathbb{R}} \varepsilon^k d\mu(\varepsilon)$  its  $k$ -th moment. In particular,  $\mu$  is finite if and only if it has a finite moment of order 0. In this case,  $\mu \in \mathcal{M}_+(\mathbb{R})$  and its 0-th moment is called the *mass* of  $\mu$ , denoted by  $\mu(\mathbb{R}) = m_0(\mu) = \int_{\mathbb{R}} d\mu$ . These notation and considerations extend to the case of matrix-valued measures, as will be discussed in the next section.

### 3.3.1 Pick functions

Our mathematical framework intersects with the realm of complex analysis pioneered by Pick [49] and Nevanlinna [45], focusing on the study of so-called Pick functions. A *Pick function* is a map  $f : \mathbb{C}_+ \rightarrow \overline{\mathbb{C}_+}$  which is analytic. In this article, we use the term Pick functions, but several terminologies coexist in the literature: Nevanlinna functions, Herglotz functions, Riesz functions, or  $R$ -functions. A *Pick matrix* is an analytic map  $f : \mathbb{C}_+ \rightarrow \mathbb{C}^{n \times n}$ ,  $n \geq 1$ , such that for all  $z \in \mathbb{C}_+$ ,  $\Im(f(z)) \geq 0$  (i.e.  $\Im(f(z)) \in \mathcal{S}_n^+(\mathbb{C})$ ). Sometimes, it is convenient to extend Pick matrices to the lower-half-plane  $\mathbb{C}_-$ . In this case, the usual convention is to set for all  $z \in \mathbb{C}_-$ ,  $f(z) = f(\bar{z})^\dagger$  [23]. One of the most important results about Pick functions is that they have an integral representation.

**Theorem 3.3.1** (Nevanlinna-Riesz representation theorem [23]). *Let  $f : \mathbb{C}_+ \rightarrow \mathbb{C}^{n \times n}$  be a Pick matrix. There exist  $a \in \mathcal{S}_n^+(\mathbb{C})$ ,  $b \in \mathcal{S}_n(\mathbb{C})$  and  $\mu$  a Borel  $\mathcal{S}_n^+(\mathbb{C})$ -valued measure on  $\mathbb{R}$  such that  $(1 + |\varepsilon|)^{-1}$  is  $\mu$ -integrable and*

$$\forall z \in \mathbb{C}_+, \quad f(z) = az + b + \int_{\mathbb{R}} \left( \frac{1}{\varepsilon - z} - \frac{\varepsilon}{1 + \varepsilon^2} \right) d\mu(\varepsilon). \quad (3.45)$$

The measure  $\mu$  is called the Nevanlinna-Riesz measure of  $f$ , and  $a = \lim_{y \rightarrow +\infty} \frac{1}{iy} f(iy)$ ,  $b = \Re(f(i)) := (f(i) + f(i)^\dagger)/2$ . In the particular case of Pick functions, i.e.  $n = 1$ , we have  $a \geq 0$ ,  $b \in \mathbb{R}$ , and  $\mu$  is a positive Borel measure on  $\mathbb{R}$ , with the same integrability condition.

The following theorem extends to Pick matrices a result on Pick functions which can be found in [15] and [2, Theorem 3.2.1]. It states that the moments of the Nevanlinna-Riesz measure of a Pick function or matrix are related to its expansion on the imaginary axis at  $+\infty$ .

**Theorem 3.3.2.** *Let  $f : \mathbb{C}_+ \rightarrow \mathbb{C}^{n \times n}$  be a Pick matrix and  $\mu$  its Nevanlinna-Riesz measure. Let  $n \in \mathbb{N}$ . The function  $f$  satisfies:*

$$-f(iy) = m_{-2}(iy) + m_{-1} + \frac{m_0}{iy} + \frac{m_1}{(iy)^2} + \frac{m_2}{(iy)^3} + \cdots + \frac{m_{2n}}{(iy)^{2n+1}} + o_{y \rightarrow +\infty} \left( \frac{1}{y^{2n+1}} \right) \quad (3.46)$$

if and only if  $\mu$  has finite moments of order less than or equal to  $2n$ , i.e. for all  $x \in \mathbb{C}^n$ ,  $\langle x, \int_{\mathbb{R}} |\varepsilon|^k d\mu(\varepsilon)x \rangle < \infty$  for  $0 \leq k \leq 2n$ . For  $0 \leq k \leq 2n$ , the coefficient  $m_k$  is then the  $k$ -th moment of  $\mu$ , i.e.  $m_k = \int_{\mathbb{R}} \varepsilon^k d\mu(\varepsilon) \in \mathcal{S}_n(\mathbb{C})$ .

*Proof.* The result for Pick functions can be found in [15] and [2, Theorem 3.2.1]. To extend the result to Pick matrices, it suffices to notice  $f$  is a Pick matrix if and only if for all  $x \in \mathbb{C}^n$ , the map  $f_x : z \in \mathbb{C}_+ \mapsto \langle x, f(z)x \rangle$  is a Pick function.  $\square$

As mentioned in the previous section, Pick matrices are related to the study of Green's functions methods in general, and to DMFT in particular because of the following result.

**Proposition 3.3.3** ( $-G, -\Delta, -\Sigma$  are Pick).

1. Let  $\hat{H}$  be a Hamiltonian on  $\text{Fock}(\mathbb{C}^n)$ , the Fock space associated to  $\mathcal{H} \simeq \mathbb{C}^n$ , and  $G : \mathbb{C}_+ \rightarrow \mathbb{C}^{n \times n}$  the one-body Green's function of  $\hat{H}$  in an equilibrium state. Then  $-G$  is a Pick matrix.

2. Let  $\hat{H}$  be a Hamiltonian on  $\text{Fock}(\mathbb{C}^n)$ , with non-interacting Hamiltonian  $d\Gamma(H^0)$ ,  $G^0$  the one-body Green's function of  $d\Gamma(H^0)$ ,  $G$  the one-body Green's function of  $\hat{H}$  in an equilibrium state of  $\hat{H}$ , and  $\Sigma : \mathbb{C}_+ \rightarrow \mathbb{C}^{n \times n}$  the self-energy defined by

$$\Sigma(z) := G^0(z)^{-1} - G(z)^{-1}.$$

Then  $-\Sigma$  is a Pick matrix.

3. Let  $\Delta : \mathbb{C}_+ \rightarrow \mathbb{C}^{n \times n}$  be the hybridization function of some Anderson Impurity Model (AIM) with impurity one-particle state space  $\mathbb{C}^n$ . Then  $-\Delta$  is a Pick matrix.

**Remark 3.3.4.** In condensed matter physics, the Nevanlinna-Riesz measure of  $-G$  is the so-called spectral function [43].

The following proposition highlights the fact that, the single-site translation-invariant IPT-DMFT equations have no solution with hybridization functions of a finite-dimensional AIM.

**Proposition 3.3.5** (Non-existence of solutions to the finite-dimensional bath single-site paramagnetic translation-invariant IPT-DMFT equations). *Apart from the limit cases described in Proposition 3.2.12, the single-site paramagnetic translation-invariant IPT-DMFT equations (3.43)-(3.44) have no finite-dimensional bath solution, that is no solution  $\Delta$  of the form*

$$\Delta(z) = \sum_{k=1}^K \frac{a_k}{z - \varepsilon_k}, \quad K \geq 1, \quad a_k > 0, \quad \varepsilon_k \in \mathbb{R}.$$

This implies that finding a solution to the DMFT equations requires considering infinite-dimensional bath hybridization functions. The appropriate function space can be characterized in terms of Nevanlinna-Riesz measures, as will be shown in the subsequent section.

### 3.3.2 Functional setting: the Bath Update and IPT maps

The DMFT map is the composition of the IPT map and the Bath Update (BU) map, which we will study separately. Before focusing on the paramagnetic single-site translation-invariant case, let us get back to the general case presented in Section 3.2.4. First, we formalize in our setting the definition of the BU map  $F^{\text{SC}}$ . It has been proved by Lindsey, Lin and Schneider [41] that the BU map is well defined when the Nevanlinna-Riesz measure of each self-energy is a finite sum of Dirac measures, which means in particular that the self-energy is a rational function. The following proposition extends this result to the case of finite  $\mathcal{S}_n^+(\mathbb{C})$ -valued measures, by using a different approach. In the following, we will denote by  $L_p := |\Lambda_p|$  the size of the  $p$ -th fragment, that is the cardinality of the subgraph  $\Lambda_p \subset \Lambda$ , and identify  $\mathcal{H}_p$  with  $\mathbb{C}^{2L_p}$  for convenience. Recall that the cardinality of the graph  $\Lambda$  is denoted by  $L = |\Lambda|$ . The spaces to which the self-energies  $\Sigma_p$  and the hybridization functions  $\Delta_p$  belong are respectively given by

$$\mathfrak{S}_p = \left\{ z \in \mathbb{C}_+ \mapsto C + \int_{\mathbb{R}} \frac{d\mu(\varepsilon)}{z - \varepsilon}; \quad C \in \mathcal{S}_{2L_p}(\mathbb{C}), \mu \in \mathcal{M}(\mathbb{R}, \mathcal{S}_{2L_p}^+(\mathbb{C})) \right\}, \quad (3.47)$$

where  $\mathcal{M}(\mathbb{R}, \mathcal{S}_n^+(\mathbb{C}))$  is the set of finite  $\mathcal{S}_n^+(\mathbb{C})$ -valued Borel measures on  $\mathbb{R}$ , and

$$\mathfrak{D}_p = \left\{ z \in \mathbb{C}_+ \mapsto \int_{\mathbb{R}} \frac{d\nu(\varepsilon)}{z - \varepsilon}; \quad \nu \in \mathcal{M}(\mathbb{R}, \mathcal{S}_{2L_p}^+(\mathbb{C})), \quad \nu(\mathbb{R}) = W_p^\dagger W_p \right\},$$

where  $W_p \in \mathbb{C}^{(L-L_p) \times 2L_p}$  is defined in (3.26)-(3.27). These definitions are motivated by the consequences of Proposition 3.3.5 and the statements of Propositions 3.3.6 and 3.3.8.

**Proposition 3.3.6** (Bath Update map:  $\Sigma \mapsto \Delta$ ). *For  $1 \leq p \leq P$ , let  $\Sigma_p \in \mathfrak{S}_p$ , and let  $\mu_p$  be the Nevanlinna-Riesz measure associated to  $\Sigma_p$ . For  $1 \leq p \leq P$ , the hybridizations functions  $\Delta_p$  given by*

$$\Delta_p(z) = W_p \left( z - H_p^0 - \bigoplus_{q \neq p} \Sigma_q(z) \right)^{-1} W_p^\dagger \quad (3.48)$$

for  $z \in \mathbb{C}_+$  are well-defined. With this definition,  $-\Delta_p$  is a Pick matrix and there exists a finite measure  $\nu_p \in \mathcal{M}(\mathbb{R}, \mathcal{S}_{2L_p}^+(\mathbb{C}))$  such that

$$\forall z \in \mathbb{C}_+, \quad \Delta_p(z) = \int_{\mathbb{R}} \frac{d\nu_p(\varepsilon)}{z - \varepsilon} \quad \text{and} \quad \nu_p(\mathbb{R}) = W_p W_p^\dagger, \quad (3.49)$$

namely  $\Delta_p \in \mathfrak{D}_p$ .

In the particular case of the single-site paramagnetic translation-invariant IPT-DMFT framework, we have  $L_p = 1$  for all  $1 \leq p \leq P$  and the Nevanlinna-Riesz measures of the self-energies and the hybridization functions are finite positive Borel measures on  $\mathbb{R}$ . The self-energy space (3.47) takes the simpler form:

$$\mathfrak{S}_p^{IPT} = \left\{ \mathbb{C}_+ \ni z \mapsto U^2 \int_{\mathbb{R}} \frac{d\mu(\varepsilon)}{z - \varepsilon} \in \mathbb{C} ; \mu \in \mathcal{M}_+(\mathbb{R}) \right\}, \quad (3.50)$$

and is therefore in one-to-one correspondence with the set  $\mathcal{M}_+(\mathbb{R})$  of finite positive Borel measures on  $\mathbb{R}$ . The hybridization space becomes

$$\mathfrak{D}_p^{IPT} = \left\{ \mathbb{C}_+ \ni z \mapsto |W|^2 \int_{\mathbb{R}} \frac{d\nu(\varepsilon)}{z - \varepsilon} \in \mathbb{C} ; \nu \in \mathcal{P}(\mathbb{R}) \right\}, \quad (3.51)$$

and is thus in one-to-one correspondence with the set  $\mathcal{P}(\mathbb{R})$  of Borel probability measures on  $\mathbb{R}$ . These one-to-one correspondences allow us to focus on the measure spaces  $\mathcal{M}_+(\mathbb{R})$  and  $\mathcal{P}(\mathbb{R})$ , and we will study the DMFT loop in terms of measures from now on. The BU map can then be defined as a function  $F^{SC}$  between measure spaces as follows.

**Corollary 3.3.7** (BU map in the IPT-DMFT framework:  $F^{SC} : \Sigma \mapsto \Delta$ ). *The Bath Update (BU) map in the paramagnetic single-site translation-invariant IPT-DMFT framework is defined as the function  $F^{SC} : \mathcal{M}_+(\mathbb{R}) \rightarrow \mathcal{P}(\mathbb{R})$  such that*

$$F^{SC}(\mu) = \nu,$$

with

$$W_p^\dagger W_p \int_{\mathbb{R}} \frac{d\nu(\varepsilon)}{z - \varepsilon} = W \left( z - H_\perp^0 - U^2 \int_{\mathbb{R}} \frac{d\mu(\varepsilon)}{z - \varepsilon} \right)^{-1} W^\dagger. \quad (3.52)$$

In the DMFT loop, the impurity solver is the focus of the second stage. Within our model, we define the IPT map  $F^{IPT}$ , which transforms a given hybridization function  $\Delta$  into a self-energy  $\Sigma$ . As well as the Bath Update map, this mapping operates across measure spaces and maps Borel probability measures to finite positive Borel measures.

**Proposition 3.3.8** (Definition of the IPT map). *Let  $\nu \in \mathcal{P}(\mathbb{R})$  and  $\Delta \in \mathfrak{D}_p^{IPT}$  the hybridization function associated with  $\nu$ : for all  $z \in \mathbb{C}_+$ ,*

$$\Delta(z) = |W|^2 \int_{\mathbb{R}} \frac{d\nu(\varepsilon)}{z - \varepsilon}.$$

*There exists  $\xi \in \mathcal{P}(\mathbb{R})$ , such that for all  $z \in \mathbb{C}_+$ ,*

$$\int_{\mathbb{R}} \frac{d\xi(\varepsilon)}{z - \varepsilon} = \frac{1}{z - \Delta(z)}. \quad (3.53)$$

*Then define*

$$\tilde{\xi}(d\varepsilon) := \frac{\xi(d\varepsilon)}{1 + e^{-\beta\varepsilon}}, \quad (3.54)$$

$$\tilde{\mu} := \tilde{\xi} * \tilde{\xi} * \tilde{\xi}, \quad (3.55)$$

*where  $*$  is the convolution product, and*

$$\mu(d\varepsilon) := (1 + e^{-\beta\varepsilon})\tilde{\mu}(d\varepsilon). \quad (3.56)$$

*Finally, define the self-energy associated to the measure  $\mu$  by*

$$\Sigma(z) = U^2 \int_{\mathbb{R}} \frac{d\mu(\varepsilon)}{z - \varepsilon}. \quad (3.57)$$

*The measure  $\mu$  is a positive finite measure:  $\mu \in \mathcal{M}_+(\mathbb{R})$ , hence  $\Sigma \in \mathfrak{S}_p^{IPT}$ , where  $\mathfrak{S}_p^{IPT}$  is defined in (3.50). The IPT map  $F^{IPT} : \mathcal{P}(\mathbb{R}) \rightarrow \mathcal{M}_+(\mathbb{R})$  is defined by*

$$F^{IPT}(\nu) = \mu.$$

*Moreover, the map  $\mathfrak{D}_p^{IPT} \ni \Delta \mapsto \Sigma \in \mathfrak{S}_p^{IPT}$  defined by (3.53)-(3.57) is continuous with respect to the weak topology of measures, and coincides with the IPT solver defined in Proposition 3.2.18 on finite-dimensional bath hybridization functions, hence it is its unique continuous extension to the set  $\mathfrak{D}_p^{IPT}$ .*

Now that we have defined the maps  $F^{\text{IPT}}$  and  $F^{\text{SC}}$ , we define the paramagnetic translation-invariant single-site IPT-DMFT map as

$$F^{\text{DMFT}} := F^{\text{SC}} \circ F^{\text{IPT}} : \mathcal{P}(\mathbb{R}) \rightarrow \mathcal{P}(\mathbb{R}).$$

For the sake of brevity, we will sometimes refer to  $F^{\text{DMFT}}$  as the IPT-DMFT map rather than restating all the assumptions: paramagnetic framework, translation-invariant and single-site. In the same way, we refer to fixed points of  $F^{\text{DMFT}}$  as IPT-DMFT solutions. Such fixed points (more precisely the associated hybridization functions and self-energies) are indeed solutions of the single-site paramagnetic translation-invariant IPT-DMFT equations (3.43)-(3.44).

### 3.3.3 Existence and properties of IPT-DMFT solutions

The main result of this paper is the existence of a solution to the DMFT equations (3.43)-(3.44) in the paramagnetic translation-invariant single-site framework, using the IPT impurity solver.

**Theorem 3.3.9** (Existence of a fixed point). *The IPT-DMFT map  $F^{\text{DMFT}}$  has a fixed point  $\nu \in \mathcal{P}(\mathbb{R})$ .*

Moreover, IPT-DMFT solutions have finite moments of all orders.

**Proposition 3.3.10.** *Let  $\nu^0 \in \mathcal{P}(\mathbb{R})$ ,  $\nu = F^{\text{DMFT}}(\nu^0)$ , and  $k \in 2\mathbb{N}$ . If  $\nu^0 \in \mathcal{P}(\mathbb{R})$  has finite  $k$ -th moment, then  $\nu$  has finite  $(k+4)$ -th moment. In particular, any fixed point of the IPT-DMFT map has finite moments of all orders.*

## 3.4 Proofs

In this section, we give the proofs of the results stated in Section 3.2 and Section 3.3. Among other things, we will make use of the results stated in Section 3.3.1 about Pick functions and of some results from measure theory, which will be recalled when needed. As we will discuss continuity of functions defined on measure spaces, we must specify the topology we are considering. Recall that a sequence  $(\mu_n)_{n \in \mathbb{N}}$  of finite Borel measures on  $\mathbb{R}$  is said to converge weakly to  $\mu$  if for all bounded continuous function  $f \in \mathcal{C}_b^0(\mathbb{R})$ ,

$$\int_{\mathbb{R}} f d\mu_n \rightarrow \int_{\mathbb{R}} f d\mu. \quad (3.58)$$

It converges vaguely to  $\mu$  if (3.58) holds for all  $f \in \mathcal{C}_0^0(\mathbb{R})$ , the space of continuous functions from  $\mathbb{R}$  to  $\mathbb{R}$  vanishing at infinity. Weak convergence clearly implies vague convergence, and the converse is also true if all the  $\mu_n$ 's are probability measures, since  $\mathbb{R}$  is locally compact [62]. We will also make use of the notions of Wasserstein distance and optimal transportation on  $\mathbb{R}$ . The Wasserstein 2-distance between two Borel probability measures  $\mu$  and  $\nu$  on  $\mathbb{R}$  is defined by

$$W_2(\mu, \nu) := \left( \inf_{\pi \in \Pi(\mu, \nu)} \int_{\mathbb{R}^2} |x - y|^2 d\pi(x, y) \right)^{\frac{1}{2}}, \quad (3.59)$$

where  $\Pi(\mu, \nu)$  is the set of all couplings of  $\mu$  and  $\nu$ , i.e. of Borel probability measures on  $\mathbb{R} \times \mathbb{R}$  whose marginals with respect to the first and second variables are respectively  $\mu$  and  $\nu$ . The infimum in the definition (3.59) is actually a minimum, and there exists in fact a unique  $\pi_{\mu, \nu} \in \Pi(\mu, \nu)$  such that  $W_2(\mu, \nu)^2 = \int |x - y|^2 d\pi_{\mu, \nu}(x, y)$  [53].

### 3.4.1 Proofs of the results in Section 3.2

Most of the results presented in Section 3.2 are known in other settings similar to ours. However, the proofs of Propositions 3.2.3 and 3.2.8 found in the literature are limited to specific states (such as ground states or Gibbs states) and do not emphasize the importance of the notion of *equilibrium* state. Our proofs overcome this artificial distinction. Additionally, Proposition 3.2.12 is often regarded as obvious in the physics literature, but it is typically proven only for translation-invariant settings. Our proof allows for the computation of the Green's function of a strictly interacting Hubbard model and facilitates understanding of the DMFT equations, which we hope will aid the reader in grasping the machinery introduced in this section. Furthermore, Theorem 3.2.15 has long been considered proven in [7] within

the physics community. However, the proof given in [7] does not utilize classical analytic continuation techniques known at the time. Our proof is entirely different and relies precisely on analytic continuation techniques. We hope it sheds light on certain aspects of [7] in this specific *finite*-dimensional Hilbert space setting. In particular, our proof of uniqueness of the analytic continuation of the Matsubara's Fourier coefficients does not rely on the asymptotic behavior of the Green's function, but on the properties of Pick functions.

### Proof of Proposition 3.2.3

Our proof is based on the time evolution of annihilation/creation propagators for ideal Fermi gases. More precisely, one has, as detailed in [12, p.46],

$$\mathbb{H}(\hat{a}_\phi)(t) = \hat{a}_{e^{itH^0}\phi}. \quad (3.60)$$

For all  $z \in \mathbb{C}_+$ , we have to show that  $(z - H^0)G(z) = (z - H^0)(G_+(z) + G_-(\bar{z})^\dagger) = \mathbf{1}$ . Integrating by parts, one has

$$(z - H^0)G_+(z) = i\tilde{G}(0^+) + \int_{\mathbb{R}_+^*} e^{izt} \left( i\frac{d}{dt}\tilde{G}(t) - H^0\tilde{G}(t) \right) dt,$$

and for  $t > 0$ ,  $i\tilde{G}(t)$  represents the sesquilinear form defined by

$$\forall \phi, \phi' \in \mathcal{H}, \quad \langle \phi, (i\tilde{G})(t)\phi' \rangle = \Omega(\mathbb{H}(\hat{a}_\phi)(t)\hat{a}_{\phi'}^\dagger),$$

so that

$$\langle \phi, (i\frac{d}{dt}\tilde{G})(t)\phi' \rangle = \Omega\left(\frac{d}{dt}(\mathbb{H}(\hat{a}_\phi))(t)\hat{a}_{\phi'}^\dagger\right) = -i\Omega(\mathbb{H}(\hat{a}_{H^0\phi})(t)\hat{a}_{\phi'}^\dagger) = \langle H^0\phi, \tilde{G}(t)\phi' \rangle = \langle \phi, H^0\tilde{G}(t)\phi' \rangle.$$

Similarly, another integration by parts leads to

$$(z - H^0)G_-(\bar{z})^\dagger = i\tilde{G}(0^-)^\dagger + \int_{\mathbb{R}_-} e^{-izt} (i\frac{d}{dt}\tilde{G}(t) - \tilde{G}(t)H^0)^\dagger dt.$$

For  $t < 0$ ,  $i\tilde{G}(t)$  represents the sesquilinear form defined by

$$\forall \phi, \phi' \in \mathcal{H}, \quad \langle \phi, (i\tilde{G})(t)\phi' \rangle = -\Omega(\hat{a}_{\phi'}^\dagger \mathbb{H}(\hat{a}_\phi)(t)).$$

Note that, because  $\Omega$  is an equilibrium state and by the cyclic property of the trace, one has

$$\langle \phi, (i\tilde{G})(t)\phi' \rangle = -\Omega(\mathbb{H}(\hat{a}_{\phi'}^\dagger)(-t)\hat{a}_\phi) \quad (3.61)$$

(equilibrium propagators are time-translation-invariant), so that

$$\langle \phi, (i\frac{d}{dt}\tilde{G})(t)\phi' \rangle = i\Omega(\mathbb{H}(\hat{a}_{H^0\phi'}^\dagger)(-t)\hat{a}_\phi) = \langle \phi, \tilde{G}(t)H^0\phi' \rangle.$$

Finally, one has for  $\phi, \phi' \in \mathcal{H}$ ,

$$\langle \phi, (z - H^0)G(z)\phi' \rangle = \langle \phi, i\tilde{G}(0^+)\phi' \rangle + \langle \phi, i\tilde{G}(0^-)^\dagger\phi' \rangle = \Omega(\hat{a}_\phi\hat{a}_{\phi'}^\dagger + \hat{a}_{\phi'}^\dagger\hat{a}_\phi) = \langle \phi, \phi' \rangle,$$

because  $\Omega$  is a state and the annihilation/creation operators satisfy the CAR.

### Proof of Theorem 3.2.8

For the simplicity of the proof, note first that an equivalent definition of an impurity problem is that there exists an *impurity space*  $\mathcal{H}_{\text{imp}} \subset \mathcal{H}$  such that the interacting part  $\hat{H}^I$  of the Hamiltonian  $\hat{H}$  as introduced in (3.9) belongs to the following subalgebra

$$\hat{H}^I \in \mathcal{A}\{\hat{a}_\phi^\dagger\hat{a}_{\phi'}, \phi, \phi' \in \mathcal{H}_{\text{imp}}\}. \quad (3.62)$$

In other words, the interacting part of the Hamiltonian is an element of the Gauge Invariant Canonical Anti-commutation Relations (GICAR) algebra generated by  $\mathcal{H}_{\text{imp}}$  (see [56] for a concise introduction to GICAR algebras).

From that, the proof is a generalization of [40]. To prove the sparsity pattern of  $\Sigma$ , we have to prove that for all  $z \in \mathbb{C}_+$ , for all  $\phi \in \mathcal{H}$ ,  $\phi' \in \mathcal{H}_{\text{imp}}^\perp$ ,

$$\langle \phi, G(z)\Sigma(z)\phi' \rangle = 0 \text{ and } \langle \phi', \Sigma(z)G(z)\phi \rangle = 0. \quad (3.63)$$

The first equality is equivalent to

$$\langle \phi, G(z)(z - H^0)\phi' \rangle = \langle \phi, \phi' \rangle,$$

and, similarly as in the previous proof, we have

$$\begin{aligned} \langle \phi, G(z)(z - H^0)\phi' \rangle &= \langle \phi, \phi' \rangle + \int_{\mathbb{R}_+} e^{izt} \left( \frac{d}{dt} \langle \phi, i\tilde{G}(t)\phi' \rangle - \langle \phi, \tilde{G}(t)H^0\phi' \rangle \right) dt \\ &\quad + \int_{\mathbb{R}_-^*} e^{-izt} \left( \frac{d}{dt} \langle i\tilde{G}(t)\phi, \phi' \rangle - \langle \tilde{G}(t)H^0\phi, \phi' \rangle \right) dt. \end{aligned}$$

Now, for all  $t \in \mathbb{R}_+$ , we have using the cyclicity of the trace, similarly as in (3.61),

$$\frac{d}{dt} \langle \phi, i\tilde{G}(t)\phi' \rangle = -i\Omega \left( \hat{a}_\phi \mathbb{H}([\hat{H}, \hat{a}_{\phi'}^\dagger])(-t) \right).$$

To compute the commutator, note first that for all  $\phi_1, \phi_2 \in \mathcal{H}_{\text{imp}}$ , we have using the CAR

$$[\hat{a}_{\phi_1}^\dagger \hat{a}_{\phi_2}, \hat{a}_{\phi'}^\dagger] = \langle \phi_2, \phi' \rangle \hat{a}_{\phi_1}^\dagger = 0$$

since  $\phi' \in \mathcal{H}_{\text{imp}}^\perp$ , so that  $\hat{a}_{\phi'}^\dagger$  commutes with the generators of the algebra to which  $\hat{H}^I$  belongs, hence with  $\hat{H}^I$ . Moreover, we have using (3.60),

$$[d\Gamma(H^0), \hat{a}_{\phi'}^\dagger] = -i \frac{d}{dt} \left( t \mapsto \mathbb{H}(\hat{a}_{\phi'}^\dagger)_{H^0} \right) (0) = \hat{a}_{H^0\phi'}^\dagger,$$

where  $\mathbb{H}(\cdot)_{H^0}$  denotes the Heisenberg picture associated to the non-interacting Hamiltonian  $d\Gamma(H^0)$ , so that we end up with

$$\frac{d}{dt} \langle \phi, i\tilde{G}(t)\phi' \rangle = -i\Omega \left( \hat{a}_\phi \mathbb{H}(\hat{a}_{H^0\phi'}^\dagger)(-t) \right) = \langle \phi, \tilde{G}(t)H^0\phi' \rangle.$$

One shows, using the same techniques, that for all  $t \in \mathbb{R}_-^*$ ,

$$\frac{d}{dt} \langle i\tilde{G}(t)\phi, \phi' \rangle = \langle \tilde{G}(t)H^0\phi, \phi' \rangle$$

hence the first equality of (3.63) is proven. The second equality can be proved similarly.

### Proof of Proposition 3.2.12

We stick to the case in Remark 3.2.10, where the AIM states are Gibbs states at inverse temperature  $\beta$  and chemical potential  $\epsilon_F$ . Now for the first case, if  $U = 0$ , the AIM are non-interacting, hence the Green's functions are the non-interacting Green's functions, the self-energies  $\Sigma_{\text{imp},p}$  are identically zero, and the hybridization functions are given by, for all  $z \in \mathbb{C}_+$ ,

$$\Delta_p(z) = W_p (z - H_p^0)^{-1} W_p^\dagger.$$

Now if the partition  $\mathfrak{P}$  is such that  $\mathcal{G}_H = \bigoplus_{p=1}^P \mathcal{G}_p$ , or if  $T = 0$ , we have

$$H_{\text{H},p,\bar{p}}^0 = 0,$$

so that the hybridization functions  $\Delta_p$  are identically zero. This is equivalent to zero-dimensional baths, and all the AIMs reduce to Hubbard models defined by  $(\mathcal{G}_p, T_p, U_p)$ . Hence the self-energies  $\Sigma_p$  are the self-energies associated to the corresponding Hubbard models.

### Proof of Theorem 3.2.15

We start by proving the equality. On the one hand, the Källén-Lehmann representation (3.7) of  $\tilde{G}$  associated to the grand canonical Hamiltonian  $\hat{H}' = \hat{H} - \epsilon_F \hat{N}$  reads for  $\phi, \phi' \in \mathcal{H}$  and  $z \in \mathbb{C}_+$ ,

$$\langle \phi, G(z)\phi' \rangle = \sum_{\psi, \psi' \in \mathcal{B}} (\rho_\psi + \rho_{\psi'}) \langle \psi, \hat{a}_\phi \psi' \rangle \langle \psi', \hat{a}_{\phi'}^\dagger \psi \rangle \frac{1}{z + \epsilon_F + (E_\psi - E_{\psi'})}.$$

On the other hand, the Källén-Lehmann representation of  $\tilde{G}^M$  reads for  $\phi, \phi' \in \mathcal{H}$  and  $n \in \mathbb{N}$ ,

$$\langle \phi, G_n^M \phi' \rangle = \sum_{\psi, \psi' \in \mathcal{B}} \left( \rho_\psi + \rho_{\psi'} e^{\beta(E_\psi - E_{\psi'} + \epsilon_F)} \right) \langle \psi, \hat{a}_\phi \psi' \rangle \langle \psi', \hat{a}_{\phi'}^\dagger \psi \rangle \frac{1}{i\omega_n + \epsilon_F + (E_\psi - E_{\psi'})}.$$

Note now that whenever  $\langle \psi, \hat{a}_\phi \psi' \rangle \neq 0$ , we have  $N_{\psi'} = N_\psi + 1$  and then

$$\rho_\psi e^{\beta(E_\psi - E_{\psi'} + \epsilon_F)} = e^{-\beta(E_{\psi'} - \epsilon_F(N_\psi + 1))} = \rho_{\psi'},$$

yielding

$$\forall n \in \mathbb{N}, \quad G(i\omega_n) = G_n^M.$$

To prove uniqueness, we use the fact that  $-G$  is a Pick function (see Proposition 3.3.3), and its Nevanlinna-Riesz measure is a weighted sum of finitely many Dirac measures. It follows that the Analytical Continuation Problem defined by  $(i\omega_n, -G_n^M)_{n \in \mathbb{N}}$  has no other solution thanks to Theorem 3.A.8, which concludes.

### Proof of Proposition 3.2.18

Proposition 3.2.18 can actually be seen as a corollary of Proposition 3.3.8, but we give at this stage a pedestrian proof, which enlightens the way the hybridization function "encapsulates" the energy of the bath orbitals and their coupling to the impurity. We have for all  $z \in \mathbb{C}_+$ ,

$$(z - \Delta(z))^{-1} = (z - H_{\text{AIM}}^0)_{1,1}^{-1}, \quad \text{where } H_{\text{AIM}}^0 = \begin{pmatrix} 0 & \sqrt{a_1} & \sqrt{a_2} & \cdots & \sqrt{a_K} \\ \sqrt{a_1} & \varepsilon_1 & 0 & \cdots & 0 \\ \sqrt{a_2} & 0 & \varepsilon_2 & \ddots & \vdots \\ \vdots & \vdots & \ddots & \ddots & 0 \\ \sqrt{a_K} & 0 & \cdots & 0 & \varepsilon_K \end{pmatrix},$$

which holds true in particular for  $z = i\omega_n$ . Note that  $H_{\text{AIM}}^0$  is self-adjoint and that for all  $z \in \mathbb{C}_+$ , using functional calculus,

$$\int_0^\beta e^{i\omega_n \tau} \frac{-e^{-\tau H_{\text{AIM}}^0}}{1 + e^{-\beta H_{\text{AIM}}^0}} d\tau = (i\omega_n - H_{\text{AIM}}^0)^{-1},$$

so that we can perform explicitly the Fourier summation :

$$\frac{1}{\beta} \sum_{n' \in \mathbb{Z}} e^{-i\omega_n \tau} (i\omega_{n'} - \Delta(i\omega_{n'}))^{-1} = \left( \frac{-e^{-\tau H_{\text{AIM}}^0}}{1 + e^{-\beta H_{\text{AIM}}^0}} \right)_{1,1} = - \sum_{k=1}^{K+1} \frac{|P_{1,k}|^2 e^{-\tau \varepsilon'_k}}{1 + e^{-\beta \varepsilon'_k}}, \quad (3.64)$$

where  $P \in \mathbb{C}^{(K+1) \times (K+1)}$  is a unitary matrix such that  $H_{\text{AIM}}^0 = P \text{diag}(\varepsilon'_1, \dots, \varepsilon'_{K+1}) P^\dagger$ . The right-hand side of (3.64) is a continuous function on  $[0, \beta]$  and the following integral is well-defined and reads

$$\begin{aligned} \int_0^\beta e^{i\omega_n \tau} \left( \frac{1}{\beta} \sum_{n' \in \mathbb{Z}} (i\omega_{n'} - \Delta(i\omega_{n'}))^{-1} e^{-i\omega_{n'} \tau} \right)^3 d\tau = \\ \sum_{k_1, k_2, k_3=1}^{K+1} \frac{1 + e^{-\beta(\varepsilon'_{k_1} + \varepsilon'_{k_2} + \varepsilon_{k_3})}}{(1 + e^{-\beta \varepsilon'_{k_1}})(1 + e^{-\beta \varepsilon'_{k_2}})(1 + e^{-\beta \varepsilon'_{k_3}})} \frac{|P_{1,k_1}|^2 |P_{1,k_2}|^2 |P_{1,k_3}|^2}{i\omega_n - (\varepsilon'_{k_1} + \varepsilon'_{k_2} + \varepsilon'_{k_3})}. \end{aligned}$$

Let us now compute the spectrum of  $H_{\text{AIM}}^0$ : a simple calculation shows that its characteristic polynomial  $\chi_{H_{\text{AIM}}^0}$  reads

$$\chi_{H_{\text{AIM}}^0}(\varepsilon) = \left( \prod_{k=1}^K (\varepsilon - \varepsilon_k) \right) \varepsilon - \sum_{k=1}^K a_k \prod_{l=1, l \neq k}^K (\varepsilon - \varepsilon_l).$$

By assumption on the  $a_k$ 's and  $\varepsilon_k$ 's, we have  $\chi_{H_{\text{AIM}}^0}(\varepsilon_k) \neq 0$ , so that

$$\chi_{H_{\text{AIM}}^0}(\varepsilon) = 0 \iff \varepsilon - \Delta(\varepsilon) = 0.$$

This in fact straightforwardly follows from the Schur complement approach. Moreover, one can compute explicitly  $|P_{1,k}|^2$ : by definition, we have for all  $k \in \llbracket 1, K+1 \rrbracket$  and  $l \in \llbracket 1, K \rrbracket$ ,

$$\sqrt{a_l} P_{1,k} + \varepsilon_l P_{l+1,k} = \varepsilon'_k P_{l+1,k} \implies \frac{a_l}{(\varepsilon'_k - \varepsilon_l)^2} |P_{1,k}|^2 = |P_{l+1,k}|^2,$$

which gives after summation on  $l$  and using the fact that  $PP^\dagger = 1$ ,

$$|P_{1,k}|^2 = (1 - \Delta'(\varepsilon'_k))^{-1}.$$

This shows that  $\Sigma^{\text{IPT}}(i\omega_n) = \Sigma_{\text{imp},n}$ , hence  $\Sigma^{\text{IPT}}$  is a solution to the Analytical Continuation Problem (ACP) defined in (3.40). Then, Theorem 3.A.8 ensures that there is no other solution, which concludes the proof.

### 3.4.2 Proof of Proposition 3.3.3 ( $-G, -\Sigma, -\Delta$ are Pick matrices)

The fact that the Green's function  $G$  is a Pick matrix readily follows from the KL representation (3.7) and inequality (3.8).

Combining (3.10) and (3.12), the self-energy can be written as

$$\forall z \in \mathbb{C}_+, \quad \Sigma(z) = z - H^0 - G(z)^{-1}.$$

Recall that we know from (3.8) that  $G(z)$  is invertible for all  $z \in \mathbb{C}_+$ . Since  $-G$  is Pick,  $G^{-1}$  is Pick. This readily implies that  $\Sigma$  is analytic. Let us now prove that  $-\Sigma$  is Pick. First, we infer from the KL representation (3.7) that for all  $k \in \mathbb{N}$ , there exists  $m_0, \dots, m_{2k} \in \mathbb{C}^{n \times n}$  such that it holds

$$G(iy) = \frac{m_0}{iy} + \frac{m_1}{(iy)^2} + \frac{m_2}{(iy)^3} + \cdots + \frac{m_{2k}}{(iy)^{2k+1}} + o_{y \rightarrow +\infty} \left( \frac{1}{y^{2k+1}} \right).$$

Using the anti-commutation relation  $\hat{a}_\phi \hat{a}_{\phi'}^\dagger + \hat{a}_{\phi'}^\dagger \hat{a}_\phi = \langle \phi, \phi' \rangle$  and the normalization condition  $\sum_{\psi \in \mathcal{B}} \rho_\psi = 1$ , we obtain that  $m_0 = I_n$ . As a consequence, we have

$$G(iy)^{-1} = (iy)I_n - m_1 + \frac{1}{iy}(m_1^2 - m_2) + o_{y \rightarrow +\infty} \left( \frac{1}{y} \right).$$

In view of Theorem 3.3.2, the Pick matrix  $G^{-1}$  has a Nevanlinna-Riesz representation of the form

$$G(z)^{-1} = z - \Sigma_\infty + \int_{\mathbb{R}} \frac{d\mu(\epsilon)}{\epsilon - z},$$

with  $\Sigma_\infty \in \mathcal{S}_n(\mathbb{C})$  and  $\mu$  a finite Borel  $\mathcal{S}_n^+(\mathbb{C})$ -valued measure on  $\mathbb{R}$ . We thus obtain that

$$\forall z \in \mathbb{C}_+, \quad \Sigma(z) = \Sigma_\infty + \int_{\mathbb{R}} \frac{d\mu(\epsilon)}{z - \epsilon},$$

from which we deduce that  $-\Sigma$  is Pick. As a matter of fact,  $\Sigma$  is a matrix-valued rational function, that is  $\mu$  is a weighted sum of finitely many Dirac measures.

Let  $\Delta$  be a hybridization function of an AIM defined as (3.18). Since  $H_{\text{bath}}^0$  is self-adjoint, its spectrum is real and (3.18) thus defines an analytic function on  $\mathbb{C}_+$ . In addition, for all  $z \in \mathbb{C}_+$ ,  $\Im(z - H_{\text{bath}}^0) = \Im(z) > 0$  hence  $\Im((z - H_{\text{bath}}^0)^{-1}) < 0$ . Since the congruence preserves the sign of the imaginary part we have  $\Im(\Delta(z)) \leq 0$ . This shows that  $-\Delta$  is a Pick matrix.

### 3.4.3 Proof of Proposition 3.3.5 (no finite-dimensional bath solution)

In this section, we prove the statement of Proposition 3.3.5, which states that there is no solution to the IPT-DMFT equations considering only hybridization functions with a finite-dimensional bath.

**Lemma 3.4.1.** *Let  $f$  and  $g$  be rational matrix-valued functions of size  $n \geq 1$  given by*

$$f(z) = \sum_{k=1}^K \frac{A_k}{z - \varepsilon_k} \quad \text{and} \quad g(z) = (z - C - f(z))^{-1},$$

where  $A_1, \dots, A_K \in \mathcal{S}_n^+(\mathbb{C}) \setminus \{0\}$  are positive semi-definite matrices,  $\varepsilon_1 < \dots < \varepsilon_K$  are real numbers and  $C \in \mathcal{S}_n(\mathbb{C})$ . Assume that the matrices  $A_1, \dots, A_K$  and  $C$  commute. Then  $g$  writes

$$g(z) = \sum_{k=1}^{K'} \frac{A'_k}{z - \varepsilon'_k}, \tag{3.65}$$

where  $K' \geq K + 1$ ,  $A'_k \in \mathcal{S}_n^+(\mathbb{C}) \setminus \{0\}$ , and  $\varepsilon'_k \in \mathbb{R}$ , with  $\varepsilon'_1 < \dots < \varepsilon'_{K'}$ .

*Proof.* The fact that  $\mathbb{C}_+ \ni z \mapsto -g(z)$  is a Pick matrix follows from the fact that  $-f$  is also a Pick matrix and that  $\Im(M) > 0$  implies that  $M$  is invertible and that  $\Im(M^{-1}) < 0$ . Indeed, for all  $z \in \mathbb{C}_+$ , we have

$$\Im(z - C - f(z)) = \Im(z) - \Im(f(z)) \geq \Im(z) > 0.$$

Theorem 3.3.1 gives a Nevanlinna-Riesz representation for  $-g$ , but since  $g$  is a rational matrix-valued function, the Nevanlinna-Riesz measure of  $-g$  is just a finite sum of Dirac measures. We thus have

$$g(z) = -\tilde{A}z - \tilde{B} + \sum_{k=1}^{K'} \frac{A'_k}{z - \varepsilon'_k},$$

with the stated properties of  $A'_k$  and  $\varepsilon'_k$ , and  $\tilde{A} \geq 0$ ,  $\tilde{B} \in \mathcal{S}_L(\mathbb{C})$ . Moreover, since  $g(iy) \xrightarrow[y \rightarrow +\infty]{} 0$  due to the definition of  $g$ , the affine part of  $-g$  is zero. This ensures that  $g$  is of the form (3.65). It remains to show that the number of poles of  $g$  is at least  $K + 1$ . Because of the assumption that the matrices  $A_1, \dots, A_K$  and  $C$  commute, they can be codiagonalized in an orthonormal basis. Let  $P$  be the unitary matrix, such that  $PA_kP^\dagger = \text{diag}(\lambda_k^1, \dots, \lambda_k^L)$  and  $PCP^\dagger = \text{diag}(c^1, \dots, c^L)$ . We have

$$g(z) = P^\dagger \text{diag} \left( \frac{1}{z - c^1 - \sum_{k=1}^K \frac{\lambda_k^1}{z - \varepsilon_k}}, \dots, \frac{1}{z - c^L - \sum_{k=1}^K \frac{\lambda_k^L}{z - \varepsilon_k}} \right) P.$$

The set of poles of  $g$  contains the union of the sets of zeros of the rational functions  $u_l(z) = z - c^l - \sum_{k=1}^K \frac{\lambda_k^l}{z - \varepsilon_k}$ , for  $1 \leq l \leq L$ . The zeros of  $u_l$  are on the real axis, because  $\Im(u_l(z)) > 0$  if  $\Im(z) > 0$  and  $\Im(u_l(z)) < 0$  if  $\Im(z) < 0$ . For  $\varepsilon \in \mathbb{R} \setminus \{\varepsilon_1, \dots, \varepsilon_K\}$ , we have  $u'_l(\varepsilon) = 1 + \sum_{k=1}^K \frac{\lambda_k^l}{(\varepsilon - \varepsilon_k)^2} > 0$  so that  $u_l$  is increasing on  $(-\infty, \varepsilon_1) \cup (\varepsilon_1, \varepsilon_2) \cup \dots \cup (\varepsilon_K, +\infty)$ . As  $u_l(\varepsilon) \xrightarrow[\varepsilon \rightarrow -\infty]{} -\infty$  and  $u_l(\varepsilon) \xrightarrow[\varepsilon \rightarrow \varepsilon_1, \varepsilon < \varepsilon_1]{} +\infty$ ,  $u_l$  has exactly 1 zero in  $(-\infty, \varepsilon_1)$  by the intermediate value theorem. The same argument shows that there is exactly one zero in each interval  $(\varepsilon_k, \varepsilon_{k+1})$  and in the interval  $(\varepsilon_K, +\infty)$ . So  $u_l$  exactly  $K + 1$  zeros. Therefore,  $g$  has more than  $K + 1$  poles, which concludes the proof of the lemma.  $\square$

Suppose  $\Delta$  is a hybridization function associated to a bath of finite dimension and which is solution to the IPT-DMFT equations. That is, there exist  $K \geq 1$ ,  $a_1, \dots, a_K > 0$  and  $\epsilon_1 < \dots < \epsilon_K$  such that

$$\Delta(z) = \sum_{k=1}^K \frac{a_k}{z - \varepsilon_k}.$$

Let  $\Sigma$  be the self-energy given by the IPT impurity solver, see Proposition 3.2.18. We have

$$\begin{aligned} \Sigma(z) &= U^2 \sum_{1 \leq k_1, k_2, k_3 \leq K'} \frac{a'_{k_1, k_2, k_3}}{z - \varepsilon'_{k_1} - \varepsilon'_{k_2} - \varepsilon'_{k_3}} \text{ and} \\ a'_{k_1, k_2, k_3} &= \left(1 + e^{-\beta(\varepsilon'_{k_1} + \varepsilon'_{k_2} + \varepsilon'_{k_3})}\right) \prod_{i=1}^3 \frac{1 - \Delta'(\varepsilon'_{k_i})}{1 + e^{-\beta\varepsilon'_{k_i}}} > 0, \end{aligned}$$

where  $\varepsilon'_1 < \dots < \varepsilon'_K$ , are the poles of the rational function  $(z - \Delta(z))^{-1}$ . The number of poles is exactly  $K + 1$  and the latter are real numbers, see the proof of Lemma 3.4.1, so that  $K' = K + 1$ . Since  $U > 0$  by

assumption,  $\Sigma$  has more than  $K + 1$  poles (we do not need a better estimation of the number of poles). So we can write

$$\Sigma(z) = U^2 \sum_{k=1}^{K''} \frac{a_k''}{z - \varepsilon_k''},$$

with  $K'' \geq K + 1$ ,  $a_k'' > 0$  and  $\varepsilon_1 < \dots < \varepsilon_{K''}$ . As  $\Delta$  is assumed to be a solution to the IPT-DMFT equations, it reads

$$\Delta(z) = W(z - H_\perp^0 - \Sigma(z))^{-1} W^\dagger.$$

Applying Lemma 3.4.1 to the matrix-valued rational function  $(z - H_\perp^0 - \Sigma(z))^{-1}$ , we know that this matrix-valued rational function has more than  $K'' + 1$  poles, hence more than  $K + 2$  poles. Now,  $W \neq 0$  since we have eliminated the limit cases described in Proposition 3.2.12, hence  $\Delta$  also has more than  $K + 2$  poles. As  $K$  is by definition the number of poles of  $\Delta$ , it is impossible and  $\Delta$  cannot be a solution to the IPT-DMFT equations.

### 3.4.4 Proof of Proposition 3.3.6 (Bath Update map)

Let  $\Sigma_p \in \mathfrak{S}_p$ , for  $1 \leq p \leq P$ , and let  $C_p \in \mathcal{S}_{2L_p}(\mathbb{C})$  and  $\mu_p \in \mathcal{M}(\mathbb{R}, \mathcal{S}_{2L_p}^+(\mathbb{C}))$  be such that for all  $z \in \mathbb{C}_+$ ,  $\Sigma_p(z) = C_p + \int_{\mathbb{R}} \frac{d\mu_p(\varepsilon)}{z - \varepsilon}$ . Since for all  $1 \leq p \leq P$ ,  $-\Sigma_p : \mathbb{C}_+ \rightarrow \mathbb{C}^{2L_p \times 2L_p}$  is a Pick matrix,

$$-\bigoplus_{q \neq p} \Sigma_q : \mathbb{C}_+ \rightarrow \mathbb{C}^{2(L-L_p) \times 2(L-L_p)}$$

is a Pick matrix. As  $H_p^0$  is Hermitian, we have for all  $z \in \mathbb{C}_+$ ,

$$\Im \left( z - H_p^0 - \bigoplus_{q \neq p} \Sigma_q(z) \right) = \Im(z) - \bigoplus_{q \neq p} \Im(\Sigma_q(z)) \geq \Im(z) > 0,$$

where  $M_1 \geq M_2$  means that  $M_1 - M_2$  is a positive semidefinite matrix. Moreover, if  $\Im(M) > 0$ , then  $M$  is invertible. Thus  $z - H_p^0 - \bigoplus_{q \neq j} \Sigma_q(z)$  is invertible and  $\Delta_p(z)$  is well defined. As  $\Im(M) > 0$  if and only if  $\Im(M^{-1}) < 0$ , and as the congruence preserves the sign of the imaginary part, we have  $\Im(\Delta_p(z)) \leq 0$  for all  $z \in \mathbb{C}_+$ , so that  $-\Delta_p$  is a Pick matrix. To show formula (3.49), we will make use of the results on Pick functions stated in Section 3.3.1. As  $\mu_q$ , the Nevanlinna-Riesz measure of  $\Sigma_q$ , is finite for  $1 \leq q \leq P$ , we have for  $x \in \mathbb{C}^{2L_q}$ , that the positive Borel measure  $\mu_q^x$  defined as the Nevanlinna-Riesz measure of the Pick function  $z \mapsto -\langle x, \Sigma_q(z)x \rangle$ , is also a finite positive measure. Then, for  $x \in \mathbb{C}^{2L_q}$  and  $y \geq 1$ ,

$$\left| \left\langle x, \int_{\mathbb{R}} \frac{d\mu_q(\varepsilon)}{iy - \varepsilon} x \right\rangle \right| = \left| \int_{\mathbb{R}} \frac{d\mu_q^x(\varepsilon)}{iy - \varepsilon} \right| \leq \int_{\mathbb{R}} \frac{d\mu_q^x(\varepsilon)}{|iy - \varepsilon|} \leq \int_{\mathbb{R}} d\mu_q^x < \infty.$$

This coarse upper bound is enough to ensure that

$$\begin{aligned} iy\Delta_p(iy) &= iyW_p \left( iy - H_p^0 - \bigoplus_{q \neq p} \Sigma_q(iy) \right)^{-1} W_p^\dagger \\ &= W_p \left( 1 - \frac{1}{iy} \left( H_p^0 + \bigoplus_{q \neq p} \left( C_q + \int_{\mathbb{R}} \frac{d\mu_q(\varepsilon)}{iy - \varepsilon} \right) \right) \right)^{-1} W_p^\dagger \\ &\xrightarrow[y \rightarrow +\infty]{} W_p W_p^\dagger. \end{aligned}$$

This gives the expansion  $\Delta_p(iy) = \frac{W_p W_p^\dagger}{iy} + o\left(\frac{1}{y}\right)$ , as  $y$  goes to  $+\infty$ . By Theorem 3.3.2, it follows that the Nevanlinna-Riesz measure of  $-\Delta_p$ , denoted by  $\nu_p$ , is finite, and its mass is precisely the quantity  $W_p^\dagger W_p$ . Thus the Nevanlinna-Riesz representation of  $-\Delta_p$  reads

$$-\Delta_p(z) = az + b - \int_{\mathbb{R}} \frac{d\nu_p(\varepsilon)}{z - \varepsilon},$$

for some  $a \in \mathcal{S}_{2L_p}^+(\mathbb{C})$  and  $b \in \mathcal{S}_{2L_p}(\mathbb{C})$ . Now, because of the aforementioned expansion, we must have  $a = b = 0$ , which concludes the proof.

### 3.4.5 Proof of Proposition 3.3.8 (IPT map)

Let  $\nu \in \mathcal{P}(\mathbb{R})$ , and define the associated hybridization function  $\Delta(z) = W_p^\dagger W_p \int_{\mathbb{R}} \frac{d\nu(\varepsilon)}{z-\varepsilon}$ . We first establish the following lemma, which we will use several times in our analysis.

**Lemma 3.4.2.** *Let  $c \in \mathbb{R}$ ,  $\mu_0 \in \mathcal{M}_+(\mathbb{R})$ . For  $z \in \mathbb{C}_+$ , we set*

$$f(z) = \int_{\mathbb{R}} \frac{d\mu_0(\varepsilon)}{z-\varepsilon} \quad \text{and} \quad g(z) = \frac{1}{z-c-f(z)}.$$

*Then  $-g$  is a Pick function and its Nevanlinna-Riesz representation reads  $g(z) = \int_{\mathbb{R}} \frac{d\mu(\varepsilon)}{z-\varepsilon}$  with  $\mu \in \mathcal{P}(\mathbb{R})$ . In particular,  $\mu$  has finite moments of order less than or equal to 2, given by*

$$m_0(\mu) = 1 \quad (\mu \text{ is a probability measure}), \quad m_1(\mu) = c \quad \text{and} \quad m_2(\mu) = \mu_0(\mathbb{R}) + c^2.$$

*Proof.* The result follows from the expansion of the function  $g(z)$  when  $z = iy$ ,  $y \rightarrow +\infty$  and Theorem 3.3.2. One has

$$g(iy) = \frac{1}{iy} \frac{1}{1 - \frac{c}{iy} - \frac{f(iy)}{iy}}.$$

Since  $f(iy) = \frac{\mu_0(\mathbb{R})}{iy} + o\left(\frac{1}{y}\right)$ , we have

$$\begin{aligned} g(iy) &= \frac{1}{iy} \frac{1}{1 - \frac{c}{iy} - \frac{\mu_0(\mathbb{R})}{(iy)^2} + o\left(\frac{1}{y^2}\right)} = \frac{1}{iy} \left(1 + \frac{c}{iy} + \frac{\mu_0(\mathbb{R}) + c^2}{(iy)^2} + o\left(\frac{1}{y^2}\right)\right) \\ &= \frac{1}{iy} + \frac{c}{(iy)^2} + \frac{\mu_0(\mathbb{R}) + c^2}{(iy)^3} + o\left(\frac{1}{y^3}\right). \end{aligned}$$

Using again Theorem 3.3.2, we obtain the desired result.  $\square$

We apply Lemma 3.4.2 with  $c = 0$  and  $f = \Delta$ . It follows that there exists  $\xi \in \mathcal{P}(\mathbb{R})$  satisfying (3.53).

Then, following equations (3.54)-(3.56), set  $\tilde{\xi}(d\varepsilon) = \frac{\xi(d\varepsilon)}{1 + e^{-\beta\varepsilon}}$ , and  $\tilde{\mu} = \tilde{\xi} * \tilde{\xi} * \tilde{\xi}$ . We must verify that, setting  $\mu(d\varepsilon) = (1 + e^{-\beta\varepsilon})\tilde{\mu}(d\varepsilon)$ ,  $\mu$  is indeed a positive finite measure, so that the self-energy  $\Sigma$  associated to the measure  $\mu$  belongs to  $\mathfrak{S}_p^{\text{IPT}}$ .

The multiplication by positive functions and the convolution preserves positivity, so  $\mu$  is a positive measure. Moreover, we have

$$\mu(\mathbb{R}) = \int_{\mathbb{R}^3} \frac{(1 + e^{-\beta(\varepsilon_1 + \varepsilon_2 + \varepsilon_3)}) d\xi(\varepsilon_1) d\xi(\varepsilon_2) d\xi(\varepsilon_3)}{(1 + e^{-\beta\varepsilon_1})(1 + e^{-\beta\varepsilon_2})(1 + e^{-\beta\varepsilon_3})} \leq \int_{\mathbb{R}^3} d\xi(\varepsilon_1) d\xi(\varepsilon_2) d\xi(\varepsilon_3) = 1. \quad (3.66)$$

Thus  $\mu$  is finite, and the map  $F^{\text{IPT}}$  is well defined. To prove that this map is actually continuous with respect to the weak topology of measures, we need to establish Lemma 3.4.3. This result states the continuity of the map  $\mathcal{M}_+(\mathbb{R}) \ni \mu_0 \mapsto \mu \in \mathcal{P}(\mathbb{R})$  defined in Lemma 3.4.2, which is central in the IPT-DMFT equations. Note that it holds

$$\forall z \in \mathbb{C}_+, \quad \int_{\mathbb{R}} \frac{d\mu(\varepsilon)}{z-\varepsilon} = \frac{1}{z-c-\int_{\mathbb{R}} \frac{d\mu_0(\varepsilon)}{z-\varepsilon}}. \quad (3.67)$$

**Lemma 3.4.3.** *The map  $\Phi : \mathcal{M}_+(\mathbb{R}) \ni \mu_0 \mapsto \mu \in \mathcal{P}(\mathbb{R})$  defined in Lemma 3.4.2 is weakly continuous. More precisely, the following stronger result holds true: if  $(\mu_0^n)_{n \in \mathbb{N}}$  converges weakly to  $\mu_0$  in  $\mathcal{M}_+(\mathbb{R})$ , then  $W_2(\Phi(\mu_0^n), \Phi(\mu)) \xrightarrow[n \rightarrow \infty]{} 0$ , where  $W_2$  is the Wasserstein distance of order 2.*

*Proof.* Let  $(\mu_0^n)_{n \in \mathbb{N}} \subset \mathcal{M}_+(\mathbb{R})$  converging weakly to  $\mu_0$  in  $\mathcal{M}_+(\mathbb{R})$ ,  $\mu^n := \Phi(\mu_0^n)$  and  $\mu := \Phi(\mu_0)$ . In view of Lemma 3.4.2,  $\mu^n$  has finite moments of orders 1 and 2, given by  $m_1(\mu^n) = c$  and  $m_2(\mu^n) = \mu_0^n(\mathbb{R}) + c^2$ .

As  $\mu_0^n$  converges weakly to  $\mu_0$ , we have  $\int_{\mathbb{R}} f d\mu_0^n \rightarrow \int_{\mathbb{R}} f d\mu_0$  for all  $f \in \mathcal{C}_b^0(\mathbb{R})$ . Taking  $f \equiv 1$ , we get  $\mu_0^n(\mathbb{R}) = \int_{\mathbb{R}} d\mu_0^n \xrightarrow[n \rightarrow \infty]{} \int_{\mathbb{R}} d\mu_0 = \mu_0(\mathbb{R})$ . Hence,  $m_2(\mu^n) = \mu_0^n(\mathbb{R}) + c^2 \xrightarrow[n \rightarrow \infty]{} \mu_0(\mathbb{R}) + c^2 = m_2(\mu)$ .

Now, for all  $z \in \mathbb{C}_+$ , the function  $\mathbb{R} \ni \varepsilon \mapsto \frac{1}{z-\varepsilon} \in \mathbb{C}$  is also bounded and continuous. Thus, we can pass to the limit in formula (3.67):

$$\int_{\mathbb{R}} \frac{d\mu^n(\varepsilon)}{z-\varepsilon} = \frac{1}{z-c-\int_{\mathbb{R}} \frac{d\mu_0^n(\varepsilon)}{z-\varepsilon}} \xrightarrow{n \rightarrow \infty} \frac{1}{z-c-\int_{\mathbb{R}} \frac{d\mu_0(\varepsilon)}{z-\varepsilon}} = \int_{\mathbb{R}} \frac{d\mu(\varepsilon)}{z-\varepsilon}. \quad (3.68)$$

This can be extended to complex numbers  $z \in \mathbb{C} \setminus \mathbb{R}$  by taking the complex conjugate of the limit (3.68). Let  $\mathcal{A}$  be the algebra generated by the functions  $\mathbb{R} \ni \varepsilon \mapsto \frac{1}{z - \varepsilon} \in \mathbb{C}$  for  $z \in \mathbb{C} \setminus \mathbb{R}$ . It is known that  $\mathcal{A}$  is dense in  $\mathcal{C}_0^0(\mathbb{R})$  (this can be shown using Helffer-Sjöstrand formula [28]). Together with (3.68), this implies that for all  $f \in \mathcal{C}_0^0(\mathbb{R})$ ,  $\int_{\mathbb{R}} f d\mu^n \xrightarrow{n \rightarrow \infty} \int_{\mathbb{R}} f d\mu$ , i.e. that  $(\mu^n)_{n \in \mathbb{N}}$  vaguely converges to  $\mu$ . Since  $\mathbb{R}$  is locally compact and the  $\mu^n$ 's are probability measures, the vague convergence is equivalent in this case to the weak convergence. The map  $\Phi$  is therefore weakly continuous. Since on the space of Borel probability measures on  $\mathbb{R}$ ,  $W_2$ -convergence is equivalent to weak convergence and the convergence of the second moment [3, Section 7.1], the proof is complete.  $\square$

Let us now prove that the impurity solver  $F^{\text{IPT}} : \mathcal{P}(\mathbb{R}) \rightarrow \mathcal{M}_+(\mathbb{R})$  is weakly continuous. Let  $(\nu^n)_{n \in \mathbb{N}} \subset \mathcal{P}(\mathbb{R})$  converging weakly to  $\nu \in \mathcal{P}(\mathbb{R})$ . Define  $\xi^n \in \mathcal{P}(\mathbb{R})$  and  $\mu^n := F^{\text{IPT}}(\nu^n)$  as in Proposition 3.3.8, see equation (3.53), as well as  $\xi \in \mathcal{P}(\mathbb{R})$  and  $\mu := F^{\text{IPT}}(\nu)$ . We want to show that  $\mu^n$  converges weakly to  $\mu$ . First, because of the definition of  $\xi$  through equation (3.53), and thanks to Lemma 3.4.3, we know that  $W_2(\xi^n, \xi) \xrightarrow{n \rightarrow \infty} 0$ . Moreover, using the same density argument as in the proof of Lemma 3.4.3, it is sufficient to show that for all  $z \in \mathbb{C}_+$ , the following convergence holds:

$$\int_{\mathbb{R}} \frac{d\mu^n(\varepsilon)}{z - \varepsilon} \xrightarrow{n \rightarrow \infty} \int_{\mathbb{R}} \frac{d\mu(\varepsilon)}{z - \varepsilon}.$$

We have for  $z \in \mathbb{C}_+$ ,

$$\int_{\mathbb{R}} \frac{d\mu^n(\varepsilon)}{z - \varepsilon} = \int_{\mathbb{R}^3} \frac{1}{z - (\varepsilon_1 + \varepsilon_2 + \varepsilon_3)} \frac{1 + e^{-\beta(\varepsilon_1 + \varepsilon_2 + \varepsilon_3)}}{(1 + e^{-\beta\varepsilon_1})(1 + e^{-\beta\varepsilon_2})(1 + e^{-\beta\varepsilon_3})} d\xi^n(\varepsilon_1) d\xi^n(\varepsilon_2) d\xi^n(\varepsilon_3).$$

Let  $\psi(\varepsilon_1, \varepsilon_2, \varepsilon_3) = \frac{1}{z - (\varepsilon_1 + \varepsilon_2 + \varepsilon_3)} \frac{1 + e^{-\beta(\varepsilon_1 + \varepsilon_2 + \varepsilon_3)}}{(1 + e^{-\beta\varepsilon_1})(1 + e^{-\beta\varepsilon_2})(1 + e^{-\beta\varepsilon_3})}$ , for  $(\varepsilon_1, \varepsilon_2, \varepsilon_3) \in \mathbb{R}^3$ . Then,

$$\begin{aligned} \left| \int_{\mathbb{R}} \frac{d\mu^n(\varepsilon)}{z - \varepsilon} - \int_{\mathbb{R}} \frac{d\mu(\varepsilon)}{z - \varepsilon} \right| &= \left| \int_{\mathbb{R}^3} \psi d\xi^n d\xi^n d\xi^n - \int_{\mathbb{R}^3} \psi d\xi d\xi d\xi \right| \\ &\leq \left| \int_{\mathbb{R}^3} \psi d\xi^n d\xi^n d\xi^n - \int_{\mathbb{R}^3} \psi d\xi^n d\xi^n d\xi \right| \end{aligned} \quad (3.69)$$

$$+ \left| \int_{\mathbb{R}^3} \psi d\xi^n d\xi^n d\xi - \int_{\mathbb{R}^3} \psi d\xi^n d\xi d\xi \right| \quad (3.70)$$

$$+ \left| \int_{\mathbb{R}^3} \psi d\xi^n d\xi d\xi - \int_{\mathbb{R}^3} \psi d\xi d\xi d\xi \right|. \quad (3.71)$$

We now prove that the last term (3.71) goes to zero when  $n$  goes to  $\infty$ . The same arguments apply to the other two terms, (3.69) and (3.70). The function  $\psi$  is smooth and a simple calculation shows that its partial derivative with respect to  $\varepsilon_1$  is bounded by

$$|\partial_1 \psi(\varepsilon_1, \varepsilon_2, \varepsilon_3)| \leq \frac{1}{|\Im(z)|^2} + \frac{2\beta}{|\Im(z)|} =: \kappa_{z, \beta}. \quad (3.72)$$

Let  $\varepsilon_2, \varepsilon_3 \in \mathbb{R}$ . Using the  $W_2$  convergence of  $\xi^n$  towards  $\xi$ , set  $\pi_n$  the optimal coupling between these two measures [53]. We have that

$$\int_{\mathbb{R}} \psi(\varepsilon_1, \varepsilon_2, \varepsilon_3) d\xi^n(\varepsilon_1) = \int_{\mathbb{R}^2} \psi(\varepsilon_1, \varepsilon_2, \varepsilon_3) d\pi_n(\varepsilon_1, \varepsilon'_1).$$

By Taylor's Theorem and since  $\psi$  is continuously derivable, we have

$$\int_{\mathbb{R}} \psi(\varepsilon_1, \varepsilon_2, \varepsilon_3) d\xi^n(\varepsilon_1) = \int_{\mathbb{R}^2} \psi(\varepsilon'_1, \varepsilon_2, \varepsilon_3) d\pi_n(\varepsilon_1, \varepsilon'_1) + \int_{\mathbb{R}^2} \int_{\varepsilon'_1}^{\varepsilon_1} (\varepsilon_1 - t) \partial_1 \psi(t, \varepsilon_2, \varepsilon_3) dt d\pi_n(\varepsilon_1, \varepsilon'_1).$$

On the one hand, the first term is exactly  $\int_{\mathbb{R}} \psi(\varepsilon_1, \varepsilon_2, \varepsilon_3) d\xi(\varepsilon_1)$  by definition of  $\pi_n$ , and on the other hand, using (3.72), we can bound the second term by

$$\begin{aligned} \left| \int_{\mathbb{R}^2} \int_{\varepsilon'_1}^{\varepsilon_1} (\varepsilon_1 - t) \partial_1 \psi(t, \varepsilon_2, \varepsilon_3) dt d\pi_n(\varepsilon_1, \varepsilon'_1) \right| &\leq \frac{1}{2} \int_{\mathbb{R}^2} |\varepsilon_1 - \varepsilon'_1|^2 \|\partial_1 \psi\|_{\infty} d\pi_n(\varepsilon_1, \varepsilon'_1) \\ &\leq \frac{\kappa_{z, \beta}}{2} \int_{\mathbb{R}^2} |\varepsilon_1 - \varepsilon'_1|^2 d\pi_n(\varepsilon_1, \varepsilon'_1) \\ &= \frac{\kappa_{z, \beta}}{2} W_2(\xi^n, \xi)^2. \end{aligned}$$

Finally, the term (3.71) can be bounded by

$$\begin{aligned} \left| \int_{\mathbb{R}^3} \psi d\xi^n d\xi d\xi - \int_{\mathbb{R}^3} \psi d\xi d\xi d\xi \right| &\leq \int_{\mathbb{R}^2} \left| \int_{\mathbb{R}} \psi(\varepsilon_1, \cdot, \cdot) d\xi^n(\varepsilon_1) - \int_{\mathbb{R}} \psi(\varepsilon_1, \cdot, \cdot) d\xi(\varepsilon_1) \right| d\xi d\xi \\ &= \int_{\mathbb{R}^2} \left| \int_{\mathbb{R}^2} \int_{\varepsilon'_1}^{\varepsilon_1} (\varepsilon_1 - t) \partial_1 \psi(t, \varepsilon_2, \varepsilon_3) dt d\pi_n(\varepsilon_1, \varepsilon'_1) \right| d\xi(\varepsilon_2) d\xi(\varepsilon_3) \\ &\leq \int_{\mathbb{R}^2} \frac{\kappa_{z,\beta}}{2} W_2(\xi^n, \xi)^2 d\xi(\varepsilon_2) d\xi(\varepsilon_3) = \frac{\kappa_{z,\beta}}{2} W_2(\xi^n, \xi)^2 \xrightarrow{n \rightarrow \infty} 0. \end{aligned}$$

This shows that the map  $F^{\text{IPT}}$  is weakly continuous. It remains to prove that the map  $\mathfrak{D}_p^{\text{IPT}} \ni \Delta \mapsto \Sigma \in \mathfrak{S}_p^{\text{IPT}}$  defined by (3.53)-(3.57) coincides on the set of discrete probability measures with finite support with the map defined in Proposition 3.2.18.

Let  $\Delta \in \mathfrak{D}_p^{\text{IPT}}$  with a Nevanlinna-Riesz measure of the form  $\nu = \sum_{k=1}^K a_k \delta_{\varepsilon_k}$ , where  $a_k > 0$ ,  $\sum a_k = W_p^\dagger W_p$  and  $\varepsilon_1 < \dots < \varepsilon_K$ . It follows that the rational function  $(z - \Delta(z))^{-1}$  is of the form  $\sum_{k=1}^{K+1} \frac{a'_k}{z - \varepsilon'_k}$  (see the proof of Lemma 3.4.1). This means by (3.53) that  $\xi = \sum_{k=1}^{K+1} a'_k \delta_{\varepsilon'_k}$ , and the  $\varepsilon'_k$ 's are the zeros of the rational function  $z - \Delta(z)$ , so that the residues are given by  $a'_k = (1 - \Delta'(\varepsilon'_k))^{-1}$ . The self-energy  $\Sigma$  given by (3.57) then reads for all  $z \in \mathbb{C}_+$ ,

$$\begin{aligned} \Sigma(z) &= U^2 \int_{\mathbb{R}^3} \frac{1 + e^{-\beta(\varepsilon_1 + \varepsilon_2 + \varepsilon_3)}}{(1 + e^{-\beta\varepsilon_1})(1 + e^{-\beta\varepsilon_2})(1 + e^{-\beta\varepsilon_3})} \frac{d\xi(\varepsilon_1) d\xi(\varepsilon_2) d\xi(\varepsilon_3)}{z - (\varepsilon_1 + \varepsilon_2 + \varepsilon_3)} \\ &= U^2 \sum_{k_1, k_2, k_3=1}^{K+1} \frac{1 + e^{-\beta(\varepsilon'_{k_1} + \varepsilon'_{k_2} + \varepsilon'_{k_3})}}{(1 + e^{-\beta\varepsilon'_{k_1}})(1 + e^{-\beta\varepsilon'_{k_2}})(1 + e^{-\beta\varepsilon'_{k_3}})} \frac{a'_{k_1} a'_{k_2} a'_{k_3}}{z - (\varepsilon'_{k_1} + \varepsilon'_{k_2} + \varepsilon'_{k_3})} \\ &= U^2 \sum_{k_1, k_2, k_3=1}^{K+1} \frac{a'_{k_1, k_2, k_3}}{z - (\varepsilon'_{k_1} + \varepsilon'_{k_2} + \varepsilon'_{k_3})}, \end{aligned}$$

where  $a'_{k_1, k_2, k_3}$  is given by (3.42). This complies with the result stated in Proposition 3.2.18.

Finally, since the set of discrete probability measures with finite support is dense in the set of probability measures  $\mathcal{P}(\mathbb{R})$  for the weak topology and since  $F^{\text{IPT}}$  is weakly continuous,  $F^{\text{IPT}}$  is the only continuous extension of the IPT map defined in Proposition 3.2.18 for a finite-dimensional bath.

### 3.4.6 Continuity of the IPT-DMFT map

The following result is central to prove the existence of a fixed point to the DMFT equations.

**Theorem 3.4.4** (Continuity of the IPT-DMFT map). *The IPT-DMFT map  $F^{\text{DMFT}}$  is weakly continuous on  $\mathcal{P}(\mathbb{R})$ . More precisely, the following stronger results holds true: if  $(\nu^n)_{n \in \mathbb{N}}$  converges weakly to  $\nu$ , then*

$$W_2(F^{\text{DMFT}}(\nu^n), F^{\text{DMFT}}(\nu)) \xrightarrow{n \rightarrow \infty} 0,$$

where  $W_2$  is the Wasserstein 2-distance.

We have proven in the previous section the continuity of the map  $F^{\text{IPT}}$ . In order to prove the continuity of  $F^{\text{SC}}$ , we need to adapt Lemma 3.4.3 to equation (3.52). Let  $\mu \in \mathcal{M}_+(\mathbb{R})$ . Applying Theorem 3.3.2 to the measure  $\mu$ , and using the definition (3.52) of the hybridization function  $\Delta$  associated to  $F^{\text{SC}}(\mu)$ , we obtain

$$\begin{aligned} \Delta(iy) &= \frac{1}{iy} W \left( \mathbf{1} - \frac{H_\perp^0}{iy} - \frac{1}{iy} U^2 \int_{\mathbb{R}} \frac{d\mu(\varepsilon)}{iy - \varepsilon} \right)^{-1} W^\dagger \\ &= \frac{1}{iy} W \left( \mathbf{1} - \frac{H_\perp^0}{iy} - \frac{1}{iy} \left( \frac{U^2 \mu(\mathbb{R})}{iy} + o\left(\frac{1}{y}\right) \right) \right)^{-1} W^\dagger \\ &= W \left[ \frac{1}{iy} + \frac{H_\perp^0}{(iy)^2} + \frac{(H_\perp^0)^2 + U^2 \mu(\mathbb{R})}{(iy)^3} \right] W^\dagger + o\left(\frac{1}{y^3}\right). \end{aligned}$$

It follows that, when  $y \rightarrow +\infty$ , we have the expansion

$$\int_{\mathbb{R}} \frac{dF^{\text{SC}}(\mu)(\varepsilon)}{iy - \varepsilon} = \frac{1}{W_p^\dagger W_p} \Delta(iy) = \frac{1}{iy} + \frac{s^1}{(iy)^2} + \frac{s^2(\mu)}{(iy)^3} + o\left(\frac{1}{y^3}\right), \quad (3.73)$$

with  $s_p^1$  and  $s_p^2(\mu)$  given by

$$s^1 = \frac{WH_{\perp}^0 W^\dagger}{W_p^\dagger W_p}, \quad (3.74)$$

$$s^2(\mu) = \frac{W((H_{\perp}^0)^2 + U^2\mu(\mathbb{R}))W^\dagger}{W_p^\dagger W_p}. \quad (3.75)$$

In view of Theorem 3.3.2, this implies that  $\nu := F^{\text{SC}}(\mu)$  has finite moments of orders 1 and 2, respectively given by  $m_1(\nu) = s^1$  and  $m_2(\nu) = s^2(\mu)$ . The arguments in the proof of Lemma 3.4.3 can then be used to show that the following result holds true.

**Proposition 3.4.5.**  $F^{\text{SC}} : \mathcal{M}_+(\mathbb{R}) \rightarrow \mathcal{P}(\mathbb{R})$  is weakly continuous. More precisely, if  $(\mu^n)_{n \in \mathbb{N}}$  converges weakly to  $\mu$  in  $\mathcal{M}_+(\mathbb{R})$ , then  $W_2(F^{\text{SC}}(\mu^n), F^{\text{SC}}(\mu)) \xrightarrow{n \rightarrow \infty} 0$ .

We are now in position to complete the proof of Theorem 3.4.4. Let  $(\nu^n)_n \subset \mathcal{P}(\mathbb{R})$  converging weakly to  $\nu$  in  $\mathcal{P}(\mathbb{R})$ . Denoting by  $\mu^n := F^{\text{IPT}}(\nu^n)$  and  $\mu := F^{\text{IPT}}(\nu)$ , we have shown in the proof of Proposition 3.3.8 that  $\mu^n$  converges weakly to  $\mu$  in  $\mathcal{M}_+(\mathbb{R})$ , see Section 3.4.5. Proposition 3.4.5 then shows that  $W_2(F^{\text{DMFT}}(\nu^n), F^{\text{DMFT}}(\nu)) = W_2(F^{\text{SC}}(\mu^n), F^{\text{SC}}(\mu)) \xrightarrow{n \rightarrow \infty} 0$ . In particular,  $F^{\text{DMFT}}(\nu^n)$  converges weakly to  $F^{\text{DMFT}}(\nu)$ .

### 3.4.7 Proof of Theorem 3.3.9: existence of a fixed point

The existence of a fixed point to the IPT-DMFT map, that is a solution to the IPT-DMFT equations, is a consequence of the following fixed point theorem [57].

**Theorem 3.4.6** (Schauder-Singbal). *Let  $E$  be a locally convex Hausdorff linear topological space,  $C$  a nonempty closed convex subset of  $E$ , and  $F$  a continuous map from  $C$  into itself, such that  $F(C)$  is contained in a compact subset of  $C$ . Then  $F$  has a fixed point.*

Let us consider the vector space  $E = \mathcal{M}(\mathbb{R})$  endowed with the Kantorovitch-Rubinstein norm  $\|\cdot\|_0$ . Recall that the latter is defined as

$$\|\mu\|_0 := \sup \left\{ \int_{\mathbb{R}} f d\mu ; f \in \text{Lip}_1, \|f\|_{\infty} \leq 1 \right\},$$

where  $\text{Lip}_1$  is the set of continuous functions on  $\mathbb{R}$  with Lipschitz constant less than or equal to 1.

Let us then set  $C := \mathcal{P}(\mathbb{R}) = \{\mu \in E \mid \mu \geq 0, \int_{\mathbb{R}} d\mu = 1\}$ . Since  $E$  is a normed vector space on  $\mathbb{R}$ , it is a locally convex Hausdorff linear topological space, and  $C$  is obviously a non-empty convex subset of  $E$ .

Besides, on the set of finite positive measures, weak convergence is equivalent to convergence for the Kantorovitch-Rubinstein norm [9, Chapter 8.3]. We can thus work with the weak topology on  $C$ .

The fact that  $C$  is weakly closed means that  $\mathcal{P}(\mathbb{R})$  is a weakly closed subset of  $\mathcal{M}(\mathbb{R})$ . This result can be found in [10, Section 3.2]. Moreover, we already proved in Theorem 3.4.4 that  $F^{\text{DMFT}} : C \rightarrow C$  was weakly continuous.

To apply Schauder-Singbal's theorem to our setting, it thus remains to show that  $F^{\text{DMFT}}(C)$  is relatively compact for the weak topology. This is in fact a consequence of Prokhorov's Theorem [10, Theorem 2.3.4].

Indeed, let  $\nu \in F^{\text{DMFT}}(C)$  and  $\nu_0 \in \mathcal{P}(\mathbb{R})$ ,  $\mu = F^{\text{IPT}}(\nu_0) \in \mathcal{M}_+(\mathbb{R})$  such that  $\nu = F^{\text{DMFT}}(\nu_0) = F^{\text{SC}}(\mu)$ . As we have seen in the proof of Proposition 3.4.5,  $\nu$  has finite moments of order 1 and 2, given respectively by  $m_1(\nu) = s^1$  and  $m_2(\nu) = s^2(\mu)$ , where  $s^1$  is defined by (3.74) and  $s^2(\mu)$  by (3.75). The inequality (3.66) states that the mass of the measure  $\mu$  is bounded by 1. Hence,  $m_2(\nu) = s^2(\mu)$  is bounded independently on  $\nu$ :

$$m_2(\nu) = s^2(\mu) \leq c := \frac{W((H_{\perp}^0)^2 + U^2)W^\dagger}{W_p^\dagger W_p}. \quad (3.76)$$

This allows us to show that  $F^{\text{DMFT}}(C)$  is tight. For  $\eta > 0$ , take  $K = [-a, a]$ , with  $a \geq 1$  large enough so that  $c/a^2 \leq \eta$ . Then for  $\nu \in F^{\text{DMFT}}(C)$ , (3.76) holds and

$$\nu(\mathbb{R} \setminus K) = \int_{\mathbb{R} \setminus K} \frac{\varepsilon^2}{\varepsilon^2} d\nu(\varepsilon) \leq \frac{1}{a^2} \int_{\mathbb{R} \setminus K} \varepsilon^2 d\nu(\varepsilon) \leq \frac{1}{a^2} \int_{\mathbb{R}} \varepsilon^2 d\nu(\varepsilon) = \frac{m_2(\nu)}{a^2} \leq \frac{c}{a^2} \leq \eta.$$

Hence  $F^{\text{DMFT}}(C)$  is tight. By Prokhorov's Theorem, it is thus weakly relatively compact.

This concludes the proof of our main result.

### 3.4.8 Proof of Proposition 3.3.10

Let  $\nu^0 \in \mathcal{P}(\mathbb{R})$  and  $k \in 2\mathbb{N}$ , and assume that  $\nu^0$  has finite  $k$ -th moment, i.e.  $\int_{\mathbb{R}} |\varepsilon|^k d\nu^0(\varepsilon) < \infty$ . By Theorem 3.3.2, the following expansion holds, with  $m_k(\nu^0) \geq 0$ :

$$\int_{\mathbb{R}} \frac{d\nu^0(\varepsilon)}{iy - \varepsilon} = \frac{1}{iy} + \cdots + \frac{m_k(\nu^0)}{(iy)^{k+1}} + o\left(\frac{1}{y^{k+1}}\right). \quad (3.77)$$

Then define  $\Delta^0(z) = W_p^\dagger W_p \int_{\mathbb{R}} \frac{d\nu^0(\varepsilon)}{z - \varepsilon}$  and  $\xi$  by (3.53):

$$\int_{\mathbb{R}} \frac{d\xi(\varepsilon)}{z - \varepsilon} = \frac{1}{z - \Delta^0(z)}.$$

This function can be asymptotically expanded to order  $k+3$  using (3.77).

$$\begin{aligned} \int_{\mathbb{R}} \frac{d\xi(\varepsilon)}{iy - \varepsilon} &= \frac{1}{iy - W_p^\dagger W_p \left( \frac{1}{iy} + \cdots + \frac{m_k(\nu^0)}{(iy)^{k+1}} + o\left(\frac{1}{y^{k+1}}\right) \right)} \\ &= \frac{1}{iy} \left( 1 - \frac{W_p^\dagger W_p}{iy} \left( \frac{1}{iy} + \cdots + \frac{m_k(\nu^0)}{(iy)^{k+1}} + o\left(\frac{1}{(iy)^{k+1}}\right) \right) \right)^{-1} \\ &= \frac{1}{iy} + \cdots + \frac{m_{k+2}(\xi)}{(iy)^{k+3}} + o\left(\frac{1}{y^{k+3}}\right). \end{aligned}$$

By Theorem 3.3.2,  $\xi$  has finite moments up to order  $k+2$ , which is even, denoted by  $m_0(\xi) = 1, \dots, m_{k+2}(\xi)$ . Now let  $\mu := F^{\text{IPT}}(\nu^0)$ , so that  $\mu \in \mathcal{M}_+(\mathbb{R})$  is given by (3.56) in the statement of Proposition 3.3.8. In particular, there exists  $C_k \in \mathbb{R}_+$  such that

$$\begin{aligned} \int_{\mathbb{R}} |\varepsilon|^{k+2} d\mu(\varepsilon) &= \int_{\mathbb{R}^3} |\varepsilon_1 + \varepsilon_2 + \varepsilon_3|^{k+2} \frac{1 + e^{-\beta(\varepsilon_1 + \varepsilon_2 + \varepsilon_3)}}{(1 + e^{-\beta\varepsilon_1})(1 + e^{-\beta\varepsilon_2})(1 + e^{-\beta\varepsilon_3})} d\xi(\varepsilon_1) d\xi(\varepsilon_2) d\xi(\varepsilon_3) \\ &\leq \int_{\mathbb{R}^3} |\varepsilon_1 + \varepsilon_2 + \varepsilon_3|^{k+2} d\xi(\varepsilon_1) d\xi(\varepsilon_2) d\xi(\varepsilon_3) \\ &\leq \int_{\mathbb{R}^3} C_k \sum_{\substack{1 \leq i_1, i_2, i_3 \leq k+2 \\ i_1 + i_2 + i_3 = k+2}} |\varepsilon_1|^{i_1} |\varepsilon_2|^{i_2} |\varepsilon_3|^{i_3} d\xi(\varepsilon_1) d\xi(\varepsilon_2) d\xi(\varepsilon_3) \\ &= C_k \sum_{\substack{1 \leq i_1, i_2, i_3 \leq k+2 \\ i_1 + i_2 + i_3 = k+2}} \int_{\mathbb{R}} |\varepsilon_1|^{i_1} d\xi(\varepsilon_1) \int_{\mathbb{R}} |\varepsilon_2|^{i_2} d\xi(\varepsilon_2) \int_{\mathbb{R}} |\varepsilon_3|^{i_3} d\xi(\varepsilon_3) < \infty, \end{aligned}$$

since for  $l \leq k+2$ ,  $\int_{\mathbb{R}} |\varepsilon|^l d\xi(\varepsilon) < \infty$ . Thus  $\mu$  has finite moments of order less than or equal to  $k+2$ . Finally, let  $\nu := F^{\text{SC}}(\mu) = F^{\text{DMFT}}(\nu^0)$ . Equations (3.48) and (3.49) read

$$\Delta(z) = W_p^\dagger W_p \int_{\mathbb{R}} \frac{d\nu(\varepsilon)}{z - \varepsilon} = W \left( z - H_{\perp}^0 - \Sigma(z) \right)^{-1} W^\dagger,$$

with  $\Sigma(z) = U^2 \int_{\mathbb{R}} \frac{d\mu(\varepsilon)}{z - \varepsilon}$ . By Theorem 3.3.2, we can expand  $\int_{\mathbb{R}} \frac{d\mu(\varepsilon)}{iy - \varepsilon}$  as  $y$  goes to  $+\infty$  and get

$$\begin{aligned} \Delta(iy) &= W \left( iy - H_{\perp}^0 - U^2 \left( \frac{m_0(\mu)}{iy} + \cdots + \frac{m_{k+2}(\mu)}{(iy)^{k+3}} + o\left(\frac{1}{y^{k+3}}\right) \right) \right)^{-1} W^\dagger \\ &= W_p^\dagger W_p \left( \frac{1}{iy} + \cdots + \frac{m_{k+4}(\nu)}{(iy)^{k+5}} \right) + o\left(\frac{1}{y^{k+5}}\right). \end{aligned}$$

This means that

$$\int_{\mathbb{R}} \frac{d\nu(\varepsilon)}{iy - \varepsilon} = \frac{1}{iy} + \cdots + \frac{m_{k+4}(\nu)}{(iy)^{k+5}} + o\left(\frac{1}{y^{k+5}}\right),$$

which proves, by Theorem 3.3.2, that  $\nu$  has finite moments up to order  $k+4$ .

## Acknowledgements

This project has received funding from the Simons Targeted Grant Award No. 896630 and from the European Research Council (ERC) under the European Union's Horizon 2020 research and innovation programme (grant agreement EMC2 No 810367). The authors thank Michel Ferrero, David Gontier and Mathias Dus for useful discussions. Part of this work was done during the IPAM program *Advancing quantum mechanics with mathematics and statistics*.

# Appendices

## 3.A Uniqueness theorem for an interpolation problem

The Nevanlinna-Pick Analytical Continuation Problem (ACP), which we will also call *interpolation problem*, has been studied in the beginning of the 20th century independently by Nevanlinna ([45], 1919) and Pick ([49], 1915). The results presented in Section 3.A.1 are gathered in the book [63]. Many other references address this problem, such as [20], [1], [55]. In Section 3.A.1, we set up the problem and then give some results that are important to our analysis. Other important results on the ACP and characterizations of the solutions are detailed in the references. For example, we will not discuss the question of extremal solutions ([47], [58]), nor the use of Blaschke products ([63], [20], [46]). The approaches of Nevanlinna and Pick are different, we chose here to focus on Nevanlinna's approach.

### 3.A.1 Introduction and some general properties

The Nevanlinna-Pick Analytical Continuation Problem (ACP) can be stated as follows. Let  $(z_n)_{n \in I}$  be a sequence of distinct points in the Poincaré upper-half-plane  $\mathbb{C}_+$  and let  $(w_n)_{n \in I}$  be a sequence in  $\overline{\mathbb{C}_+}$ . We want to answer the following question.

**Question 3.A.1.** *Is there an analytic function  $f : \mathbb{C}_+ \rightarrow \overline{\mathbb{C}_+}$  interpolating the given values at the prescribed points? In other words, we look for a Pick function  $f$  such that*

$$\forall n \in I, \quad f(z_n) = w_n, \tag{3.78}$$

where  $I$  is a (at most) countable set.

Without loss of generality, we can assume that  $I = \{1, 2, \dots\}$ . We denote by  $AC_{\mathbb{C}_+}(z_n, w_n)_I$  the set of solutions to this problem (we will omit the dependence on  $I$  unless when needed). Both sets  $\mathbb{C}_+$  and  $\overline{\mathbb{C}_+}$  are invariant under the action of the subset  $\mathcal{T}$  of affine transformations of  $\overline{\mathbb{C}_+}$  given by  $\mathcal{T} = \{\tau : \overline{\mathbb{C}_+} \rightarrow \overline{\mathbb{C}_+}, z \mapsto az + b, b \in \mathbb{R}, a > 0\}$ , and we have

$$\forall \tau_1, \tau_2 \in \mathcal{T}, \quad AC_{\mathbb{C}_+}(\tau_1(z_n), \tau_2(w_n)) = \tau_2 \circ AC_{\mathbb{C}_+}(z_n, w_n) \circ \tau_1^{-1}. \tag{3.79}$$

Moreover, question 3.A.1 can equivalently be stated in the unit disc instead of the upper-half-plane:

**Question 3.A.2.** *Let  $(z_n)$  and  $(w_n)$  be sequences in the unit disc  $\mathbb{D} = \{z \in \mathbb{C}, |z| < 1\}$  and the closed disc  $\overline{\mathbb{D}}$  respectively. Is there an analytic function  $f : \mathbb{D} \rightarrow \overline{\mathbb{D}}$  such that  $\forall n \in I, \quad f(z_n) = w_n$ ?*

The reason for the equivalence between both formulations is simply the upper-half-plane can be mapped to the unit disc through the Cayley transform, which is biholomorphic between these sets. The Cayley transform  $\mathcal{W}$  and its reciprocal  $\mathcal{W}^{-1}$  are given by:

$$\begin{array}{rcl} \mathcal{W} : \mathbb{C} \setminus \{-i\} & \longrightarrow & \mathbb{C} \setminus \{1\} \\ z & \mapsto & \frac{z-i}{z+i} \end{array} \quad \begin{array}{rcl} \mathcal{W}^{-1} : \mathbb{C} \setminus \{1\} & \longrightarrow & \mathbb{C} \setminus \{-i\} \\ z & \mapsto & i \frac{1+z}{1-z}. \end{array}$$

As the Cayley transform  $\mathcal{W}$  is biholomorphic from  $\mathbb{C}_+$  to  $\mathbb{D}$  and maps the real line  $\mathbb{R}$  to the unit circle deprived of the point 1, we have the equivalence of the following statements, with  $F : \mathbb{C}_+ \rightarrow \overline{\mathbb{C}_+}$ ,  $(z_n) \subset \mathbb{C}_+$ ,  $(w_n) \subset \overline{\mathbb{C}_+}$ ,  $f = \mathcal{W} \circ F \circ \mathcal{W}^{-1} : \mathbb{D} \rightarrow \overline{\mathbb{D}}$ ,  $\tilde{z}_n = \mathcal{W}(z_n) \in \mathbb{D}$  and  $\tilde{w}_n = \mathcal{W}(w_n) \in \overline{\mathbb{D}}$ .

$$\forall n \geq 1, \quad F(z_n) = w_n \iff \forall n \geq 1, \quad f(\tilde{z}_n) = \tilde{w}_n.$$

In other words, denoting by  $AC_{\mathbb{D}}(z_n, w_n)$  the set of solutions to Question 3.A.2, we have

$$AC_{\mathbb{D}}(\mathcal{W}(z_n), \mathcal{W}(w_n)) = \mathcal{W} \circ AC_{\mathbb{C}_+}(z_n, w_n) \circ \mathcal{W}^{-1}. \tag{3.80}$$

As a matter of fact, we can answer Question 3.A.2 when the sequence  $(w_n)$  is constant and of modulus 1, as a direct consequence of the maximum modulus principle.

**Lemma 3.A.3.** *Given  $C \in \overline{\mathbb{D}} \setminus \mathbb{D}$ ,  $AC_{\mathbb{D}}(z_n, C) = \{C\}$ .*

Combined with equation (3.80), we have a first statement about the set of solutions  $AC_{\mathbb{C}_+}$  to the interpolation problem (3.78).

**Corollary 3.A.4.** *Given  $C \in \mathbb{R}$ ,  $AC_{\mathbb{C}_+}(z_n, C) = \{C\}$ .*

The next definition introduces the functions  $b_a$  (the notation suggests Blaschke products, see [47] and [20]), which will be useful for our analysis of  $AC_{\mathbb{D}}(z_n, w_n)$ .

**Definition 3.A.5.** *Let  $a \in \mathbb{D}$ . Define for  $z \in \mathbb{D}$ ,  $b_a(z) = \frac{z-a}{1-\bar{a}z} \in \mathbb{D}$ .*

These functions are in fact biholomorphic from  $\mathbb{D}$  to itself and  $b_a$  only vanishes in  $a \in \mathbb{D}$ . This zero is of order 1. The function  $b_a$  can actually be extended to the closed disc  $\overline{\mathbb{D}}$ , and we will also denote this extension  $b_a$ . Considering our interpolation problem, we notice the following. If  $f$  is a solution to the interpolation problem stated in question 3.A.2, we have  $f(z_1) = w_1$ , with  $|w_1| \leq 1$ . If the modulus of  $w_1$  is 1, then  $f$  is constant because of the maximum modulus principle. Suppose this is not the case and define the function  $f^{(1)}$  by

$$f^{(1)}(z) = \frac{b_{w_1}(f(z))}{b_{z_1}(z)}. \quad (3.81)$$

$f^{(1)}$  is then well-defined on  $\mathbb{D}$ , because the only zero of  $b_{z_1}$  is  $z_1$  and is of order 1, and  $z_1$  is also a zero of order at least 1 of  $b_{w_1} \circ f$ . One can check that  $f^{(1)}$  takes values in  $\overline{\mathbb{D}}$ , so that  $f^{(1)}$  is analytic from  $\mathbb{D}$  to  $\overline{\mathbb{D}}$  if and only if  $f = b_{w_1}^{-1} \circ (b_{z_1} f^{(1)})$  is analytic from  $\mathbb{D}$  to  $\overline{\mathbb{D}}$ .

Now suppose  $|I| \geq 2$  and define for all  $n \in I \setminus \{1\}$ ,  $w_n^{(1)} := \frac{b_{w_1}(w_n)}{b_{z_1}(z_n)}$ . We notice that  $f^{(1)}(z_n) = \frac{b_{w_1}(f(z_n))}{b_{z_1}(z_n)} = \frac{b_{w_1}(w_n)}{b_{z_1}(z_n)} = w_n^{(1)}$ . This means that  $f^{(1)}$  is the solution to the Nevanlinna-Pick interpolation problem

$$g(z_n) = w_n^{(1)}, \quad \forall n \in I \setminus \{1\}. \quad (3.82)$$

We have proven the following lemma, which is the main element of the Schur interpolation algorithm [25].

**Lemma 3.A.6** (Schur iteration). *Assume  $|I| \geq 2$  and  $w_1 \in \mathbb{D}$ . We then have the following equivalence:*

$$f \in AC_{\mathbb{D}}(z_n, w_n)_I \iff f^{(1)} : z \mapsto \frac{b_{w_1}(f(z))}{b_{z_1}(z)} \in AC_{\mathbb{D}}(z_n, w_n^{(1)})_{I \setminus \{1\}}.$$

In other words,

$$AC_{\mathbb{D}}(z_n, w_n)_I = b_{w_1}^{-1} \circ \left( b_{z_1} \cdot AC_{\mathbb{D}}(z_n, w_n^{(1)})_{I \setminus \{1\}} \right).$$

Both previous lemmas give the intuition about the following theorem, which can be found in any reference dealing with the issue of Nevanlinna-Pick interpolation, e.g. [63], [20], [46]. Refinements of this result and characterizations of the solutions are detailed in the references given at the beginning of this section.

**Theorem 3.A.7.** *Let  $(z_n)_{n \geq 1}$  and  $(w_n)_{n \geq 1}$  be sequences in the unit disc  $\mathbb{D}$  and the closed disc  $\overline{\mathbb{D}}$  respectively. Define by induction, for  $1 \leq l$  and  $k > l$ ,*

$$w_k^{(l)} := \frac{w_k^{(l-1)} - w_l^{(l-1)}}{1 - \overline{w_l^{(l-1)}} w_k^{(l-1)}} \frac{1 - \bar{z}_l z_k}{z_k - z_l} = \frac{b_{w_l^{(l-1)}}(w_k^{(l-1)})}{b_{z_l}(z_k)}, \quad (3.83)$$

with  $w_k^{(0)} = w_k$  for  $k \geq 1$ .

There are three distinct cases.

1. If there exists  $k \geq 1$  such that  $|w_k^{(k-1)}| > 1$ , then there is no solution to the interpolation problem (3.78).
2. Else, if there exists  $K \geq 1$  such that for all  $1 \leq k < K$ ,  $|w_k^{(k-1)}| < 1$ ,  $|w_K^{(K-1)}| = 1$  and for all  $l \geq K$ ,  $w_l^{(K-1)} = w_K^{(K-1)}$ , then there exists a unique solution to the interpolation problem (3.78).
3. Else, we have for all  $k \geq 1$ ,  $|w_k^{(k-1)}| < 1$  and there is either 1 or infinitely many solutions to the interpolation problem.

### 3.A.2 A uniqueness result for ACPs with a rational solution

In our mathematical framework, we need the following uniqueness theorem (Theorem 3.A.8). In this section, we are tackling the uniqueness of the interpolation problem (3.78), in the case where we have already found one solution of some specific form. We assume that we have found a solution  $f$  such that its Nevanlinna-Riesz measure in the integral representation (3.45) is a finite sum of weighted Dirac measures, that is  $f$  is a rational function. This means that we have  $f(z) = \alpha z + C + \sum_{k=1}^K \frac{a_k}{z - \varepsilon_k}$ , with  $\alpha \geq 0$ ,  $C \in \mathbb{R}$ ,  $K \in \mathbb{N}$ , the  $a_k$ 's are negative numbers and the  $\varepsilon_k$ 's are distinct real numbers. The following theorem states that it is then the only solution to the interpolation problem (3.78).

**Theorem 3.A.8.** *Let  $f : \mathbb{C}_+ \rightarrow \overline{\mathbb{C}_+}$  be a Pick function such that its Nevanlinna-Riesz measure  $\mu$  is a finite sum of Dirac measures: there exist  $K \in \mathbb{N}$ ,  $a_1, \dots, a_K < 0$  and distinct real numbers  $\varepsilon_1, \dots, \varepsilon_K$  such that*

$$\mu = \sum_{k=1}^K a_k \delta_{\varepsilon_k}.$$

*Then, if  $f$  is a solution to an interpolation problem  $AC_{\mathbb{C}_+}(z_n, w_n)_I$  with  $|I| \geq K + 2$ , this problem has no other solution.*

*Proof.* We prove this result by strong induction on  $K$ , for  $K \in \mathbb{N}$ . If  $K = 0$ , the expression of  $f$  reads  $f(z) = \alpha z + C$ , with  $\alpha \geq 0$  and  $C \in \mathbb{R}$ . Now suppose  $f \in AC_{\mathbb{C}_+}(z_n, w_n)$ . Then for all  $n \in I$ , we have  $\alpha z_n + C = w_n$ , so that

$$AC_{\mathbb{C}_+}(z_n, w_n) = AC_{\mathbb{C}_+}(z_n, \alpha z_n + C).$$

If  $\alpha = 0$ , then  $AC_{\mathbb{C}_+}(z_n, C) = \{C\}$  by corollary 3.A.4. Else, we extend continuously  $f$  to  $\overline{\mathbb{C}_+}$  into the affine transformation  $\tilde{f} \in \mathcal{T}$  and we have

$$AC_{\mathbb{C}_+}(z_n, w_n) = \tilde{f} \circ \mathcal{W}^{-1} \circ AC_{\mathbb{D}}(\mathcal{W}(z_n), \mathcal{W}(z_n)) \circ \mathcal{W}.$$

Denoting by  $\tilde{z}_n = \tilde{w}_n = \mathcal{W}(z_n)$ , we find that for all  $n \in I \setminus \{1\}$ ,  $\tilde{w}_n^{(1)} = 1$ . Hence by Theorem 3.A.7,  $AC_{\mathbb{D}}(\mathcal{W}(z_n), \mathcal{W}(z_n)) = \{z \mapsto z\}$  and  $AC_{\mathbb{C}_+}(z_n, w_n) = \{f\}$ .

Now assume the result holds for  $l \leq K$  and take  $f$  such that its Nevanlinna-Riesz measure is a sum of  $K+1$  Dirac measures. Now consider an ACP  $AC_{\mathbb{C}}(z_n, w_n)_I$  with  $|I| \geq K+3$  to which  $f$  is a solution, namely  $f(z_n) = w_n$  and there exist  $\alpha \geq 0$ ,  $C \in \mathbb{R}$ ,  $a_1, \dots, a_{K+1} < 0$  and real numbers  $\varepsilon_1 < \dots < \varepsilon_{K+1}$ , such that for all  $z \in \mathbb{C}_+$ ,

$$f(z) = \alpha z + C + \sum_{k=1}^{K+1} \frac{a_k}{z - \varepsilon_k}.$$

We start by making use of the property (3.79) to simplify the problem. It is possible to chose two affine transformations  $\tau_{z_1}$  and  $\check{\tau}_{z_1}$  in  $\mathcal{T}$  such that, setting  $\tilde{f} = \check{\tau}_{z_1} \circ f \circ \tau_{z_1}^{-1}$ , we have

$$\tilde{f}(z) = \tilde{C} + \tilde{\alpha}z + \sum_{k=1}^{K+1} \frac{\tilde{a}_k}{z - \tilde{\varepsilon}_k},$$

where the parameters  $\tilde{C}$ ,  $\tilde{\alpha}$ ,  $\tilde{a}_k$ , and  $\tilde{\varepsilon}_k$  satisfy the same properties as their counterparts without the tildes, and such that

$$\tau_{z_1}(z_1) = i, \quad \Re(\tilde{f}(\tilde{z}_1)) = 0 \quad \text{and} \quad \sum_{k=1}^{K+1} \frac{-\tilde{a}_k}{1 + \tilde{\varepsilon}_k^2} = 1. \quad (3.84)$$

Using (3.79), we have

$$AC_{\mathbb{C}_+}(z_n, w_n) = \check{\tau}_{z_1}^{-1} \circ AC_{\mathbb{C}_+}(\underbrace{\tau_{z_1}(z_n)}_{\tilde{z}_n}, \underbrace{(\check{\tau}_{z_1} \circ f \circ \tau_{z_1}^{-1})(\tau_{z_1}(z_n))}_{\tilde{f}}) \circ \tau_{z_1}.$$

For the remaining of the proof, we will then focus on  $AC_{\mathbb{C}_+}(\tilde{z}_n, \tilde{f}(\tilde{z}_n))$ . We will omit the tildes for the sake of simplicity, and assume that  $z_1 = i$  and that (3.84) holds. With that being said, notice that  $\Im(f(z_1)) = \Im(f(i)) = \alpha + \sum_{k=1}^{K+1} \frac{-a_k}{1 + \varepsilon_k^2} > 0$ , hence  $\mathcal{W}(f(z_1)) \in \mathbb{D}$ . Therefore, using Lemma 3.A.6 equation (3.80), we have

$$AC_{\mathbb{D}}(\mathcal{W}(z_n), \mathcal{W}(f(z_n)))_I = b_{\mathcal{W}(f(z_1))}^{-1} \circ \left( b_{z_1} \cdot AC_{\mathbb{D}}(\mathcal{W}(z_n), \mathcal{W}(f(z_n))^{(1)})_{I \setminus \{1\}} \right).$$

and

$$AC_{\mathbb{D}}(\mathcal{W}(z_n), \mathcal{W}(f(z_n))^{(1)})_{I \setminus \{1\}} = \mathcal{W} \circ AC_{\mathbb{C}_+} \left( z_n, \mathcal{W}^{-1}([\mathcal{W}(f(z_n))]^{(1)}) \right)_{I \setminus \{1\}} \circ \mathcal{W}^{-1}.$$

We now compute  $g(z) = \mathcal{W}^{-1} \circ [\mathcal{W} \circ f]^{(1)}(z)$ , for  $z \in \mathbb{C}_+ \setminus \{i\}$ . Since  $\mathcal{W}(z_1) = \mathcal{W}(i) = 0$  and  $z \neq i$ , we have  $b_{\mathcal{W}(z_1)}(\mathcal{W}(z)) = \mathcal{W}(z) \neq 0$  and  $g(z)$  is well defined. The computation reads

$$g(z) = i \frac{(f(z_1) + i) \frac{\overline{f(z_1) - f(z)}}{z+i} + (\overline{f(z_1) + i}) \frac{f(z) - f(z_1)}{z-i}}{(f(z_1) + i) \frac{\overline{f(z_1) - f(z)}}{z+i} - (\overline{f(z_1) + i}) \frac{f(z) - f(z_1)}{z-i}}.$$

We used the fact that since  $\overline{\mathcal{W}(f(z_1))}\mathcal{W}(f(z)) \in \mathbb{D}$ , it is not equal to 1 and that  $\frac{1}{2i}(f(z)+i)|(f(z_1)+i)|^2 \neq 0$ . Now, realize that, since  $z_1 = i$ , we have

$$\frac{f(z) - f(z_1)}{z - i} = \alpha + \sum_{k=1}^{K+1} \frac{1}{\varepsilon_k - i} \frac{a_k}{z - \varepsilon_k},$$

and similarly

$$\frac{\overline{f(z_1)} - f(z)}{z + i} = -\alpha - \sum_{k=1}^{K+1} \frac{1}{\varepsilon_k + i} \frac{a_k}{z - \varepsilon_k},$$

so that

$$g(z) = -\frac{\alpha(\Im(f(z_1)) + 1) + \sum_{k=1}^{K+1} \Im\left(\frac{f(z_1) + i}{\varepsilon_k + i}\right) \frac{a_k}{z - \varepsilon_k}}{\alpha \Re(f(z_1)) + \sum_{k=1}^{K+1} \Re\left(\frac{f(z_1) + i}{\varepsilon_k + i}\right) \frac{a_k}{z - \varepsilon_k}}, \quad (3.85)$$

which holds for  $z = i$  as well. As we set  $\Re(f(z_1)) = 0$ , we have

$$\Re\left(\frac{f(z_1) + i}{\varepsilon_k + i}\right) = \frac{\Im(f(z_1)) + 1}{1 + \varepsilon_k^2} > 0 \quad \text{and} \quad \Im\left(\frac{f(z_1) + i}{\varepsilon_k + i}\right) = \varepsilon_k \frac{\Im(f(z_1)) + 1}{1 + \varepsilon_k^2}.$$

Multiplying the numerator and denominator in (3.85) by  $\frac{1}{\Im(f(z_1)) + 1} \prod_{k=1}^{K+1} (z - \varepsilon_k)$ , we end up with  $g(z) = \frac{P(z)}{Q(z)}$ , with

$$P(z) := \alpha \prod_{k=1}^{K+1} (z - \varepsilon_k) + \sum_{k=1}^{K+1} \varepsilon_k \frac{a_k}{1 + \varepsilon_k^2} \prod_{l=1, l \neq k}^{K+1} (z - \varepsilon_l),$$

and

$$Q(z) := \sum_{k=1}^{K+1} \frac{-a_k}{1 + \varepsilon_k^2} \prod_{l=1, l \neq k}^{K+1} (z - \varepsilon_l).$$

We have  $Q(\varepsilon_k) = \frac{-a_k}{1 + \varepsilon_k^2} \prod_{l=1, l \neq k}^{K+1} (\varepsilon_k - \varepsilon_l) \neq 0$  by hypothesis on the  $\varepsilon_k$ 's, so that

$$Q(z) = 0 \iff \sum_{k=1}^{K+1} \frac{\frac{-a_k}{1 + \varepsilon_k^2}}{z - \varepsilon_k} = 0,$$

hence  $Q$  admits exactly  $K$  distinct roots  $\varepsilon'_k \in (\varepsilon_k, \varepsilon_{k+1}) \subset \mathbb{R}$  by the intermediate value theorem (as in the proof of Lemma 3.4.1), and it is unitary due to (3.84). The partial fraction decomposition of  $g$  finally reads

$$g(z) = \alpha' z + C' + \sum_{k=1}^K \frac{a'_k}{z - \varepsilon'_k},$$

where

$$\begin{aligned} \alpha' &= \alpha, \\ C' &= \lim_{y \rightarrow \infty} g(iy) - i\alpha'y = (1 - \alpha) \sum_{k=1}^{L+1} \varepsilon_k \frac{a_k}{1 + \varepsilon_k^2} \in \mathbb{R}, \\ a'_k &= \lim_{y \rightarrow 0^+} iy g(\varepsilon'_k + iy) \\ &= \left( \prod_{l=1, l \neq k}^K \underbrace{\left( \frac{\varepsilon'_k - \varepsilon_l}{\varepsilon'_k - \varepsilon'_l} \right)}_{>0} \right) \underbrace{(\varepsilon'_k - \varepsilon_k)}_{<0} \underbrace{(\varepsilon'_k - \varepsilon_{L+1})}_{>0} \underbrace{(\alpha + 1)}_{>0} < 0. \end{aligned}$$

This computation shows that the Nevanlinna-Riesz measure of  $g$  is a sum of  $K$  Dirac measures as described in the statement of the theorem. It is a solution to the Analytical Continuation Problem

$$AC_{\mathbb{C}_+} \left( z_n, \mathcal{W}^{-1}([\mathcal{W}(f(z_n))]^{(1)}) \right)_{I \setminus \{1\}},$$

where  $|I \setminus \{1\}| \geq K + 2$  by assumption. By the induction hypothesis,  $g$  is the only solution to this ACP, and therefore  $f$  is the only solution to the ACP  $AC_{\mathbb{C}_+}(w_n, z_n)_I$ .  $\square$

### 3.B Paramagnetic IPT-DMFT equations

In this appendix, we detail the spin independence of the paramagnetic IPT-DMFT equations.

As detailed in Remark 3.2.9, the Hamiltonian  $\hat{H}_{AI}$  commutes with the total spin operator  $\hat{S}_{AI}$ . More precisely,  $\mathcal{H}_{AI}$  is  $\hat{S}_{AI}$ -invariant, and in the decomposition

$$\mathcal{H}_{AI} = \mathcal{H}_\uparrow \oplus \mathcal{H}_\downarrow, \quad \mathcal{H}_\sigma = \text{Span} \left( |\emptyset\rangle \otimes \cdots \otimes |\emptyset\rangle \otimes \underset{m-\text{th}}{\langle \sigma |} \otimes |\emptyset\rangle \otimes \cdots \otimes |\emptyset\rangle, m \in \Lambda \sqcup [\![1, B]\!] \right) \quad (3.86)$$

the total spin operators reads  $\hat{S}_{AI} = \mathbf{1}_\uparrow \oplus (-\mathbf{1}_\downarrow)$ :

$$\hat{S}_{AI} = \begin{pmatrix} \mathbf{1} & 0 \\ 0 & -\mathbf{1} \end{pmatrix}.$$

Writing in this decomposition  $H^0 = H_\uparrow^0 \oplus H_\downarrow^0$ , we then have

$$G^0(z) = (z - H_\uparrow^0)^{-1} \oplus (z - H_\downarrow^0)^{-1}.$$

Since no magnetic field is included in the model,  $H_\uparrow^0$  and  $H_\downarrow^0$  act the same way on their respective domains: denoting by  $\hat{F} \in \mathcal{L}(\mathcal{H}_{AI})$  the *spin flip* isomorphism defined by linearity with  $\forall m \in \Lambda \sqcup [\![1, B]\!], \forall \sigma \in \{\uparrow, \downarrow\}$

$$\hat{F} \left( |\emptyset\rangle \otimes \cdots \otimes |\emptyset\rangle \otimes \underset{m-\text{th}}{\langle \sigma |} \otimes |\emptyset\rangle \otimes \cdots \otimes |\emptyset\rangle \right) = |\emptyset\rangle \otimes \cdots \otimes |\emptyset\rangle \otimes \underset{m-\text{th}}{\langle \bar{\sigma} |} \otimes |\emptyset\rangle \otimes \cdots \otimes |\emptyset\rangle,$$

we have

$$H_\uparrow^0 = \hat{F}_{\uparrow, \downarrow} H_\downarrow^0 \hat{F}_{\downarrow, \uparrow}.$$

Now in the impurity-spin decomposition

$$\mathcal{H} = \mathcal{H}_{\uparrow, \text{imp}} \oplus \mathcal{H}_{\uparrow, \text{bath}} \oplus \mathcal{H}_{\downarrow, \text{imp}} \oplus \mathcal{H}_{\downarrow, \text{bath}} \quad (3.87)$$

$$\mathcal{H}_{\sigma, \text{imp}} = \text{Span} \left( |\emptyset\rangle \otimes \cdots \otimes |\emptyset\rangle \otimes \underset{i-\text{th}}{\langle \sigma |} \otimes |\emptyset\rangle \otimes \cdots \otimes |\emptyset\rangle, i \in \Lambda \right) \quad (3.88)$$

$$\mathcal{H}_{\sigma, \text{bath}} = \text{Span} \left( |\emptyset\rangle \otimes \cdots \otimes |\emptyset\rangle \otimes \underset{k-\text{th}}{\langle \sigma |} \otimes |\emptyset\rangle \otimes \cdots \otimes |\emptyset\rangle, k \in [\![1, B]\!] \right) \quad (3.89)$$

we have  $\hat{S}_{AI} = \mathbf{1} \oplus \mathbf{1} \oplus (-\mathbf{1}) \oplus (-\mathbf{1})$  and  $\hat{N}_{\text{imp}} = \mathbf{1} \oplus 0 \oplus \mathbf{1} \oplus 0$ :

$$\hat{S}_{AI} = \begin{pmatrix} \mathbf{1} & 0 & 0 & 0 \\ 0 & \mathbf{1} & 0 & 0 \\ 0 & 0 & -\mathbf{1} & 0 \\ 0 & 0 & 0 & -\mathbf{1} \end{pmatrix}, \quad \hat{N}_{\text{imp}} = \begin{pmatrix} \mathbf{1} & 0 & 0 & 0 \\ 0 & 0 & 0 & 0 \\ 0 & 0 & \mathbf{1} & 0 \\ 0 & 0 & 0 & 0 \end{pmatrix}$$

and we have for the impurity orthogonal restriction of the non-interacting Green's function  $G_{\text{imp}}^0$ :

$$G_{\text{imp}}^0(z) = (z - H_{\uparrow, \text{imp}}^0 - \Delta_\uparrow(z)) \oplus (z - H_{\downarrow, \text{imp}}^0 - \Delta_\downarrow(z))$$

Indeed, as it is the case for the non-interacting Hamiltonian and the non-interacting Green's function,  $\Delta_\uparrow$  acts similarly as  $\Delta_\downarrow$  on their respective domain, and are related by conjugation with the spin flip operator

$$\Delta_\uparrow = \hat{F}_{\uparrow, \downarrow} \Delta_\downarrow \hat{F}_{\downarrow, \uparrow}$$

With that being said, in the IPT approximation outlined in this document, we have for  $n \in \mathbb{Z}$ ,

$$\Sigma_{\text{imp},n}^M = \Sigma_{\uparrow,\text{imp},n}^M \oplus \Sigma_{\downarrow,\text{imp},n}^M,$$

with for all  $\sigma \in \{\uparrow, \downarrow\}$ ,

$$\Sigma_{\sigma,\text{imp},n}^M = U^2 \int_0^\beta e^{i\omega_n \tau} \left( \frac{1}{\beta} \sum_{n' \in \mathbb{Z}} (i\omega_{n'} - \Delta_\sigma(i\omega_{n'})^{-1}) \right)^3 d\tau.$$

And indeed, we have the conjugation relation

$$\Sigma_{\uparrow,\text{imp},n}^M = \hat{F}_{\uparrow,\downarrow} \Sigma_{\downarrow,\text{imp},n}^M \hat{F}_{\downarrow,\uparrow}.$$

These last equations show that the impurity-spin orthogonal restrictions of the Matsubara self-energy Fourier coefficients are copies one of another. Since we assume that the partition  $\mathfrak{P}$  is in singletons, it follows that  $|\Lambda| = 1$  and  $\dim(\mathcal{H}_{\sigma,\text{imp}}) = 1$ , so that using the bases  $\mathcal{B}_{\sigma,\text{imp}}$  given by

$$\forall \sigma \in \{\uparrow, \downarrow\}, \quad \mathcal{B}_{\sigma,\text{imp}} = \{|\sigma\rangle \otimes |\emptyset\rangle \otimes \cdots \otimes |\emptyset\rangle\},$$

we have for all  $n \in \mathbb{Z}$ ,

$$\text{mat}_{\mathcal{B}_{\uparrow,\text{imp}}}(\Sigma_{\uparrow,\text{imp},n}^M) = \text{mat}_{\mathcal{B}_{\downarrow,\text{imp}}}(\Sigma_{\downarrow,\text{imp},n}^M) := \Sigma_n.$$

Finally, we have for  $z \in \mathbb{C}_+$ ,

$$\text{mat}_{\mathcal{B}_{\uparrow,\text{imp}}}(\Delta_{\uparrow}(z)) = \text{mat}_{\mathcal{B}_{\downarrow,\text{imp}}}(\Delta_{\downarrow}(z)) = \sum_{k=1}^B \frac{V_k V_k^\dagger}{z - \epsilon_k},$$

so that we indifferently refer to  $\Delta(z)$  by abuse of notation.

## Bibliography

- [1] M. B. Abrahamse. The Pick interpolation theorem for finitely connected domains. *Michigan Mathematical Journal*, 26(2):195–203, January 1979. Publisher: University of Michigan, Department of Mathematics.
- [2] Naum I. Akhiezer. *The Classical Moment Problem and Some Related Questions in Analysis*. Society for Industrial and Applied Mathematics, Philadelphia, PA, 2020.
- [3] Luigi Ambrosio, Nicola Gigli, and Giuseppe Savaré. *Gradient flows: in metric spaces and in the space of probability measures*. Springer Science & Business Media, 2005.
- [4] Philip W. Anderson. Localized Magnetic States in Metals. *Physical Review*, 124(1):41–53, 1961.
- [5] Louis-François Arsenault, Patrick Sémon, and André-Marie S. Tremblay. Benchmark of a modified iterated perturbation theory approach on the fcc lattice at strong coupling. *Physical Review B*, 86(8):085133, 2012.
- [6] Volker Bach, Elliott H. Lieb, and Jan Philip Solovej. Generalized Hartree-Fock theory and the Hubbard model. *Journal of Statistical Physics*, 76(1):3–89, July 1994.
- [7] Gordon Baym and N. David Mermin. Determination of Thermodynamic Green's Functions. *Journal of Mathematical Physics*, 2(2):232–234, March 1961.
- [8] Johannes G. Bednorz and Karl A. Müller. Possible highTc superconductivity in the Ba-La-Cu-O system. *Zeitschrift für Physik B Condensed Matter*, 64(2):189–193, June 1986.
- [9] Vladimir I. Bogačev. *Measure theory*. Springer, Berlin, 2007.
- [10] Vladimir I. Bogačev. *Weak convergence of measures*. Number volume 234 in Mathematical surveys and monographs. American Mathematical Society, Providence, Rhode Island, 2018.
- [11] Ola Bratteli and Derek William Robinson. *Operator algebras and quantum statistical mechanics 1. C\*-and W\*-Algebras. Symmetry Groups. Decomposition of States*. Theoretical and Mathematical Physics. Springer Berlin, Heidelberg, 2 edition, 1987.

- [12] Ola Bratteli and Derek William Robinson. *Operator algebras and quantum statistical mechanics 2. Equilibrium States. Models in Quantum Statistical Mechanics*. Theoretical and Mathematical Physics. Springer Berlin Heidelberg, 2 edition, 1997.
- [13] Eric Cancès, David Gontier, and Gabriel Stoltz. A mathematical analysis of the GW0 method for computing electronic excited energies of molecules. *Reviews in Mathematical Physics*, 28(04):1650008, 2016.
- [14] Éric Cancès, Fabian M. Faulstich, Alfred Kirsch, Eloïse Letournel, and Antoine Levitt. Some mathematical insights on Density Matrix Embedding Theory, 2023. arXiv:2305.16472.
- [15] Jonathan Eckhardt. Continued fraction expansions of Herglotz–Nevanlinna functions and generalized indefinite strings of Stieltjes type. *Bulletin of the London Mathematical Society*, 54(2):737–759, 2022. eprint: <https://londmathsoc.onlinelibrary.wiley.com/doi/pdf/10.1112/blms.12598>.
- [16] Fabian M. Faulstich, Raehyun Kim, Zhi-Hao Cui, Zaiwen Wen, Garnet Kin-Lic Chan, and Lin Lin. Pure State v-Representability of Density Matrix Embedding Theory. *Journal of Chemical Theory and Computation*, 18(2):851–864, 2022.
- [17] Jiani Fei, Chia-Nan Yeh, Dominika Zgid, and Emanuel Gull. Analytical continuation of matrix-valued functions: Carathéodory formalism. *Physical Review B*, 104(16):165111, 2021.
- [18] Edoardo Fertitta and George H. Booth. Energy-weighted density matrix embedding of open correlated chemical fragments. *The Journal of Chemical Physics*, 151(1):014115, 2019.
- [19] Richard P Feynman and Frank L Vernon. The theory of a general quantum system interacting with a linear dissipative system. *Annals of Physics*, 24:118–173, 1963.
- [20] John Garnett. *Bounded Analytic Functions*. Springer Science & Business Media, 2006.
- [21] Antoine Georges. Lectures at Collège de France. Fermions en interaction : Introduction à la théorie du champ moyen dynamique, 2018.
- [22] Antoine Georges, Gabriel Kotliar, Werner Krauth, and Marcelo J. Rozenberg. Dynamical mean-field theory of strongly correlated fermion systems and the limit of infinite dimensions. *Reviews of Modern Physics*, 68(1):13–125, January 1996.
- [23] Fritz Gesztesy and Eduard Tsekanovskii. On Matrix–Valued Herglotz Functions. *Mathematische Nachrichten*, 218(1):61–138, 2000.
- [24] David Gontier. *Contributions mathématiques aux calculs de structures électroniques*. Thèse de doctorat, Paris Est, 2015.
- [25] Emanuel Gull, Andrew J. Millis, Alexander I. Lichtenstein, Alexey N. Rubtsov, Matthias Troyer, and Philipp Werner. Continuous-time Monte Carlo methods for quantum impurity models. *Reviews of Modern Physics*, 83(2):349–404, 2011.
- [26] Martin C. Gutzwiller. Effect of Correlation on the Ferromagnetism of Transition Metals. *Physical Review Letters*, 10(5):159–162, March 1963.
- [27] Karsten Held, Georg Keller, Volker Eyert, Dieter Vollhardt, and Vladimir I Anisimov. Mott-Hubbard Metal-Insulator Transition in Paramagnetic V\$<sub>2</sub>\$ O\$<sub>3</sub>\$: An LDA+DMFT (QMC) Study. *Physical review letters*, 86(23):5345, 2001.
- [28] Bernard Helffer and Johannes Sjöstrand. Equation de Schrödinger avec champ magnétique et équation de Harper. In *Schrödinger Operators: Proceedings of the Nordic Summer School in Mathematics Held at Sandbjerg Slot, Sønderborg, Denmark, August 1–12, 1988*, pages 118–197. Springer, 2005.
- [29] John Hubbard. Electron correlations in narrow energy bands. *Proceedings of the Royal Society of London. Series A. Mathematical and Physical Sciences*, 276(1365):238–257, 1963.
- [30] Henrik Kajueter and Gabriel Kotliar. New Iterative Perturbation Scheme for Lattice Models with Arbitrary Filling. *Physical Review Letters*, 77(1):131–134, 1996.

- [31] Junjiro Kanamori. Electron Correlation and Ferromagnetism of Transition Metals. *Progress of Theoretical Physics*, 30(3):275–289, 1963.
- [32] Gerald Knizia and Garnet Kin-Lic Chan. Density Matrix Embedding: A Simple Alternative to Dynamical Mean-Field Theory. *Physical Review Letters*, 109(18):186404, November 2012.
- [33] Jun Kondo. Resistance Minimum in Dilute Magnetic Alloys. *Progress of Theoretical Physics*, 32(1):37–49, 1964.
- [34] Gunnar Källén. On the Definition of the Renormalization Constants in Quantum Electrodynamics. June 1952. Medium: text/html,application/pdf,text/html Publisher: Birkhäuser.
- [35] Frank Lechermann, Antoine Georges, Gabriel Kotliar, and Olivier Parcollet. Rotationally invariant slave-boson formalism and momentum dependence of the quasiparticle weight. *Physical Review B*, 76(15):155102, 2007.
- [36] Harry Lehmann. Über Eigenschaften von Ausbreitungsfunktionen und Renormierungskonstanten quantisierter Felder. *Il Nuovo Cimento*, 11(4):16, April 1954.
- [37] Elliott H. Lieb. The Hubbard model: Some Rigorous Results and Open Problems. In *Condensed Matter Physics and Exactly Soluble Models: Selecta of Elliott H. Lieb*. Berlin, Heidelberg, 2004.
- [38] Elliott H. Lieb and F. Y. Wu. Absence of Mott Transition in an Exact Solution of the Short-Range, One-Band Model in One Dimension. *Physical Review Letters*, 20(25):1445–1448, June 1968.
- [39] Elliott H. Lieb and F.Y. Wu. The one-dimensional Hubbard model: a reminiscence. *Physica A: Statistical Mechanics and its Applications*, 321(1-2):1–27, April 2003.
- [40] Lin Lin and Michael Lindsey. Sparsity Pattern of the Self-energy for Classical and Quantum Impurity Problems. *Annales Henri Poincaré*, 21(7):2219–2257, 2020.
- [41] Michael Lindsey. *The Quantum Many-Body Problem: Methods and Analysis*. PhD thesis, University of California, Berkeley, 2019.
- [42] He Ma, Nan Sheng, Marco Govoni, and Giulia Galli. Quantum Embedding Theory for Strongly Correlated States in Materials. *Journal of Chemical Theory and Computation*, 17(4):2116–2125, 2021.
- [43] Richard M. Martin, Lucia Reining, and David M. Ceperley. *Interacting Electrons: Theory and Computational Approaches*. Cambridge University Press, Cambridge, 2016.
- [44] Walter Metzner and Dieter Vollhardt. Correlated Lattice Fermions in  $d = \infty$  Dimensions. *Physical Review Letters*, 62(3):324–327, January 1989.
- [45] Rolf Nevanlinna. Über beschränkte Funktionen, die in gegeben Punkten vorgeschrieben Werte annehmen. *Ann. Acad. Sci. Fenn. Ser. A 1 Mat. Dissertationes*, 1919.
- [46] Artur Nicolau. Interpolating Blaschke products solving Pick-Nevanlinna problems. *Journal d'Analyse Mathématique*, 62(1):199–224, December 1994.
- [47] Artur Nicolau. The Nevanlinna-Pick Interpolation Problem. 2015.
- [48] Rudolph Pariser and Robert G. Parr. A Semi-Empirical Theory of the Electronic Spectra and Electronic Structure of Complex Unsaturated Molecules. II. *The Journal of Chemical Physics*, 21(5):767–776, 1953.
- [49] Georg Pick. Über die Beschränkungen analytischer Funktionen, welche durch vorgegebene Funktionswerte bewirkt werden. *Mathematische Annalen*, 77(1):7–23, March 1915.
- [50] John A. Pople. Electron interaction in unsaturated hydrocarbons. *Transactions of the Faraday Society*, 49(0):1375–1385, 1953.
- [51] Marcello J. Rozenberg, Gabriel Kotliar, and X. Y. Zhang. Mott-Hubbard transition in infinite dimensions. II. *Physical Review B*, 49(15):10181–10193, 1994.

- [52] A. N. Rubtsov, V. V. Savkin, and A. I. Lichtenstein. Continuous-time quantum Monte Carlo method for fermions. *Physical Review B*, 72(3):035122, July 2005.
- [53] Filippo Santambrogio. *Optimal Transport for Applied Mathematicians: Calculus of Variations, PDEs, and Modeling*, volume 87 of *Progress in Nonlinear Differential Equations and Their Applications*. Springer International Publishing, Cham, 2015.
- [54] Myriam P. Sarachik. Resistivity of Some 5d Elements and Alloys Containing Iron. *Physical Review*, 170(3):679–682, 1968.
- [55] Donald Sarason. Generalized interpolation in  $H^\infty$ . *Transactions of the American Mathematical Society*, 127(2):179–203, 1967.
- [56] Ryosuke Sato. GICAR Algebras and Dynamics on Determinantal Point Processes: Discrete Orthogonal Polynomial Ensemble Case. *Communications in Mathematical Physics*, 405(5):115, May 2024.
- [57] Joel H. Shapiro. *A Fixed-Point Farrago*. Universitext. Springer International Publishing, Cham, 2016.
- [58] Arne Stray. Interpolating Sequences and the Nevanlinna Pick Problem. *Publicacions Matemàtiques*, 35(2):507–516, 1991. Publisher: Universitat Autònoma de Barcelona.
- [59] Ping Sun and Gabriel Kotliar. Extended dynamical mean-field theory and GW method. *Physical Review B*, 66(8):085120, 2002.
- [60] Yuting Tan, Pak Ki Henry Tsang, Vladimir Dobrosavljević, and Louk Rademaker. Doping a Wigner-Mott insulator: Exotic charge orders in transition metal dichalcogenide moiré heterobilayers. *Physical Review Research*, 5(4):043190, 2023.
- [61] E. C. Titchmarsh. *Introduction to the Theory of Fourier Integrals*. Clarendon Press, Oxford, 1948.
- [62] Cédric Villani. *Optimal transport. Old and New*, volume 338 of *Grundlehren der mathematischen Wissenschaften*. Springer Berlin Heidelberg, 1 edition, 2009.
- [63] J. L. Walsh. *Interpolation and Approximation by Rational Functions in the Complex Domain*. American Mathematical Soc., December 1935. Google-Books-ID: Pyz3AwAAQBAJ.
- [64] Steven R. White. Density matrix formulation for quantum renormalization groups. *Physical Review Letters*, 69(19):2863–2866, 1992.
- [65] Gian-Carlo Wick. Properties of Bethe-Salpeter Wave Functions. *Physical Review*, 96(4):1124–1134, 1954.
- [66] Xiaojie Wu, Michael Lindsey, Tiangang Zhou, Yu Tong, and Lin Lin. Enhancing robustness and efficiency of density matrix embedding theory via semidefinite programming and local correlation potential fitting. *Phys. Rev. B*, 102(8):085123, August 2020. Publisher: American Physical Society.
- [67] Yijun Yu, Liguo Ma, Peng Cai, Ruidan Zhong, Cun Ye, Jian Shen, G. D. Gu, Xian Hui Chen, and Yuanbo Zhang. High-temperature superconductivity in monolayer  $\text{Bi}_2\text{Sr}_2\text{Ca}\text{Cu}_2\text{O}_8+\delta$ . *Nature*, 575(7781):156–163, November 2019.
- [68] X. Y. Zhang, M. J. Rozenberg, and G. Kotliar. Mott transition in the  $d=\infty$  Hubbard model at zero temperature. *Physical Review Letters*, 70(11):1666–1669, March 1993.
- [69] Jianqiang Sky Zhou, Lucia Reining, Alessandro Nicolaou, Azzedine Bendounan, Kari Ruotsalainen, Marco Vanzini, J. J. Kas, J. J. Rehr, Matthias Muntwiler, Vladimir N. Strocov, Fausto Sirotti, and Matteo Gatti. Unraveling intrinsic correlation effects with angle-resolved photoemission spectroscopy. *Proceedings of the National Academy of Sciences*, 117(46):28596–28602, 2020.

# Chapter 4

## A mathematical analysis of the discretized IPT-DMFT equations.

### Contents

---

<b>4.1</b>	<b>IPT-DMFT on the Matsubara's frequencies</b>	<b>129</b>
4.1.1	Analytic continuation	130
4.1.2	Matsubara's formalism	131
<b>4.2</b>	<b>Existence of solutions to the discretized equations</b>	<b>132</b>
4.2.1	Main result	132
4.2.2	Proof of Theorem 4.2.1	133
<b>4.3</b>	<b>Iterative scheme and Mott transition</b>	<b>135</b>
4.3.1	Mott transition	135
4.3.2	Linear convergence for small and large on-site repulsion	137
4.3.3	Continuation method and metastable solution	141
<b>4.4</b>	<b>Uniqueness of the solution in perturbative regimes.</b>	<b>143</b>
4.4.1	Main result	143
4.4.2	Proof of Theorem 4.4.1	144
	<b>Bibliography</b>	<b>145</b>

---

In the previous chapter, we have proven the existence of a solution to the IPT-DMFT equations. In view of practical purposes, this result needs to be adapted to a set of discretized equations on which realistic computations can be performed. In this chapter, we are interested in the discretization of the DMFT functional equations based on the restriction of the hybridization function and self-energy to the collection of points in the upper half-plane  $z = i\omega_n$ , where  $\omega_n = (2n + 1)\pi/\beta$  is the  $n$ -th Matsubara frequency. After a presentation of these equations, we start by proving the existence of a solution to these equations, which is an adaptation of [3, Theorem 3.9] to this setting. We then show numerically, using an iterative scheme for the Hubbard dimer based on these equations, that global uniqueness is guaranteed for small and large on-site repulsion  $U$ . In accordance with these numerical insights, we finally prove uniqueness of the solution for small on-site repulsion  $U$  or small hopping parameter  $T$ .

### 4.1 IPT-DMFT on the Matsubara's frequencies

The success of the Dynamical Mean-Field Theory (DMFT) in the strongly correlated condensed matter community lies in its ability to provide with good approximations of local Green's functions for very large systems [7]. As already mentioned in the previous chapter, the computationally expensive part in a DMFT algorithm is the *impurity solver* step, which provides for each Anderson Impurity Model (AIM) (labeled by  $p \in \mathfrak{P}$ ) the impurity self-energy  $\Sigma_{\text{imp},p}$  given the hybridization function  $\Delta_p$  and the impurity parameters  $(\mathcal{G}_p, T_p, U_p)$ , as detailed in [3, Section 2.4]. Most of practical implementations of DMFT are based on the *translation-invariant* setting [3, Remark 2.11], for which the set of equations scales down to only two equations in the translation invariant quantities  $(\Delta, \Sigma)$ : in this setting, only one impurity model remains, which reduces the computational cost. Still, the impurity solver is the practical bottleneck of a DMFT computation (even ground-state computations are known to be very expensive

[2]): accurate computations are performed using Continuous Time Quantum Monte Carlo (CTQMC) [10, 17, 22, 23, 13, 19], which are exact up to statistical noise. Nevertheless, their computational price is too high and for specific applications such as moiré heterobilayers [21], computations are performed using *approximate solvers*. One of them is the Iterated Perturbation Theory (IPT) solver, which we are interested in in this chapter.

IPT is one of the most computationally cheap (and one of the least accurate) solvers [6, 24, 7]. We have studied its analytical properties in [3], in the *single-site translation-invariant paramagnetic* setting: recall that in this setting, for a given inverse temperature  $\beta$ , on-site repulsion  $U \in \mathbb{R}$  and hopping parameter  $T \in \mathbb{R}$ , the IPT-DMFT equations read

$$\forall z \in \mathbb{C}_+, \quad \Delta(z) = W(z - H_\perp^0 - \Sigma(z))^{-1} W^\dagger \quad (4.1)$$

$$\Sigma = \text{IPT}_\beta(U, \Delta) \quad (4.2)$$

where  $\text{IPT}_\beta(U, \Delta)$  is the *IPT solver* introduced in [3, Section 2.5.2],  $-\Delta, -\Sigma$  are analytic functions from  $\mathbb{C}_+$  to  $\overline{\mathbb{C}_+}$ , and  $H_\perp^0 \in \mathcal{S}_{L-1}(\mathbb{R})$  and  $W^\dagger \in \mathbb{R}^{L-1}$  are given by

$$T\text{Adj} = \begin{pmatrix} 0 & W \\ W^\dagger & H_\perp^0 \end{pmatrix},$$

with  $\text{Adj}$  the adjacency matrix of the original Hubbard graph  $\mathcal{G}_H = (\Lambda, E)$ ,  $|\Lambda| = L$ .

We have shown in particular that this solver is well-defined for hybridization functions representing finite dimensional baths [3, Proposition 2.18], and that it extends continuously (for the appropriate distance) to the closure if this set, which represents thermodynamic limits of finite dimensional baths [3, Proposition 3.6]. Nevertheless, the very quantities  $\Delta, \Sigma$  this solver is dealing with are functions defined on the whole upper half-plane: any practical computational scheme requires discretizations of these two objects.

In this chapter, we focus on the set of equations obtained when discretizing  $\Delta$  and  $\Sigma$  by their values on a finite subset of the so-called Matsubara's frequencies  $(i\omega_n)_{n \in \mathbb{N}}$  where  $\omega_n = (2n + 1)\frac{\pi}{\beta}$  [3, Section 2.5.1]. More precisely, we are interested in the following discretization: for given  $\Delta, \Sigma$ , we construct the following finite dimensional objects

$$(\Delta_n)_{n \in [\![0, N_\omega]\!]}, \quad -\Delta_n = -\Delta(i\omega_n) \in \overline{\mathbb{C}_+} \quad (4.3)$$

$$(\Sigma_n)_{n \in [\![0, N_\omega]\!]}, \quad -\Sigma_n = -\Sigma(i\omega_n) \in \overline{\mathbb{C}_+} \quad (4.4)$$

where  $N_\omega \in \mathbb{N}$  is the *Matsubara's frequency cutoff*. Note that we extend this definition to negative Matsubara's frequencies with for all  $n \in [\![0, N_\omega]\!]$

$$\Delta_{-(n+1)} = \overline{\Delta_n} \in \overline{\mathbb{C}_+}, \quad \Sigma_{-(n+1)} = \overline{\Sigma_n} \in \overline{\mathbb{C}_+} \quad (4.5)$$

in accordance with the conventional extension of a Pick function to the lower half-plane [8] ( $\forall z \in \mathbb{C}_-, f(z) = \overline{f(\bar{z})}$ ) and the fact that  $\omega_{-(n+1)} = -\omega_n$ . The set  $(i\omega_n)_{n \in [\![0, N_\omega]\!]}$  of points in  $\mathbb{C}_+$ , represented in Figure 1, is motivated by two reasons that we discuss below.

#### 4.1.1 Analytic continuation

Let us first recall that, given a Green's function  $G$  as defined in [3, Definition 2.2], it is theoretically enough to know the sequence  $(G(i\omega_n))_{n \in \mathbb{N}}$  to reconstruct the whole Green's function: as proven in [3, Theorem 2.15] and already established in [1],  $-G$  is the only Pick matrix which is solution to the analytic continuation problem  $\text{AC}_{\mathbb{C}_+}(i\omega_n, -G(i\omega_n))_{n \in \mathbb{N}}$ . One proves similarly, using [3, Theorem A.8] and the Källen-Lehmann representation [3, Equation 7] that this result holds true for the self-energy  $\Sigma$  and hybridization function  $\Delta$ .

In practice, several algorithms exist to perform this analytic continuation [9, 12, 4, 5, 11]. In most cases, the output of these methods are the values of the analytic continuation on the real axis  $\mathbb{R}$ , from which one can extract the Nevanlinna-Riesz measure of the associated Pick function using the Stieltjes inversion formula [8]: recall that for  $f$  a Pick Matrix given for all  $z \in \mathbb{C}_+$  by

$$f(z) = \int_{\mathbb{R}} \frac{1}{\varepsilon - z} d\mu(\varepsilon)$$

with  $\mu$  a positive-matrix-valued Borel finite measure, then we have for all  $x, y \in \mathbb{R}$ ,

$$\frac{1}{2}\mu(\{x\}) + \frac{1}{2}\mu(\{y\}) + \mu((x, y)) = \frac{1}{\pi} \lim_{\eta \rightarrow 0} \int_x^y \Im(f(\varepsilon + i\eta)) d\varepsilon.$$

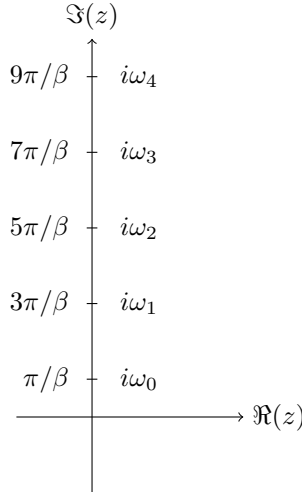


Figure 1: The set  $(i\omega_n)_{n \in \llbracket 0, N_\omega \rrbracket}$  of points in  $\mathbb{C}_+$  used for the discretization of  $\Delta$  and  $\Sigma$  with  $N_\omega = 4$

In particular, the Nevanlinna-Riesz measure associated to  $-G$  is the so-called *spectral function A* [15], which allows to determine whether the system is a conductor or not: more precisely, the system is an electrical conductor if 0 is in the support of  $A$ .

Based on this property, a strategy to study the conduction properties using a DMFT algorithm is as follows :

- Run the DMFT algorithm on  $(\Delta_n, \Sigma_n)_{n \in \llbracket 0, N_\omega \rrbracket}$  until convergence is reached.
- Get the spectral function  $A$  by analytic continuation of the sequence  $(G(i\omega_n))_{n \in \llbracket 0, N_\omega \rrbracket}$ , and check for the conduction criterion.

In this chapter, we will show numerically in Section 4.3 that for the Hubbard dimer ( $|\mathcal{G}_H| = 2$ ), the system hosts a metal-to-insulator Mott transition for a fixed inverse temperature  $\beta$ , while varying the on-site repulsion  $U$ . This result, already established in the seminal paper [7] for truncated lattices made the fame of this method, and is related to uniqueness of the solution for specific parameters, as we will discuss in Section 4.3.

For now, let us mention that analytic continuation, if theoretically well founded, suffers from ill-conditioning issues [9, 12]. For this reason, we will use it only for illustrative purposes in Section 4.3.

#### 4.1.2 Matsubara's formalism

The second justification of this discretization lies in the proper definition of the IPT-DMFT equations. We note first that equation (4.1) relates the value of  $\Delta$  in  $z \in \mathbb{C}_+$  to the value of  $\Sigma$  on the same  $z \in \mathbb{C}_+$ . More precisely, given  $-\Delta, -\Sigma : \mathbb{C}_+ \rightarrow \overline{\mathbb{C}_+}$  satisfying (4.1), their values  $\Delta_n, \Sigma_n$  on the points  $(i\omega_n)_{n \in \llbracket 0, N_\omega \rrbracket}$  are related by for all  $n \in \llbracket 0, N_\omega \rrbracket$ ,

$$\Delta_n = \Delta(i\omega_n) = W(i\omega_n - H_\perp^0 - \Sigma(i\omega_n))^{-1} W^\dagger = W(i\omega_n - H_\perp^0 - \Sigma_n)^{-1} W^\dagger.$$

so that we will impose this condition on the discretized quantities. This property holds for all  $z \in \mathbb{C}_+$ , and the prescription  $i\omega_n$  is best motivated by the second equation we will impose.

Now for the discretization of (4.2), recall that by definition [3, Proposition 2.18], given  $-\Delta : \mathbb{C}_+ \rightarrow \overline{\mathbb{C}_+}$ ,  $-\text{IPT}_\beta(U, \Delta) : \mathbb{C}_+ \rightarrow \overline{\mathbb{C}_+}$  is a solution to the interpolation problem  $\text{AC}(i\omega_n, \Sigma_n)$  (we have proven uniqueness for hybridization functions associated to finite dimensional baths), where

$$\Sigma_n = U^2 \int_0^\beta e^{i\omega_n \tau} \left( \frac{1}{\beta} \sum_{n' \in \mathbb{Z}} e^{-i\omega_{n'} \tau} (i\omega_{n'} - \Delta(i\omega_{n'}))^{-1} \right)^3 d\tau.$$

In our discretized scheme, we only consider finite sequences, so that we need to truncate the above sum: we will impose that, given  $(\Delta_n)_{n \in \llbracket 0, N_\omega \rrbracket}$ ,  $\Sigma_n$  is defined as

$$\Sigma_n = U^2 \int_0^\beta e^{i\omega_n \tau} \left( \frac{1}{\beta} \sum_{n'=-(N_\omega+1)}^{N_\omega} e^{-i\omega_{n'} \tau} (i\omega_{n'} - \Delta_{n'})^{-1} \right)^3 d\tau,$$

which, contrary to the discretization of (4.1), provides a given  $\Sigma_n$  from  $(\Delta_n)_{n \in \llbracket 0, N_\omega \rrbracket}$ . For now on, we will denote  $(\Delta_n)_{n \in \llbracket 0, N_\omega \rrbracket}$  by  $\Delta$ , and  $(\Sigma_n)_{n \in \llbracket 0, N_\omega \rrbracket}$  by  $\Sigma$ . We consolidate the content of this section into the following definition.

**Definition 4.1.1** (Matsubara's frequencies discretized IPT-DMFT equations). *Given  $N_\omega \in \mathbb{N}$  a Matsubara's frequencies cutoff, the Matsubara's frequencies discretized IPT-DMFT equations are the set of equations defined for all  $n \in \llbracket 0, N_\omega \rrbracket$  by*

$$\Delta_n = W (i\omega_n - H_\perp^0 - \Sigma_n)^{-1} W^\dagger \quad (4.6)$$

$$\Sigma_n = U^2 \int_0^\beta e^{i\omega_n \tau} \left( \frac{1}{\beta} \sum_{n'=-\left(N_\omega+1\right)}^{N_\omega} e^{-i\omega_{n'} \tau} (i\omega_{n'} - \Delta_{n'})^{-1} \right)^3 d\tau \quad (4.7)$$

with  $-\Delta = (-\Delta_n)_{n \in \llbracket 0, N_\omega \rrbracket} \in \overline{\mathbb{C}_+}^{N_\omega+1}$ ,  $-\Sigma = (-\Sigma_n)_{n \in \llbracket 0, N_\omega \rrbracket} \subset \overline{\mathbb{C}_+}^{N_\omega+1}$ .

We prove in the next section the existence of a solution to these equations, and will show numerically that uniqueness is not always guaranteed.

**Remark 4.1.2.** *The requirement that  $-\Delta, -\Sigma \in \overline{\mathbb{C}_+}^{N_\omega+1}$  is a minimal condition for the solution to represent physical quantities. Nevertheless, nothing ensures a priori that a solution to these equations admits an analytic continuation, nor if they do, that this solution is unique. This point makes the strategy we have followed to prove existence completely different from [3] (we will not make use of results associated to Pick functions). We refer the reader to [5], and to Section 4.3.2 for a numerical discussion about this topic.*

## 4.2 Existence of solutions to the discretized equations

### 4.2.1 Main result

In this section, we present and prove our main result about existence of solutions: using Brouwer's fixed-point theorem [20], we show that the above defined equations admit a solution for specific range of parameters. The space  $\overline{\mathbb{C}_+}^{N_\omega+1}$  is equipped with the norm topology, and for all  $u \in \overline{\mathbb{C}_+}^{N_\omega+1}$ , we denote by  $\|u\|_2 = \left(\sum_{n=0}^{N_\omega} |u_n|^2\right)^{1/2}$  the usual Euclidean norm and by  $B(u, R)$  the closed Euclidean ball of radius  $R$  centered in  $u$ . For all Matsubara's frequency cutoff  $N_\omega \in \mathbb{N}$ , we introduce the critical radius  $R_{N_\omega}$  defined as

$$\sup \left\{ R \in \mathbb{R}_+ \text{ s.t. } \forall z \in B(0, R) \cap \overline{\mathbb{C}_+}^{N_\omega+1}, \forall n \in \llbracket 0, N_\omega \rrbracket, \quad \Im(F_{n, N_\omega}(z)) \leq 0 \right\}, \quad (4.8)$$

where

$$F_{n, N_\omega}(z) = \sum_{\substack{n_1, n_2, n_3 = -(N_\omega+1) \\ n_1 + n_2 + n_3 = n-1}}^{N_\omega} \prod_{i=1}^3 (i(2n_i + 1)/\pi + z_{n_i})^{-1}, \quad (4.9)$$

where for all  $n \in \llbracket -N_\omega + 1, -1 \rrbracket$ ,  $z_n = \overline{z_{-(n+1)}}$  (as in (4.5)). Note that the set described in (4.8) is closed.

**Theorem 4.2.1** (Existence of solution to the discretized IPT-DMFT equations.). *For all Matsubara's frequencies cutoff  $N_\omega \in \mathbb{N}$ , the critical radius  $R_{N_\omega}$  is well-defined and strictly positive. Moreover, for all inverse temperature  $\beta \in \mathbb{R}_+^*$  and  $W^\dagger \in \mathbb{R}_{L-1}$  satisfying*

$$\beta \|W\|_2 \leq \sqrt{2\sqrt{2}R_{N_\omega}}, \quad (4.10)$$

and for all on-site repulsion  $U \in \mathbb{R}$ , the set of equations given by (4.6), (4.7) admits a solution  $(\Delta, \Sigma) \in \mathfrak{D}_{\beta, N_\omega} \times \mathfrak{S}_{\beta, N_\omega, U}$  where

$$\mathfrak{D}_{\beta, N_\omega} = B(0, R_{N_\omega}/\beta) \cap \left(-\overline{\mathbb{C}_+}^{N_\omega+1}\right), \quad \mathfrak{S}_{\beta, N_\omega, U} = \text{IPT}_{N_\omega}(\mathfrak{D}_{\beta, N_\omega}) \quad (4.11)$$

### 4.2.2 Proof of Theorem 4.2.1

We introduce  $\text{BU}_{N_\omega}$  and  $\text{IPT}_{N_\omega}$  defined for all  $n \in \llbracket 0, N_\omega \rrbracket$  by

$$\begin{aligned}\text{BU}_{N_\omega}(\Sigma)_n &= W(i\omega_n - H_\perp^0 - \Sigma_n)^{-1} W^\dagger \\ \text{IPT}_{N_\omega}(\Delta)_n &= U^2 \int_0^\beta e^{i\omega_n \tau} \left( \frac{1}{\beta} \sum_{n'=-\lfloor N_\omega + 1 \rfloor}^{N_\omega} e^{-i\omega_{n'} \tau} (i\omega_{n'} - \Delta_{n'})^{-1} \right)^3 d\tau\end{aligned}$$

so that

$$(4.6) \iff \Delta = \text{BU}_{N_\omega}(\Sigma)$$

$$(4.7) \iff \Sigma = \text{IPT}_{N_\omega}(\Delta).$$

We show in Lemmata 4.2.2 and 4.2.3 below that these maps are well-defined on the right sets. We start by the following lemma:

**Lemma 4.2.2** (Boundedness of  $\text{BU}_{N_\omega}$ ). *If  $-\Sigma \in \overline{\mathbb{C}_+}^{N_\omega+1}$ , then  $-\text{BU}_{N_\omega}(\Sigma) \in \overline{\mathbb{C}_+}^{N_\omega+1}$ , namely  $\text{BU}_{N_\omega} : -\overline{\mathbb{C}_+}^{N_\omega+1} \rightarrow -\overline{\mathbb{C}_+}^{N_\omega+1}$  is well defined, and*

$$\|\text{BU}_{N_\omega}(\Sigma)\|_2 \leq \beta \frac{\|W\|_2^2}{2\sqrt{2}}.$$

*Proof.* The sign of the imaginary part is a direct consequence of the definition of the imaginary part of matrices and of the fact that if  $f$  is a Pick matrix, so is  $-f^{-1}$ . Recall that  $H_\perp^0 \in \mathcal{S}_{L-1}(\mathbb{R})$ , so that there exists  $P \in \mathcal{M}_{L-1}(\mathbb{C})$  unitary with  $H_\perp^0 = P \text{diag}(\varepsilon_1, \dots, \varepsilon_{L-1}) P^\dagger$ : from that, we have for all  $n \in \llbracket 0, N_\omega \rrbracket$ ,

$$\begin{aligned}|W(i\omega_n - H_\perp^0 - \Sigma_n)^{-1} W^\dagger|^2 &\leq \sum_{k=1}^{L-1} \frac{|(WP)_k|^2}{|i\omega_n - \Sigma_n - \varepsilon_k|^2} \\ &\leq \frac{1}{(\omega_n - \Im(\Sigma_n))^2} \|W\|_2^2 \leq \frac{\|W\|_2^2}{\omega_n^2},\end{aligned}$$

hence we finally have

$$\|\text{BU}_{N_\omega}(\Sigma)\|_2 \leq \|W\|_2^2 \left( \sum_{n=0}^{N_\omega} \frac{1}{\omega_n^2} \right)^{1/2} = \|W\|_2^2 \frac{\beta}{\pi} \left( \sum_{n=0}^{N_\omega} \frac{1}{(2n+1)^2} \right)^{1/2} \leq \beta \frac{\|W\|_2^2}{2\sqrt{2}}.$$

□

The analogue of this lemma for  $\text{IPT}_{N_\omega}$  is more restrictive as we state now, together with the well-definiteness of the critical radius  $R_{N_\omega}$ . We use the convention  $B(0, +\infty) = \mathbb{C}^{N_\omega+1}$  in the case  $R_{N_\omega}$  is not reached.

**Lemma 4.2.3** (Alternative formula for  $\text{IPT}_{N_\omega}$ ). *Given  $-\Delta \in \overline{\mathbb{C}_+}^{N_\omega+1}$ ,  $\text{IPT}_{N_\omega}(\Delta)$  reads for all  $n \in \llbracket 0, N_\omega \rrbracket$ ,*

$$\text{IPT}_{N_\omega}(\Delta)_n = \beta U^2 F_{n, N_\omega}(-\beta \Delta), \quad (4.12)$$

where  $F_{n, N_\omega}$  is given in (4.9). Moreover, for all Matsubara's frequency cutoff  $N_\omega$ , the critical radius  $R_{N_\omega}$  defined in (4.8) is well defined, and  $\text{IPT}_{N_\omega} : B(0, R_{N_\omega}/\beta) \cap (-\overline{\mathbb{C}_+}^{N_\omega+1}) \rightarrow -\overline{\mathbb{C}_+}^{N_\omega+1}$  is well defined.

*Proof.* We have for all  $n \in \llbracket 0, N_\omega \rrbracket$ ,

$$\begin{aligned}\text{IPT}_{N_\omega}(\Delta)_n &= \frac{U^2}{\beta^3} \sum_{n_1, n_2, n_3 = -(N_\omega+1)}^{N_\omega} \prod_{i=1}^3 (i\omega_{n_i} - \Delta_{n_i})^{-1} \int_0^\beta e^{i(\omega_n - \omega_{n_1} - \omega_{n_2} - \omega_{n_3})\tau} d\tau \\ &= \frac{U^2}{\beta^2} \sum_{\substack{n_1, n_2, n_3 = -(N_\omega+1) \\ n_1 + n_2 + n_3 = n-1}}^{N_\omega} \prod_{i=1}^3 (i\omega_{n_i} - \Delta_{n_i})^{-1}\end{aligned}$$

as

$$\int_0^\beta e^{i(\omega_n - \omega_{n_1} - \omega_{n_2} - \omega_{n_3})\tau} d\tau = \begin{cases} \beta & \text{if } n_1 + n_2 + n_3 = n - 1 \\ 0 & \text{else.} \end{cases}$$

For the second part, we first prove that  $\Im(F_{n,N_\omega}(0)) \leq 0$ : for all  $n \in \llbracket 0, N_\omega \rrbracket$ , we define

$$A(n, N_\omega) = \frac{1}{\pi^3} \Im(F_{n,N_\omega}(0)) = \sum_{\substack{n_1, n_2, n_3 = -(N_\omega+1) \\ n_1 + n_2 + n_3 = n-1}}^{N_\omega} \prod_{i=1}^3 \frac{1}{2n_i + 1}$$

Let us show that the quantity  $A(n, N_\omega)$  is increasing in  $N_\omega$ : by enumerating, we have for all  $n \in \llbracket 0, N_\omega \rrbracket$ ,

$$A(n, N_\omega + 1) - A(n, N_\omega) = \frac{3}{2N_\omega + 3} \sum_{\substack{n_1, n_2 = -(N_\omega+1) \\ n_1 + n_2 + N_\omega + 1 = n-1}}^{N_\omega} \frac{1}{(2n_1 + 1)(2n_2 + 1)} \quad (4.13)$$

$$- \frac{3}{2N_\omega + 3} \sum_{\substack{n_1, n_2 = -(N_\omega+1) \\ n_1 + n_2 - (N_\omega+2) = n-1}}^{N_\omega} \frac{1}{(2n_1 + 1)(2n_2 + 1)} \quad (4.14)$$

$$- \frac{6}{(2N_\omega + 3)^2(2n + 1)}.$$

Now for the first term (4.13) of the r.h.s., we have for all  $n_1, n_2 \in \llbracket -(N_\omega + 1), N_\omega \rrbracket$  satisfying  $n_1 + n_2 + N_\omega + 1 = n - 1$ ,

$$\frac{1}{(2n_1 + 1)(2n_2 + 1)} = \frac{1}{2(n - (N_\omega + 1))} \left( \frac{1}{2n_1 + 1} + \frac{1}{2n_2 + 1} \right)$$

so that

$$\begin{aligned} \sum_{\substack{n_1, n_2 = -(N_\omega+1) \\ n_1 + n_2 + N_\omega + 1 = n-1}}^{N_\omega} \frac{1}{(2n_1 + 1)(2n_2 + 1)} &= \frac{1}{n - (N_\omega + 1)} \sum_{n_1 = -(N_\omega+1)}^{n-1} \frac{1}{2n_1 + 1} \\ &= \frac{1}{N_\omega + 1 - n} \sum_{n_1 = n}^{N_\omega} \frac{1}{2n_1 + 1}, \end{aligned}$$

where the last equality comes from the fact that  $\sum_{n_1 = -(N_\omega+1)}^{N_\omega} \frac{1}{2n_1 + 1} = 0$ . For the second term (4.14), we also have for all  $n_1, n_2 \in \llbracket -(N_\omega + 1), N_\omega \rrbracket$  satisfying  $n_1 + n_2 - (N_\omega + 2) = n - 1$ ,

$$\frac{1}{(2n_1 + 1)(2n_2 + 1)} = \frac{1}{2(n + N_\omega + 2)} \left( \frac{1}{2n_1 + 1} + \frac{1}{2n_2 + 1} \right),$$

so that

$$\sum_{\substack{n_1, n_2 = -(N_\omega+1) \\ n_1 + n_2 - (N_\omega+2) = n-1}}^{N_\omega} \frac{1}{(2n_1 + 1)(2n_2 + 1)} = \frac{1}{n + N_\omega + 2} \sum_{n_1 = n+1}^{N_\omega} \frac{1}{2n_1 + 1}.$$

We end up with

$$\begin{aligned} A(n, N_\omega + 1) - A(n, N_\omega) &= \frac{3}{2N_\omega + 3} \left( \frac{1}{N_\omega + 1 - n} - \frac{1}{n + N_\omega + 2} \right) \sum_{n_1 = n+1}^{N_\omega} \frac{1}{2n_1 + 1} \\ &\quad + \frac{3}{(2N_\omega + 3)(2n + 1)} \left( \frac{1}{(N_\omega + 1 - n)} - \frac{2}{2N_\omega + 3} \right) \end{aligned}$$

which is positive, hence  $A(n, N_\omega)$  is increasing in  $N_\omega$  and so is  $\Im(F_{n,N_\omega}(0))$ . Note also that by Dirichlet theorem on Fourier series and dominated convergence (see [3, Equation (64)]), we have

$$\lim_{N_\omega \rightarrow \infty} F_{n,N_\omega}(0) = \frac{1}{\beta} \text{IPT}_\beta(U = 1, 0)(i\omega_n)$$

as defined in [3, Proposition 2.18], which we have shown to be of negative imaginary part. Therefore,

$$\Im(F_{n,N_\omega}(0)) \leq \frac{1}{\beta} \Im(\text{IPT}_\beta(U=1,0)(i\omega_n)) < 0.$$

Since for all  $n \in \llbracket 0, N_\omega \rrbracket$ , the map  $F_{n,N_\omega}$  is continuous in 0 (see equation (4.9)), the set described in (4.8) is not empty and closed, such that  $R_c^{N_\omega}$  is well-defined, which concludes.  $\square$

We conclude from the two above lemmata, that for  $\beta \|W\|_2 < \sqrt{2\sqrt{2}R_{N_\omega}}$ , the map  $\text{DMFT}_{N_\omega} = \text{BU}_{N_\omega} \circ \text{IPT}_{N_\omega}$  is well-defined from  $B(0, R_{N_\omega}/\beta)$  to itself: indeed, for all  $\Delta \in B(0, R_{N_\omega}/\beta)$ ,  $\beta\Delta \in B(0, R_{N_\omega})$  so that  $-\text{IPT}_{N_\omega}(\Delta) \in \overline{\mathbb{C}_+}^{N_\omega+1}$ , hence

$$\|\text{BU}_{N_\omega}(\text{IPT}_{N_\omega}(\Delta))\|_2 \leq \beta \frac{\|W\|_2^2}{2\sqrt{2}} \leq R_{N_\omega}/\beta.$$

Since  $\text{DMFT}_{N_\omega}$  is continuous, it admits a fixed-point by the Brouwer fixed-point theorem, which concludes the proof.

### 4.3 Iterative scheme and Mott transition

As emphasized in the proof of Theorem 4.2.1, a natural formulation of the Matsubara's frequency discretized IPT-DMFT equations is based on the introduction of the  $\text{DMFT}_{N_\omega}$  map, which is defined so that

$$(4.6), (4.7) \iff \begin{cases} \Delta = \text{DMFT}_{N_\omega}(\Delta) \\ \Sigma = \text{IPT}_{N_\omega}(\Delta) \end{cases}.$$

The existence (and uniqueness) of a solution is therefore equivalent to the existence (and uniqueness) of a fixed point of  $\text{DMFT}_{N_\omega}$ . In this section, we make use of this formulation to come up with a DMFT algorithm based on the implementation of the naive fixed-point algorithm (we will not consider more elaborate methods such as Anderson acceleration). It proceeds as follows: given  $-\Delta^{(0)} \in \overline{\mathbb{C}_+}^{N_\omega+1}$ , we define by recursion for all  $n \in \mathbb{N}$

$$\Delta^{(n+1)} = \text{DMFT}_{N_\omega}(\Delta^{(n)}).$$

To make the setting as simple as possible, we focus on the implementation of this algorithm for the Hubbard dimer  $|\mathcal{G}_H| = 2$ , still in the *single-site translation-invariant paramagnetic* case: in this setting,  $H_\perp^0 = 0$  and  $W = T \in \mathbb{R}$  (see (4.3)), so that equation (4.6) amounts to, for all  $n \in \llbracket 0, N_\omega \rrbracket$ ,

$$\Delta_n = T^2 (i\omega_n - \Sigma_n)^{-1} \tag{4.15}$$

This example, in spite of its simplicity, is enough to exhibit Mott transition (Section 4.3.1) and to discuss the uniqueness of fixed points for specific range of parameters (Section 4.3.2).

**Discretization parameters** The simulations are performed using the Python/C++ library **TRIQS**, version 3.1.0 [16]. Discretization parameters are chosen such that the discretization error due to the integral performed in (4.7) can be considered as negligible: we always take a number of points  $N_\tau$  associated to the discretization of  $(0, \beta)$  large compared to  $N_\omega$ . Another reason for considering errors related to this integral negligible is that this integral is actually performed using the **Fourier** method (see **TRIQS** web page for the documentation), which performs tail-fitting on top. For all the simulations to come, we took the following parameters:

$$N_\tau = 10000, \quad N_\omega = 1000 \quad \left( \frac{N_\tau}{N_\omega} = 10 \right)$$

#### 4.3.1 Mott transition

As announced in Section 4.1, we provide numerical illustration to the existence of a metal-to-insulator Mott transition as predicted by DMFT for the Hubbard dimer. It is known [14] that the ground-state of such a system shall not exhibit such a phase transition, but DMFT focuses on the Gibbs state [3] for non-zero temperatures. The procedure is as follows for a given set of parameters  $T, U, \beta$ :

- For an initialization  $\Delta^{(0)}$ , we run  $N_{\text{iter}}$  iterations of  $\text{DMFT}_{N_\omega}$  to reach a converged solution  $\Delta^\infty$ .

- We then compute the associated self-energy  $\Sigma^\infty = \text{IPT}_{N_\omega}(\Delta^\infty)$ , and the corresponding discretized impurity Green's function  $-G^\infty \in \overline{\mathbb{C}_+}^{N_\omega+1}$  as explained below. Recall that in DMFT, the later is an approximation of the original Hubbard model Green's function restricted to the subgraph induced by the DMFT partition  $\mathfrak{P}$ . Recall also that by definition of the hybridization function  $\Delta$  and due to the sparsity pattern of the self-energy  $\Sigma$  [3, Theorem 2.8], the impurity Green's function of an AIM reads

$$G_{\text{imp}} = (z - H_{\text{imp}}^0 - \Delta(z) - \Sigma_{\text{imp}}(z))^{-1}$$

For a partition in singletons,  $H_{\text{imp}}^0 = 0$ , so that we finally define  $G^\infty$  by setting, for all  $n \in \llbracket 0, N_\omega \rrbracket$ ,

$$G_n^\infty = (i\omega_n - \Delta_n^\infty - \Sigma_n^\infty)^{-1}$$

- Finally we solve numerically the analytic continuation problem  $(i\omega_n, -G_n^\infty)_{n \in \llbracket 0, N_\omega \rrbracket}$  using the method `set_from_pade`, which is based on Pade approximants, and returns the values  $G_{\mathbb{R}}$  of this interpolation on a given set of points on the real line. This set is a regular mesh of  $[\varepsilon_{\min}, \varepsilon_{\max})$  consisting in  $N_{\text{mesh}} \in \mathbb{N}$  points. As already mentioned in Section 4.1, these analytic continuation methods are ill-conditioned and we use them only for illustration purposes.

Assuming the analytic continuation is a Pick function with Nevanlinna-Riesz measure absolutely continuous (with respect to Lebesgue measure), we get the density  $\rho$  of the spectral function  $A$  by

$$\rho = -\frac{1}{\pi} \Im(G_{\mathbb{R}})$$

Let us mention that, contrary to other methods developed recently in [4], `set_from_pade` does not ensure *a priori* that the analytic continuation is a Pick function, and may lead to results with negative signs.

We plot in Figure 2 the results of this algorithm for the following parameters:

$$\beta = 1, \quad T = 1, \quad N_{\text{iter}} = 50, \quad \Delta^{(0)} = (i\omega_n)_{n \in \llbracket 0, N_\omega \rrbracket}^{-1}, \quad -\varepsilon_{\min} = \varepsilon_{\max} = 10, \quad N_{\text{mesh}} = 1000 \quad (4.16)$$

while varying  $U$  from 2 to 10. The big picture is similar to what is obtained for the so-called Bethe lattice [7] and requires some comments:

- As  $U$  increases,  $\rho(0)$  decreases to reach approximately 0 between  $U = 6$  and  $8$ : for  $U < 6$ , the system is a conductor according to the conduction criterion provided in Section 4.3, and insulating for  $U > 8$ . In between these values, `set_from_pade` returns negative values of  $\rho(0)$ , which refrains this study from determining more precisely the value of  $U$  for which the Mott transition occurs, nor if this transition really exists or if it only consists of a crossover [18].
- The density  $\rho$  is even: this is a consequence of the fact that, given a purely imaginary initialization  $-\Delta^{(0)} \in (i\mathbb{R}_+)^{N_\omega+1}$ , the iterates are purely imaginary as well:  $\forall n \in \mathbb{N}, -\Delta^{(n)} \in (i\mathbb{R}_+)^{N_\omega+1}$  (this is a direct consequence of Lemma 4.2.3 and Equation (4.15)). Note that this property also holds true at convergence, for non-even initializations.

This property is in relation with the fact we are dealing with *half-filled* systems, and a Hubbard graph for which particle-hole symmetry holds, as detailed in [7].

For all these simulations to make sense, we need to check that convergence is reached: in the next section, we study how this iterative scheme converges for different sets of parameters, showing how Mott transition is affected by temperature, and how the result depends on the initial condition.

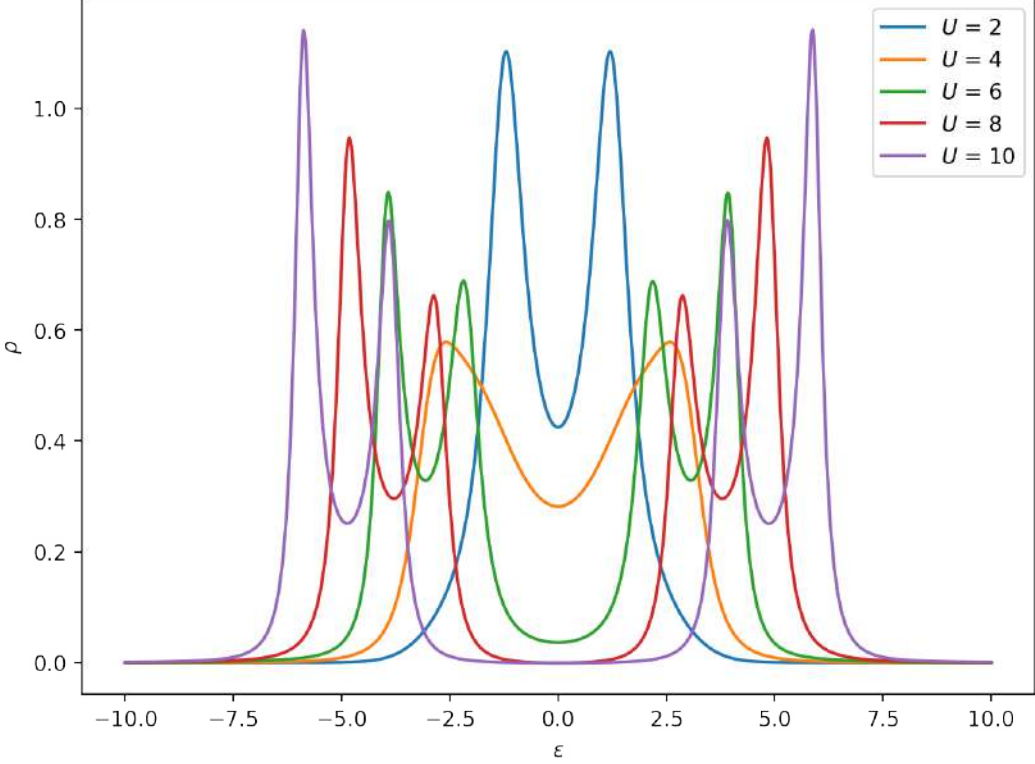


Figure 2: Density  $\rho$  of the spectral function  $A$  obtained by analytic continuation using Pade approximants, for different values of the on-site repulsion  $U$ . Other parameters are fixed as in (4.16).

#### 4.3.2 Linear convergence for small and large on-site repulsion

In this section, we explore numerically the convergence of the basic fixed-point algorithm already introduced. To do so, we compute the norm of the residual  $\|\Delta^{(n+1)} - \Delta^{(n)}\|_2$  as a function of the iteration  $n$ . We fix  $T = 1$  for all the simulations, which amounts to consider  $\beta, U, \Delta, \Sigma$  to be adimensional quantities: the inverse temperature  $\beta$  is fixed while the on-site repulsion  $U$  varies from 0.5 to 18. We also take two radically different initial guess  $\Delta^{(0)} = (i\omega_n)_{n \in \llbracket 0, N_\omega \rrbracket}^{-1}$ ,  $\Delta^{(0)} = 0$  which correspond to the two solutions in the limit cases  $U = 0$  and  $U = \infty$  respectively. We will consider two temperatures: first, we take  $\beta = 1$ , to ensure the simulations done in the previous section are converged, then  $\beta = 10$  to show the coexistence of a physical solution and an unphysical one. We summarize in Figure 3 the settings for which we run the simulations.

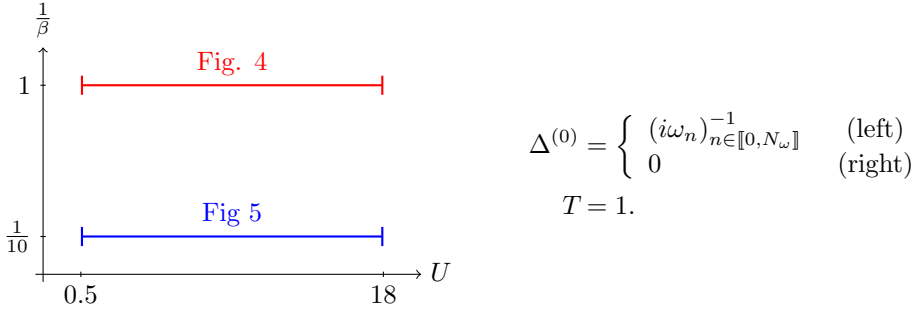


Figure 3: Schematic of the two scans in  $U$  at fixed  $\beta$ , with the associated parameters.

**High-temperature ( $\beta = 1$ ) simulations.** We report in Figure 4 the simulations performed for inverse temperature  $\beta = 1$ , which corresponds to the setting established in Section 4.3.1. For all values of  $U$ , the algorithm converges linearly to a solution, regardless of the choice of one of the two initial guesses, which validates simulations performed in Section 4.3.1. The rate of convergence first increases with  $U$  to

reach a maximum between 6 and 8, where the Mott transition takes place, and then decreases. These simulations show that the convergence is affected by the parameters  $\beta, U$ : we now present what happens for larger  $\beta$ , which corresponds to smaller temperatures.

**Low-temperature ( $\beta = 10$ ) simulations.** Results for  $\beta = 10$  are reported in Figure 5. The general picture is quite different: for small and high on-site repulsion  $U$ , the algorithm still converges linearly for the two initial guesses to the same solution, but for intermediate values of  $U$  (between 3 and 5), the residual does not decay monotonously and requires much more iterations to converge. Moreover, for  $U = 3$  and with the initial guess  $\Delta^{(0)} = (i\omega_n)_{n \in \llbracket 0, N_\omega \rrbracket}^{-1}$  (center left in Figure 5), the algorithm reaches a stationary solution with a much larger residual compared to the simulations with  $\Delta^{(0)} = 0$ : this converged solution, represented in Figure 6, is not in  $-\overline{\mathbb{C}_+}^{N_\omega+1}$ , hence cannot correspond to the values of a negative of a Pick function on the given Matsubara's frequencies.

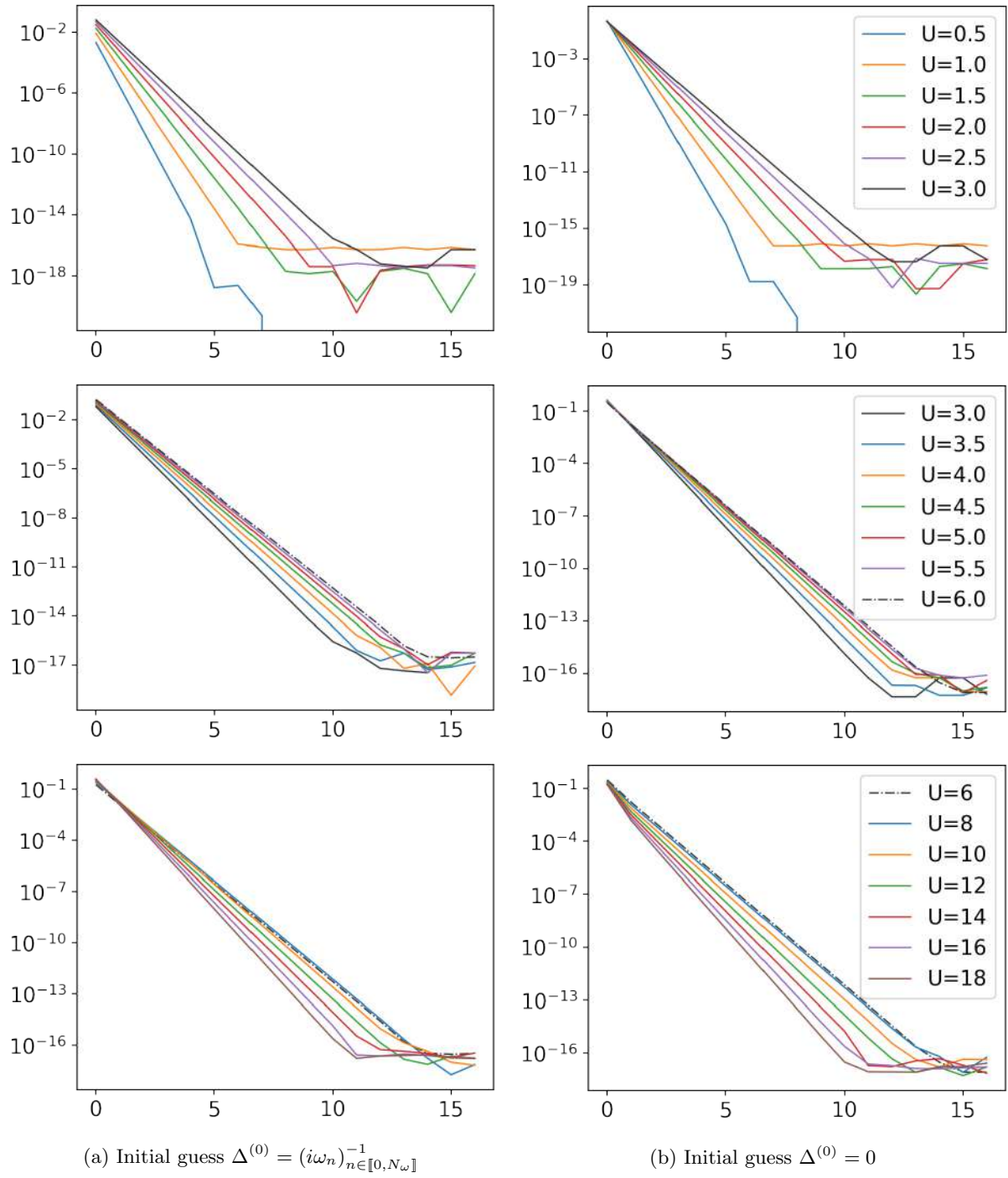


Figure 4: Residual  $\|\Delta^{(n+1)} - \Delta^{(n)}\|_2$  in log scale, as a function of the iteration  $n \in \llbracket 0, N_{\text{iter}} \rrbracket$ , for high temperature  $\beta = 1$  and several values of  $U$ . Left and right sides differ in the initial guess  $\Delta^{(0)}$ .

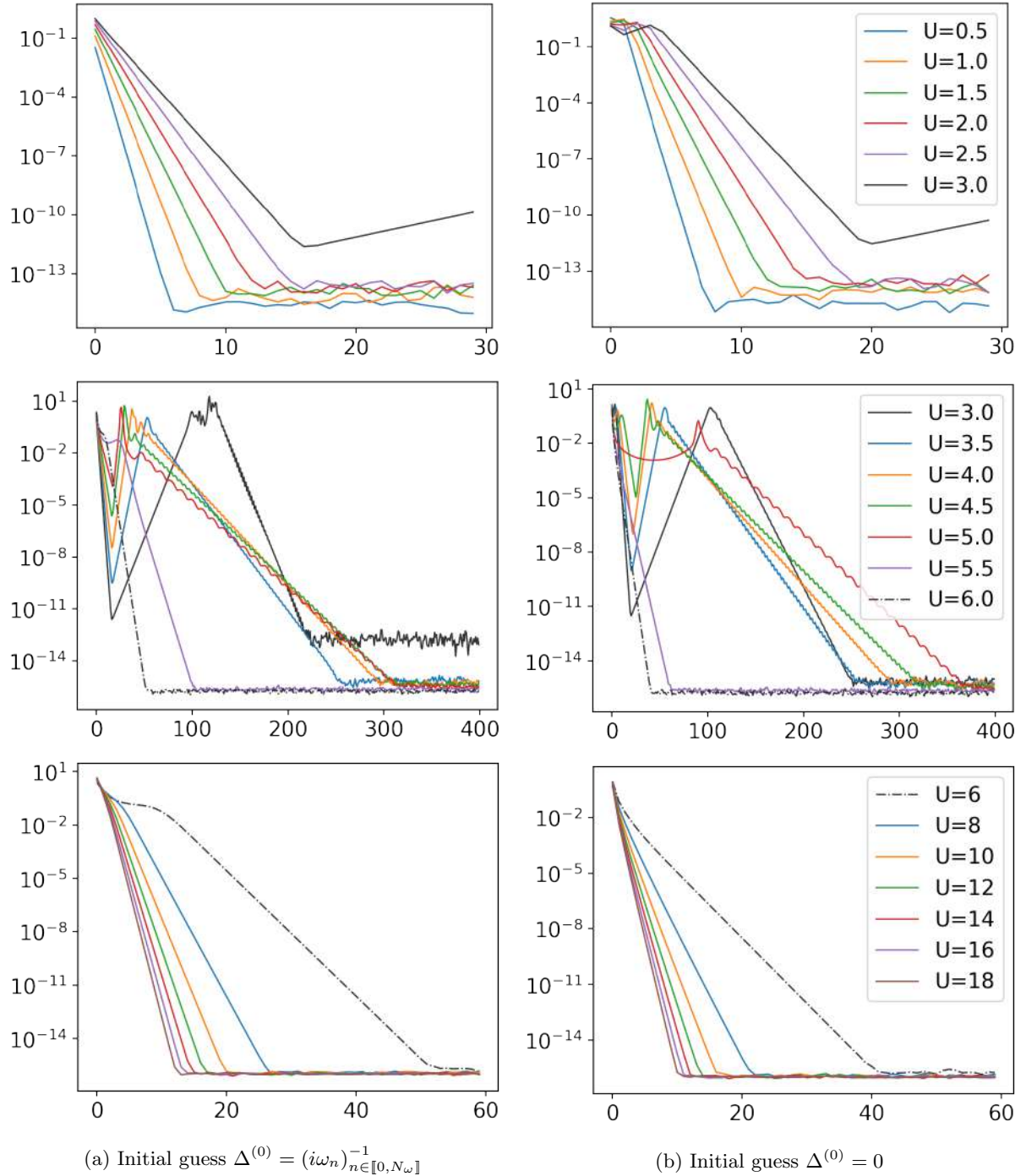
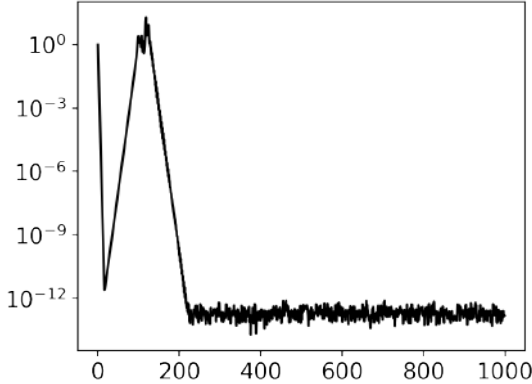
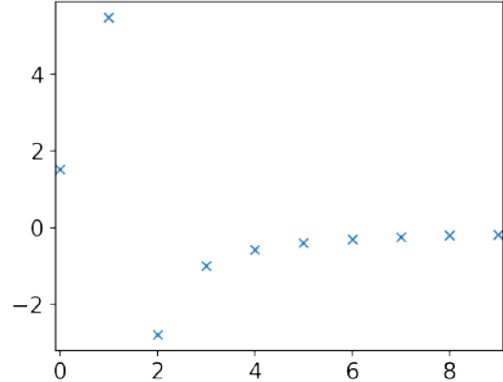


Figure 5: Residual  $\|\Delta^{(n+1)} - \Delta^{(n)}\|_2$  in log scale, as a function of the iteration  $n \in [0, N_{\text{iter}}]$ , for low temperature  $\beta = 10$  and several values of  $U$ . Left and right sides differ in the initial guess  $\Delta^{(0)}$ .



(a) Residual  $\|\Delta^{(n+1)} - \Delta^{(n)}\|_2$  in log scale, as a function of the iteration  $n \in \llbracket 0, N_{\text{iter}} \rrbracket$ , for  $\beta = 10$  and  $U = 3.0$ , with  $\Delta^{(0)} = (i\omega_n)^{-1}_{n \in \llbracket 0, N_\omega \rrbracket}$ . The residual is stationary after  $\approx 200$  iterations.



(b) Representation of the first 10 components of  $\Im(\Delta^\infty)$ . The first 2 are positive, hence there is no negative of Pick function which interpolates  $\Delta^\infty$  at the Matsubara's frequencies  $(i\omega_n)_{n \in \llbracket 0, N_\omega \rrbracket}$ .

Figure 6: Residual convergence (left) and plot of the imaginary part of the converged solution  $\Delta^\infty$  (right). The naïve fixed-point algorithm does not always converge to a physical solution (see Remark 4.1.2).

This result shows that convergence toward a physical solution is not guaranteed for intermediate values of  $U$  for  $\beta = 10$  and depends on the initialization: to overcome this issue, we will run simulations using continuation method in the next section, starting from small/large  $U$  where the algorithm seems to converge better. For now, let us mention that these convergences advocate for uniqueness in the small and large on-site repulsion  $U$  regimes : we will show in Section 4.4 that it holds by perturbative arguments.

### 4.3.3 Continuation method and metastable solution

In this section, we give a last numerical insight about the convergence of the algorithm we have introduced: for high temperature  $\beta = 10$  and intermediary on-site repulsion  $U$ , it does not converge monotonously, and not always toward a physical solution. These issues seem to depend on the initial guess, and to overcome them, we use a continuation method:

- We start by running the algorithm for on-site repulsion  $U$  small/large enough: as depicted in Figure 5, the algorithm seems to converge globally regardless of the initial condition, so that we take the initial guess  $\Delta^{(0)} = (i\omega_n)^{-1}_{n \in \llbracket 0, N_\omega \rrbracket}$ .
- Once the algorithm is converged, we change slightly the value of  $U$  and take as initial condition the converged solution  $\Delta^\infty$  for the prior value of  $U$ .
- We repeat until we get to the values of interest in  $U$ .

We run this continuation method with two starting values of the on-site repulsion: one starts with  $U = 1$  and increases by steps of 1 until 4 is reached (namely  $U = 1, 2, 3, 4$ ), the other starts from  $U = 6$  and decreases by the same steps until 2 is reached (namely  $U = 6, 5, 4, 3, 2$ ). We then plot the values of  $\Delta^{N_{\text{iter}}}$  for the values of  $U$  common to both the increasing and decreasing sequences (namely  $U \in \{2, 3, 4\}$ ). In order to provide insights on the convergence, we run these simulations with increasing number of iterations  $N_{\text{iter}}$ : we start by  $N_{\text{iter}} = 60$ , which is required so that the first simulations of the continuation method at  $U = 1$  and  $U = 6$  give a converged solution  $\Delta^\infty$  (see Figure 5). We then take  $N_{\text{iter}} = 100$  and finally  $N_{\text{iter}} = 400$  for which the residual is fully converged. We summarize in Figure 7 the setting.

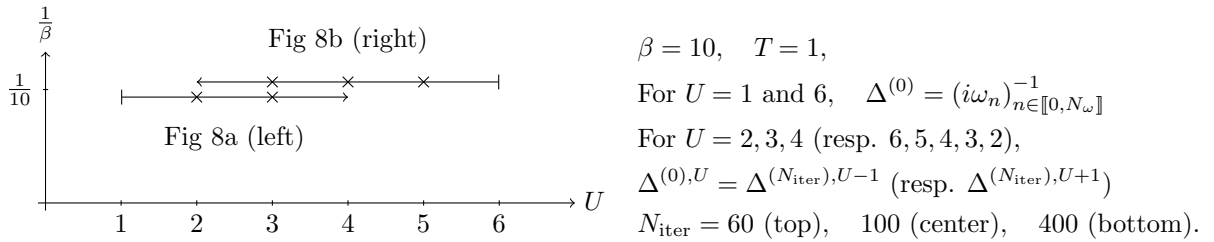
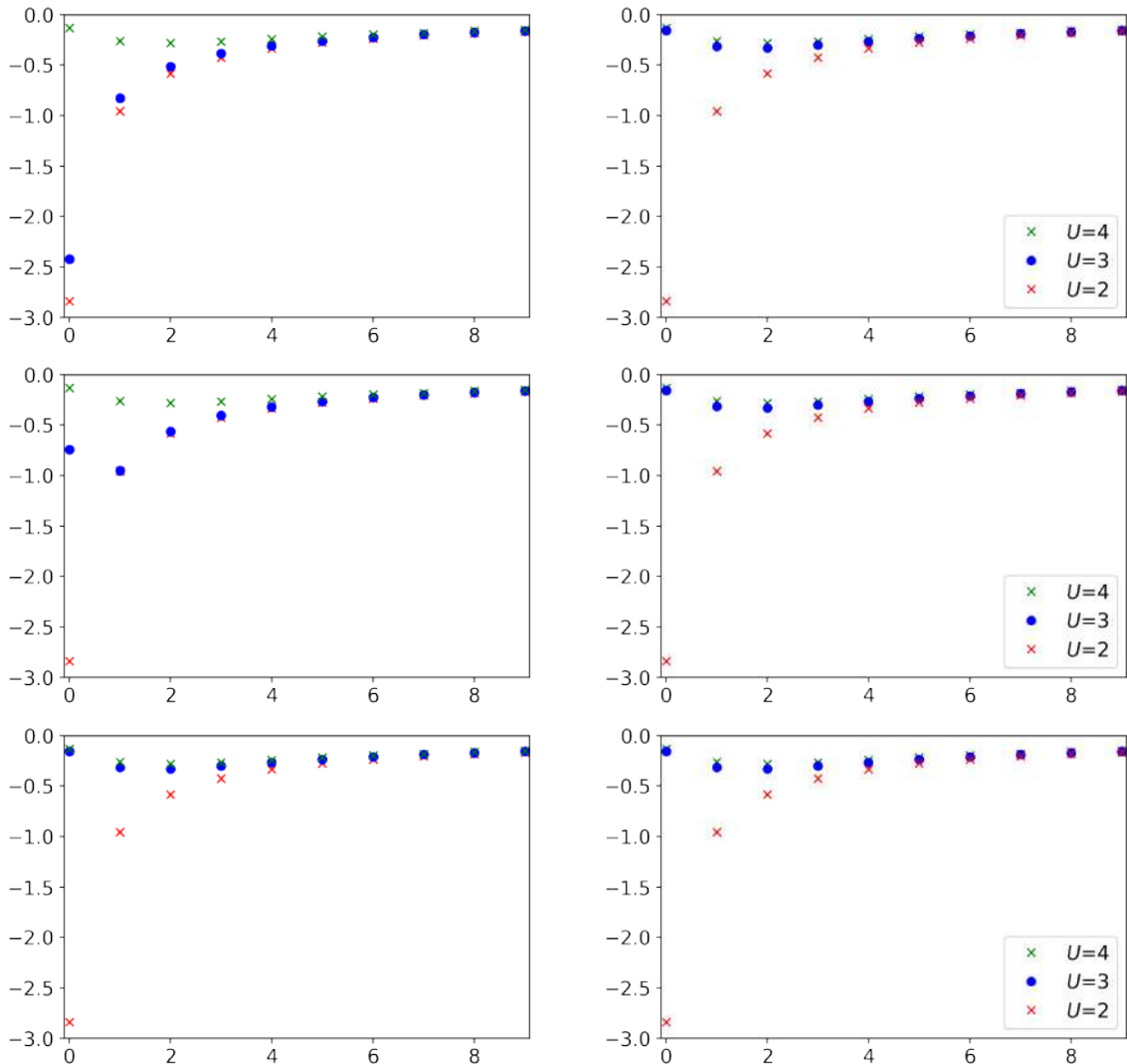


Figure 7: Schematic of the increasing-in- $U$  (Figure 8a) and decreasing-in- $U$  (Figure 8b) simulations, and recap of the parameters used for the simulations.



(a) Performed with  $\Delta^{(0)} = (i\omega_n)_{n \in [0, N_\omega]}$  at  $U = 1$ , and then recursively for  $U = 2, 3, 4$  increasingly, with  $\Delta^{(0),U} = \Delta^{(N_{\text{iter}}), U-1}$ .

(b) Performed with  $\Delta^{(0)} = (i\omega_n)_{n \in [0, N_\omega]}$  at  $U = 6$ , and then recursively for  $U = 5, 4, 3, 2$  decreasingly, with  $\Delta^{(0),U} = \Delta^{(N_{\text{iter}}), U+1}$ .

Figure 8: Plot of the first 10 components of  $\Im(\Delta^{(N_{\text{iter}}),U})$  with  $U \in \{2, 3, 4\}$ , for both the increasing sequence (left) and decreasing sequence (right), with  $N_{\text{iter}} = 60$  (top), 100 (center), 200 (bottom).

The results are presented in Figure 8 and commented on below:

- For  $U = 2$  and  $U = 4$ , the simulations are converged for  $N_{\text{iter}} = 60$  and the increasing-in- $U$  and decreasing-in- $U$  simulations solutions agree on these values of  $U$ . If each of these finite sequences can be analytically continued into a Pick function, the case  $U = 2$  would have a Nevanlinna-Riesz measure concentrated in 0, while  $U = 4$  would have a symmetric profile with small mass in 0. This also holds for the associated Green's functions values: as for  $\beta = 1$  (see Section 4.3.1), we observe a Mott transition but for a smaller interval in  $U$ , the case  $U = 2$  corresponding to a conductor, while  $U = 4$  corresponds to an insulator.
- The case  $U = 3$  is more delicate: for  $N_{\text{iter}} = 60$ , the increasing-in- $U$  exhibits a conductive-like solution, while the decreasing-in- $U$  solution is resembles an insulator. We also see that when increasing  $N_{\text{iter}}$ , the increasing-in- $U$  simulation eventually reaches the insulating solution predicted by the decreasing-in- $U$  for  $N_{\text{iter}} = 200$ . In the literature [7], this effect is not reported: on the opposite, it is stated that for  $\beta$  high-enough, there is a range in  $U$  for which two solutions coexist. This phenomenon would be a signature of the existence of a phase transition of order 1. The present simulations are performed on an other system (the Hubbard dimer) and for much bigger  $N_{\text{iter}}$ . They rather support for the scenario of a "metastable" solution, meaning it requires much more iterations to converge than for other values of the parameters  $\beta, U$ .

In light of these results, it would be desirable to implement acceleration methods on this fixed-point iteration algorithm in order to avoid this slow convergence for intermediate values of  $U$ , and a stabilization procedure which would help in understanding the discrepancy of the increasing/decreasing sequences detailed above. A great candidate for these two improvements is Anderson mixing. From a mathematical perspective, a first affordable result is the uniqueness of the fixed point in the perturbative regime, as we state now.

## 4.4 Uniqueness of the solution in perturbative regimes.

### 4.4.1 Main result

The previous simulations indicate that uniqueness of the solution, if not elucidated for arbitrary values of the parameters  $T, U, \beta$ , holds perturbatively around the regimes  $U = 0$  and  $T = 0$ , the later corresponding to the formal limit case  $U = \infty$ . From a mathematical perspective, it is best seen from the fact that, similarly as with the DMFT equations [3, Proposition 2.12], the discretized IPT-DMFT equations (4.6),(4.7) admit a unique solution in the following trivial limits:

- For  $U = 0$ ,  $\text{IPT}_{N_\omega} = 0$ , hence the only solution is given by, for all  $n \in \llbracket 0, N_\omega \rrbracket$ ,

$$\Sigma_n = 0, \quad \Delta_n = \text{BU}_{N_\omega}(0) = W(i\omega_n - H_\perp^0)W^\dagger$$

- Conversely, for  $T = 0$ ,  $\text{BU}_{N_\omega} = 0$ , hence the only solution is given by, for all  $n \in \llbracket 0, N_\omega \rrbracket$ ,

$$\Sigma_n = \text{IPT}_{N_\omega}(0)_n, \quad \Delta_n = 0$$

Note moreover that the fixed-point algorithm we have implemented converges in one iteration in these limits. In both cases, these solutions satisfy with the physicality criterion  $-\Delta, -\Sigma \in \overline{\mathbb{C}_+}^{N_\omega+1}$  (see the proof of Lemma 4.2.3). The following theorem covers the perturbative regime around these two above limit cases  $T = 0$  or  $U = 0$ , showing the existence of a unique solution in the sets introduced in Theorem 4.2.1. It also proves the linear convergence observed for these two regimes, using a Picard fixed point theorem. As it holds for Theorem 1, our analysis relies on the properties of  $F_{n, N_\omega}$ : let us introduce  $L_{N_\omega}$  the (finite) largest Lipschitz constant of the  $F_{n, N_\omega}$  over  $\overline{\mathbb{C}_+}^{N_\omega+1}$ , for  $n \in \llbracket 0, N_\omega \rrbracket$ ,

$$L_{N_\omega} = \max_{n \in \llbracket 0, N_\omega \rrbracket} \text{Lip}_{\mathbb{C}_+}(F_{n, N_\omega}). \quad (4.17)$$

Note incidentally that, since  $F_{n, N_\omega}$  is a sum of rational function in the  $(\Delta_n)_{n \in \llbracket 0, N_\omega \rrbracket}$  with poles on the negative imaginary axis  $i\mathbb{R}_-^*$ , we have for all  $R > 0$ ,  $\text{Lip}_{\overline{\mathbb{C}_+}^{N_\omega+1}}(F_{n, N_\omega}) = \text{Lip}_{B(0, R) \cap \overline{\mathbb{C}_+}^{N_\omega+1}}(F_{n, N_\omega})$ .

**Theorem 4.4.1** (Uniqueness of the solution to the discretized IPT-DMFT equations). *For all Matsubara's frequencies cutoff  $N_\omega \in \mathbb{N}$ , inverse temperature  $\beta \in \mathbb{R}_+^*$ ,  $W^\dagger \in \mathbb{R}_{L-1}$ , and on-site repulsion  $U \in \mathbb{R}$  satisfying with the assumption of Theorem 1 (4.10) and*

$$\left( \frac{\beta^2 \|W\|_2 U}{\pi} \right)^2 L_{N_\omega} < 1, \quad (4.18)$$

*the discretized IPT-DMFT equations (4.6) (4.7) admits a unique solution in  $\mathfrak{D}_\beta \times \mathfrak{S}_{\beta, N_\omega, U}$ . Moreover, the fixed point algorithm sequence  $(\Delta^{(n)})_{n \in \mathbb{N}}$*

$$\Delta^{(0)} \in \mathfrak{D}_\beta, \quad \forall n \in \mathbb{N}, \quad \Delta^{(n+1)} = \text{DMFT}_{N_\omega}(\Delta^{(n)}) \quad (4.19)$$

*converges linearly toward this solution.*

In particular, Assumption (4.18) holds true for  $T$  or  $U$  small enough.

#### 4.4.2 Proof of Theorem 4.4.1

As announced, the proof is based on Picard fixed-point theorem on  $\mathfrak{D}_{\beta, N_\omega}$ . The first estimate is the following.

**Lemma 4.4.2** (Estimate on  $\text{BU}_{N_\omega}$ ). *Given  $-\Sigma_1, -\Sigma_2 \in \overline{\mathbb{C}_+}$ , the following estimate holds*

$$\|\text{BU}_{N_\omega}(\Sigma_1) - \text{BU}_{N_\omega}(\Sigma_2)\|_2 \leq \beta^2 \frac{\|W\|_2^2}{\pi^2} \|\Sigma_1 - \Sigma_2\|_2$$

*Proof.* Note that the resolvent identity yields for all  $n \in \llbracket 0, N_\omega \rrbracket$

$$\begin{aligned} \text{BU}_{N_\omega}(\Sigma_1)(i\omega_n) - \text{BU}_{N_\omega}(\Sigma_2)(i\omega_n) &= (\Sigma_1(i\omega_n) - \Sigma_2(i\omega_n)) \\ &\quad W(i\omega_n - \Sigma_1(i\omega_n) - H_\perp^0)^{-1} (i\omega_n - \Sigma_2(i\omega_n) - H_\perp^0)^{-1} W^\dagger \end{aligned}$$

and we have similarly as in the proof of lemma 4.2.2

$$|W(i\omega_n - \Sigma_1(i\omega_n) - H_\perp^0)^{-1} (i\omega_n - \Sigma_2(i\omega_n) - H_\perp^0)^{-1} W^\dagger|^2 \leq (WW^\dagger)^2 \frac{1}{\omega_n^4} \leq \beta^4 \frac{(WW^\dagger)^2}{\pi^4},$$

so that we end up with

$$\|\text{BU}_{N_\omega}(\Sigma_1)(i\omega_n) - \text{BU}_{N_\omega}(\Sigma_2)(i\omega_n)\| \leq \beta^2 \frac{WW^\dagger}{\pi^2} \left( \sum_{n=0}^{N_\omega} |\Sigma_1(i\omega_n) - \Sigma_2(i\omega_n)|^2 \right)^{1/2}$$

which concludes the proof.  $\square$

Now for  $\text{IPT}_{N_\omega}$ , we have the following estimate.

**Lemma 4.4.3** (Estimate on  $\text{IPT}_{N_\omega}$ ). *For all Matsubara's frequency cutoff  $N_\omega \in \mathbb{N}$ ,  $\text{IPT}_{N_\omega}$  is  $C^\infty$  on  $-\overline{\mathbb{C}_+}^{N_\omega+1}$ , and for all  $\Delta_1, \Delta_2 \in -\overline{\mathbb{C}_+}^{N_\omega+1}$ ,*

$$\|\text{IPT}_{N_\omega}(\Delta_1) - \text{IPT}_{N_\omega}(\Delta_2)\|_2 \leq (\beta U)^2 L_{N_\omega} \|\Delta_1 - \Delta_2\|_2 \quad (4.20)$$

where

*Proof.* This follows directly from Lemma 4.2.3 and the definition of the corresponding constants: for all  $\Delta_1, \Delta_2 \in -\overline{\mathbb{C}_+}^{N_\omega+1}$ , we have

$$\|\text{IPT}_{N_\omega}(\Delta_1) - \text{IPT}_{N_\omega}(\Delta_2)\|_2 = \beta U^2 \left( \sum_{n=0}^{N_\omega} |F_{n, N_\omega}(-\beta \Delta_1) - F_{n, N_\omega}(-\beta \Delta_2)|^2 \right)^{1/2} \quad (4.21)$$

$$\leq (\beta U)^2 L_{N_\omega} \|\Delta_1 - \Delta_2\| \quad (4.22)$$

$\square$

Now, under the assumption that (4.10) holds,  $\text{DMFT}_{N_\omega}$  is well defined from  $\mathfrak{D}_{\beta, N_\omega}$  to itself. Moreover, using Lemmata 4.2.3, 4.4.2 and 4.4.3, we have for all  $\Delta_1, \Delta_2 \in \mathfrak{D}_{\beta, N_\omega}$

$$\|\text{DMFT}_{N_\omega}(\Delta_1) - \text{DMFT}_{N_\omega}(\Delta_2)\|_2 \leq \left( \frac{\beta^2 \|W\|_2 U}{\pi} \right)^2 L_{N_\omega} \|\Delta_1 - \Delta_2\|_2, \quad (4.23)$$

and we conclude using Picard fixed-point theorem.

## Bibliography

- [1] Gordon Baym and N. David Mermin. Determination of Thermodynamic Green's Functions. *Journal of Mathematical Physics*, 2(2):232–234, March 1961.
- [2] Sergey Bravyi and David Gosset. Complexity of quantum impurity problems. *Communications in Mathematical Physics*, 356(2):451–500, December 2017. arXiv:1609.00735 [cond-mat, physics:math-ph, physics:quant-ph].
- [3] Éric Cancès, Alfred Kirsch, and Solal Perrin-Roussel. A mathematical analysis of IPT-DMFT, June 2024. arXiv:2406.03384.
- [4] Jiani Fei, Chia-Nan Yeh, and Emanuel Gull. Nevanlinna Analytical Continuation. *Physical Review Letters*, 126(5):056402, February 2021.
- [5] Jiani Fei, Chia-Nan Yeh, Dominika Zgid, and Emanuel Gull. Analytical continuation of matrix-valued functions: Carathéodory formalism. *Physical Review B*, 104(16):165111, 2021.
- [6] Antoine Georges and Gabriel Kotliar. Hubbard model in infinite dimensions. *Physical Review B*, 45(12):6479–6483, March 1992.
- [7] Antoine Georges, Gabriel Kotliar, Werner Krauth, and Marcelo J. Rozenberg. Dynamical mean-field theory of strongly correlated fermion systems and the limit of infinite dimensions. *Reviews of Modern Physics*, 68(1):13–125, January 1996.
- [8] Fritz Gesztesy and Eduard Tsekanovskii. On Matrix–Valued Herglotz Functions. *Mathematische Nachrichten*, 218(1):61–138, 2000.
- [9] J. E. Gubernatis, Mark Jarrell, R. N. Silver, and D. S. Sivia. Quantum Monte Carlo simulations and maximum entropy: Dynamics from imaginary-time data. *Physical Review B*, 44(12):6011–6029, 1991.
- [10] Emanuel Gull, Andrew J. Millis, Alexander I. Lichtenstein, Alexey N. Rubtsov, Matthias Troyer, and Philipp Werner. Continuous-time Monte Carlo methods for quantum impurity models. *Reviews of Modern Physics*, 83(2):349–404, 2011.
- [11] Zhen Huang, Emanuel Gull, and Lin Lin. Robust analytic continuation of Green's functions via projection, pole estimation, and semidefinite relaxation. *Physical Review B*, 107(7):075151, February 2023. arXiv:2210.04187 [cond-mat, physics:physics].
- [12] Mark Jarrell and J. E. Gubernatis. Bayesian inference and the analytic continuation of imaginary-time quantum Monte Carlo data. *Physics Reports*, 269(3):133–195, May 1996.
- [13] Jia Li, Yang Yu, Emanuel Gull, and Guy Cohen. Interaction-expansion inchworm Monte Carlo solver for lattice and impurity models. *Physical Review B*, 105(16):165133, 2022.
- [14] Elliott H. Lieb and F. Y. Wu. Absence of Mott Transition in an Exact Solution of the Short-Range, One-Band Model in One Dimension. *Physical Review Letters*, 20(25):1445–1448, June 1968.
- [15] Richard M. Martin, Lucia Reining, and David M. Ceperley. *Interacting Electrons: Theory and Computational Approaches*. Cambridge University Press, Cambridge, 2016.
- [16] Olivier Parcollet, Michel Ferrero, Thomas Ayral, Hartmut Hafermann, Igor Krivenko, Laura Messio, and Priyanka Seth. TRIQS: A toolbox for research on interacting quantum systems. *Computer Physics Communications*, 196:398–415, 2015.
- [17] A. N. Rubtsov, V. V. Savkin, and A. I. Lichtenstein. Continuous-time quantum Monte Carlo method for fermions. *Physical Review B*, 72(3):035122, July 2005.
- [18] Thomas Schäfer, Nils Wentzell, Fedor Šimkovic, Yuan-Yao He, Cornelia Hille, Marcel Klett, Christian J. Eckhardt, Behnam Arzhang, Viktor Harkov, François-Marie Le Régent, Alfred Kirsch, Yan Wang, Aaram J. Kim, Evgeny Kozik, Evgeny A. Stepanov, Anna Kauch, Sabine Andergassen, Philipp Hansmann, Daniel Rohe, Yuri M Vilk, James P. F. LeBlanc, Shiwei Zhang, A.-M. S. Tremblay, Michel Ferrero, Olivier Parcollet, and Antoine Georges. Tracking the Footprints of Spin Fluctuations: A MultiMethod, MultiMessenger Study of the Two-Dimensional Hubbard Model. *Physical Review X*, 11(1):011058, March 2021.

- [19] Priyanka Seth, Igor Krivenko, Michel Ferrero, and Olivier Parcollet. TRIQS/CTHYB: A continuous-time quantum Monte Carlo hybridisation expansion solver for quantum impurity problems. *Computer Physics Communications*, 200:274–284, 2016.
- [20] Joel H. Shapiro. *A Fixed-Point Farrago*. Universitext. Springer International Publishing, Cham, 2016.
- [21] Yuting Tan, Pak Ki Henry Tsang, Vladimir Dobrosavljević, and Louk Rademaker. Doping a Wigner-Mott insulator: Exotic charge orders in transition metal dichalcogenide moiré heterobilayers. *Physical Review Research*, 5(4):043190, 2023.
- [22] Philipp Werner, Armin Comanac, Luca de' Medici, Matthias Troyer, and Andrew J. Millis. Continuous-Time Solver for Quantum Impurity Models. *Physical Review Letters*, 97(7):076405, 2006.
- [23] Philipp Werner and Andrew J. Millis. Hybridization expansion impurity solver: General formulation and application to Kondo lattice and two-orbital models. *Physical Review B*, 74(15):155107, 2006.
- [24] X. Y. Zhang, M. J. Rozenberg, and G. Kotliar. Mott transition in the  $d = \infty$  Hubbard model at zero temperature. *Physical Review Letters*, 70(11):1666–1669, March 1993.